

Discovery of the Leinamycin Family of Natural Products by Mining Actinobacterial Genomes

Guohui Pan^{a,1}, Zhengren Xu^{a,1}, Zhikai Guo^a, Hindra^a, Ming Ma^a, Dong Yang^{a,b}, Hao Zhou^a, Yannick Gansemans^c, Xiangcheng Zhu^{d,e}, Yong Huang^d, Li-Xing Zhao^f, Yi Jiang^f, Jinhua Cheng^{g,h}, Filip Van Nieuwerburgh^c, Joo-Won Sun^{g,h}, Yanwen Duan^{d,e}, and Ben Shen^{a,b,i,*}

^aDepartment of Chemistry, The Scripps Research Institute, Jupiter, FL 33458, USA; ^bNatural Products Library Initiatives at The Scripps Research Institute, The Scripps Research Institute, Jupiter, FL 33458, USA; ^cLaboratory of Pharmaceutical Biotechnology, Ghent University, Ghent, Belgium; ^dXiangya International Academy of Translational Medicine, Central South University, Changsha, Hunan 410013, China; ^eHunan Engineering Research Center of Combinatorial Biosynthesis and Natural Product Drug Discovery, Changsha, Hunan 410013, China; ^fYunnan Institute of Microbiology, Yunnan University, Kunming, Yunnan 650091, China; ^gDivision of Bioscience and Bioinformatics, College of Natural Science, Myongji University, Yongin, Gyeonggi-Do 17058, Korea; ^hCenter for Neutraceutical and Pharmaceutical Materials, Myongji University, Yongin, Gyeonggi-Do 17058, Korea; ⁱDepartment of Molecular Medicine, The Scripps Research Institute, Jupiter, FL 33458, USA;

*Correspondence to E-mail: shenb@scripps.edu, Tel: (561) 228-2456; Fax: (561) 228-2472

Short title: Discovery of the Leinamycin Family of Natural Products

¹These authors contributed equally

Supporting Online Materials

Table of Contents

Materials and general experimental procedures	S4-S10
Physicochemical properties of new compounds	S11-S12
Table S1. Summary of the 19 hits from public databases and the 30 hits from TSRI collection	S13-S14
Table S2. Strains and plasmids used in this study	S15-S16
Table S3. Primers used in this study	S17-S20
Tables S4-S22. Annotation of the 19 <i>Inm</i> -type gene clusters from public databases in comparison to LNM	S21-S41
Tables S23-S31. Annotation of the 9 <i>Inm</i> -type gene clusters from the TSRI collection in comparison to LNM	S42-S51
Tables S32-S36. Comparison of <i>Inm</i> -type gene clusters within the same clades	S52-S57
Table S37. Substrate specificity-conferring codes and predicted substrates of the adenylation proteins/domains from the LNM-type biosynthetic pathways	S58
Table S38. ^1H and ^{13}C NMR data of GNM A	S59
Table S39. ^1H and ^{13}C NMR data of GNM B and GNM B3	S60
Table S40. ^1H and ^{13}C NMR data of (<i>R</i>)- and (<i>S</i>)-PGME-GNM B2	S61
Table S41. ^1H and ^{13}C NMR data of (<i>R</i>)- and (<i>S</i>)-PGME-LNM E2	S62
Table S42. ^1H and ^{13}C NMR data of WSM A1, A2, A3	S63
Table S43. ^1H and ^{13}C NMR data of (<i>R</i>)- and (<i>S</i>)-PGME-WSM A2	S64
Table S44. ^1H and ^{13}C NMR data of GNM B1 and GNM B2	S65
Fig. S1. Proposed pathway for LNM biosynthesis in <i>S. atroolivaceus</i> S-140 and the modes of action of LNM and LNM E1	S66-67
Fig. S2. Discovery-based approach to combinatorial biosynthesis for the LNM family of natural products by genome mining for the <i>Inm</i> -type gene clusters	S68
Fig. S3. Phylogenetic analysis of the hit strains, and domain organization and the proposed/identified nascent products of LNM-type biosynthetic machineries from 17 different clades.	S69-S73
Fig. S4. Pathways for β -alkylation in LNM-type natural product biosynthesis	S74-S75
Fig. S5. Phylogenetic analysis of HCSs suggesting acetyl- or propyl-S-ACP as the preferred substrate	S76-S77
Fig. S6. Phylogenetic analysis of DUF or SH domain suggesting correlation with the preferred substrate (acetyl- or propyl-S-ACP) used for β -alkylation.	S78
Fig. S7. Genome neighborhood network (GNN) analysis for the prediction of novel chemistry for the biosynthesis of the LNM family of natural products	S79
Fig. S8. Construction of the $\Delta gnmB$ mutant strain SB21001 in <i>S. sp.</i> CB01883	S80
Fig. S9. Proposed pathway for GNM biosynthesis in <i>S. sp.</i> CB01883	S81
Fig. S10. Key COSY, HMBC and ROESY correlations supporting the structural elucidation of the GNMs	S82
Figs. S11-12. 1D and 2D NMR spectra of GNM A and B	S83-S95

Fig. S13. Key COSY, HMBC and ROESY correlations of (<i>R</i>)- and (<i>S</i>)-PGME derivatives of GNM B2, LNM E2, and WSM A2	S96
Fig. S14. Determination of the absolute stereochemistry of GNMs by measuring the chemical shift differences of (<i>R</i>)- and (<i>S</i>)-PGME derivatives of GNM B2	S97
Fig. S15. 1D and 2D NMR spectra of (<i>R</i>)- and (<i>S</i>)-PGME-GNM B2	S98-S105
Fig. S16. Validating the method for absolute stereochemistry determination for GNMs and WSMs with LNM E2 as a positive control	S106-S107
Fig. S17. 1D and 2D NMR spectra of (<i>R</i>)- and (<i>S</i>)-PGME-LNM E2	S108-S115
Fig. S18. Construction of the $\Delta wsmW$ mutant strain SB22001 in <i>S. sp.</i> CB02120-2	S116
Fig. S19. Proposed pathway for WSM biosynthesis in <i>S. sp.</i> CB02120-2	S117
Fig. S20. Key COSY, HMBC and ROESY correlations supporting the structural elucidation of the WSMs	S118
Figs. S21-23. 1D and 2D NMR spectra of WSM A1, A2, and A3	S119-S130
Fig. S24. Determination of the absolute stereochemistry of WSMs by measuring the chemical shift differences of (<i>R</i>)- and (<i>S</i>)-PGME-WSM A2	S131
Fig. S25. 1D and 2D NMR spectra of (<i>R</i>)- and (<i>S</i>)-PGME-WSM A2	S132-S39
Fig. S26. Construction of the $\Delta wsmZ3$ mutant (SB22002) and $\Delta wsmZ4$ mutant (SB22004) in <i>S. sp.</i> CB02120-2 and confirmation of their genotypes	S140
Fig. S27. Discovery of <i>S. sp.</i> CB01635 as an alternative LNM producer	S141
Fig. S28. Discovery of NRRL F-5630 and NRRL B-2183 as alternative GNM producers	S142
Fig. S29. In vitro characterization of selected A domains or proteins from the newly discovered LNM-type biosynthetic machineries	S143-S144
Fig. S30. Construction of the $\Delta gnmO$ mutant strain SB21003 in <i>S. sp.</i> CB01883.	S145
Fig. S31. 1D and 2D NMR spectra of GNM B1, B2, and B3	S146-S157
Fig. S34. Conversion of GNM B to GNM B1, B2, B3 upon oxidative activation	S158
References	S159-S160

Materials and Methods

Bacterial strains, plasmids, chemicals

Strains, plasmids, and PCR primers used in this study are listed in **Tables S2** and **S3**, respectively. PCR primers were purchased from Sigma-Aldrich. Q5 high-fidelity DNA polymerase, restriction endonucleases, and T4 DNA ligase were purchased from New England Biolabs (NEB) and reactions were performed according to the manufacturer's protocols. DNA gel extraction and plasmid preparation kits were purchased from Omega Bio-Tek. DNA sequencing was conducted by Eton Bioscience. Other common chemicals, bio-chemical, and media components were purchased from standard commercial sources.

General procedures

E. coli strains harboring plasmids or cosmids were grown in lysogeny broth (LB) with appropriate antibiotics (1). *E. coli* ET12567/pUZ8002 was used for intergeneric conjugation with *Streptomyces* sp. CB01883 and *Streptomyces* sp. CB02120-2, and the conjugations were carried out following typical procedures (2). *Streptomyces* sp. NRRL F-5630 and *S. aureofaciens* NRRL B-2183 were obtained from NRRL (Agricultural Research Service Culture Collection). *Streptomyces* sp. NRRL F-5630 was cultivated on solid ISP2 medium for sporulation, while all the other *Streptomyces* strains used in this study were cultivated on solid ISP4 medium for sporulation. *Streptomyces* strains were cultivated in liquid tryptic soy broth (TSB) at 28 °C and 250 rpm to prepare the mycelium for genomic DNA (gDNA) isolation. Isolation of gDNA from *Streptomyces* strains were performed using the salting out protocol (2). Cosmid libraries of *Streptomyces* sp. CB01883 and *Streptomyces* sp. CB02120-2 were constructed based on SuperCos 1 cosmid following standard protocols (Agilent Technologies). Screening of the cosmid libraries were performed by PCR with primers shown in **Table S3** using OneTaq® 2X Master Mix with GC buffer (NEB). For Southern analysis, digoxigenin labeled DNA probes preparation, hybridization, and detection were performed according to the manufacturer's protocols (Roche Diagnostics Corp.).

ClustalW was used for multiple sequence alignment (3). All the phylogenetic trees (Figs. 2A and 3A in the main text, Figs. S3A, S3B, S5, and S6 in the SI) in this study were generated by MEGA6 using the maximum likelihood method with a bootstrap test of 500 replicates (4). Numbers next to the branches represent the percentage of replicate trees in which the shown topology was reached. Annotation of the new *Inm*-type gene clusters were done by using antiSMASH 3.0 (5) and 2ndFind (<http://biosyn.nih.go.jp/2ndFind/>). Construction of GNN of the LNM-type pathways was carried out as described previously (6).

Optical rotation values were measured using an Autopol IV automatic polarimeter. UV spectra were recorded with a NanoDrop 2000C spectrophotometer (Thermo Scientific). IR spectra were collected with a Spectrum One FT-IR spectrometer (PerkinElmer). All ¹H, ¹³C, and 2D-NMR (HSQC, ¹H-¹H COSY, HMBC, ROESY) spectra were collected at room temperature (25 °C) with a Bruker Avance III Ultrashield 700 at 700 MHz for ¹H and 175 MHz for ¹³C nuclei. ¹H-NMR spectra at higher temperatures were measured using Bruker Avance 400 MHz ULTRASHield instrument. HR-ESI-MS data were acquired on Agilent 6230 TOF LC/MS instrument.

Genome survey of 5,000 strains from the actinomycetes collection at TSRI for producers of the leinamycin (LNM) family of natural products

Real-time PCR was performed using an Applied Biosystems 7900HT Fast Real-Time PCR system. To identify strains harboring *Inm*-type gene clusters, the conserved DUF-SH didomain was chosen as the screening target. Degenerate primers DUF-F (derived from the conserved sequences within DUF domains) and SH-sub-R (derived from the conserved sequences

predicted to be involved in substrate and potassium binding within SH domains), aiming to amplify a 500 bp DNA fragment from DUF-SH didomain, were used in the screening with final concentrations of 1 μ M. Preparation of gDNA arrays and application of the real-time PCR screening followed a published protocol (7). Specifically, gDNA samples were arrayed in 384-well plates and subjected to real-time PCR. Each plate contained a positive control, with the gDNA of *S. atroolivaceus* S-140 (LNM producer) as the template which will give PCR products with a theoretical T_m of 93.1 °C, and a negative control without template. The PCR conditions consisted of a background check at 50 °C for 2 min; initial denaturation at 95 °C for 7 min; 35 cycles of denaturation at 95 °C for 30 s, primer annealing at 52 °C for 15 s, extension at 68 °C for 45 s; and melting steps with a ramp rate of 2%. Samples with T_m between 91.6 to 93.5 °C were considered as potential hits (**Fig. S2**).

To verify the identity of hit strains obtained from the real-time PCR screening, another round of PCR was performed with degenerate primers Seq-DUF-F and Seq-SH-R/Seq-SH-2120-R, aiming to amplify a 1.2 kb DNA fragment from DUF-SH didomain, using the gDNAs of the hit strains as templates. The resultant PCR products were subjected to DNA sequencing and the sequence results have been deposited into GenBank with their accession numbers summarized in **Table S1**. For taxonomic analysis, three housekeeping genes (16S rRNA, *recA*, and *trpB*) were amplified, sequenced, and analyzed. All the DNA sequences have been deposited into GenBank (**Table S1**).

DNA Sequencing and Genome Assembly

Genome sequencing of the representative hit strains was performed using an Illumina MiSeq sequencer (2 x 300 paired end sequencing) at the Next Generation Sequencing and Microarray Core Facility, The Scripps Research Institute. Read quality filtering was performed using an in-house developed tool. Adapter trimming and de novo assembly were done with CLC Genomics Workbench version 7.5.1 (CLC Bio.) using default settings. The resulting contigs were further extended and joined into a final scaffold by SSPACE version 2.0 using all quality filtered reads (8). The remaining gaps within the final scaffold were partially or completely filled using the quality filtered reads by GapFiller version 1.10 (9). Genome sequences (under BioProject PRJNA393980) have been deposited into GenBank with accession numbers summarized in **Table S1**.

Inactivation and complementation of *gnmB* (encoding hybrid NRPS/PKS) and *gnmO* (encoding N-acetylglucosamine deacetylase) in Strain *Streptomyces* sp. CB01883

To construct a plasmid for inactivation of *gnmB*, a 1555 bp DNA fragment upstream of *gnmB* was amplified with primers 1883orf155-I5 and 1883orf155-I3, and a 1483 bp DNA fragment downstream of *gnmB* was amplified with primers 1883orf155-II5 and 1883orf155-II3, using cosmid pBS21001 (1C4) of strain CB01883 as template. The two DNA fragments were trimmed with appropriate enzymes and cloned into the *Hind*III and *Eco*RI sites of pOJ260 to obtain pBS21004 (10). Then pBS21004 was transformed into *E. coli* ET12567(pUZ8002) and introduced into strain CB01883 by intergeneric conjugation. After several rounds of passaging the exconjugants on solid ISP4 medium, apramycin sensitive double-crossover mutants were obtained. The genotype of the in-frame deletion mutant strain SB21001 (i.e. $\Delta gnmB$) was verified by Southern analysis (**Fig. S8**).

For complementation of SB21001, a 7687 bp DNA fragment containing *gnmB* was amplified with primers orf155-kasO-5 and orf155-kasO-3 using cosmid pBS21001 as template, and then cloned into the *Af*II and *Spel* sites of pBS21003 (pSET-KasO*: constructed by digestion of PCR products obtained with primers PSET-kasO-F and PSET-kasO-R using pSETTurdR as template with *Nsi*I followed by self-ligation) (11) to obtain pBS21005, in which *gnmB* was under the

control of the strong promoter *kasO** (12). Then pBS21005 was introduced into SB21001 by intergeneric conjugation to afford the complementation strain SB21002 (i.e. $\Delta gnmB/gnmB$). Similar strategy was used to generate the in-frame deletion mutant strain SB21003 (i.e. $\Delta gnmO$). An upstream 3085 bp DNA fragment was amplified with primers 1883orf132-I5 and 1883orf132-I3, and a downstream 3070 bp DNA fragment was amplified with primers 1883orf132-II5 and 1883orf132-II3, using cosmid pBS21001 as template. The two DNA fragments were digested with appropriate enzymes and cloned into the *HindIII* and *EcoRI* sites of pOJ260. The resultant plasmid pBS21006 was introduced into strain CB01883 by intergeneric conjugation. After several rounds of screening, apramycin sensitive double-crossover mutants were obtained. The genotype of the in-frame deletion mutant strain SB21003 was verified by Southern analysis (**Fig. S30**).

For complementation of SB21003, a 1007 bp DNA fragment containing *gnmO* obtained by PCR with primers orf132-com-F and orf132-com-R using cosmid pBS21001 as template, was cloned into the *AfII* and *Spel* sites of pBS21003 to generate pBS21007, which was then introduced into SB21003 by intergeneric conjugation to afford the complementation strain SB21004 (i.e. $\Delta gnmO/gnmO$).

Inactivation of *wsmW* (encoding hybrid NRPS/PKS), *wsmZ3* (encoding 3-oxyacyl-ACP synthase, KASIII) and *wsmZ4* (encoding 3-hydroxylacyl-CoA dehydrogenase, HBDH) in *Streptomyces* sp. CB02120-2

To construct a plasmid for inactivation of *wsmW*, an upstream 3038 bp DNA fragment was amplified with primers 2120orf25-I5 and 2120orf25-I3, and a downstream 3033 bp DNA fragment was amplified with primers 2120orf25-II5 and 2120orf25-II3 using cosmid pBS22001 (8E4) of strain CB02120-2 as template. The two DNA fragments were then cloned into the *HindIII* and *EcoRI* sites of pOJ260. The resultant plasmid pBS22004 was introduced into strain CB02120-2 by intergeneric conjugation. After several rounds of passaging the exconjugants on solid ISP4 medium, apramycin sensitive double-crossover mutants were obtained. The genotype of the in-frame deletion mutant strain SB22001 (i.e. $\Delta wsmW$) was verified by Southern analysis (**Fig. S18**).

Similar strategy was used to generate the in-frame deletion mutant strains SB22002 (i.e. $\Delta wsmZ3$) and SB22004 (i.e. $\Delta wsmZ4$). For knock out of *wsmZ3*, an upstream 3165 bp DNA fragment was amplified with primers 2120orfZ3-I5 and 2120orfZ3-I3, and a downstream 3182 bp DNA fragment was amplified with primers 2120orfZ3-II5 and 2120orfZ3-II3, using cosmid pBS22001 as template. The two DNA fragments were then cloned into the *HindIII* and *EcoRI* sites of pOJ260 to obtain pBS22005. For knock out of *wsmZ4*, an upstream 3155 bp DNA fragment was amplified with primers 2120orfZ4-I5 and 2120orfZ4-I3, and a downstream 3170 bp DNA fragment was amplified with primers 2120orfZ4-II5 and 2120orfZ4-II3, using cosmid pBS22001 as template. And then the two DNA fragments were cloned into the *HindIII* and *EcoRI* sites of pOJ260 to obtain pBS22007. The plasmids pBS22005 and pBS22007 were introduced into strain CB02120-2, respectively, through intergeneric conjugation. After several rounds of screening, apramycin sensitive double-crossover mutant strains SB22002 and SB22004 were obtained, and their genotypes were verified by Southern analysis (**Fig. S26**).

For complementation of SB22002, a 1283 bp DNA fragment containing *wsmZ3* was amplified with primers orfZ3-kasO-5 and orfZ3-kasO-3 using cosmid pBS22001 as template, and then cloned into the *AfII* and *Spel* sites of pBS21003 to obtain pBS22006. For complementation of SB22004, a 1264 bp DNA fragment containing *wsmZ4* was amplified with primers orfZ4-kasO-5 and orfZ4-kasO-3 using cosmid pBS22001 as template, and then cloned into the *AfII* and *Spel* sites of pBS21003 to generate pBS22008. Then pBS22006 and pBS22008 were introduced into

SB22002 and SB22004, respectively, to afford the complementation strains SB22003 (i.e. $\Delta wsmZ3/wsmZ3$) and SB22005 (i.e. $\Delta wsmZ4/wsmZ4$), by intergeneric conjugation.

Fermentation, HPLC analysis and isolation of guangnanmycin (GNM) A, GNM B, GNM B1, GNM B2 and GNM B3

Fresh spores of strain CB01883, its derivative mutant and complementation strains were individually inoculated into 250-mL baffled flasks containing 50 mL TSB seed medium and cultured for 36 h at 28 °C and 250 rpm. For small-scale fermentations, seed culture was inoculated (10%, v/v) into 250-mL baffled flasks each containing 50 mL production medium LM1 (soluble starch 3%, soy flour 1%, CaCO₃ 0.5%, KH₂PO₄ 0.05%, MgSO₄ 0.025%, ZnSO₄·7H₂O 0.004 %, L-methionine 0.01%, vitamin B₁₂ 0.0001%, pH 7.2), a medium modified from the one for the production of LNM by *S. atroolivaceus* S-140 (13). Amberlite XAD-16 resin (Sigma) was added to each flask (4%, w/v) at 24 h after inoculation, and the fermentation was allowed for another 72 h. The resin was harvested from the fermentation broth, washed with water and allowed to air dry. The dry resin was extracted with 6 mL methanol, and the methanol extract was directly used for HPLC and LC-MS analysis. HPLC analysis was carried out on an Agilent 1260 Infinity LC System with an Agilent SB-C18 column (5 µm, 250 × 4.6 mm) at a flow rate of 1 mL/min. The column was equilibrated with 100% solvent A (20% acetonitrile with acetic acid, pH 3.6), and developed with a 56 min analytical program consisting of a 40 min linear gradient from 0% to 68% of solvent B (80% acetonitrile with acetic acid, pH 3.6); 68–100% of solvent B from 40 to 42 min; 100% of solvent B from 42 to 50 min; 100–0% of solvent B from 50 to 51 min; and 0% of solvent B for further 5 min. HPLC-MS was performed on an Agilent 1260 Infinity LC coupled to a 6230 TOF (HRESI) equipped with an Agilent Poroshell 120 EC-C18 column (2.7 µm, 250 × 4.6 mm). Chromatography for LC-MS was conducted using an 18 min solvent gradient from 5–100% acetonitrile containing 0.1% formic acid in H₂O containing 0.1% formic acid at a flow rate of 0.4 mL/min.

For isolation of GNM A and GNM B1, a large scale fermentation (12 L) of *Streptomyces* sp. CB01883 was performed with medium LM1. The resins were harvested, and extracted with methanol (2 L × 3). The solvent was evaporated to give the crude extract, which was suspended with water (500 mL), and extracted with ethyl acetate (1 L × 3). The combined organic phases were evaporated to dryness, and the residue was fractionated with Agilent 1260 Infinity LC System using an Eclipse XDB-C18 column (7 µm, 212 × 250 mm). The mobile phase consisted of solvent A (20% acetonitrile with acetic acid, pH 3.6) and B (80% acetonitrile with acetic acid, pH 3.6). The crude extract was eluted with a linear gradient of 0% B to 100% B for 20 min, followed with 100% B for 5 min at a flow rate of 17 mL/min. The fractions containing compounds of interest were combined and concentrated. The residue was subjected to a Sephadex LH-20 column, and eluted with methanol. The fractions containing compounds of interest were combined and finally purified by Varian LC system with a Zorbax SB-C13 column (5 µm, 9.4 × 250 mm) to give GNM A (5.9 mg) as a white powder, and GNM B1 (1.2 mg) as a yellowish oil.

For isolation of GNM B, GNM B2 and GNM B3, a large scale fermentation (20 L) of the mutant strain SB21003 was performed with medium LM3 (soluble starch 0.5%, malt extract 1.5%, glucose 1%, tryptone 0.4%, K₂HPO₄ 0.05%, MgSO₄·7H₂O 0.02%, methionine 0.01%, vitamin B₁₂ 0.0001%, pH 7.2). The fermentation was carried out for 6 days at 28 °C and 250 rpm, with 3% (w/v) Amberlite XAD-16 resin added after 1 day of fermentation. The mixture of the resin and mycelia were harvested by centrifugation and extracted by acetone. The solvent was removed under reduced pressure. The crude extract was suspended with water, and extracted with ethyl acetate. The combined organic phases were concentrated in vacuum, and the residue was subjected to Sephadex LH-20 column chromatography and eluted with methanol. The fractions with compounds of interest were combined, and further purified with Varian LC system

with a Zorbax SB-C13 column (5 μ m, 9.4 \times 250 mm) to afford GNM B (53.2 mg), GNM B2 (1.1 mg), and GNM B3 (0.8 mg).

Fermentation of *Streptomyces* sp. CB01635, *Streptomyces* sp. NRRL F-5630 and *S. aureofaciens* NRRL B-2183, and analysis of their metabolite profiles

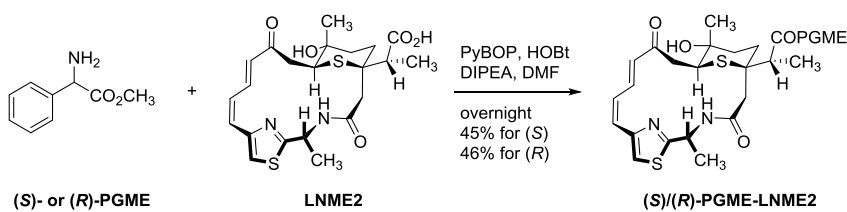
Strain CB01635 and LNM original producing strain *S. atroolivaceus* S-140 were cultivated using a two-stage fermentation similar to the previously published procedure (13). Briefly, fresh spores were inoculated into 250-mL baffled flasks containing 50 mL seed medium (glucose 1%, soluble starch 1%, beef extract 0.3%, yeast extract 0.5%, tryptone 0.5%, CaCO_3 0.2%, pH 7.2), and cultured for 48 h at 28 °C and 250 rpm. Seed culture (5 mL) was then inoculated into 250-mL baffled flasks containing 50 mL production medium LM1. Amberlite XAD-16 resin (Sigma) were added to each flask (4%, w/v) at 16 h after inoculation, and the fermentation was continued for another 72 h. Crude extracts were analyzed with HPLC and LC-MS by the same procedures as those used for strain CB01883.

Streptomyces sp. NRRL F-5630 and *S. aureofaciens* NRRL B-2183 were cultivated and fermented in a similar way to that of strain CB01883 except for the production medium, in which medium LM3 was used. The HPLC and LC-MS analysis were carried out using the same procedures described previously for strain CB01883.

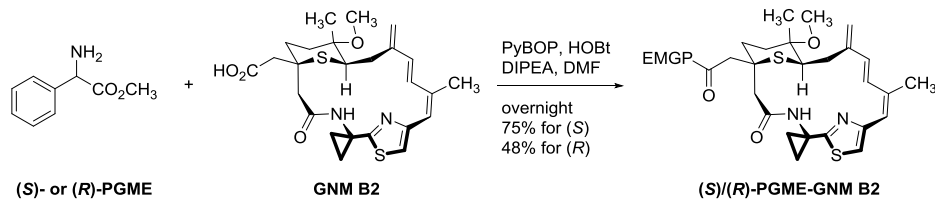
Fermentation of *Streptomyces* sp. CB02120-2, HPLC analysis of its metabolite profiles and isolation of weishanmycin (WSM) A1-A3

Small-scale fermentations and HPLC-MS analysis of strain CB02120-2, its derivative mutant and complementation strains were carried out using the same procedure for the production of guangnanmycins by strain CB01883. For isolation of WSM A1-A3, a large-scale (12 L) fermentation of strain CB02120-2 was performed with medium LM1. The resins were harvest, and extracted with methanol (2 L \times 3). The solvent was evaporated to give the crude extract, which was suspended with water (500 mL), and extracted with ethyl acetate (1 L \times 3). The combined organic phases were evaporated to dryness, and the residue was fractionated with Agilent 1260 Infinity LC System using an Eclipse XDB-C18 column (7 μ m, 212 \times 250 mm). The mobile phase consisted of solvent A (20% acetonitrile with acetic acid, pH 3.6) and B (80% acetonitrile with acetic acid, pH 3.6). The crude extract was eluted with a linear gradient of 0% B to 100% B for 20 min, followed with 100% B for 15 min at a flow rate of 17 mL/min. The fractions containing compounds of interest were combined and concentrated. The residue was subjected to a Sephadex LH-20 column, and eluted with methanol. The fractions containing compounds of interest were combined and finally purified by Varian LC system with a Zorbax SB-C13 column (5 μ m, 9.4 \times 250 mm) to give WSM A1 (18.1 mg) as a yellowish oil, WSM A2 (16.8 mg) as a yellowish oil, and WSM A3 (2.4 mg) as a yellowish oil.

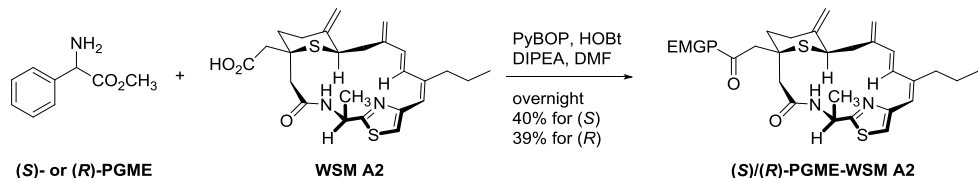
Chemical transformations of leinamycin E2 (LNM E2), GNM B2 and WSM A2 to their phenylglycine methyl ester (PGME) derivatives for absolute configuration determination (14)



(S)/(R)-PGME-LNM E2. To a stirring solution of LNM E2 (1.0 equiv) in DMF (0.01 M) was added (S)/(R)-PGME (1.3 equiv), PyBOP (1.3 equiv), HOBt (1.3 equiv) and DIPEA (20 equiv), and the reaction mixture was allowed to stir at room temperature overnight. The desired product was purified with Agilent 1260 Infinity LC System using an Eclipse XDB-C18 column (7 μ m, 212 \times 250 mm) with the mobile phase containing A (water) and B (acetonitrile), and eluted with a linear gradient of 5% B to 80% B for 20 min, followed with 80% B for 5 min at a flow rate of 17 mL/min. (S)-PGME-LNM E2 (45%) and (R)-PGME-LNM E2 (46%) were obtained as white powders.



(S)/(R)-PGME-GNM B2. To a stirring solution of GNM B2 (1.0 equiv) in DMF (0.01 M) was added (S)/(R)-PGME (1.3 equiv), PyBOP (1.3 equiv), HOBt (1.3 equiv) and DIPEA (20 equiv), and the reaction mixture was allowed to stir at room temperature overnight. The desired product was purified with Agilent 1260 Infinity LC System using an Eclipse XDB-C18 column (7 μ m, 212 \times 250 mm) with the mobile phase containing A (H_2O) and B (CH_3CN), and eluted with a linear gradient of 5% B to 100% B for 20 min, followed with 100% B for 7 min at a flow rate of 17 mL/min. (S)-PGME-GNM B2 (75%) and (R)-PGME-GNM B2 (48%) were obtained as white powders.



(S)/(R)-PGME-WSM A2. To a stirring solution of WSM A2 (1.0 equiv) in DMF (0.01 M) was added (S)/(R)-PGME (1.3 equiv), PyBOP (1.3 equiv), HOBt (1.3 equiv) and DIPEA (20 equiv), and the reaction mixture was allowed to stir at room temperature overnight. The desired product was purified with Agilent 1260 Infinity LC System using an Eclipse XDB-C18 column (7 μ m, 212 \times 250 mm) with the mobile phase containing A (H_2O) and B (CH_3CN), and eluted with a linear gradient of 5% B to 100% B for 20 min, followed with 100% B for 7 min at a flow rate of 17 mL/min. (S)-PGME-WSM A2 (40%) and (R)-PGME-WSM A2 (39%) were obtained as white powder.

Cloning and production of adenylation domains from *Streptomyces* sp. CB01883 (GnmS), *Micromonospora aurantiaca* (Maur_X), *Streptomyces* sp. CB02120-2 (WsmQ), *Streptomyces* sp. CB01373 (CB01373_Q) and *Streptomyces* sp. CB02613 (CB02613_Z17 and CB02613_M)

To construct a plasmid for production of GnmS, the region coding *gnmS* was amplified by PCR from the cosmid pBS21001 of strain CB01883 using primers 1883orf127-F and 1883orf127-R, and then cloned into the *Nde*I and *Hind*III sites of pET28a(+) (Novagen) to afford pBS21008.

To construct a plasmid for production of WsmQ, the region coding *wsmQ* was amplified by PCR from the cosmid pBS22002 (7F6) of strain CB02120-2 using primers 2120orf32-N-5 and

2120orf32-N-3, and then cloned into pBS3080 (15) according to the ligation independent procedures (16) to afford pBS22009.

The DNA region encoding the adenylation domain of Maur_X was amplified by PCR from gDNA of *Micromonospora aurantiaca* with primers MaurX-Ad-N5 and MaurX-Ad-N3, and cloned into the *Bam*HI and *Hind*III sites of pBS3082 (15) to obtain pBS21009.

The DNA region encoding the adenylation domain of CB01373_Q was obtained by PCR from gDNA of strain CB01373 with primers 1373Q-Ad-N5 and 1373Q-Ad-N3, and cloned into pBS3080 according to the ligation independent procedures to give pBS21010.

The DNA regions encoding the adenylation domains CB02613_Z17 and CB02613_M were amplified by PCR from gDNA of strain CB02613 with primers 2613Z17-Ad-N5/2613Z17-Ad-N3, and 2613M-Ad-N5/2613M-Ad-N3, respectively. The two PCR products were cloned into pBS3080 according to the ligation independent procedures to give pBS21011 and pBS21012, respectively.

For protein production, plasmids containing the desired gene fragments were transformed into *E. coli* BL21(DE3) (Life Technologies). The resultant recombinant strains were cultivated in LB at 37 °C and 250 rpm until an OD₆₀₀ of 0.6 was reached, and then induced by 0.2 mM isopropyl-β-D-thiogalactopyranoside (IPTG) for 20 h at 18 °C. The cells were harvested by centrifugation, resuspended in lysis buffer (100 mM Tris, pH 8.0, containing 300 mM NaCl, 15 mM imidazole, and 10% glycerol) and lysed by sonication. After centrifugation at 15,000g for 20 min at 4 °C, the supernatants containing the corresponding proteins were first purified by nickel-affinity chromatography using an ÄKTA FPLC system (GE Healthcare Biosciences) equipped with a HisTrap HP column. The fractions containing the target protein (with an N-terminal His₆-tag) were combined and further purified by ion exchange chromatography using a HiTrap Q HP column (GE Healthcare Biosciences). The purified proteins were desalted using a HiPrep desalting column (GE Healthcare Biosciences) and concentrated using an Amicon Ultra-15 concentrator (Millipore) in 25 mM Tris, pH 7.5, containing 25 mM NaCl, and 10% glycerol. The resultant proteins were stored at -80 °C until use.

Hydroxylamine-trapping assay of adenylation proteins (17)

A typical 150 µl reaction mixture contained 25 mM Tris-HCl (pH 8.0), 15 mM MgCl₂, 2.25 mM ATP, 150 mM hydroxylamine (stock solution was prepared as 2 M hydroxylamine in 3.5 M NaOH, and pH adjusted to 8 with concentrated HCl), 3 mM amino acid, and purified A protein (final concentrations of GnmS and WsmQ were 2.5 µM, and the final concentrations of the other adenylation proteins were 7.5 µM). The reaction with boiled enzyme was used as the negative control. The reactions were performed in 96-well plates at 30 °C for 1 h, and stopped by addition of 150 µl of stopping solution containing 10% (w/v) FeCl₃ 6H₂O, 3.3% (v/v) trichloroacetic acid, and 0.7 M HCl. The absorbance at 540 nm of each reaction was recorded on a SpectraMax M5 Multi-Mode Microplate Reader (Molecular Devices).

Physicochemical properties of new compounds

Guangnanmycin A. White powder; $[\alpha]_D^{25} +15.3$ (*c* 0.32, CHCl₃/MeOH, 1:1); IR (neat) ν_{\max} 3277, 2921, 1669, 1515, 1422, 1201, 1025 cm⁻¹; UV (DMSO) λ_{\max} (log ϵ) 259 (4.09) nm; ¹H and ¹³C NMR data see **Table S38**; HR-ESI-MS *m/z* 505.1647 [M + H]⁺ (calcd for C₂₅H₃₃N₂O₃S₃, 505.1648).

Guangnanmycin B. White powder; $[\alpha]_D^{25} +66.3$ (*c* 0.21, CHCl₃); IR (neat) ν_{\max} 3303, 2925, 1660, 1504, 1445, 1260, 1082 cm⁻¹; UV (DMSO) λ_{\max} (log ϵ) 300 (3.97) nm; ¹H and ¹³C NMR data see **Table S39**; HR-ESI-MS *m/z* 459.1772 [M + H]⁺ (calcd for C₂₄H₃₁N₂O₃S₂, 459.1771).

Guangnanmycin B1. Yellowish oil; $[\alpha]_D^{25} +54.2$ (*c* 0.16, CHCl₃/MeOH, 1:1); IR (neat) ν_{\max} 3264, 2927, 1665, 1535, 1379, 1027 cm⁻¹; UV (DMSO) λ_{\max} (log ϵ) 258 (4.02) nm; 304 (4.06) nm; ¹H and ¹³C NMR data see **Table S44**; HR-ESI-MS *m/z* 475.1719 [M + H]⁺ (calcd for C₂₄H₃₁N₂O₄S₂, 475.1720).

Guangnanmycin B2. Yellowish oil; $[\alpha]_D^{25} +18.2$ (*c* 0.06, CHCl₃/MeOH, 1:1); IR (neat) ν_{\max} 3257, 2925, 1663, 1446, 1377, 1259, 1092 cm⁻¹; UV (DMSO) λ_{\max} (log ϵ) 313 (4.08) nm; ¹H and ¹³C NMR data see **Table S44**; HR-ESI-MS *m/z* 489.1875 [M + H]⁺ (calcd for C₂₅H₃₃N₂O₄S₂, 489.1876).

Guangnanmycin B3. Yellowish oil; $[\alpha]_D^{25} -0.69$ (*c* 0.15, CHCl₃); IR (neat) ν_{\max} 3365, 2925, 1708, 1661, 1451, 1260, 1023, 799 cm⁻¹; UV (DMSO) λ_{\max} (log ϵ) 298 (4.13) nm; ¹H and ¹³C NMR data see **Table S39**; HR-ESI-MS *m/z* 915.3314 [M + H]⁺ (calcd for C₄₈H₅₉N₄O₆S₄, 915.3312).

Weishanmycin A1. Colorless oil; $[\alpha]_D^{25} +35.6$ (*c* 0.93, CHCl₃/MeOH, 1:1); IR (neat) ν_{\max} 3378, 2929, 1713, 1647, 1524, 1444, 1023 cm⁻¹; UV (DMSO) λ_{\max} (log ϵ) 279 (4.09) nm; ¹H and ¹³C NMR data see **Table S42**; HR-ESI-MS *m/z* 491.2029 [M + H]⁺ (calcd for C₂₅H₃₅N₂O₄S₂, 491.2033).

Weishanmycin A2. Yellowish oil; $[\alpha]_D^{25} +206$ (*c* 0.84, CHCl₃/MeOH, 1:1); IR (neat) ν_{\max} 3336, 2932, 1712, 1647, 1021 cm⁻¹; UV (DMSO) λ_{\max} (log ϵ) 267 (4.21) nm, 303 (3.89) nm; ¹H and ¹³C NMR data see **Table S42**; HR-ESI-MS *m/z* 473.1928 [M + H]⁺ (calcd for C₂₅H₃₃N₂O₃S₂, 473.1927).

Weishanmycin A3. Yellowish oil; $[\alpha]_D^{25} -140.8$ (*c* 0.12, CHCl₃/MeOH, 1:1); IR (neat) ν_{\max} 3367, 2941, 1653, 1017 cm⁻¹; UV (DMSO) λ_{\max} (log ϵ) 287 (4.49) nm; ¹H and ¹³C NMR data see **Table S42**; HR-ESI-MS *m/z* 507.1984 [M + H]⁺ (calcd for C₂₅H₃₅N₂O₅S₂, 507.1982).

(S)-PGME-LNM E2. White powder; $[\alpha]_D^{25} +89.8$ (*c* 0.32, CHCl₃/MeOH, 1:1); IR (neat) ν_{\max} 3288, 2926, 1742, 1645, 1525, 1023, 1003, 699 cm⁻¹; ¹H and ¹³C NMR data see **Table S41**; HR-ESI-MS *m/z* 612.2194 [M + H]⁺ (calcd for C₃₁H₃₈N₃O₆S₂, 612.2197).

(R)-PGME-LNM E2. White powder; $[\alpha]_D^{25} +0.7$ (*c* 0.31, CHCl₃/MeOH, 1:1); IR (neat) ν_{\max} 3295, 2968, 1739, 1644, 1525, 1269, 1023, 1003, 699 cm⁻¹; ¹H and ¹³C NMR data see **Table S41**; HR-ESI-MS *m/z* 612.2199 [M + H]⁺ (calcd for C₃₁H₃₈N₃O₆S₂, 612.2197).

(S)-PGME-GNM B2. White powder; $[\alpha]_D^{25} +87.0$ (*c* 0.20, CHCl₃/MeOH, 1:1); IR (neat) ν_{\max} 3263, 2937, 1743, 1646, 1531, 1436, 1051, 1025, 1005, 697 cm⁻¹; ¹H and ¹³C NMR data see **Table S40**; HR-ESI-MS *m/z* 636.2559 [M + H]⁺ (calcd for C₃₄H₄₂N₃O₅S₂, 636.2560).

(R)-PGME-GNM B2. White powder; $[\alpha]_D^{25} +19.3$ (*c* 0.14, CHCl₃/MeOH, 1:1); IR (neat) ν_{\max} 3253, 2940, 1742, 1645, 1532, 1436, 1211, 1052, 1024, 1005, 697 cm⁻¹; ¹H and ¹³C NMR data see **Table S40**; HR-ESI-MS *m/z* 636.2562 [M + H]⁺ (calcd for C₃₄H₄₂N₃O₅S₂, 636.2560).

(S)-PGME-WSM A2. White powder; $[\alpha]_D^{25} +51.0$ (*c* 0.54, CHCl₃/MeOH, 1:1); IR (neat) ν_{\max} 3253, 2929, 1744, 1669, 1644, 1521, 1439, 1209, 1169, 1053, 1026, 977, 891, 731, 697 cm⁻¹; ¹H and ¹³C NMR data see **Table S43**; HR-ESI-MS *m/z* 620.2612 [M + H]⁺ (calcd for C₃₄H₄₂N₃O₄S₂, 620.2611).

(R)-PGME-WSM A2. White powder; $[\alpha]_D^{25} -40.7$ (*c* 0.29, CHCl₃/MeOH, 1:1); IR (neat) ν_{\max} 3247, 2927, 1743, 1671, 1642, 1521, 1496, 1440, 1212, 1170, 1053, 1026, 976, 890, 731, 696 cm⁻¹; ¹H and ¹³C NMR data see **Table S43**; HR-ESI-MS *m/z* 620.2610 [M + H]⁺ (calcd for C₃₄H₄₂N₃O₄S₂, 620.2611).

Table S1A. Taxonomy, geography, and genome sequence information of the 19 hit strains from public databases.

Strain name ^a	location ^b	clade ^c	NCBI Genome accession number
<i>Micromonospora tulbaghiae</i> DSM 45142	South Africa	IV	NZ_FMCMQ00000000
<i>Streptomyces leeuwenhoekii</i> DSM 42122	Chile	V	NZ_AZSD01000122
<i>Streptomyces hygroscopicus</i> NBRC 16556	Japan	V	NZ_BBOU00000000
<i>Streptomyces</i> sp. NBRC 109436	Japan	V	NZ_BBON00000000
<i>Salinispora arenicola</i> CNH964	Gulf of Mexico	XVII	2515154125 (IMG genome ID) ^d
<i>Streptomyces canus</i> ATCC 12647	USA	VII	NZ_LQCG00000000
<i>Catenulispora acidiphila</i> DSM 44928	Italy	VIII	NC_013131
<i>Streptomyces</i> sp. NRRL F-5630	unknown	IX	NZ_JOGO00000000
<i>Streptomyces aureofaciens</i> NRRL B-2183	USA	IX	NZ_JODU00000000
<i>Saccharothrix</i> sp. ST-888	Japan	XI	NZ_JYJF01000000
<i>Streptomyces</i> sp. NBRC 110035	Japan	XII	NZ_BBNN00000000
<i>Streptomyces novaecaesareae</i> NRRL B-1267	USA	XIII	NZ_JNWQ01000000
<i>Saccharothrix espanaensis</i> DSM 44229	Spain	XIV	NC_019673
<i>Micromonospora</i> sp. L5	Mexico	XV	NC_014815
<i>Micromonospora marina</i> DSM 45555	Thailand	XV	NZ_FMCMV00000000
<i>Micromonospora</i> sp. CNB394	unknown	XV	NZ_ARGW00000000
<i>Micromonospora globosa</i> NRRL B-2673	unknown	XV	NZ_JNZR00000000
<i>Micromonospora aurantiaca</i> ATCC 27029	Russia	XV	NC_014391
<i>Burkholderia ubonensis</i> RF25-BP1	Thailand	XVIII	NZ_LOTL01000000

^a*Burkholderia ubonensis* RF25-BP1 is Gram-negative bacteria, while all the others are actinomycetes (Gram-positive).

^bGeographic distribution of the 19 hits.

^cSee Fig. 2 and Fig. S3B for detailed clade information.

^dThe IMG genome ID of *Salinispora arenicola* CNH964 is provided, as the NCBI genome accession number of this strain is not available. IMG: Integrated Microbial Genomes (<https://jgi.doe.gov/data-and-tools/img/>).

Table S1B. Taxonomy, geography, accession numbers of partial DUF-SH didomain sequences and selected housekeeping genes of 30 hit strains from the actinomycetes collections at TSRI, and genome sequence information of the nine selected hits.

strain	location ^a	clade ^b	Taxonomy ^c	NCBI accession number				
				DUF-SH ^d	16S rRNA	recA	trpB	genome
CB01635	China	I	<i>Streptomyces</i> sp.	MF455337	MF455323	MF455352	MF455367	NNBL00000000
MJM2585 ^f	Korea	I	<i>Streptomyces</i> sp.	MF925449	MF925434	MF925464	MF925479	--
CB02930	China	II	<i>Streptomyces</i> sp.	MF455335	MF455321	MF455350	MF455365	--
CB02959	China	II	<i>Streptomyces</i> sp.	MF455336	MF455322	MF455351	MF455366	NNBP00000000
CB02891	China	III	<i>Kitasatospora</i> sp.	MF455338	MF455324	MF455353	MF455368	NNBO00000000
TSRI0384-2	TSRI	V	<i>Streptomyces</i> sp.	MF455339	MF455325	MF455354	MF455369	NOWW00000000
MJM2046 ^f	Korea	V	<i>Streptomyces</i> sp.	MF925446	MF925431	MF925461	MF925476	--
MJM2478 ^f	Korea	V	<i>Streptomyces</i> sp.	MF925447	MF925432	MF925462	MF925477	--
MJM2479 ^f	Korea	V	<i>Streptomyces</i> sp.	MF925448	MF925433	MF925463	MF925478	--
CB02613	UAE	XVI	<i>Streptomyces</i> sp.	MF455340	MF455326	MF455355	MF455370	NNBN00000000
CB04103	USA	VI	<i>Streptomyces</i> sp.	MF925441	MF925426	MF925456	MF925471	--
CB04055	USA	VII	<i>Streptomyces</i> sp.	MF925436	MF925421	MF925451	MF925466	--
I-43184 ^g	Italy	VII	<i>Streptomyces</i> sp.	MF925445	MF925430	MF925460	MF925475	--
CB04056	USA	VII	<i>Streptomyces</i> sp.	MF925437	MF925422	MF925452	MF925467	--
CB04069	USA	VII	<i>Streptomyces</i> sp.	MF925438	MF925423	MF925453	MF925468	--
CB04083	USA	VII	<i>Streptomyces</i> sp.	MF925439	MF925424	MF925454	MF925469	--
CB04370	China	VII	<i>Streptomyces</i> sp.	MF925443	MF925428	MF925458	MF925473	--
MJM7752 ^f	Korea	VII	<i>Streptomyces</i> sp.	MF925450	MF925435	MF925465	MF925480	--
CB02209	China	VII	<i>Streptomyces</i> sp.	MF455343	MF455329	MF455358	MF455373	--
CB01373	TSRI	VII	<i>Streptomyces</i> sp.	MF455341	MF455327	MF455356	MF455371	NNBK00000000
CB01318	China	VII	<i>Streptomyces</i> sp.	MF455342	MF455328	MF455357	MF455372	--
CB02274	China	VII	<i>Streptomyces</i> sp.	MF455344	MF455330	MF455359	MF455374	--
CB01883	China	IX	<i>Streptomyces</i> sp.	MF455349	KT722854	MF455364	KT793843	LIWA00000000
CB04099	USA	IX	<i>Streptomyces</i> sp.	MF925440	MF925425	MF925455	MF925470	--
CB01201	China	X	<i>Streptomyces</i> sp.	MF455348	MF455334	MF455363	MF455378	NNBJ00000000
CB05481	China	XII	<i>Streptomyces</i> sp.	MF925444	MF925429	MF925459	MF925474	--
TSRI0429	TSRI	XII	<i>Streptomyces</i> sp.	MF455347	MF455333	MF455362	MF455377	--
CB02120-2	China	XII	<i>Streptomyces</i> sp.	MF455346	MF455332	MF455361	MF455376	NNBM00000000
CB04134	China	XII	<i>Streptomyces</i> sp.	MF925442	MF925427	MF925457	MF925472	--
TSRI0370	TSRI	XV	<i>Micromonospora</i> sp.	MF455345	MF455331	MF455360	MF455375	--
S-140 ^g	Japan	I	<i>Streptomyces</i> sp.	--	MF511767	MF511768	MF511769	--

^aGeographic distribution of the 30 hits, UAE abbreviated for United Arab Emirates, and TSRI denoted legacy strains in the TSRI strain collection whose geographic origins are not available (also see Fig. S2).

^bSee Fig. 2 and Fig. S3B for detailed clade information.

^cTaxonomy classification based on the three housekeeping genes including 16S rRNA, recA, and trpB (also see Fig. S3A).

^dThe partial DUF-SH didomain sequences used to construct the phylogenetic tree (Fig. 2 and Fig. S3B).

^eOriginal leinamycin producing strain *Streptomyces atroolivaceus* S-140.

^fHit strains from Myongji University.

^gHit strain from the Naicons' collection.

Table S2. Strains and plasmids used in this study

Strains/Plasmids	Genotype description	Source
<i>E. coli</i> strains		
DH5α	<i>E. coli</i> host for general cloning	Life Technologies
ET12567/pUZ8002	Methylation-deficient <i>E. coli</i> host for intergeneric conjugation	2
XL1-Blue MRF	<i>E. coli</i> host for cosmid library construction	Epicentre
BL21(DE3)	<i>E. coli</i> host for protein production	Life Technologies
<i>Streptomyces</i> strains		
<i>Streptomyces</i> sp. CB01883	Producing strain of guangnanmycins (GNM), wild-type	This study
SB21001 ($\Delta gnmB$)	$gnmB$ in-frame deletion mutant strain of CB01883	This study
SB21002 ($\Delta gnmB/gnmB$)	mutant strain SB21001 harboring plasmid pBS21005 (pSETgnmB)	This study
SB21003 ($\Delta gnmO$)	$gnmO$ in-frame deletion mutant strain of CB01883	This study
SB21004 ($\Delta gnmO/gnmO$)	mutant strain SB21003 harboring plasmid pBS21007 (pSETgnmO)	This study
<i>Streptomyces</i> sp. NRRL F-5630	Alternative producer of GNM, wild-type	NRRL
<i>Streptomyces aureofaciens</i>	Alternative producer of GNM, wild-type	NRRL
NRRL B-2183		
<i>Streptomyces atroolivaceus</i>	Producing strain of LNM, wild-type	Kyowa Hakko Kogyo Co. Ltd.
S-140		
<i>Streptomyces</i> sp. CB01635	Alternative producer of LNM E1, wild-type	This study
<i>Streptomyces</i> sp. CB02120-2	Producing strain of weishanmycin (WSM) A1-A3, wild-type	This study
SB22001 ($\Delta wsmW$)	$wsmW$ in-frame deletion mutant strain of CB02120-2	This study
SB22002 ($\Delta wsmZ3$)	$wsmZ3$ in-frame deletion mutant strain of CB02120-2	This study
SB22003 ($\Delta wsmZ3/wsmZ3$)	mutant strain SB22002 harboring plasmid pBS22006 (pSETwsmZ3)	This study
SB22004 ($\Delta wsmZ4$)	$wsmZ4$ in-frame deletion mutant strain of CB02120-2	This study
SB22005 ($\Delta wsmZ4/wsmZ4$)	mutant strain SB22004 harboring plasmid pBS22008 (pSETwsmZ4)	This study
Plasmids		
SuperCos 1	Vector for the construction of cosmid library, Kana ^R	Agilent Technologies
pOJ260	<i>E. coli</i> - <i>Streptomyces</i> shuttle vector, Am ^R	10
pSETTurdR	pSET152 derived plasmid containing the promoter <i>kasO*</i> , Am ^R	11
pBS3080	pRSFDuet-1 derived plasmid containing <i>BsmI</i> site for ligation-independent cloning	15
pBS3082	pRSFDuet-1 derived plasmid with insert encodes a TEV protease site after the His ₆ -tag	15
pBS21001	Cosmid 1C4 containing partial <i>gnm</i> gene cluster	This study
pBS21002	Cosmid 1B9 containing partial <i>gnm</i> gene cluster	This study
pBS21003 (pSET-kasO*)	pSETTurdR derived plasmid containing the promoter <i>kasO*</i> , Am ^R	This study
pBS21004 (pOJgnmB)	pOJ260 derived plasmid for inactivation of <i>gnmB</i> in CB01883	This study
pBS21005 (pSETgnmB)	pBS21003 derived plasmid for over-expression of <i>gnmB</i>	This study
pBS21006 (pOJgnmO)	pOJ260 derived plasmid for inactivation of <i>gnmO</i> in CB01883	This study
pBS21007 (pSETgnmO)	pBS21003 derived plasmid for over-expression of <i>gnmO</i>	This study
pBS21008 (pET28a-GnmS)	pET28a derived plasmid for production of GnmS	This study
pBS21009 (pBS3082-Maur_X-Ad)	pBS3082 derived plasmid for protein production of the A domain of Maur_X	This study
pBS21010 (pRSF-1373Q-Ad)	pBS3080 derived plasmid for protein production of the A domain of CB01373_Q	This study

pBS21011 (pRSF-2613Z17-Ad)	pBS3080 derived plasmid for protein production of the A domain of CB02613_Z17	This study
pBS21012 (pRSF-2613M-Ad)	pBS3080 derived plasmid for protein production of the A domain of CB02613_M	This study
pBS22001	Cosmid 8E4 containing partial <i>wsm</i> gene cluster	This study
pBS22002	Cosmid 7F6 containing partial <i>wsm</i> gene cluster	This study
pBS22003	Cosmid 3F12 containing partial <i>wsm</i> gene cluster	This study
pBS22004 (pOJwsmW)	pOJ260 derived plasmid for inactivation of <i>wsmW</i> in CB02120-2	This study
pBS22005 (pOJwsmZ3)	pOJ260 derived plasmid for inactivation of <i>wsmZ3</i> in CB02120-2	This study
pBS22006 (pSETwsmZ3)	pBS21003 derived plasmid for over-expression of <i>wsmZ3</i>	This study
pBS22007 (pOJwsmZ4)	pOJ260 derived plasmid for inactivation of <i>wsmZ4</i> in CB02120-2	This study
pBS22008 (pSETwsmZ4)	pBS21003 derived plasmid for over-expression of <i>wsmZ4</i>	This study
pBS22009 (pRSF-WsmQ)	pBS3080 derived plasmid for protein production of WsmQ	This study

Table S3. Primers used in this study

Name	Sequence (from 5' to 3') (restriction sites underlined)	Function
DUF-F	AYCTGCTSGACSTGGAGTTCTA	Real-time PCR screening
SH-sub-R	CSMGBTCSGMCCASGAGTCGGT	Real-time PCR screening
Seq-DUF-F	TGTAAAACGACGCCAGTAYCTGCTSGACSTGGAGTTCTA	Amplifying partial sequence from DUF-SH didomain
Seq-SH-R	CAGGAAACAGCTATGACCCGSHGTCGASRCCGAAGTCCTT	Amplifying partial sequence from DUF-SH didomain
Seq-SH-2120-R	CAGGAAACAGCTATGACACGCCGAAGTCCTTSGASAGRCT	Amplifying partial sequence from DUF-SH didomain
16SrRNA_for	AGAGTTTGATCCTGGCTCAG	Amplifying partial 16S rRNA
16SrRNA_rev	ACGGCTACCTTGTACGACTT	Amplifying partial 16S rRNA
recA-for	TAATACGACTCACTATAAGGCCGCRCCTCGCACARATTGAACG	Amplifying partial <i>recA</i>
recA-rev	GCTAGTTATTGCTCAGCGGCGTCGGGTTGTCCTSAGGAAG	Amplifying partial <i>recA</i>
recA-micromono-F	TAATACGACTCACTATAAGGAGACGCCGGCGAAGGCAGG	Amplifying partial <i>recA</i> from <i>Micromonospora</i> sp. strains
recA-micromono-R	GCTAGTTATTGCTCAGCGGCCGACGCCGAGCTTCTCCA	Amplifying partial <i>recA</i> from <i>Micromonospora</i> sp. strains
recA-kitasatospora-F	TAATACGACTCACTATAAGGGYNCYDGRSRCCGSHCTYGC	Amplifying partial <i>recA</i> from <i>Kitasatospora</i> sp. strains
recA-kitasatospora-R	GCTAGTTATTGCTCAGCGGSRGCTGGWMSCCMTSGYAGG	Amplifying partial <i>recA</i> from <i>Kitasatospora</i> sp. strains
trpB-for	TAATACGACTCACTATAAGGGCGCGAGGACCTGAACCACAC	Amplifying partial <i>trpB</i>
trpB-rev	GCTAGTTATTGCTCAGCGGCATGCCGGGATGATGCC	Amplifying partial <i>trpB</i>
trpB-micromono-Fn	TAATACGACTCACTATAAGGACCGGCTCCGGCCCAGCT	Amplifying partial <i>trpB</i> from <i>Micromonospora</i> sp. strains
trpB-micromono-Rn	GCTAGTTATTGCTCAGCGGCGSCTGCTGCCGACTAC	Amplifying partial <i>trpB</i> from <i>Micromonospora</i> sp. strains
1883-screen-U5	TACATGACCTGCCTGGAGCG	Screening for cosmids containing <i>gnm</i> gene cluster
1883-screen-U3	GGTCGAGGATCAGCAGTCCC	Screening for cosmids containing <i>gnm</i> gene cluster
1883-screen-M5	AGCACGCCAGAAAAGTCCT	Screening for cosmids containing <i>gnm</i> gene cluster
1883-screen-M3	GTGTAGGTCCAGCTCCGGTC	Screening for cosmids containing <i>gnm</i> gene cluster
1883-screen-D5	CTACGTCGAGACACACGGCA	Screening for cosmids containing <i>gnm</i> gene cluster
1883-screen-D3	CAAGGGTTCTCCGTCTCG	Screening for cosmids containing <i>gnm</i> gene cluster
1883orf155-I5	CCCA <u>AGCTTGGCACCGCCGGAGTGGCATC</u> (<i>Hind</i> III)	Inactivation of <i>gnmB</i> in CB01883
1883orf155-I3	GCT <u>CTAGACCTGGCGACCAGCGGCTC</u> (<i>Xba</i> I)	Inactivation of <i>gnmB</i> in CB01883
1883orf155-II5	GCT <u>CTAGACCCCTGGTCAACGCGGTCTCG</u> (<i>Xba</i> I)	Inactivation of <i>gnmB</i> in CB01883
1883orf155-II3	GGA <u>ATTCCGCTGCGTGCCCCGATGTC</u> (<i>Eco</i> RI)	Inactivation of <i>gnmB</i> in

			CB01883
orf155-SBlot-5n	CTGGAGCACCGGCAGGACCC		Southern blot analysis of SB21001 ($\Delta gnmB$)
orf155-SBlot-3n	AAGTGCTCCGCGAACCGGC		Southern blot analysis of SB21001 ($\Delta gnmB$)
orf155-kasO-5	<u>CCCTTAAGCCTGCGGTGGTGCACAAAGTTGA</u> ($Af\ I$)		Complementation of SB21001 ($\Delta gnmB$)
orf155-kasO-3	<u>ACGTACTAGTCGGTGTCCCCTCACTCGGTTCC</u> ($Spel$)		Complementation of SB21001 ($\Delta gnmB$)
PSET-kasO-F	<u>TGCATGCATA</u> CGTACTAGTCTGACATATGACGTGAATTGTAATC (<i>Nsi</i> I)		Construction of pBS21003 (pSET-kasO*)
PSET-kasO-R	<u>TGCATGCATA</u> CGTCTTAAGAACTCCCCAGTCCTGCA (<i>Nsi</i> I)		Construction of pBS21003 (pSET-kasO*)
1883orf132-I5	<u>CCCAAGCTTTCTGTGTCGAGGGGGACTC</u> (<i>Hind</i> III)		Inactivation of <i>gnmO</i> in CB01883
1883orf132-I3	<u>GCTCTAGAATTCCATGTCGTCGGGATGC</u> (<i>Xba</i> I)		Inactivation of <i>gnmO</i> in CB01883
1883orf132-II5	<u>GCTCTAGACGATGCCTTCGAGCTGATA</u> (<i>Xba</i> I)		Inactivation of <i>gnmO</i> in CB01883
1883orf132-II3	<u>GGAATTCACTTTCTGGCGTGCTCAGT</u> (<i>Eco</i> RI)		Inactivation of <i>gnmO</i> in CB01883
orf132-SBlot-5nn	AGAACTCCGCGAGAGCCTTC		Southern blot analysis of SB21003 ($\Delta gnmO$)
orf132-SBlot-3nn	CCCGTTCGAGCAGACCGAC		Southern blot analysis of SB21003 ($\Delta gnmO$)
orf132-kasO-5	<u>CCCTTAAGCCTCTCGCTCACGGGAC</u> ($Af\ I$)		Complementation of SB21003 ($\Delta gnmO$)
orf132-kasO-3	<u>ACGTACTAGTGTCTACGCCAAGCGGTGA</u> ($Spel$)		Complementation of SB21003 ($\Delta gnmO$)
2120-screen-U5	CCCTGACCCCGCTCAC		Screening for cosmids containing <i>wsm</i> gene cluster
2120-screen-U3	GTTGCTCGGTGAAGTCGTCG		Screening for cosmids containing <i>wsm</i> gene cluster
2120-screen-M5	CCGTCGAACGCGTACACATC		Screening for cosmids containing <i>wsm</i> gene cluster
2120-screen-M3	ATGGAGTCGAGCCCCATGTC		Screening for cosmids containing <i>wsm</i> gene cluster
2120-screen-D5	TTCGGCTTCGGAGGGTTCAA		Screening for cosmids containing <i>wsm</i> gene cluster
2120-screen-D3	ACACCAGGATGACGGACCTG		Screening for cosmids containing <i>wsm</i> gene cluster
2120orf25-I5	<u>CCCAAGCTTGCGCAGGAACTCGGCCTTG</u> (<i>Hind</i> III)		Inactivation of <i>wsmW</i> in CB02120-2
2120orf25-I3	<u>GCTCTAGACGCAACCACCGTCATCGAGTC</u> (<i>Xba</i> I)		Inactivation of <i>wsmW</i> in CB02120-2
2120orf25-II5	<u>GCTCTAGAGTGGACTGGCGAACCGGAC</u> (<i>Xba</i> I)		Inactivation of <i>wsmW</i> in

			CB02120-2
2120orf25-II3	<u>GGAATTCTCGAGACGATGGACACCGC</u> (<i>EcoRI</i>)	Inactivation of <i>wsmW</i> in CB02120-2	
orf25-SBlot-5	GTCAGCCACTGCGACCTCAT	Southern blot analysis of SB22001 ($\Delta wsmW$)	
orf25-SBlot-3	TGCGGAAGCGTTCGTCGTC	Southern blot analysis of SB22001 ($\Delta wsmW$)	
2120orfZ3-I5	<u>GTAACAAGCTTGCTCGTACATCGTCACCGC</u> (<i>HindIII</i>)	Inactivation of <i>wsmZ3</i> in CB02120-2	
2120orfZ3-I3	<u>GCTCTAGATGCGCTCCTCGATCCATTG</u> (<i>XbaI</i>)	Inactivation of <i>wsmZ3</i> in CB02120-2	
2120orfZ3-II5	<u>GCTCTAGACGGAGACCTCGTCGTACGG</u> (<i>XbaI</i>)	Inactivation of <i>wsmZ3</i> in CB02120-2	
2120orfZ3-II3	<u>GGAATTCGACCAGAGCCGGACCTACGA</u> (<i>EcoRI</i>)	Inactivation of <i>wsmZ3</i> in CB02120-2	
orfZ3-SBlot-5	CTTCGACTACGTCGGCCGGG	Southern blot analysis of SB22002 ($\Delta wsmZ3$)	
orfZ3-SBlot-3	TCCATTGGCGGGTATGCCG	Southern blot analysis of SB22002 ($\Delta wsmZ3$)	
orfZ3-kasO-5	<u>CCCTTAAGCTCGTCCAGGAGAACCGGCAC</u> (<i>AflII</i>)	Complementation of SB22002 ($\Delta wsmZ3$)	
orfZ3-kasO-3	<u>ACGTACTAGTTGGCACGGGAGAACGACCACG</u> (<i>SpeI</i>)	Complementation of SB22002 ($\Delta wsmZ3$)	
2120orfZ4-I5	<u>GTAACAAGCTTCTCCTCGCCTACCTGAGCAT</u> (<i>HindIII</i>)	Inactivation of <i>wsmZ4</i> in CB02120-2	
2120orfZ4-I3	<u>GCTCTAGATGGCACGGGAGACGACCA</u> (<i>XbaI</i>)	Inactivation of <i>wsmZ4</i> in CB02120-2	
2120orfZ4-II5	<u>GCTCTAGAGAGTTGCCGAGCCGCAGTA</u> (<i>XbaI</i>)	Inactivation of <i>wsmZ4</i> in CB02120-2	
2120orfZ4-II3	<u>GGAATTCAAGCATGCTTCCCCGGTGC</u> (<i>EcoRI</i>)	Inactivation of <i>wsmZ4</i> in CB02120-2	
orfZ4-SBlot-5	ACCTCAAGCGGGTCATCGGC	Southern blot analysis of SB22004 ($\Delta wsmZ4$)	
orfZ4-SBlot-3	CGCAGGGCCGAGGTGAGG	Southern blot analysis of SB22004 ($\Delta wsmZ4$)	
orfZ4-kasO-5	<u>CCCTTAAGAAGATCGGGATGTCCCACGC</u> (<i>AflII</i>)	Complementation of SB22004 ($\Delta wsmZ4$)	
orfZ4-kasO-3	<u>ACGTACTAGTGTCTCGGCCTGGCTGTACG</u> (<i>SpeI</i>)	Complementation of SB22004 ($\Delta wsmZ4$)	
1883orf127-F	<u>GGAATTCCATATGACGGCCGACGCCGGCGGT</u> (<i>NdeI</i>)	Production of GnmS	
1883orf127-R	<u>GTAACAAGCTTACCCGGTCCGCCAGGCAGC</u> (<i>HindIII</i>)	Production of GnmS	
2120orf32-N-5	AAAACCTCTATTCAGTCGGTCTGCTGGACCAAGTGGTTC	Production of WsmQ	
2120orf32-N-3	TACTTACTAAATGTCACGAGGACGGAGTGGGG	Production of WsmQ	
MaurX-Ad-N5	<u>CGGGATCC</u> ATGCCCGTGACTGACTGCCAC (<i>BamHI</i>)	Production of the A domain Maur_X	
MaurX-Ad-N3	<u>CCCAAGCTTACTCGGCCGGCTGGCCAGA</u> (<i>HindIII</i>)	Production of the A domain	

		Maur_X
1373Q-Ad-N5	AAAACCTCTATTCCAGTCGATGGTTCCGGCAAGACGCTG	Production of the A domain CB01373_Q
1373Q-Ad-N3	TACTTACTTAAATGTTATCACGTCAGTCCCGCGCCGGC	Production of the A domain CB01373_Q
2613Z17-Ad-N5	AAAACCTCTATTCCAGTCGGTGAGCGCACCAACCGACCC	Production of the A domain CB02613_Z17
2613Z17-Ad-N3	TACTTACTTAAATGTTATCAGCTCTCGGGATCCCCGCCG	Production of the A domain CB02613_Z17
2613M-Ad-N5	AAAACCTCTATTCCAGTCGATGACCGACACGCAGCCGCTC	Production of the A domain CB02613_M
2613M-Ad-N3	TACTTACTTAAATGTTATCACAGGTACGCCGACGCCCT	Production of the A domain CB02613_M

Table S4. Predicted functions of ORFs in the *Inm*-type gene cluster from *Micromonospora tulbaghiae* DSM 45142 (Clade IV)

gene ^a	aa ^b	putative function ^c	protein homologue (accession #)	% identity/ % similarity
<i>Mtul_orf(-1)</i>	274	hypothetical protein	(WP_043960781)	86/90
<i>Mtul_A</i>	552	4-coumarate:CoA ligase	LnmW (AAN85536)	35/48
<i>Mtul_B</i>	193	Crp/Fnr family transcriptional regulator	LnmO (AAN85528)	46/67
<i>Mtul_C</i>	602	NRPS (A-PCP)	SyrB1 (AKF46132)	45/59
<i>Mtul_D</i>	315	halogenase	SyrB2 (AKF46131)	69/79
<i>Mtul_E</i>	379	alpha/beta hydrolase	ADZ36_03165 (KNE83935)	46/55
<i>Mtul_F</i>	244	Crp/Fnr family transcriptional regulator	LnmO (AAN85528)	50/60
<i>Mtul_G</i>	306	unknown	LnmE (AAN85518)	49/61
<i>Mtul_H</i>	257	enoyl-CoA hydratase	LnmF (AAN85519)	53/64
<i>Mtul_I</i>	778	AT-less acyltransferase/oxidoreductase	LnmG (AAN85520)	65/76
<i>Mtul_J</i>	314	unknown	LnmH (AAN85521)	44/61
<i>Mtul_K</i>	4285	AT-less type I PKS	LnmI (AAN85522)	50/60
<i>Mtul_L</i>	7078	AT-less type I PKS	LnmJ (AAN85523)	50/60
<i>Mtul_M</i>	329	acyltransferase/decarboxylase	LnmK (AAN85524)	55/70
<i>Mtul_N</i>	86	acyl carrier protein	LnmL (AAN85525)	58/73
<i>Mtul_O</i>	413	HMG-CoA-synthase	LnmM (AAN85526)	65/79
<i>Mtul_P</i>	250	type II thioesterase	LnmN (AAN85527)	55/65
<i>Mtul_Q</i>	134	unknown	LnmZ' (AAN85540)	33/47
<i>Mtul_R</i>	476	dTDP-hexose 2,3-dehydratase	JadO (AAK01936)	45/56
<i>Mtul_S</i>	333	oxidoreductase	(WP_060727604)	49/60
<i>Mtul_T</i>	203	dTDP-4-dehydrorhamnose 3,5-epimerase	NivL (AGZ78381)	45/57
<i>Mtul_U</i>	374	dTDP-sugar aminotransferase	(SEP57347)	60/73
<i>Mtul_V</i>	214	TetR family transcriptional regulator	(WP_062008487)	46/57
<i>Mtul_W</i>	510	antibiotic efflux protein	LnmY (AAN85538)	44/61
<i>Mtul_X</i>	256	sugar O-methyltransferase	(WP_009950022)	64/77
<i>Mtul_Y</i>	411	glycosyltransferase, MGT family	(WP_063747047)	43/54
<i>Mtul_Z1</i>	378	hypothetical protein	(WP_054026420)	30/50
<i>Mtul_Z2</i>	403	cytochrome P450 oxygenase	LnmA (AAN85514)	40/55
<i>Mtul_Z3</i>	405	cytochrome P450 oxygenase	LnmA (AAN85514)	49/65
<i>Mtul_Z4</i>	126	glyoxalase/bleomycin resistance protein	BN971_01690 (CPR09988)	44/54
<i>Mtul_Z5</i>	527	ABC transporter component, periplasmic oligopeptide binding protein	LnmU (AAN85534)	34/50
<i>Mtul_Z6</i>	331	ABC transporter component, membrane spanning protein	LnmT (AAN85533)	45/59
<i>Mtul_Z7</i>	803	ABC transporter component, ATP hydrolase	LnmR (AAN85531)	43/55
<i>Mtul_Z8</i>	419	cytochrome P450 oxygenase	LnmA (AAN85514)	35/52
<i>Mtul_Z9</i>	261	methyltransferase	(WP_031183778)	32/44
<i>Mtul_Z10</i>	238	N-acetylglucosaminyl deacetylase	LnmX (AAN85537)	58/68
<i>Mtul_Z11</i>	469	sodium:proton exchanger	(WP_020553490)	34/52
<i>Mtul_Z12</i>	522	4-coumarate:CoA ligase	LnmW (AAN85536)	36/67
<i>Mtul_Z13</i>	138	unknown, NTF2 family protein	LnmV (AAN85535)	46/65
<i>Mtul_Z14</i>	432	hypothetical protein	(WP_067304298)	43/62
<i>Mtul_Z15</i>	229	4'-phosphopantetheinyl transferase	Sfp (P39135)	24/40

MtuL_orf(+1) 308 transcriptional regulator (WP_009713296) 51/64

^a*orf(-1)* and *orf(+1)* are predicted to represent the upstream and downstream boundaries of the *Inm*-type gene cluster.

^bNumber of amino acids. ^cAlso see **Fig. 2** for the genetic organization of the *Inm*-type gene cluster.

Table S5. Predicted functions of ORFs in the *lnm*-type gene cluster from *Streptomyces* sp. NBRC 109436 (Clade V)

gene ^a	aa ^b	putative function ^c	protein homologue (accession #)	% identity/ % similarity
S109_orf(-1)	230	TetR family transcriptional regulator	(WP_062008487)	99/99
S109_A	572	4-coumarate:CoA ligase	LnmW (AAN85536)	40/56
S109_B	252	methyltransferase	(WP_031183778)	35/45
S109_C	293	unknown	LnmE (AAN85518)	49/63
S109_D	411	HMG-CoA-synthase	LnmM (AAN85526)	47/63
S109_E	261	enoyl-CoA hydratase	LnmF (AAN85519)	51/63
S109_F	845	AT-less acyltransferase/oxidoreductase	LnmG (AAN85520)	67/78
S109_G	297	unknown	LnmH (AAN85521)	43/59
S109_H	626	adenylation protein-peptidyl carrier protein	SyrB1 (AKF46132)	45/59
S109_I	316	halogenase	SyrB2 (AKF46131)	65/75
S109_J	387	alpha/beta hydrolase	ADZ36_03165 (KNE83935)	44/55
S109_K	4266	AT-less type I PKS	LnmI (AAN85522)	47/57
S109_L	6593	AT-less type I PKS	LnmJ (AAN85523)	50/61
S109_M	327	acyltransferase/decarboxylase	LnmK (AAN85524)	52/64
S109_N	86	acyl carrier protein	LnmL (AAN85525)	63/77
S109_O	410	HMG-CoA synthase	LnmM (AAN85526)	64/76
S109_P	82	acyl carrier protein	(WP_062008561)	99/100
S109_Q	424	beta-ketoacyl-ACP synthase	SiaA (AFS33443)	46/58
S109_R	260	type II thioesterase	LnmN (AAN85527)	54/65
S109_S	139	unknown, NTF2 family protein	LnmV (AAN85535)	43/61
S109_T	133	unknown	LnmZ' (AAN85540)	34/49
S109_U	396	cytochrome P450 oxygenase	LnmA (AAN85514)	44/58
S109_V	411	cytochrome P450 oxygenase	LnmA (AAN85514)	50/66
S109_W	144	glyoxalase/bleomycin resistance protein	BN971_01690 (CPR09988)	41/53
S109_X	238	N-acetylglucosaminyl deacetylase	LnmX (AAN85537)	53/64
S109_Y	530	ABC transporter component, periplasmic oligopeptide binding protein	LnmU (AAN85534)	32/46
S109_Z1	333	ABC transporter component, membrane spanning protein	LnmT (AAN85533)	44/60
S109_Z2	817	ABC transporter component, ATP hydrolase	LnmR (AAN85531)	42/54
S109_Z3	226	Crp/Fnr family transcriptional regulator	LnmO (AAN85528)	48/68
S109_orf(+1)	209	dTDP-4-dehydrorhamnose 3,5-epimerase	NivL (AGZ78381)	67/79

^aorf(-1) and orf(+1) are predicted to represent the upstream and downstream boundaries of the *lnm*-type gene cluster.

^bNumber of amino acids. ^cAlso see Fig. 2 for the genetic organization of the *lnm*-type gene cluster.

Table S6. Predicted functions of ORFs in the *lnm*-type gene cluster from *S. hygroscopicus* sp. NBRC 16556 (Clade V)

gene ^a	aa ^b	putative function ^c	protein homologue (accession #)	% identity/ % similarity
<i>Shyg_orf(-1)</i>	230	TetR family transcriptional regulator	(WP_062008487)	99/99
<i>Shyg_A</i>	572	4-coumarate:CoA ligase	LnmW (AAN85536)	40/56
<i>Shyg_B</i>	252	methyltransferase	(WP_031183778)	35/45
<i>Shyg_C</i>	293	unknown	LnmE (AAN85518)	49/63
<i>Shyg_D</i>	411	HMG-CoA-synthase	LnmM (AAN85526)	47/63
<i>Shyg_E</i>	261	enoyl-CoA hydratase	LnmF (AAN85519)	51/63
<i>Shyg_F</i>	845	AT-less acyltransferase/oxidoreductase	LnmG (AAN85520)	67/78
<i>Shyg_G</i>	337	unknown	LnmH (AAN85521)	43/59
<i>Shyg_H</i>	626	adenylation protein-peptidyl carrier protein	SyrB1 (AKF46132)	45/59
<i>Shyg_I</i>	316	halogenase	SyrB2 (AKF46131)	65/75
<i>Shyg_J</i>	397	alpha/beta hydrolase	ADZ36_03165 (KNE83935)	44/55
<i>Shyg_K</i>	4258	AT-less type I PKS	LnmI (AAN85522)	47/57
<i>Shyg_L</i>	6571	AT-less type I PKS	LnmJ (AAN85523)	50/61
<i>Shyg_M</i>	327	acyltransferase/decarboxylase	LnmK (AAN85524)	52/64
<i>Shyg_N</i>	86	acyl carrier protein	LnmL (AAN85525)	63/77
<i>Shyg_O</i>	410	HMG-CoA synthase	LnmM (AAN85526)	64/76
<i>Shyg_P</i>	82	acyl carrier protein	(WP_062008561)	99/100
<i>Shyg_Q</i>	424	beta-ketoacyl-ACP synthase	SiaA (AFS33443)	46/58
<i>Shyg_R</i>	260	type II thioesterase	LnmN (AAN85527)	54/65
<i>Shyg_S</i>	139	unknown, NTF2 family protein	LnmV (AAN85535)	43/61
<i>Shyg_T</i>	133	unknown	LnmZ' (AAN85540)	34/49
<i>Shyg_U</i>	396	cytochrome P450 oxygenase	LnmA (AAN85514)	44/58
<i>Shyg_V</i>	411	cytochrome P450 oxygenase	LnmA (AAN85514)	50/66
<i>Shyg_W</i>	144	glyoxalase/bleomycin resistance protein	BN971_01690 (CPR09988)	41/53
<i>Shyg_X</i>	238	N-acetylglucosaminyl deacetylase	LnmX (AAN85537)	53/64
<i>Shyg_Y</i>	530	ABC transporter component, periplasmic oligopeptide binding protein	LnmU (AAN85534)	32/46
<i>Shyg_Z1</i>	333	ABC transporter component, membrane spanning protein	LnmT (AAN85533)	44/60
<i>Shyg_Z2</i>	817	ABC transporter component, ATP hydrolase	LnmR (AAN85531)	42/54
<i>Shyg_Z3</i>	226	Crp/Fnr family transcriptional regulator	LnmO (AAN85528)	48/68
<i>Shyg_orf(+1)</i>	209	dTDP-4-dehydrorhamnose 3,5-epimerase	NivL (AGZ78381)	67/79

^a*orf(-1)* and *orf(+1)* are predicted to represent the upstream and downstream boundaries of the *lnm*-type gene cluster.

^bNumber of amino acids. ^cAlso see Fig. 2 for the genetic organization of the *lnm*-type gene cluster.

Table S7. Predicted functions of ORFs in the *lnm*-type gene cluster from *S. leeuwenhoeekii* DSM 42122 (Clade V)

gene ^a	aa ^b	putative function ^c	protein homologue (accession #)	% identity/ % similarity
<i>Slee_orf(-1)</i>	187	TetR family transcriptional regulator	(WP_062008487)	98/98
<i>Slee_A</i>	479	4-coumarate:CoA ligase	LnmW (AAN85536)	40/56
<i>Slee_B</i>	234	methyltransferase	(WP_031183778)	37/46
<i>Slee_C</i>	293	unknown	LnmE (AAN85518)	48/62
<i>Slee_D</i>	411	HMG-CoA-synthase	LnmM (AAN85526)	47/64
<i>Slee_E</i>	255	enoyl-CoA hydratase	LnmF (AAN85519)	50/63
<i>Slee_F</i>	808	AT-less acyltransferase/oxidoreductase	LnmG (AAN85520)	67/78
<i>Slee_G</i>	303	unknown	LnmH (AAN85521)	44/60
<i>Slee_H</i>	630	adenylation protein-peptidyl carrier protein	SyrB1 (AKF46132)	45/59
<i>Slee_I</i>	316	halogenase	SyrB2 (AKF46131)	65/75
<i>Slee_J</i>	376	alpha/beta hydrolase	ADZ36_03165 (KNE83935)	44/56
<i>Slee_K</i>	4212	AT-less type I PKS	LnmI (AAN85522)	49/59
<i>Slee_L</i>	6495	AT-less type I PKS	LnmJ (AAN85523)	50/61
<i>Slee_M</i>	310	acyltransferase/decarboxylase	LnmK (AAN85524)	52/64
<i>Slee_N</i>	86	acyl carrier protein	LnmL (AAN85525)	50/67
<i>Slee_O</i>	410	HMG-CoA synthase	LnmM (AAN85526)	64/76
<i>Slee_P</i>	82	acyl carrier protein	(WP_062008561)	96/97
<i>Slee_Q</i>	424	beta-ketoacyl-ACP synthase	SiaA (AFS33443)	46/58
<i>Slee_R</i>	260	type II thioesterase	LnmN (AAN85527)	52/64
<i>Slee_S</i>	139	unknown, NTF2 family protein	LnmV (AAN85535)	43/61
<i>Slee_T</i>	120	unknown	LnmZ' (AAN85540)	36/51
<i>Slee_U</i>	396	cytochrome P450 oxygenase	LnmA (AAN85514)	43/57
<i>Slee_V</i>	387	cytochrome P450 oxygenase	LnmA (AAN85514)	51/66
<i>Slee_W</i>	124	glyoxalase/bleomycin resistance protein	BN971_01690 (CPR09988)	43/53
<i>Slee_X</i>	238	N-acetylglucosaminyl deacetylase	LnmX (AAN85537)	53/65
<i>Slee_Y</i>	530	ABC transporter component, periplasmic oligopeptide binding protein	LnmU (AAN85534)	32/46
<i>Slee_Z1</i>	315	ABC transporter component, membrane spanning protein	LnmT (AAN85533)	44/60
<i>Slee_Z2</i>	778	ABC transporter component, ATP hydrolase	LnmR (AAN85531)	42/55
<i>Slee_Z3</i>	226	Crp/Fnr family transcriptional regulator	LnmO (AAN85528)	49/68
<i>Slee_orf(+1)</i>	203	dTDP-4-dehydrorhamnose 3,5-epimerase	NivL (AGZ78381)	68/80

^a*orf(-1)* and *orf(+1)* are predicted to represent the upstream and downstream boundaries of the *lnm*-type gene cluster.

^bNumber of amino acids. ^cAlso see Fig. 2 for the genetic organization of the *lnm*-type gene cluster.

Table S8. Predicted functions of ORFs in the *lnm*-type gene cluster from *Streptomyces canus* ATCC 12647 (Clade VII)

gene ^a	aa ^b	putative function ^c	protein homologue	% identity/ % similarity
<i>Scan_orf(-1)</i>	205	TetR family transcriptional regulator	(WP_058852673)	41/62
<i>Scan_A</i>	191	Ydel-like protein	SAVERM_307 (BAC68016)	71/80
<i>Scan_B</i>	454	cytochrome P450 oxygenase	VR46_04425 (KJY47279)	38/55
<i>Scan_C</i>	228	Crp/Fnr family transcriptional regulator	LnmO (AAN85528)	42/59
<i>Scan_D</i>	236	4'-phosphopantetheinyl transferase	Sfp (P39135)	22/41
<i>Scan_E</i>	433	cytochrome P450 oxygenase	LnmA (AAN85514)	36/57
<i>Scan_F</i>	238	Crp/Fnr family transcriptional regulator	LnmO (AAN85528)	43/62
<i>Scan_G</i>	437	sodium:proton exchanger	(WP_020553490)	58/74
<i>Scan_H</i>	298	unknown	LnmE (AAN85518)	46/63
<i>Scan_I</i>	410	HMG-CoA synthase	LnmM (AAN85526)	46/62
<i>Scan_J</i>	263	enoyl-CoA hydratase	LnmF (AAN85519)	51/65
<i>Scan_K</i>	867	AT-less acyltransferase/oxidoreductase	LnmG (AAN85520)	57/69
<i>Scan_L</i>	316	unknown	LnmH (AAN85521)	43/59
<i>Scan_M</i>	599	adenylation protein-peptidyl carrier protein	SyrB1 (AKF46132)	46/62
<i>Scan_N</i>	311	halogenase	SyrB2 (AKF46131)	67/79
<i>Scan_O</i>	391	alpha/beta hydrolase	ADZ36_03165 (KNE83935)	43/54
<i>Scan_P</i>	4242	hybrid NRPS/type I PKS	LnmI (AAN85522)	51/61
<i>Scan_Q</i>	7157	AT-less type I PKS	LnmJ (AAN85523)	49/61
<i>Scan_R</i>	329	acyltransferase/decarboxylase	LnmK (AAN85524)	55/67
<i>Scan_S</i>	87	acyl carrier protein	LnmL (AAN85525)	60/69
<i>Scan_T</i>	412	HMG-CoA synthase	LnmM (AAN85526)	63/77
<i>Scan_U</i>	80	acyl carrier protein	(WP_062008561)	53/71
<i>Scan_V</i>	422	beta-ketoacyl-ACP synthase	SiaA (AFS33443)	43/53
<i>Scan_W</i>	253	type II thioesterase	LnmN (AAN85527)	53/65
<i>Scan_X</i>	239	N-acetylglucosaminyl deacetylase	LnmX (AAN85537)	55/65
<i>Scan_Y</i>	132	unknown	LnmZ' (AAN85540)	38/57
<i>Scan_Z1</i>	488	4-coumarate:CoA ligase	LnmW (AAN85536)	44/57
<i>Scan_Z2</i>	395	FAD-dependent oxidoreductase	(WP_010982689)	61/70
<i>Scan_Z3</i>	121	glyoxalase/bleomycin resistance protein	(WP_062700437)	41/60
<i>Scan_Z4</i>	491	4-coumarate:CoA ligase	LnmW (AAN85536)	42/55
<i>Scan_Z5</i>	414	cytochrome P450 oxygenase	LnmA (AAN85514)	34/50
<i>Scan_orf(+1)</i>	1157	Repeat domain-containing protein	STTU_5173 (EGJ77962)	64/75

^a*orf(-1)* and *orf(+1)* are predicted to represent the upstream and downstream boundaries of the *lnm*-type gene cluster.

^bNumber of amino acids. ^cAlso see Fig. 2 for the genetic organization of the *lnm*-type gene cluster.

Table S9. Predicted functions of ORFs in the *lnm*-type gene cluster from *Catenulispora acidiphila* DSM 44928 (Clade VIII)

gene ^a	aa ^b	putative function ^c	protein homologue	% identity/ % similarity
<i>Caci_orf(-1)</i>	311	Hypothetical protein	Not found	
<i>Caci_A</i>	397	FAD-dependent oxidoreductase	(WP_010982689)	44/58
<i>Caci_B</i>	483	amidase	(WP_011874565)	86/92
<i>Caci_C</i>	503	4-coumarate:CoA ligase	LnmW (AAN85536)	33/45
<i>Caci_D</i>	539	antibiotic efflux protein	LnmY (AAN85538)	29/48
<i>Caci_E</i>	360	oxidoreductase	(WP_026583996)	45/60
<i>Caci_F</i>	404	cytochrome P450 oxygenase	LnmA (AAN85514)	39/53
<i>Caci_G</i>	308	unknown	LnmH (AAN85521)	43/60
<i>Caci_H</i>	132	unknown	LnmZ' (AAN85540)	34/49
<i>Caci_I</i>	179	hypothetical protein	(WP_053707566)	50/65
<i>Caci_J</i>	80	ferredoxin	LnmB (AAN85515)	36/47
<i>Caci_K</i>	865	acyltransferase/oxidoreductase	LnmG	51/62
<i>Caci_L</i>	622	NRPS (A-PCP)	SyrB1 (AKF46132)	43/59
<i>Caci_M</i>	332	halogenase	SyrB2 (AKF46131)	67/79
<i>Caci_N</i>	397	alpha/beta hydrolase	ADZ36_03165 (KNE83935)	46/58
<i>Caci_O</i>	221	Crp/Fnr family transcriptional regulator	LnmO (AAN85528)	46/66
<i>Caci_P</i>	2454	AT-less type I PKS	LnmI (AAN85522)	46/58
<i>Caci_Q</i>	264	type II thioesterase	LnmN (AAN85527)	56/67
<i>Caci_R</i>	325	unknown	LnmE (AAN85518)	44/63
<i>Caci_S</i>	413	HMG-CoA synthase	LnmM (AAN85526)	45/61
<i>Caci_T</i>	268	enoyl-CoA hydratase	LnmF (AAN85519)	46/58
<i>Caci_U</i>	2284	AT-less type I PKS	LnmI (AAN85522)	49/58
<i>Caci_V</i>	7149	AT-less type I PKS	LnmJ (AAN85523)	44/56
<i>Caci_W</i>	324	acyltransferase/decarboxylase	LnmK (AAN85524)	50/68
<i>Caci_X</i>	89	acyl carrier protein	LnmL (AAN85525)	50/72
<i>Caci_Y</i>	424	HMG-CoA synthase	LnmM (AAN85526)	62/75
<i>Caci_Z1</i>	83	acyl carrier protein	(WP_062008561)	48/57
<i>Caci_Z2</i>	428	beta-ketoacyl-ACP synthase	SiaA (AFS33443)	41/53
<i>Caci_Z3</i>	241	N-acetylglucosaminyl deacetylase	LnmX (AAN85537)	54/64
<i>Caci_orf(+1)</i>	98	aminotransferase	(WP_051733654)	50/59

^a*orf(-1)* and *orf(+1)* are predicted to represent the upstream and downstream boundaries of the *lnm*-type gene cluster.

^bNumber of amino acids. ^cAlso see Fig. 2 for the genetic organization of the *lnm*-type gene cluster.

Table S10. Predicted functions of ORFs in the *gnm*-like gene cluster from *Streptomyces* sp. F5630 (Clade IX)

gene ^a	aa ^b	putative function ^c	protein homologue (accession #)	% identity/ % similarity
<i>Sf56_orf(-1)</i>	196	putative lanthionine synthetase	SAVERM_307 (BAC68016)	59/74
<i>Sf56_A</i>	145	truncated hemoglobin	SAVERM_3316 (BAC71027)	36/50
<i>Sf56_B</i>	2390	hybrid NRPS/type I PKS	LnmI (AAN85522)	47/56
<i>Sf56_C</i>	252	type II thioesterase	LnmN (AAN85527)	55/65
<i>Sf56_D</i>	246	4'-phosphopantetheinyl transferase	Sfp (P39135)	28/49
<i>Sf56_E</i>	410	HMG-CoA synthase	LnmM (AAN85526)	48/63
<i>Sf56_F</i>	262	enoyl-CoA hydratase	LnmF (AAN85519)	48/60
<i>Sf56_G</i>	759	acyltransferase/oxidoreductase	LnmG (AAN85520)	47/62
<i>Sf56_H</i>	2052	AT-less type I PKS	LnmI (AAN85522)	50/58
<i>Sf56_I</i>	518	antibiotic efflux protein	LnmY (AAN85538)	30/47
<i>Sf56_J</i>	279	unknown	LnmE (AAN85518)	48/62
<i>Sf56_K</i>	765	AT-less acyltransferase/oxidoreductase	LnmG (AAN85520)	63/74
<i>Sf56_L</i>	310	unknown	LnmH (AAN85521)	40/56
<i>Sf56_M</i>	121	glyoxalase/bleomycin resistance protein	(WP_062700437)	47/67
<i>Sf56_N</i>	135	unknown	LnmZ' (AAN85540)	35/52
<i>Sf56_O</i>	237	N-acetylglucosaminyl deacetylase	LnmX (AAN85537)	54/67
<i>Sf56_P</i>	248	methyltransferase	(WP_031183778)	37/47
<i>Sf56_Q</i>	665	putative alpha/beta hydrolase	LnmD (AAN85517)	35/45
<i>Sf56_R</i>	84	peptidyl carrier protein	LnmP (AAN85529)	47/57
<i>Sf56_S</i>	542	discrete adenylation protein	LnmQ (AAN85530)	55/66
<i>Sf56_T</i>	7148	AT-less type I PKS	LnmJ (AAN85523)	47/57
<i>Sf56_U</i>	411	HMG-CoA-synthase	LnmM (AAN85526)	59/76
<i>Sf56_V</i>	74	acyl carrier protein	Fr9M (ADH01494)	40/65
<i>Sf56_W</i>	433	beta-ketoacyl-ACP synthase	SiaA (AFS33443)	43/54
<i>Sf56_X</i>	413	cytochrome P450 oxygenase	LnmA (AAN85514)	42/53
<i>Sf56_Y</i>	434	aminotransferase	(KMS73037)	40/55
<i>Sf56_Z</i>	229	Crp/Fnr family transcriptional regulator	LnmO (AAN85528)	44/63
<i>Sf56_orf(+1)</i>	297	LysR family transcriptional regulator	(WP_031032372)	77/83

^a*orf(-1)* and *orf(+1)* are predicted to represent the upstream and downstream boundaries of the *gnm*-like gene cluster.

^bNumber of amino acids. ^cAlso see Fig. 2 for the genetic organization of the *gnm*-like gene cluster.

Table S11. Predicted functions of ORFs in the *gnm*-like gene cluster from *S. aureofaciens* NRRL B-2183 (Clade IX)

gene ^a	aa ^b	putative function ^c	protein homologue (accession #)	% identity/ % similarity
<i>Saur_orf(-1)</i>	195	putative lanthionine synthetase	SAVERM_307 (BAC68016)	60/77
<i>Saur_A</i>	145	truncated hemoglobin	SAVERM_3316 (BAC71027)	39/50
<i>Saur_B</i>	2271	hybrid NRPS/type I PKS	LnmI (AAN85522)	47/57
<i>Saur_C</i>	252	type II thioesterase	LnmN (AAN85527)	54/63
<i>Saur_D</i>	245	4'-phosphopantetheinyl transferase	Sfp (P39135)	28/47
<i>Saur_E</i>	410	HMG-CoA synthase	LnmM (AAN85526)	48/62
<i>Saur_F</i>	264	enoyl-CoA hydratase	LnmF (AAN85519)	49/61
<i>Saur_G</i>	738	acyltransferase/oxidoreductase	LnmG (AAN85520)	46/63
<i>Saur_H</i>	2042	AT-less type I PKS	LnmI (AAN85522)	49/58
<i>Saur_I</i>	489	antibiotic efflux protein	LnmY (AAN85538)	31/49
<i>Saur_J</i>	264	unknown	LnmE (AAN85518)	48/63
<i>Saur_K</i>	767	AT-less acyltransferase/oxidoreductase	LnmG (AAN85520)	56/68
<i>Saur_L</i>	310	unknown	LnmH (AAN85521)	40/56
<i>Saur_M</i>	121	glyoxalase/bleomycin resistance protein	(WP_062700437)	45/66
<i>Saur_N</i>	133	unknown	LnmZ' (AAN85540)	31/47
<i>Saur_O</i>	238	N-acetylglucosaminyl deacetylase	LnmX (AAN85537)	54/67
<i>Saur_P</i>	248	methyltransferase	(WP_031183778)	54/67
<i>Saur_Q</i>	684	putative alpha/beta hydrolase	LnmD (AAN85517)	44/56
<i>Saur_R</i>	84	peptidyl carrier protein	LnmP (AAN85529)	46/58
<i>Saur_S</i>	542	discrete adenylation protein	LnmQ (AAN85530)	54/64
<i>Saur_T</i>	7020	AT-less type I PKS	LnmJ (AAN85523)	47/56
<i>Saur_U</i>	411	HMG-CoA-synthase	LnmM (AAN85526)	59/75
<i>Saur_V</i>	73	acyl carrier protein	Fr9M (ADH01494)	36/62
<i>Saur_W</i>	433	beta-ketoacyl-ACP synthase	SiaA (AFS33443)	42/55
<i>Saur_X</i>	413	cytochrome P450 oxygenase	LnmA (AAN85514)	42/54
<i>Saur_Y</i>	433	aminotransferase	(KMS73037)	42/55
<i>Saur_Z</i>	193	Crp/Fnr family transcriptional regulator	LnmO (AAN85528)	44/61
<i>Saur_orf(+1)</i>	367	transposase	SAVERM_309 (BAC68018)	57/65

^a*orf(-1)* and *orf(+1)* are predicted to represent the upstream and downstream boundaries of the *gnm*-like gene cluster.

^bNumber of amino acids. ^cAlso see Fig. 2 for the genetic organization of the *gnm*-like gene cluster.

Table S12. Predicted functions of ORFs in the *lnm*-type gene cluster from *Saccharothrix* sp. ST-888 (Clade XI)

gene ^a	aa ^b	putative function ^c	protein homologue	% identity/ % similarity
<i>Sast_orf(-1)</i>	607	glucoamylase	(WP_010983371)	81/87
<i>Sast_A</i>	126	glyoxalase/bleomycin resistance protein	(WP_062700437)	34/48
<i>Sast_B</i>	411	cytochrome P450 oxygenase	LnmA (AAN85514)	36/50
<i>Sast_C</i>	464	ferredoxin reductase	SCO2106 (NP_626364)	35/49
<i>Sast_D</i>	78	ferredoxin	LnmB (AAN85515)	32/51
<i>Sast_E</i>	144	truncated hemoglobin	SAVERM_3316 (BAC71027)	37/50
<i>Sast_F</i>	2290	hybrid NRPS/type I PKS	LnmI (AAN85522)	50/60
<i>Sast_G</i>	251	thioesterase type II	LnmN (AAN85527)	56/67
<i>Sast_H</i>	410	HMG-CoA synthase	LnmM (AAN85526)	48/63
<i>Sast_I</i>	260	enoyl-CoA hydratase	LnmF (AAN85519)	48/58
<i>Sast_J</i>	769	acyltransferase/oxidoreductase	LnmG (AAN85520)	42/55
<i>Sast_K</i>	2063	AT-less type I PKS	LnmI (AAN85522)	50/59
<i>Sast_L</i>	503	antibiotic efflux protein	LnmY (AAN85538)	33/49
<i>Sast_M</i>	301	unknown	LnmE (AAN85518)	45/61
<i>Sast_N</i>	764	AT-less acyltransferase/oxidoreductase	LnmG (AAN85520)	66/78
<i>Sast_O</i>	306	unknown	LnmH (AAN85521)	43/59
<i>Sast_P</i>	375	hypothetical protein	(WP_054026420)	45/67
<i>Sast_Q</i>	119	glyoxalase/bleomycin resistance protein	(WP_062700437)	50/65
<i>Sast_R</i>	135	unknown	LnmZ' (AAN85540)	35/45
<i>Sast_S</i>	238	N-acetylglucosaminyl deacetylase	LnmX (AAN85537)	55/68
<i>Sast_T</i>	248	methyltransferase	(WP_031183778)	37/50
<i>Sast_U</i>	424	putative alpha/beta hydrolase	LnmD (AAN85517)	46/55
<i>Sast_V</i>	193	hypothetical protein	NA	NA
<i>Sast_W</i>	82	peptidyl carrier protein	LnmP (AAN85529)	43/59
<i>Sast_X</i>	531	discrete adenylation protein	LnmQ (AAN85530)	56/66
<i>Sast_Y</i>	7401	AT-less type I PKS	LnmJ (AAN85523)	48/58
<i>Sast_Z1</i>	411	HMG-CoA-synthase	LnmM (AAN85526)	63/76
<i>Sast_Z2</i>	82	acyl carrier protein	Fr9M (ADH01494)	31/60
<i>Sast_Z3</i>	412	beta-ketoacyl-ACP synthase	SiaA (AFS33443)	45/58
<i>Sast_Z4</i>	419	cytochrome P450 oxygenase	LnmA (AAN85514)	43/56
<i>Sast_Z5</i>	64	ferredoxin	LnmB (AAN85515)	32/47
<i>Sast_Z6</i>	212	Crp/Fnr family transcriptional regulator	LnmO (AAN85528)	49/67
<i>Sast_orf(+1)</i>	179	SMI1/KNR4 family protein	(WP_030749561)	44/52

^a*orf(-1)* and *orf(+1)* are predicted to represent the upstream and downstream boundaries of the *lnm*-type gene cluster.

^bNumber of amino acids. ^cAlso see Fig. 2 for the genetic organization of the *lnm*-type gene cluster.

Table S13. Predicted functions of ORFs in the *lnm*-type gene cluster from *Streptomyces* sp. NBRC 110035 (Clade XII)

gene ^a	aa ^b	putative function ^c	protein homologue	% identity/ % similarity
S110_orf(-1)	132	transposase	(ANZ13531)	89/90
S110_A	237	Crp/Fnr/Fnr family transcriptional regulator	LnmO (AAN85528)	37/58
S110_B	189	Ydel-like protein	SAVERM_307 (BAC68016)	55/71
S110_C	244	phosphopantetheinyl transferase	(WP_059300333)	36/47
S110_D	409	HMG-CoA-synthase	LnmM (AAN85526)	44/59
S110_E	255	enoyl-CoA hydratase	LnmF (AAN85519)	47/59
S110_F	290	acyltransferase	LnmG (AAN85520)	42/54
S110_G	1993	AT-less type I PKS	Lnml (AAN85522)	47/56
S110_H	274	transposase	(WP_011029009)	79/85
S110_I	131	glyoxalase/bleomycin resistance protein	(WP_062700437)	28/46
S110_J	496	antibiotic efflux protein	LnmY (AAN85538)	32/49
S110_K	233	unknown	LnmE (AAN85518)	38/54
S110_L	776	AT-less acyltransferase/oxidoreductase	LnmG (AAN85520)	60/72
S110_M	307	unknown	LnmH (AAN85521)	35/52
S110_N	120	glyoxalase/bleomycin resistance protein	(WP_062700437)	42/62
S110_O	236	N-acetylglucosaminyl deacetylase	LnmX (AAN85537)	50/62
S110_P	249	methyltransferase	(WP_031183778)	41/49
S110_Q	418	putative alpha/beta hydrolase	LnmD (AAN85517)	36/46
S110_R	81	peptidyl carrier protein	LnmP (AAN85529)	45/60
S110_S	525	discrete adenylation protein	LnmQ (AAN85530)	52/62
S110_T	7438	AT-less type I PKS	LnmJ (AAN85523)	43/54
S110_U	416	HMG-CoA-synthase	LnmM (AAN85526)	56/69
S110_V	81	acyl carrier protein	Fr9M (ADH01494)	31/53
S110_W	408	beta-ketoacyl-ACP synthase	SiaA (AFS33443)	41/54
S110_X	248	type II thioesterase	LnmN (AAN85527)	55/64
S110_Y	2337	hybrid NRPS/type I PKS	Lnml (AAN85522)	45/54
S110_Z1	143	truncated hemoglobin	SAVERM_3316 (BAC71027)	35/48
S110_Z2	408	cytochrome P450 oxygenase	LnmA (AAN85514)	39/55
S110_Z3	74	ferredoxin	LnmB (AAN85515)	31/55
S110_Z4	453	crotonyl-CoA carboxylase/reductase	DivR (CCP20056)	63/77
S110_Z5	330	ketoacyl-acyl carrier protein synthase III (KASIII)	DivS (CCP20057)	56/77
S110_Z6	289	3-hydroxyacyl-CoA dehydrogenase	DivT (CCP20058)	48/66
S110_orf(+1)	127	transposase	(WP_069173729)	75/82

^aorf(-1) and orf(+1) are predicted to represent the upstream and downstream boundaries of the *lnm*-type gene cluster.

^bNumber of amino acids. ^cAlso see Fig. 2 for the genetic organization of the *lnm*-type gene cluster.

Table S14. Predicted functions of ORFs in the *lnm*-type gene cluster from *S. novaecaesareae* NRRL B-1267 (Clade XIII)

gene ^a	aa ^b	putative function ^c	protein homologue	% identity/ % similarity
<i>Snov_orf(-1)</i>	126	glyoxalase/bleomycin resistance protein	(WP_062700437)	37/54
<i>Snov_A</i>	408	HMG-CoA-synthase	LnmM (AAN85526)	44/62
<i>Snov_B</i>	278	enoyl-CoA hydratase	LnmF (AAN85519)	45/59
<i>Snov_C</i>	764	acyltransferase/oxidoreductase	LnmG (AAN85520)	63/79
<i>Snov_D</i>	281	unknown	LnmH (AAN85521)	41/58
<i>Snov_E</i>	193	Ydel-like protein	SAVERM_307 (BAC68016)	61/74
<i>Snov_F</i>	150	truncated hemoglobin	SAVERM_3316 (BAC71027)	43/59
<i>Snov_G</i>	404	cytochrome P450 oxygenase	LnmA (AAN85514)	46/61
<i>Snov_H</i>	402	cytochrome P450 oxygenase	LnmA (AAN85514)	39/55
<i>Snov_I</i>	70	ferredoxin	LnmB (AAN85515)	39/50
<i>Snov_J</i>	223	Crp/Fnr family transcriptional regulator	LnmO (AAN85528)	41/59
<i>Snov_K</i>	542	putative alpha/beta hydrolase	LnmD (AAN85517)	40/52
<i>Snov_L</i>	83	peptidyl carrier protein	LnmP (AAN85529)	37/50
<i>Snov_M</i>	406	diaminopimelate decarboxylase	(WP_064072918)	54/62
<i>Snov_N</i>	495	discrete adenylation protein	LnmQ (AAN85530)	28/47
<i>Snov_O</i>	341	hypothetical protein	(WP_012392161)	46/61
<i>Snov_P</i>	376	hypothetical protein	(WP_040258597)	58/71
<i>Snov_Q</i>	340	hypothetical protein	(WP_052482831)	49/64
<i>Snov_R</i>	564	acyl-CoA synthetase	(WP_052482829)	45/59
<i>Snov_S</i>	82	ACP-like PKS domain	LnmJ (AAN85523)	38/54
<i>Snov_T</i>	973	KS-AT-ACP	(WP_052482825)	52/62
<i>Snov_U</i>	798	KS-ACP	(WP_052482823)	48/58
<i>Snov_V</i>	803	putative class-III aminotransferase	(AJE87366)	54/68
<i>Snov_W</i>	594	oxidoreductase	(AJE87364)	55/74
<i>Snov_X</i>	2844	AT-less type I PKS	LnmI (AAN85522)	48/57
<i>Snov_Y</i>	7724	AT-less type I PKS	LnmJ (AAN85523)	45/56
<i>Snov_Z1</i>	408	HMG-CoA synthase	LnmM (AAN85526)	55/70
<i>Snov_Z2</i>	82	acyl carrier protein	Fr9M (ADH01494)	29/56
<i>Snov_Z3</i>	405	beta-ketoacyl-ACP synthase	SiaA (AFS33443)	41/54
<i>Snov_Z4</i>	258	type II thioesterase	LnmN (AAN85527)	48/60
<i>Snov_Z5</i>	266	ABC transporter	(WP_069169226)	49/64
<i>Snov_Z6</i>	314	ABC transporter component, ATP hydrolase	LnmR (AAN85531)	33/48
<i>Snov_Z7</i>	152	RDD family protein, transporter	WP_011730428	35/49
<i>Snov_Z8</i>	451	sodium:proton exchanger	(WP_020553490)	28/47
<i>Snov_Z9</i>	263	methyltransferase	(WP_051803680)	46/63
<i>Snov_orf(+1)</i>	280	transglutaminase	(WP_052145777)	64/74

^a*orf(-1)* and *orf(+1)* are predicted to represent the upstream and downstream boundaries of the *lnm*-type gene cluster.

^bNumber of amino acids. ^cAlso see Fig. 2 for the genetic organization of the *lnm*-type gene cluster.

Table S15. Predicted functions of ORFs in the *lnm*-type gene cluster from *Saccharothrix espanaensis* DSM 44229 (Clade XIV)

gene ^a	aa ^b	putative function ^c	protein homologue	% identity/ % similarity
Saes_orf(-1)	314	RNA polymerase sigma24 factor	(WP_009948905)	78/86
Saes_A	136	unknown	LnmZ' (AAN85540)	35/56
Saes_B	121	glyoxalase/bleomycin resistance protein	(WP_062700437)	37/53
Saes_C	270	Crp/Fnr family transcriptional regulator	LnmO (AAN85528)	42/61
Saes_D	500	4-coumarate:CoA ligase	LnmW (AAN85536)	40/56
Saes_E	183	hypothetical protein	(WP_053707566)	48/60
Saes_F	741	acyltransferase/oxidoreductase	LnmG (AAN85520)	49/60
Saes_G	254	enoyl-CoA hydratase	LnmF (AAN85519)	51/62
Saes_H	412	HMG-CoA synthase	LnmM (AAN85526)	46/62
Saes_I	264	unknown	LnmE (AAN85518)	43/59
Saes_J	1999	hybrid NRPS/type I PKS	LnmI (AAN85522)	49/57
Saes_K	6706	AT-less type I PKS	LnmJ (AAN85523)	46/57
Saes_L	312	acyltransferase/decarboxylase	LnmK (AAN85524)	51/63
Saes_M	92	acyl carrier protein	LnmL (AAN85525)	50/66
Saes_N	412	HMG-CoA synthase	LnmM (AAN85526)	63/77
Saes_O	406	alpha/beta hydrolase	ADZ36_03165 (KNE83935)	45/57
Saes_P	416	hypothetical protein	(WP_067304298)	43/59
Saes_Q	267	ABC transporter	(WP_069169226)	37/59
Saes_R	333	ABC transporter component, ATP hydrolase	LnmR (AAN85531)	33/43
Saes_S	412	cytochrome P450 oxygenase	LnmA (AAN85514)	40/55
Saes_T	499	putative class-III aminotransferase	(AJE87366)	33/47
Saes_U	202	thioesterase type II	LnmN (AAN85527)	53/61
Saes_V	2223	AT-less type I PKS	LnmI (AAN85522)	50/61
Saes_W	784	AT-less acyltransferase/oxidoreductase	LnmG (AAN85520)	60/72
Saes_X	313	unknown	LnmH (AAN85521)	43/59
Saes_Y	600	NRPS (A-PCP)	SyrB1 (AKF46132)	45/59
Saes_Z1	318	halogenase	SyrB2 (AKF46131)	67/78
Saes_Z2	76	acyl carrier protein	(WP_062008561)	53/70
Saes_Z3	409	beta-ketoacyl-ACP synthase	SiaA (AFS33443)	41/54
Saes_Z4	404	FAD-dependent oxidoreductase	(WP_010982689)	58/69
Saes_Z5	520	ABC transporter component, periplasmic oligopeptide binding protein	LnmU (AAN85534)	51/65
Saes_Z6	315	ABC transporter component, membrane spanning protein	LnmT (AAN85533)	58/70
Saes_Z7	263	ABC transporter component, membrane spanning protein	LnmS (AAN85532)	60/70
Saes_Z8	516	ABC transporter component, ATP hydrolase	LnmR (AAN85531)	57/67
Saes_Z9	246	methyltransferase	(WP_026218883)	46/62
Saes_Z10	640	Radical SAM superfamily protein	(SED67026)	54/68
Saes_orf(+1)	271	lipase	(WP_040253406)	68/79

^aorf(-1) and orf(+1) are predicted to represent the upstream and downstream boundaries of the *lnm*-type gene cluster.

^bNumber of amino acids. ^cAlso see Fig. 2 for the genetic organization of the *lnm*-type gene cluster.

Table S16. Predicted functions of ORFs in the *Inm*-type gene cluster from *Micromonospora* sp. CNB394 (Clade XV)

gene ^a	aa ^b	putative function ^c	protein homologue	% identity/ % similarity
<i>Mcnb_orf(-1)</i>	210	peptidase 23	(SCL52691)	82/88
<i>Mcnb_A</i>	494	4-coumarate:CoA ligase	LnmW (AAN85536)	41/57
<i>Mcnb_B</i>	413	HMG-CoA-synthase	LnmM (AAN85526)	49/63
<i>Mcnb_C</i>	179	hypothetical protein	(WP_053707566)	42/57
<i>Mcnb_D</i>	426	sodium:proton exchanger	(WP_020553490)	33/51
<i>Mcnb_E</i>	253	Crp/Fnr family transcriptional regulator	LnmO (AAN85528)	46/59
<i>Mcnb_F</i>	744	acyltransferase/oxidoreductase	LnmG (AAN85520)	45/57
<i>Mcnb_G</i>	252	enoyl-CoA hydratase	LnmF (AAN85519)	52/63
<i>Mcnb_H</i>	292	unknown	LnmE (AAN85518)	43/60
<i>Mcnb_I</i>	1960	hybrid NRPS/type I PKS	Lnml (AAN85522)	50/58
<i>Mcnb_J</i>	6709	AT-less type I PKS	LnmJ (AAN85523)	46/57
<i>Mcnb_K</i>	310	acyltransferase/decarboxylase	LnmK (AAN85524)	55/67
<i>Mcnb_L</i>	80	acyl carrier protein	LnmL (AAN85525)	62/75
<i>Mcnb_M</i>	411	HMG-CoA synthase	LnmM (AAN85526)	61/75
<i>Mcnb_N</i>	397	putative alpha/beta hydrolase	LnmD (AAN85517)	27/36
<i>Mcnb_O</i>	418	hypothetical protein	(WP_067304298)	41/59
<i>Mcnb_P</i>	266	ABC transporter	(WP_069169226)	38/59
<i>Mcnb_Q</i>	328	ABC transporter component, ATP hydrolase	LnmR (AAN85531)	33/45
<i>Mcnb_R</i>	412	cytochrome P450 oxygenase	LnmA (AAN85514)	42/58
<i>Mcnb_S</i>	453	putative class-III aminotransferase	(AJE87366)	33/49
<i>Mcnb_T</i>	245	thioesterase type II	LnmN (AAN85527)	56/63
<i>Mcnb_U</i>	2161	AT-less type I PKS	Lnml (AAN85522)	48/58
<i>Mcnb_V</i>	752	AT-less acyltransferase/oxidoreductase	LnmG (AAN85520)	60/74
<i>Mcnb_W</i>	313	unknown	LnmH (AAN85521)	44/59
<i>Mcnb_X</i>	629	NRPS (A-PCP)	SyrB1 (AKF46132)	43/58
<i>Mcnb_Y</i>	321	halogenase	SyrB2 (AKF46131)	66/79
<i>Mcnb_Z1</i>	76	acyl carrier protein	LnmL (AAN85525)	37/63
<i>Mcnb_Z2</i>	412	beta-ketoacyl-ACP synthase	SiaA (AFS33443)	42/56
<i>Mcnb_Z3</i>	394	FAD-dependent oxidoreductase	(WP_010982689)	59/70
<i>Mcnb_Z4</i>	518	ABC transporter component, periplasmic oligopeptide binding protein	LnmU (AAN85534)	53/65
<i>Mcnb_Z5</i>	318	ABC transporter component, membrane spanning protein	LnmT (AAN85533)	60/73
<i>Mcnb_Z6</i>	263	ABC transporter component, membrane spanning protein	LnmS (AAN85532)	60/71
<i>Mcnb_Z7</i>	518	ABC transporter component, ATP hydrolase	LnmR (AAN85531)	57/69
<i>Mcnb_Z8</i>	136	unknown	LnmZ' (AAN85540)	34/55
<i>Mcnb_Z9</i>	121	glyoxalase/bleomycin resistance protein	(WP_062700437)	37/53
<i>Mcnb_Z10</i>	245	methyltransferase	(WP_026218883)	44/61
<i>Mcnb_Z11</i>	644	Radical SAM superfamily protein	(SED67026)	52/66
<i>Mcnb_orf(+1)</i>	1028	transcriptional regulator	(WP_073892172)	60/68

^a*orf(-1)* and *orf(+1)* are predicted to represent the upstream and downstream boundaries of the *Inm*-type gene cluster.

^bNumber of amino acids. ^cAlso see Fig. 2 for the genetic organization of the *Inm*-type gene cluster.

Table S17. Predicted functions of ORFs in the *Inm*-type gene cluster from *Micromonospora marina* DSM 45555 (Clade XV)

gene ^a	aa ^b	putative function ^c	protein homologue	% identity/ % similarity
<i>Mmar_orf(-1)</i>	214	peptidase 23	(SCL52691)	82/88
<i>Mmar_A</i>	494	4-coumarate:CoA ligase	LnmW (AAN85536)	41/57
<i>Mmar_B</i>	413	HMG-CoA-synthase	LnmM (AAN85526)	49/63
<i>Mmar_C</i>	161	hypothetical protein	(WP_053707566)	41/55
<i>Mmar_D</i>	426	sodium:proton exchanger	(WP_020553490)	33/51
<i>Mmar_E</i>	253	Crp/Fnr family transcriptional regulator	LnmO (AAN85528)	46/59
<i>Mmar_F</i>	744	acyltransferase/oxidoreductase	LnmG (AAN85520)	38/51
<i>Mmar_G</i>	252	enoyl-CoA hydratase	LnmF (AAN85519)	52/63
<i>Mmar_H</i>	292	unknown	LnmE (AAN85518)	43/60
<i>Mmar_I</i>	1954	hybrid NRPS/type I PKS	LnmI (AAN85522)	49/57
<i>Mmar_J</i>	6700	AT-less type I PKS	LnmJ (AAN85523)	46/57
<i>Mmar_K</i>	313	acyltransferase/decarboxylase	LnmK (AAN85524)	54/67
<i>Mmar_L</i>	82	acyl carrier protein	LnmL (AAN85525)	62/75
<i>Mmar_M</i>	411	HMG-CoA synthase	LnmM (AAN85526)	61/75
<i>Mmar_N</i>	397	putative alpha/beta hydrolase	LnmD (AAN85517)	27/36
<i>Mmar_O</i>	418	hypothetical protein	(WP_067304298)	41/59
<i>Mmar_P</i>	266	ABC transporter	(WP_069169226)	38/59
<i>Mmar_Q</i>	328	ABC transporter component, ATP hydrolase	LnmR (AAN85531)	33/46
<i>Mmar_R</i>	412	cytochrome P450 oxygenase	LnmA (AAN85514)	42/58
<i>Mmar_S</i>	453	putative class-III aminotransferase	(AJE87366)	33/49
<i>Mmar_T</i>	245	thioesterase type II	LnmN (AAN85527)	55/63
<i>Mmar_U</i>	2165	AT-less type I PKS	LnmI (AAN85522)	48/58
<i>Mmar_V</i>	749	AT-less acyltransferase/oxidoreductase	LnmG (AAN85520)	59/74
<i>Mmar_W</i>	313	unknown	LnmH (AAN85521)	44/59
<i>Mmar_X</i>	635	NRPS (A-PCP)	SyrB1 (AKF46132)	42/58
<i>Mmar_Y</i>	321	halogenase	SyrB2 (AKF46131)	66/79
<i>Mmar_Z1</i>	76	acyl carrier protein	LnmL (AAN85525)	37/63
<i>Mmar_Z2</i>	412	beta-ketoacyl-ACP synthase	SiaA (AFS33443)	41/56
<i>Mmar_Z3</i>	394	FAD-dependent oxidoreductase	(WP_010982689)	59/70
<i>Mmar_Z4</i>	519	ABC transporter component, periplasmic oligopeptide binding protein	LnmU (AAN85534)	53/66
<i>Mmar_Z5</i>	318	ABC transporter component, membrane spanning protein	LnmT (AAN85533)	60/73
<i>Mmar_Z6</i>	263	ABC transporter component, membrane spanning protein	LnmS (AAN85532)	60/71
<i>Mmar_Z7</i>	518	ABC transporter component, ATP hydrolase	LnmR (AAN85531)	57/69
<i>Mmar_Z8</i>	136	unknown	LnmZ' (AAN85540)	34/55
<i>Mmar_Z9</i>	121	glyoxalase/bleomycin resistance protein	(WP_062700437)	37/53
<i>Mmar_Z10</i>	253	methyltransferase	(WP_026218883)	44/61
<i>Mmar_Z11</i>	644	Radical SAM superfamily protein	(SED67026)	52/66
<i>Mmar_orf(+1)</i>	1028	transcriptional regulator	(WP_073892172)	60/68

^a*orf(-1)* and *orf(+1)* are predicted to represent the upstream and downstream boundaries of the *Inm*-type gene cluster.

^bNumber of amino acids. ^cAlso see Fig. 2 for the genetic organization of the *Inm*-type gene cluster.

Table S18. Predicted functions of ORFs in the *Inm*-type gene cluster from *Micromonospora* sp. L5 (Clade XV)

gene ^a	aa ^b	putative function ^c	protein homologue	% identity/ % similarity
<i>MI5_orf(-1)</i>	213	peptidase 23	(SCL52691)	83/90
<i>MI5_A</i>	494	4-coumarate:CoA ligase	LnmW (AAN85536)	42/57
<i>MI5_B</i>	413	HMG-CoA-synthase	LnmM (AAN85526)	49/63
<i>MI5_C</i>	179	hypothetical protein	(WP_053707566)	41/58
<i>MI5_D</i>	426	sodium:proton exchanger	(WP_020553490)	33/50
<i>MI5_E</i>	253	Crp/Fnr family transcriptional regulator	LnmO (AAN85528)	46/59
<i>MI5_F</i>	717	acyltransferase/oxidoreductase	LnmG (AAN85520)	38/50
<i>MI5_G</i>	252	enoyl-CoA hydratase	LnmF (AAN85519)	52/63
<i>MI5_H</i>	292	unknown	LnmE (AAN85518)	43/60
<i>MI5_I</i>	2006	hybrid NRPS/type I PKS	LnmI (AAN85522)	65/74
<i>MI5_J</i>	6765	AT-less type I PKS	LnmJ (AAN85523)	45/57
<i>MI5_K</i>	311	acyltransferase/decarboxylase	LnmK (AAN85524)	54/66
<i>MI5_L</i>	82	acyl carrier protein	LnmL (AAN85525)	59/71
<i>MI5_M</i>	411	HMG-CoA synthase	LnmM (AAN85526)	61/75
<i>MI5_N</i>	397	putative alpha/beta hydrolase	LnmD (AAN85517)	27/37
<i>MI5_O</i>	418	hypothetical protein	(WP_067304298)	43/61
<i>MI5_P</i>	266	ABC transporter	(WP_069169226)	38/59
<i>MI5_Q</i>	327	ABC transporter component, ATP hydrolase	LnmR (AAN85531)	33/45
<i>MI5_R</i>	412	cytochrome P450 oxygenase	LnmA (AAN85514)	41/58
<i>MI5_S</i>	453	putative class-III aminotransferase	(AJE87366)	32/48
<i>MI5_T</i>	246	thioesterase type II	LnmN (AAN85527)	55/63
<i>MI5_U</i>	2174	AT-less type I PKS	LnmI (AAN85522)	48/58
<i>MI5_V</i>	767	AT-less acyltransferase/oxidoreductase	LnmG (AAN85520)	59/73
<i>MI5_W</i>	313	unknown	LnmH (AAN85521)	44/58
<i>MI5_X</i>	621	NRPS (A-PCP)	SyrB1 (AKF46132)	43/59
<i>MI5_Y</i>	321	halogenase	SyrB2 (AKF46131)	66/79
<i>MI5_Z1</i>	76	acyl carrier protein	LnmL (AAN85525)	37/63
<i>MI5_Z2</i>	412	beta-ketoacyl-ACP synthase	SiaA (AFS33443)	42/56
<i>MI5_Z3</i>	394	FAD-dependent oxidoreductase	(WP_010982689)	58/70
<i>MI5_Z4</i>	519	ABC transporter component, periplasmic oligopeptide binding protein	LnmU (AAN85534)	53/65
<i>MI5_Z5</i>	318	ABC transporter component, membrane spanning protein	LnmT (AAN85533)	59/72
<i>MI5_Z6</i>	263	ABC transporter component, membrane spanning protein	LnmS (AAN85532)	60/71
<i>MI5_Z7</i>	518	ABC transporter component, ATP hydrolase	LnmR (AAN85531)	57/69
<i>MI5_Z8</i>	136	unknown	LnmZ' (AAN85540)	34/55
<i>MI5_Z9</i>	121	glyoxalase/bleomycin resistance protein	(WP_062700437)	37/53
<i>MI5_Z10</i>	245	methyltransferase	(WP_026218883)	44/61
<i>MI5_Z11</i>	644	Radical SAM superfamily protein	(SED67026)	52/66
<i>MI5_orf(+1)</i>	1030	transcriptional regulator	(WP_073892172)	60/68

^a*orf(-1)* and *orf(+1)* are predicted to represent the upstream and downstream boundaries of the *Inm*-type gene cluster.

^bNumber of amino acids. ^cAlso see Fig. 2 for the genetic organization of the *Inm*-type gene cluster.

Table S19. Predicted functions of ORFs in the *Inm*-type gene cluster from *Micromonospora globosa* NRRL B-2673 (Clade XV)

gene ^a	aa ^b	putative function ^c	protein homologue	% identity/ % similarity
<i>Mglo_orf(-1)</i>	213	peptidase 23	(SCL52691)	83/90
<i>Mglo_A</i>	494	4-coumarate:CoA ligase	LnmW (AAN85536)	42/57
<i>Mglo_B</i>	413	HMG-CoA-synthase	LnmM (AAN85526)	49/63
<i>Mglo_C</i>	179	hypothetical protein	(WP_053707566)	41/58
<i>Mglo_D</i>	426	sodium:proton exchanger	(WP_020553490)	33/50
<i>Mglo_E</i>	253	Crp/Fnr family transcriptional regulator	LnmO (AAN85528)	46/59
<i>Mglo_F</i>	735	acyltransferase/oxidoreductase	LnmG (AAN85520)	38/50
<i>Mglo_G</i>	252	enoyl-CoA hydratase	LnmF (AAN85519)	52/63
<i>Mglo_H</i>	292	unknown	LnmE (AAN85518)	43/60
<i>Mglo_I</i>	1986	hybrid NRPS/type I PKS	LnmI (AAN85522)	65/73
<i>Mglo_J</i>	6771	AT-less type I PKS	LnmJ (AAN85523)	46/55
<i>Mglo_K</i>	308	acyltransferase/decarboxylase	LnmK (AAN85524)	55/67
<i>Mglo_L</i>	82	acyl carrier protein	LnmL (AAN85525)	59/71
<i>Mglo_M</i>	411	HMG-CoA synthase	LnmM (AAN85526)	61/75
<i>Mglo_N</i>	397	putative alpha/beta hydrolase	LnmD (AAN85517)	27/36
<i>Mglo_O</i>	418	hypothetical protein	(WP_067304298)	43/61
<i>Mglo_P</i>	266	ABC transporter	(WP_069169226)	38/59
<i>Mglo_Q</i>	328	ABC transporter component, ATP hydrolase	LnmR (AAN85531)	33/45
<i>Mglo_R</i>	412	cytochrome P450 oxygenase	LnmA (AAN85514)	41/59
<i>Mglo_S</i>	453	putative class-III aminotransferase	(AJE87366)	32/48
<i>Mglo_T</i>	246	thioesterase type II	LnmN (AAN85527)	55/63
<i>Mglo_U</i>	2186	AT-less type I PKS	LnmI (AAN85522)	48/59
<i>Mglo_V</i>	767	AT-less acyltransferase/oxidoreductase	LnmG (AAN85520)	59/73
<i>Mglo_W</i>	313	unknown	LnmH (AAN85521)	44/58
<i>Mglo_X</i>	614	NRPS (A-PCP)	SyrB1 (AKF46132)	43/60
<i>Mglo_Y</i>	321	halogenase	SyrB2 (AKF46131)	66/79
<i>Mglo_Z1</i>	76	acyl carrier protein	LnmL (AAN85525)	37/63
<i>Mglo_Z2</i>	412	beta-ketoacyl-ACP synthase	SiaA (AFS33443)	42/56
<i>Mglo_Z3</i>	394	FAD-dependent oxidoreductase	(WP_010982689)	58/70
<i>Mglo_Z4</i>	519	ABC transporter component, periplasmic oligopeptide binding protein	LnmU (AAN85534)	53/65
<i>Mglo_Z5</i>	318	ABC transporter component, membrane spanning protein	LnmT (AAN85533)	59/72
<i>Mglo_Z6</i>	263	ABC transporter component, membrane spanning protein	LnmS (AAN85532)	60/71
<i>Mglo_Z7</i>	518	ABC transporter component, ATP hydrolase	LnmR (AAN85531)	57/69
<i>Mglo_Z8</i>	136	unknown	LnmZ' (AAN85540)	34/55
<i>Mglo_Z9</i>	121	glyoxalase/bleomycin resistance protein	(WP_062700437)	37/53
<i>Mglo_Z10</i>	245	methyltransferase	(WP_026218883)	44/61
<i>Mglo_Z11</i>	644	Radical SAM superfamily protein	(SED67026)	52/66
<i>Mglo_orf(+1)</i>	1030	transcriptional regulator	(WP_073892172)	60/68

^a*orf(-1)* and *orf(+1)* are predicted to represent the upstream and downstream boundaries of the *Inm*-type gene cluster.

^bNumber of amino acids. ^cAlso see Fig. 2 for the genetic organization of the *Inm*-type gene cluster.

Table S20. Predicted functions of ORFs in the *Inm*-type gene cluster from *Micromonospora aurantiaca* ATCC 27029 (Clade XV)

gene ^a	aa ^b	putative function ^c	protein homologue	% identity/ % similarity
<i>Maur_orf(-1)</i>	213	peptidase 23	(SCL52691)	83/89
<i>Maur_A</i>	494	4-coumarate:CoA ligase	LnmW (AAN85536)	42/57
<i>Maur_B</i>	413	HMG-CoA-synthase	LnmM (AAN85526)	49/63
<i>Maur_C</i>	179	hypothetical protein	(WP_053707566)	41/58
<i>Maur_D</i>	426	sodium:proton exchanger	(WP_020553490)	33/50
<i>Maur_E</i>	253	Crp/Fnr family transcriptional regulator	LnmO (AAN85528)	46/59
<i>Maur_F</i>	735	acyltransferase/oxidoreductase	LnmG (AAN85520)	38/50
<i>Maur_G</i>	252	enoyl-CoA hydratase	LnmF (AAN85519)	52/63
<i>Maur_H</i>	292	unknown	LnmE (AAN85518)	43/60
<i>Maur_I</i>	2005	hybrid NRPS/type I PKS	Lnml (AAN85522)	65/73
<i>Maur_J</i>	6727	AT-less type I PKS	LnmJ (AAN85523)	46/56
<i>Maur_K</i>	311	acyltransferase/decarboxylase	LnmK (AAN85524)	55/67
<i>Maur_L</i>	82	acyl carrier protein	LnmL (AAN85525)	59/71
<i>Maur_M</i>	411	HMG-CoA synthase	LnmM (AAN85526)	61/75
<i>Maur_N</i>	397	putative alpha/beta hydrolase	LnmD (AAN85517)	27/36
<i>Maur_O</i>	418	hypothetical protein	(WP_067304298)	43/60
<i>Maur_P</i>	266	ABC transporter	(WP_069169226)	38/59
<i>Maur_Q</i>	328	ABC transporter component, ATP hydrolase	LnmR (AAN85531)	33/45
<i>Maur_R</i>	412	cytochrome P450 oxygenase	LnmA (AAN85514)	41/59
<i>Maur_S</i>	453	putative class-III aminotransferase	(AJE87366)	32/48
<i>Maur_T</i>	246	thioesterase type II	LnmN (AAN85527)	55/63
<i>Maur_U</i>	2174	AT-less type I PKS	Lnml (AAN85522)	48/58
<i>Maur_V</i>	767	AT-less acyltransferase/oxidoreductase	LnmG (AAN85520)	59/73
<i>Maur_W</i>	313	unknown	LnmH (AAN85521)	44/58
<i>Maur_X</i>	621	NRPS (A-PCP)	SyrB1 (AKF46132)	43/59
<i>Maur_Y</i>	321	halogenase	SyrB2 (AKF46131)	67/80
<i>Maur_Z1</i>	76	acyl carrier protein	LnmL (AAN85525)	37/63
<i>Maur_Z2</i>	412	beta-ketoacyl-ACP synthase	SiaA (AFS33443)	42/56
<i>Maur_Z3</i>	394	FAD-dependent oxidoreductase	(WP_010982689)	58/70
<i>Maur_Z4</i>	519	ABC transporter component, periplasmic oligopeptide binding protein	LnmU (AAN85534)	53/65
<i>Maur_Z5</i>	318	ABC transporter component, membrane spanning protein	LnmT (AAN85533)	59/72
<i>Maur_Z6</i>	263	ABC transporter component, membrane spanning protein	LnmS (AAN85532)	60/71
<i>Maur_Z7</i>	518	ABC transporter component, ATP hydrolase	LnmR (AAN85531)	57/69
<i>Maur_Z8</i>	136	unknown	LnmZ' (AAN85540)	34/55
<i>Maur_Z9</i>	121	glyoxalase/bleomycin resistance protein	(WP_062700437)	37/53
<i>Maur_Z10</i>	245	methyltransferase	(WP_026218883)	44/61
<i>Maur_Z11</i>	644	Radical SAM superfamily protein	(SED67026)	52/66
<i>Maur_orf(+1)</i>	1030	transcriptional regulator	(WP_073892172)	60/68

^a*orf(-1)* and *orf(+1)* are predicted to represent the upstream and downstream boundaries of the *Inm*-type gene cluster.

^bNumber of amino acids. ^cAlso see Fig. 2 for the genetic organization of the *Inm*-type gene cluster.

Table S21. Predicted functions of ORFs in the *Inm*-type gene cluster from *Salinispora arenicola* CNH964 (Clade XVII)

gene ^a	aa ^b	putative function ^c	protein homologue	% identity/ % similarity
<i>Sal964_orf(-1)</i>	101	hypothetical protein	(WP_040795638)	66/79
<i>Sal964_A</i>	513	4-coumarate:CoA ligase	LnmW (AAN85536)	43/59
<i>Sal964_B</i>	278	hypothetical protein	(AGP55856)	38/52
<i>Sal964_C</i>	468	serine hydroxymethyltransferase	AmiS (AEF16058)	61/73
<i>Sal964_D</i>	802	NRPS (A-PCP)	SyrB1 (AKF46132)	35/52
<i>Sal964_E</i>	236	N-acetylglucosaminyl deacetylase	LnmX (AAN85537)	52/67
<i>Sal964_F</i>	504	4-coumarate:CoA ligase	LnmW (AAN85536)	38/52
<i>Sal964_G</i>	431	hypothetical protein	(WP_067304298)	46/64
<i>Sal964_H</i>	308	unknown	LnmH (AAN85521)	44/59
<i>Sal964_I</i>	405	FAD-dependent oxidoreductase	(WP_010982689)	61/70
<i>Sal964_J</i>	120	glyoxalase/bleomycin resistance protein	(WP_062700437)	44/60
<i>Sal964_K</i>	133	unknown	LnmZ' (AAN85540)	39/56
<i>Sal964_L</i>	291	phosphopantetheinyl transferase	(WP_059300333)	41/50
<i>Sal964_M</i>	287	unknown	LnmE (AAN85518)	37/52
<i>Sal964_N</i>	410	HMG-CoA-synthase	LnmM (AAN85526)	48/64
<i>Sal964_O</i>	262	enoyl-CoA hydratase	LnmF (AAN85519)	51/64
<i>Sal964_P</i>	783	AT-less acyltransferase/oxidoreductase	LnmG (AAN85520)	63/75
<i>Sal964_Q</i>	4311	hybrid NRPS/AT-less PKS	LnmI (AAN85522)	49/59
<i>Sal964_R</i>	336	taurine dioxygenase-like protein	(WP_060732555)	55/65
<i>Sal964_S</i>	311	kinase	(WP_040836916)	66/77
<i>Sal964_T</i>	1086	NRPS (A-PCP)	SyrB1 (AKF46132)	31/45
<i>Sal964_U</i>	81	peptidyl carrier protein	SyrB1 (AKF46132)	30/56
<i>Sal964_V</i>	317	halogenase	SyrB2 (AKF46131)	60/74
<i>Sal964_W</i>	381	putative alpha/beta hydrolase	LnmD (AAN85517)	26/37
<i>Sal964_X</i>	7105	AT-less type I PKS	LnmJ (AAN85523)	47/59
<i>Sal964_Y</i>	320	acyltransferase/decarboxylase	LnmK (AAN85524)	56/67
<i>Sal964_Z1</i>	90	acyl carrier protein	LnmL (AAN85525)	59/69
<i>Sal964_Z2</i>	407	HMG-CoA-synthase	LnmM (AAN85526)	64/76
<i>Sal964_Z3</i>	86	acyl carrier protein	Fr9M (ADH01494)	32/61
<i>Sal964_Z4</i>	433	beta-ketoacyl-ACP synthase	SiaA (AFS33443)	41/55
<i>Sal964_Z5</i>	270	thioesterase type II	LnmN (AAN85527)	56/69
<i>Sal964_Z6</i>	511	ABC transporter component, periplasmic oligopeptide binding protein	LnmU (AAN85534)	58/74
<i>Sal964_Z7</i>	318	ABC transporter component, membrane spanning protein	LnmT (AAN85533)	55/72
<i>Sal964_Z8</i>	263	ABC transporter component, membrane spanning protein	LnmS (AAN85532)	62/72
<i>Sal964_Z9</i>	547	ABC transporter component, ATP hydrolase	LnmR (AAN85531)	57/69
<i>Sal964_Z10</i>	297	unknown	LnmE (AAN85518)	44/59
<i>Sal964_Z11</i>	499	4-coumarate:CoA ligase	LnmW (AAN85536)	41/54
<i>Sal964_Z12</i>	407	diaminobutyric acid synthase C	DabC (AEG64688)	53/64
<i>Sal964_Z13</i>	485	diaminobutyric acid synthase B	DabB (AEG64687)	56/67
<i>Sal964_Z14</i>	354	diaminobutyric acid synthase A	DabA (AEG64686)	62/75

Sal964_orf(+1)

349

LuxR family transcriptional regulator

(WP_063766468)

37/56

^a*orf(-1)* and *orf(+1)* are predicted to represent the upstream and downstream boundaries of the *Inm*-type gene cluster.

^bNumber of amino acids. ^cAlso see **Fig. 2** for the genetic organization of the *Inm*-type gene cluster.

Table S22. Predicted functions of ORFs in the *Inm*-type gene cluster from *Burkholderia ubonensis* RF25-BP1 (Clade XVIII)

gene ^a	aa ^b	putative function ^c	protein homologue	% identity/ % similarity
<i>Bubo_orf(-1)</i>	503	outer membrane efflux protein	OprM (WP_057405643)	49/64
<i>Bubo_A</i>	330	unknown	LnmH (AAN85521)	43/60
<i>Bubo_B</i>	396	FAD-dependent oxidoreductase	(WP_010982689)	54/69
<i>Bubo_C</i>	510	4-coumarate:CoA ligase	LnmW (AAN85536)	34/51
<i>Bubo_D</i>	130	unknown	LnmZ' (AAN85540)	36/53
<i>Bubo_E</i>	298	unknown	LnmE (AAN85518)	36/55
<i>Bubo_F</i>	176	hypothetical protein	(WP_053707566)	39/52
<i>Bubo_G</i>	129	transposase	WQE_51432 (EIM93082)	56/77
<i>Bubo_H</i>	134	hypothetical protein	(WP_060317165)	95/96
<i>Bubo_I</i>	267	4'-phosphopantetheinyl transferase	Sfp (P39135)	25/40
<i>Bubo_J</i>	410	HMG-CoA synthase	LnmM (AAN85526)	45/65
<i>Bubo_K</i>	268	enoyl-CoA hydratase	LnmF (AAN85519)	44/57
<i>Bubo_L</i>	295	acyltransferase/oxidoreductase	LnmG (AAN85520)	50/63
<i>Bubo_M</i>	769	AT-less acyltransferase/oxidoreductase	LnmG (AAN85520)	53/66
<i>Bubo_N</i>	609	adenylation protein-peptidyl carrier protein	SyrB1 (AKF46132)	41/57
<i>Bubo_O</i>	313	halogenase	SyrB2 (AKF46131)	66/79
<i>Bubo_P</i>	365	alpha/beta hydrolase	ADZ36_03165 (KNE83935)	36/48
<i>Bubo_Q</i>	4169	AT-less type I PKS	LnmI (AAN85522)	39/49
<i>Bubo_R</i>	6941	AT-less type I PKS	LnmJ (AAN85523)	42/54
<i>Bubo_S</i>	318	acyltransferase/decarboxylase	LnmK (AAN85524)	44/58
<i>Bubo_T</i>	89	acyl carrier protein	LnmL (AAN85525)	49/67
<i>Bubo_U</i>	409	HMG-CoA synthase	LnmM (AAN85526)	58/72
<i>Bubo_V</i>	88	acyl carrier protein	LnmL (AAN85525)	29/57
<i>Bubo_W</i>	419	beta-ketoacyl-ACP synthase	SiaA (AFS33443)	38/52
<i>Bubo_X</i>	419	type II thioesterase	LnmN (AAN85527)	50/65
<i>Bubo_orf(+1)</i>	712	methylmalonyl-CoA mutase	(WP_060136708)	97/98

^a*orf(-1)* and *orf(+1)* are predicted to represent the upstream and downstream boundaries of the *Inm*-type gene cluster.

^bNumber of amino acids. ^cAlso see Fig. 2 for the genetic organization of the *Inm*-type gene cluster.

Table S23. Predicted functions of ORFs in the *lnm*-type gene cluster from *Streptomyces* sp. CB01635 (Clade I) in comparison with the known LNM producer *S. atroolivaceus* S-140

gene ^a	aa ^b	putative function ^c	protein homologue (accession #)	% identity/ % similarity
CB01635_orf(-1)	462	NRPS	Orf(-1) (AAN85513)	96/99
CB01635_A	399	cytochrome P450 oxygenase	LnmA (AAN85514)	99/99
CB01635_B	78	ferredoxin	LnmB (AAN85515)	99/100
CB01635_C	115	unknown	LnmC (AAN85516)	100/100
CB01635_D	438	putative alpha/beta hydrolase	LnmD (AAN85517)	97/98
CB01635_E	305	unknown	LnmE (AAN85518)	99/99
CB01635_F	265	enoyl-CoA hydratase	LnmF (AAN85519)	99/99
CB01635_G	795	AT-less acyltransferase/oxidoreductase	LnmG (AAN85520)	99/99
CB01635_H	274	unknown	LnmH (AAN85521)	100/100
CB01635_I	4447	hybrid NRPS/AT-less PKS	LnmI (AAN85522)	98/98
CB01635_J	7351	AT-less PKS	LnmJ (AAN85523)	97/97
CB01635_K	319	acyltransferase/decarboxylase	LnmK (AAN85524)	99/99
CB01635_L	86	acyl carrier protein	LnmL (AAN85525)	99/100
CB01635_M	416	HMG-CoA-synthase	LnmM (AAN85526)	99/99
CB01635_N	267	type II thioesterase	LnmN (AAN85527)	99/99
CB01635_O	227	Crp/Fnr family transcriptional regulator	LnmO (AAN85528)	100/100
CB01635_P	82	peptidyl carrier protein	LnmP (AAN85529)	99/99
CB01635_Q	516	discrete adenylation protein	LnmQ (AAN85530)	99/99
CB01635_R	575	ABC transporter component, ATP hydrolase	LnmR (AAN85531)	98/98
CB01635_S	291	ABC transporter component, membrane spanning protein	LnmS (AAN85532)	98/98
CB01635_T	321	ABC transporter component, membrane spanning protein	LnmT (AAN85533)	99/99
CB01635_U	513	ABC transporter component, periplasmic oligopeptide binding protein	LnmU (AAN85534)	99/99
CB01635_V	120	unknown, NTF2 family protein	LnmV (AAN85535)	98/100
CB01635_W	516	4-coumarate:CoA ligase	LnmW (AAN85536)	99/99
CB01635_X	243	N-acetylglucosaminyl deacetylase	LnmX (AAN85537)	99/100
CB01635_Y	474	antibiotic efflux protein	LnmY (AAN85538)	99/99
CB01635_Z1	400	cytochrome P450 oxygenase	LnmZ (AAN85539)	99/100
CB01635_Z2	134	unknown	LnmZ' (AAN85540)	99/99
CB01635_orf(+1)	216	unknown	Orf(+1) (AAN85541)	97/97

^aorf(-1) and orf(+1) are predicted to represent the upstream and downstream boundaries of the *lnm*-type gene cluster.

^bNumber of amino acids. ^cAlso see Fig. 2 for the genetic organization of the *lnm*-type gene cluster.

Table S24. Predicted functions of ORFs in the *Inm*-type gene cluster from *Streptomyces* sp. CB02959 (Clade II)

gene ^a	aa ^b	putative function ^c	protein homologue (accession #)	% identity/ % similarity
<i>CB02959_orf(-1)</i>	174	hypothetical protein	(WP_018488465)	84/89
<i>CB02959_A</i>	402	cytochrome P450 oxygenase	LnmA (AAN85514)	49/64
<i>CB02959_B</i>	247	N-acetylglucosaminyl deacetylase	LnmX (AAN85537)	54/66
<i>CB02959_C</i>	446	putative alpha/beta hydrolase	LnmD (AAN85517)	62/68
<i>CB02959_D</i>	321	unknown	LnmE (AAN85518)	74/81
<i>CB02959_E</i>	271	enoyl-CoA hydratase	LnmF (AAN85519)	82/88
<i>CB02959_F</i>	762	acyltransferase/oxidoreductase	LnmG (AAN85520)	69/76
<i>CB02959_G</i>	280	unknown	LnmH (AAN85521)	83/89
<i>CB02959_H</i>	4391	AT-less type I PKS	LnmI (AAN85522)	68/74
<i>CB02959_I</i>	7490	AT-less type I PKS	LnmJ (AAN85523)	68/75
<i>CB02959_J</i>	328	acyltransferase/decarboxylase	LnmK (AAN85524)	74/83
<i>CB02959_K</i>	86	acyl carrier protein	LnmL (AAN85525)	76/81
<i>CB02959_L</i>	419	HMG-CoA-synthase	LnmM (AAN85526)	83/88
<i>CB02959_M</i>	264	thioesterase type II	LnmN (AAN85527)	70/79
<i>CB02959_N</i>	228	Crp/Fnr family transcriptional regulator	LnmO (AAN85528)	76/85
<i>CB02959_O</i>	377	glucosyltransferase	Cpz31 (ACQ63639)	45/59
<i>CB02959_P</i>	87	peptidyl carrier protein	LnmP (AAN85529)	61/68
<i>CB02959_Q</i>	517	discrete adenylation protein	LnmQ (AAN85530)	76/81
<i>CB02959_R</i>	586	ABC transporter component, ATP hydrolase	LnmR (AAN85531)	69/76
<i>CB02959_S</i>	289	ABC transporter component, membrane spanning protein	LnmS (AAN85532)	85/90
<i>CB02959_T</i>	331	ABC transporter component, membrane spanning protein	LnmT (AAN85533)	81/87
<i>CB02959_U</i>	514	ABC transporter component, periplasmic oligopeptide binding protein	LnmU (AAN85534)	75/84
<i>CB02959_V</i>	305	glucose-1-phosphate thymidylyltransferase	MydA (BAC57039)	75/82
<i>CB02959_W</i>	323	mycothiol conjugate amidase McA	(WP_003974009)	56/70
<i>CB02959_X</i>	634	methoxymalonyl-ACP biosynthesis protein FkbH	ChID1 (AAZ77703)	56/63
<i>CB02959_Y</i>	524	oxygenase	OxyS (AAZ78342)	43/52
<i>CB02959_orf(+1)</i>	209	type III effector protein	SVEN_3170 (CCA56456)	85/89

^a*orf(-1)* and *orf(+1)* are predicted to represent the upstream and downstream boundaries of the *Inm*-type gene cluster.

^bNumber of amino acids. ^cAlso see Fig. 2 for the genetic organization of the *Inm*-type gene cluster.

Table S25. Predicted functions of ORFs in the *Inm*-type gene cluster from *Streptomyces* sp. CB02891 (Clade III)

gene ^a	aa ^b	putative function ^c	protein homologue	% identity/ % similarity
<i>CB02891_orf(-1)</i>	220	peptidase S51	ABB07_38760 (AKJ15883)	70/81
<i>CB02891_A</i>	304	unknown	LnmE (AAN85518)	65/74
<i>CB02891_B</i>	514	ABC transporter component, periplasmic oligopeptide binding protein	LnmU (AAN85534)	66/75
<i>CB02891_C</i>	324	ABC transporter component, membrane spanning protein	LnmT (AAN85533)	67/77
<i>CB02891_D</i>	272	ABC transporter component, membrane spanning protein	LnmS (AAN85532)	72/85
<i>CB02891_E</i>	543	ABC transporter component, ATP hydrolase	LnmR (AAN85531)	65/73
<i>CB02891_F</i>	528	discrete adenylation protein	LnmQ (AAN85530)	63/71
<i>CB02891_G</i>	91	peptidyl carrier protein	LnmP (AAN85529)	55/70
<i>CB02891_H</i>	228	Crp/Fnr family transcriptional regulator	LnmO (AAN85528)	60/73
<i>CB02891_I</i>	76	ferredoxin	LnmB (AAN85515)	71/80
<i>CB02891_J</i>	399	cytochrome P450 oxygenase	LnmA (AAN85514)	82/90
<i>CB02891_K</i>	449	putative alpha/beta hydrolase	LnmD (AAN85517)	53/63
<i>CB02891_L</i>	277	enoyl-CoA hydratase	LnmF (AAN85519)	61/73
<i>CB02891_M</i>	757	acyltransferase/oxidoreductase	LnmG (AAN85520)	67/77
<i>CB02891_N</i>	290	unknown	LnmH (AAN85521)	73/83
<i>CB02891_O</i>	4535	AT-less type I PKS	LnmI (AAN85522)	62/70
<i>CB02891_P</i>	7244	AT-less type I PKS	LnmJ (AAN85523)	61/69
<i>CB02891_Q</i>	328	acyltransferase/decarboxylase	LnmK (AAN85524)	67/77
<i>CB02891_R</i>	87	acyl carrier protein	LnmL (AAN85525)	65/78
<i>CB02891_S</i>	418	HMG-CoA synthase	LnmM (AAN85526)	77/85
<i>CB02891_T</i>	251	thioesterase type II	LnmN (AAN85527)	62/71
<i>CB02891_U</i>	266	4'-phosphopantetheinyl transferase	Sfp (P39135)	25/43
<i>CB02891_V</i>	136	unknown	LnmZ' (AAN85540)	82/85
<i>CB02891_W</i>	400	cytochrome P450 oxygenase	LnmZ (AAN85539)	75/86
<i>CB02891_X</i>	130	hypothetical protein	(WP_052398215)	36/53
<i>CB02891_Y</i>	475	antibiotic efflux protein	LnmY (AAN85538)	77/87
<i>CB02891_Z1</i>	242	N-acetylglucosaminyl deacetylase	LnmX (AAN85537)	79/88
<i>CB02891_Z2</i>	512	4-coumarate:CoA ligase	LnmW (AAN85536)	74/80
<i>CB02891_Z3</i>	120	unknown, NTF2 family protein	LnmV (AAN85535)	83/93
<i>CB02891_orf(+1)</i>	191	hypothetical protein	SAZU_6586 (GAP51713)	65/73

^a*orf(-1)* and *orf(+1)* are predicted to represent the upstream and downstream boundaries of the *Inm*-type gene cluster.

^bNumber of amino acids. ^cAlso see Fig. 2 for the genetic organization of the *Inm*-type gene cluster.

Table S26. Predicted functions of ORFs in the *lnm*-type gene cluster from *Streptomyces* sp. TSRI0384-2 (Clade V)

gene ^a	aa ^b	putative function ^c	protein homologue (accession #)	% identity/ % similarity
<i>TSRI0384-2_orf(-1)</i>	229	TetR family transcriptional regulator	(WP_062008487)	77/83
<i>TSRI0384-2_A</i>	572	4-coumarate:CoA ligase	LnmW (AAN85536)	41/56
<i>TSRI0384-2_B</i>	252	methyltransferase	(WP_031183778)	34/45
<i>TSRI0384-2_C</i>	292	unknown	LnmE (AAN85518)	47/61
<i>TSRI0384-2_D</i>	411	HMG-CoA-synthase	LnmM (AAN85526)	47/63
<i>TSRI0384-2_E</i>	268	enoyl-CoA hydratase	LnmF (AAN85519)	49/62
<i>TSRI0384-2_F</i>	764	AT-less acyltransferase/oxidoreductase	LnmG (AAN85520)	65/78
<i>TSRI0384-2_G</i>	303	unknown	LnmH (AAN85521)	43/58
<i>TSRI0384-2_H</i>	623	adenylation protein-peptidyl carrier protein	SyrB1 (AKF46132)	45/58
<i>TSRI0384-2_I</i>	316	halogenase	SyrB2 (AKF46131)	65/76
<i>TSRI0384-2_J</i>	397	alpha/beta hydrolase	ADZ36_03165 (KNE83935)	42/53
<i>TSRI0384-2_K</i>	4202	AT-less type I PKS	LnmI (AAN85522)	48/58
<i>TSRI0384-2_L</i>	6510	AT-less type I PKS	LnmJ (AAN85523)	51/61
<i>TSRI0384-2_M</i>	327	acyltransferase/decarboxylase	LnmK (AAN85524)	50/64
<i>TSRI0384-2_N</i>	86	acyl carrier protein	LnmL (AAN85525)	51/67
<i>TSRI0384-2_O</i>	410	HMG-CoA synthase	LnmM (AAN85526)	64/76
<i>TSRI0384-2_P</i>	82	acyl carrier protein	(WP_062008561)	84/93
<i>TSRI0384-2_Q</i>	425	beta-ketoacyl-ACP synthase	SiaA (AFS33443)	44/57
<i>TSRI0384-2_R</i>	249	type II thioesterase	LnmN (AAN85527)	52/63
<i>TSRI0384-2_S</i>	139	unknown, NTF2 family protein	LnmV (AAN85535)	44/61
<i>TSRI0384-2_T</i>	133	unknown	LnmZ' (AAN85540)	37/54
<i>TSRI0384-2_U</i>	397	cytochrome P450 oxygenase	LnmA (AAN85514)	42/57
<i>TSRI0384-2_V</i>	410	cytochrome P450 oxygenase	LnmA (AAN85514)	49/66
<i>TSRI0384-2_W</i>	125	glyoxalase/bleomycin resistance protein	BN971_01690 (CPR09988)	43/55
<i>TSRI0384-2_X</i>	238	N-acetylglucosaminyl deacetylase	LnmX (AAN85537)	55/65
<i>TSRI0384-2_Y</i>	528	ABC transporter component, periplasmic oligopeptide binding protein	LnmU (AAN85534)	33/47
<i>TSRI0384-2_Z1</i>	328	ABC transporter component, membrane spanning protein	LnmT (AAN85533)	44/60
<i>TSRI0384-2_Z2</i>	811	ABC transporter component, ATP hydrolase	LnmR (AAN85531)	43/55
<i>TSRI0384-2_Z3</i>	201	Crp/Fnr family transcriptional regulator	LnmO (AAN85528)	47/68
<i>TSRI0384-2_orf(+1)</i>	209	dTDP-4-dehydrorhamnose 3,5-epimerase	NivL (AGZ78381)	69/80

^a*orf(-1)* and *orf(+1)* are predicted to represent the upstream and downstream boundaries of the *lnm*-type gene cluster.

^bNumber of amino acids. ^cAlso see Fig. 2 for the genetic organization of the *lnm*-type gene cluster.

Table S27. Predicted functions of ORFs in the *lnm*-type gene cluster from *Streptomyces* sp. CB01373 (Clade VII)

gene ^a	aa ^b	putative function ^c	protein homologue	% identity/ % similarity
<i>CB01373_orf(-1)</i>	140	hypothetical protein	(WP_059300313)	63/72
<i>CB01373_A</i>	486	antibiotic efflux protein	LnmY (AAN85538)	41/58
<i>CB01373_B</i>	205	TetR family transcriptional regulator	(WP_058852673)	42/63
<i>CB01373_C</i>	75	hypothetical protein	(WP_062204104)	45/52
<i>CB01373_D</i>	191	Ydel-like protein	SAVERM_307 (BAC68016)	71/78
<i>CB01373_E</i>	454	cytochrome P450 oxygenase	VR46_04425 (KJY47279)	38/54
<i>CB01373_F</i>	97	hypothetical protein	(WP_028566161)	38/50
<i>CB01373_G</i>	222	Crp/Fnr family transcriptional regulator	LnmO (AAN85528)	43/59
<i>CB01373_H</i>	250	phosphopantetheinyl transferase	(WP_059300333)	87/88
<i>CB01373_I</i>	433	cytochrome P450 oxygenase	LnmA (AAN85514)	35/56
<i>CB01373_J</i>	252	Crp/Fnr family transcriptional regulator	LnmO (AAN85528)	43/62
<i>CB01373_K</i>	437	sodium:proton exchanger	(WP_020553490)	57/73
<i>CB01373_L</i>	299	unknown	LnmE (AAN85518)	45/60
<i>CB01373_M</i>	410	HMG-CoA-synthase	LnmM (AAN85526)	45/61
<i>CB01373_N</i>	264	enoyl-CoA hydratase	LnmF (AAN85519)	53/67
<i>CB01373_O</i>	808	AT-less acyltransferase/oxidoreductase	LnmG (AAN85520)	63/77
<i>CB01373_P</i>	316	unknown	LnmH (AAN85521)	43/59
<i>CB01373_Q</i>	602	NRPS (A-PCP)	SyrB1 (AKF46132)	46/61
<i>CB01373_R</i>	314	halogenase	SyrB2 (AKF46131)	67/80
<i>CB01373_S</i>	391	alpha/beta hydrolase	ADZ36_03165 (KNE83935)	42/54
<i>CB01373_T</i>	4209	AT-less type I PKS	LnmI (AAN85522)	51/61
<i>CB01373_U</i>	7120	AT-less type I PKS	LnmJ (AAN85523)	50/61
<i>CB01373_V</i>	329	acyltransferase/decarboxylase	LnmK (AAN85524)	55/66
<i>CB01373_W</i>	87	acyl carrier protein	LnmL (AAN85525)	63/71
<i>CB01373_X</i>	413	HMG-CoA synthase	LnmM (AAN85526)	62/76
<i>CB01373_Y</i>	80	acyl carrier protein	(WP_062008561)	55/72
<i>CB01373_Z1</i>	423	beta-ketoacyl-ACP synthase	SiaA (AFS33443)	43/56
<i>CB01373_Z2</i>	253	thioesterase type II	LnmN (AAN85527)	54/64
<i>CB01373_Z3</i>	239	N-acetylglucosaminyl deacetylase	LnmX (AAN85537)	54/65
<i>CB01373_Z4</i>	132	unknown	LnmZ' (AAN85540)	38/58
<i>CB01373_Z5</i>	488	4-coumarate:CoA ligase	LnmW (AAN85536)	45/58
<i>CB01373_Z6</i>	226	antibiotic efflux protein	LnmY (AAN85538)	30/43
<i>CB01373_Z7</i>	201	TetR family transcriptional regulator	(WP_058852673)	42/65
<i>CB01373_Z8</i>	395	FAD-dependent oxidoreductase	(WP_010982689)	61/70
<i>CB01373_Z9</i>	121	glyoxalase/bleomycin resistance protein	(WP_062700437)	42/59
<i>CB01373_Z10</i>	491	4-coumarate:CoA ligase	LnmW (AAN85536)	42/56
<i>CB01373_Z11</i>	414	cytochrome P450 oxygenase	LnmA (AAN85514)	38/54
<i>CB01373_orf(+1)</i>	169	hypothetical protein	(WP_053707566)	60/69

^a*orf(-1)* and *orf(+1)* are predicted to represent the upstream and downstream boundaries of the *lnm*-type gene cluster.

^bNumber of amino acids. ^cAlso see Fig. 2 for the genetic organization of the *lnm*-type gene cluster.

Table S28. Predicted functions of ORFs in the *gnm* gene cluster (accession number: MF925481) from *Streptomyces* sp. CB01883 (Clade IX)

gene ^a	aa ^b	putative function ^c	protein homologue (accession #)	% identity/ % similarity
<i>gnm_orf(-1)</i>	441	putative lanthionine synthetase	AQJ30_24115 (KUN35765)	77/85
<i>gnmA</i>	145	truncated hemoglobin	SAVERM_3316 (BAC71027)	37/51
<i>gnmB</i>	2339	hybrid NRPS/type I PKS	LnmI (AAN85522)	46/56
<i>gnmC</i>	252	type II thioesterase	LnmN (AAN85527)	53/63
<i>gnmD</i>	255	4'-phosphopantetheinyl transferase	Sfp (P39135)	26/45
<i>gnmE</i>	410	HMG-CoA synthase	LnmM (AAN85526)	49/63
<i>gnmF</i>	268	enoyl-CoA hydratase	LnmF (AAN85519)	47/58
<i>gnmG</i>	829	acyltransferase/oxidoreductase	LnmG (AAN85520)	45/62
<i>gnmH</i>	2175	AT-less type I PKS	LnmI (AAN85522)	49/58
<i>gnmI</i>	518	antibiotic efflux protein	LnmY (AAN85538)	31/49
<i>gnmJ</i>	299	unknown	LnmE (AAN85518)	45/60
<i>gnmK</i>	803	AT-less acyltransferase/oxidoreductase	LnmG (AAN85520)	61/73
<i>gnmL</i>	310	unknown	LnmH (AAN85521)	39/56
<i>gnmM</i>	121	glyoxalase/bleomycin resistance protein	(WP_062700437)	51/66
<i>gnmN</i>	135	unknown	LnmZ' (AAN85540)	34/48
<i>gnmO</i>	238	N-acetylglucosaminyl deacetylase	LnmX (AAN85537)	53/67
<i>gnmP</i>	248	methyltransferase	(WP_031183778)	39/51
<i>gnmQ</i>	702	putative alpha/beta hydrolase	LnmD (AAN85517)	47/57
<i>gnmR</i>	84	peptidyl carrier protein	LnmP (AAN85529)	45/59
<i>gnmS</i>	542	discrete adenylation protein	LnmQ (AAN85530)	55/66
<i>gnmT</i>	7422	AT-less type I PKS	LnmJ (AAN85523)	46/56
<i>gnmU</i>	415	HMG-CoA-synthase	LnmM (AAN85526)	60/75
<i>gnmV</i>	91	acyl carrier protein	Fr9M (ADH01494)	36/68
<i>gnmW</i>	423	beta-ketoacyl-ACP synthase	SiaA (AFS33443)	44/57
<i>gnmX</i>	417	cytochrome P450 oxygenase	LnmA (AAN85514)	41/53
<i>gnmY</i>	433	aminotransferase	(KMS73037)	41/56
<i>gnmZ</i>	229	Crp/Fnr family transcriptional regulator	LnmO (AAN85528)	42/62
<i>gnm_orf(+1)</i>	761	AfsR-like regulatory protein	(AKN70481)	78/84

^a*orf(-1)* and *orf(+1)* are predicted to represent the upstream and downstream boundaries of the *gnm* gene cluster.

^bNumber of amino acids. ^cAlso see Fig. 2 for the genetic organization of the *gnm* gene cluster.

Table S29. Predicted functions of ORFs in the *lnm*-type gene cluster from *Streptomyces* sp. CB01201 (Clade X)

gene ^a	aa ^b	putative function ^c	protein homologue (accession #)	% identity/ % similarity
<i>CB01201_orf(-1)</i>	367	hypothetical protein	(WP_045300259)	63/74
<i>CB01201_A</i>	145	truncated hemoglobin	SAVERM_3316 (BAC71027)	36/52
<i>CB01201_B</i>	2338	hybrid NRPS/type I PKS	LnmI (AAN85522)	46/57
<i>CB01201_C</i>	252	thioesterase type II	LnmN (AAN85527)	53/62
<i>CB01201_D</i>	290	4'-phosphopantetheinyl transferase	Sfp (P39135)	27/45
<i>CB01201_E</i>	410	HMG-CoA synthase	LnmM (AAN85526)	47/62
<i>CB01201_F</i>	257	enoyl-CoA hydratase	LnmF (AAN85519)	50/62
<i>CB01201_G</i>	727	acyltransferase/oxidoreductase	LnmG (AAN85520)	48/62
<i>CB01201_H</i>	2063	AT-less type I PKS	LnmI (AAN85522)	51/60
<i>CB01201_I</i>	515	antibiotic efflux protein	LnmY (AAN85538)	32/49
<i>CB01201_J</i>	299	unknown	LnmE (AAN85518)	43/59
<i>CB01201_K</i>	756	AT-less acyltransferase/oxidoreductase	LnmG (AAN85520)	57/67
<i>CB01201_L</i>	310	unknown	LnmH (AAN85521)	42/58
<i>CB01201_M</i>	121	glyoxalase/bleomycin resistance protein	(WP_062700437)	45/66
<i>CB01201_N</i>	135	unknown	LnmZ' (AAN85540)	35/49
<i>CB01201_O</i>	231	N-acetylglucosaminyl deacetylase	LnmX (AAN85537)	53/66
<i>CB01201_P</i>	248	methyltransferase	(WP_031183778)	38/48
<i>CB01201_Q</i>	664	putative alpha/beta hydrolase	LnmD (AAN85517)	36/47
<i>CB01201_R</i>	85	peptidyl carrier protein	LnmP (AAN85529)	43/60
<i>CB01201_S</i>	516	discrete adenylation protein	LnmQ (AAN85530)	55/66
<i>CB01201_T</i>	7016	AT-less type I PKS	LnmJ (AAN85523)	47/58
<i>CB01201_U</i>	418	HMG-CoA-synthase	LnmM (AAN85526)	62/78
<i>CB01201_V</i>	97	acyl carrier protein	Fr9M (ADH01494)	38/63
<i>CB01201_W</i>	433	beta-ketoacyl-ACP synthase	SiaA (AFS33443)	44/57
<i>CB01201_X</i>	412	cytochrome P450 oxygenase	LnmA (AAN85514)	41/54
<i>CB01201_Y</i>	446	aminotransferase	(KMS73037)	42/57
<i>CB01201_Z</i>	229	Crp/Fnr family transcriptional regulator	LnmO (AAN85528)	42/60
<i>CB01201_orf(+1)</i>	581	methylthioribulose 1-phosphate dehydratase	(WP_014143993)	63/72

^a*orf(-1)* and *orf(+1)* are predicted to represent the upstream and downstream boundaries of the *lnm*-type gene cluster.

^bNumber of amino acids. ^cAlso see Fig. 2 for the genetic organization of the *lnm*-type gene cluster.

Table S30. Predicted functions of ORFs in the *wsm* gene cluster (accession number: MF925482) from *Streptomyces* sp. CB02120-2 (Clade XII)

gene ^a	aa ^b	putative function ^c	protein homologue (accession #)	% identity/ % similarity
<i>wsm_orf(-1)</i>	294	SAM-dependent methyltransferase	ADK53_27075 (KOU30977)	
<i>wsmA</i>	219	Crp/Fnr/Fnr family transcriptional regulator	LnmO (AAN85528)	38/57
<i>wsmB</i>	190	Ydel-like protein	SAVERM_307 (BAC68016)	54/72
<i>wsmC</i>	251	phosphopantetheinyl transferase	(WP_059300333)	37/48
<i>wsmD</i>	398	HMG-CoA-synthase	LnmM (AAN85526)	46/59
<i>wsmE</i>	268	enoyl-CoA hydratase	LnmF (AAN85519)	52/61
<i>wsmF</i>	290	acyltransferase	LnmG (AAN85520)	42/55
<i>wsmG</i>	2147	AT-less type I PKS	LnmI (AAN85522)	45/54
<i>wsmH</i>	521	antibiotic efflux protein	LnmY (AAN85538)	35/52
<i>wsmI</i>	268	unknown	LnmE (AAN85518)	37/53
<i>wsmJ</i>	773	AT-less acyltransferase/oxidoreductase	LnmG (AAN85520)	61/72
<i>wsmK</i>	302	unknown	LnmH (AAN85521)	38/54
<i>wsmL</i>	121	glyoxalase/bleomycin resistance protein	(WP_062700437)	44/63
<i>wsmM</i>	236	N-acetylglucosaminyl deacetylase	LnmX (AAN85537)	49/60
<i>wsmN</i>	249	methyltransferase	(WP_031183778)	36/44
<i>wsmO</i>	455	putative alpha/beta hydrolase	LnmD (AAN85517)	35/45
<i>wsmP</i>	83	peptidyl carrier protein	LnmP (AAN85529)	46/68
<i>wsmQ</i>	526	discrete adenylation protein	LnmQ (AAN85530)	52/61
<i>wsmR</i>	7443	AT-less type I PKS	LnmJ (AAN85523)	43/53
<i>wsmS</i>	414	HMG-CoA-synthase	LnmM (AAN85526)	57/71
<i>wsmT</i>	81	acyl carrier protein	Fr9M (ADH01494)	31/50
<i>wsmU</i>	408	beta-ketoacyl-ACP synthase	SiaA (AFS33443)	43/56
<i>wsmV</i>	251	type II thioesterase	LnmN (AAN85527)	55/62
<i>wsmW</i>	2244	hybrid NRPS/type I PKS	LnmI (AAN85522)	45/54
<i>wsmX</i>	141	truncated hemoglobin	SAVERM_3316 (BAC71027)	32/45
<i>wsmY</i>	408	cytochrome P450 oxygenase	LnmA (AAN85514)	39/55
<i>wsmZ1</i>	74	ferredoxin	LnmB (AAN85515)	36/54
<i>wsmZ2</i>	452	crotonyl-CoA carboxylase/reductase	DivR (CCP20056)	64/77
<i>wsmZ3</i>	330	ketoacyl-acyl carrier protein synthase III (KASIII)	DivS (CCP20057)	56/73
<i>wsmZ4</i>	294	3-hydroxyacyl-CoA dehydrogenase	DivT (CCP20058)	52/67
<i>wsm_orf(+1)</i>	475	peptidase M1	VR46_04345 (KJY47303)	86/90

^a*orf(-1)* and *orf(+1)* are predicted to represent the upstream and downstream boundaries of the *wsm* gene cluster.

^bNumber of amino acids. ^cAlso see Fig. 2 for the genetic organization of the *wsm* gene cluster.

Table S31. Predicted functions of ORFs in the *lnm*-type gene cluster from *Streptomyces* sp. CB02613 (Clade XVI)

gene ^a	aa ^b	putative function ^c	protein homologue	% identity/ % similarity
<i>CB02613_orf(-1)</i>	188	phosphotransferase	SPW_1180 (EHM30421)	91/93
<i>CB02613_A</i>	514	ABC transporter component, periplasmic oligopeptide binding protein	LnmU (AAN85534)	59/74
<i>CB02613_B</i>	321	ABC transporter component, membrane spanning protein	LnmT (AAN85533)	53/67
<i>CB02613_C</i>	269	ABC transporter component, membrane spanning protein	LnmS (AAN85532)	62/74
<i>CB02613_D</i>	551	ABC transporter component, ATP hydrolase	LnmR (AAN85531)	54/66
<i>CB02613_E</i>	426	cytochrome P450 oxygenase	LnmA (AAN85514)	40/57
<i>CB02613_F</i>	391	methyltransferase domain of nonribosomal peptide synthetase	(WP_052853671)	41/50
<i>CB02613_G</i>	289	hypothetical protein	TrdC (ADY38535)	33/49
<i>CB02613_H</i>	271	unknown	LnmE (AAN85518)	33/50
<i>CB02613_I</i>	783	AT-less acyltransferase/oxidoreductase	LnmG (AAN85520)	64/77
<i>CB02613_J</i>	4128	AT-less type I PKS	Lnml (AAN85522)	50/59
<i>CB02613_K</i>	315	SyrP-like protein	(BAB69364)	54/64
<i>CB02613_L</i>	306	kinase	PduX_2 (GAQ50744)	64/73
<i>CB02613_M</i>	1059	NRPS (A-PCP-TE)	(ADK54899)	55/65
<i>CB02613_N</i>	402	diaminobutyric acid synthase C	DabC (AEG64688)	58/66
<i>CB02613_O</i>	487	diaminobutyric acid synthase B	DabB (AEG64687)	62/72
<i>CB02613_P</i>	360	diaminobutyric acid synthase A	DabA (AEG64686)	62/71
<i>CB02613_Q</i>	111	peptidyl carrier protein	(WP_059300325)	39/61
<i>CB02613_R</i>	317	halogenase	SyrB2 (AKF46131)	63/77
<i>CB02613_S</i>	283	alpha/beta hydrolase	ADZ36_03165 (KNE83935)	52/64
<i>CB02613_T</i>	6970	AT-less type I PKS	LnmJ (AAN85523)	50/60
<i>CB02613_U</i>	299	acyltransferase/decarboxylase	LnmK (AAN85524)	54/67
<i>CB02613_V</i>	86	acyl carrier protein	LnmL (AAN85525)	58/68
<i>CB02613_W</i>	406	HMG-CoA synthase	LnmM (AAN85526)	66/77
<i>CB02613_X</i>	79	acyl carrier protein	LnmL (AAN85525)	39/61
<i>CB02613_Y</i>	418	beta-ketoacyl-ACP synthase	SiaA (AFS33443)	43/55
<i>CB02613_Z1</i>	266	thioesterase type II	LnmN (AAN85527)	53/64
<i>CB02613_Z2</i>	212	phosphatidylethanolamine-binding protein	Mesil_1512 (ADH63402)	50/64
<i>CB02613_Z3</i>	127	unknown	LnmZ' (AAN85540)	37/55
<i>CB02613_Z4</i>	261	enoyl-CoA hydratase	LnmF (AAN85519)	50/66
<i>CB02613_Z5</i>	415	HMG-CoA synthase	LnmM (AAN85526)	47/63
<i>CB02613_Z6</i>	457	sodium:proton exchanger	(WP_020553490)	56/70
<i>CB02613_Z7</i>	242	Crp/Fnr family transcriptional regulator	LnmO (AAN85528)	43/61
<i>CB02613_Z8</i>	134	unknown	LnmZ' (AAN85540)	39/55
<i>CB02613_Z9</i>	314	unknown	LnmH (AAN85521)	44/59
<i>CB02613_Z10</i>	514	4-coumarate:CoA ligase	LnmW (AAN85536)	42/55
<i>CB02613_Z11</i>	236	N-acetylglucosaminyl deacetylase	LnmX (AAN85537)	52/65
<i>CB02613_Z12</i>	294	unknown	LnmE (AAN85518)	47/65
<i>CB02613_Z13</i>	94	peptidyl carrier protein	PyrB (AFV71306)	53/62
<i>CB02613_Z14</i>	293	hypothetical protein	TrdC (ADY38535)	37/49

<i>CB02613_Z15</i>	500	4-coumarate:CoA ligase	LnmW (AAN85536)	43/57
<i>CB02613_Z16</i>	470	serine hydroxymethyltransferase	AmiS (AEF16058)	62/75
<i>CB02613_Z17</i>	824	nonribosomal peptide synthetase (A-PCP)	LnmQ (AAN85530)	36/46
<i>CB02613_Z18</i>	118	hypothetical protein	SSHG_04587 (EFE84146)	60/66
<i>CB02613_Z19</i>	362	hypothetical protein	(WP_028812750)	78/87
<i>CB02613_Z20</i>	975	4-coumarate:CoA ligase	LnmW (AAN85536)	41/55
<i>CB02613_Z21</i>	400	FAD-dependent oxidoreductase	(WP_010982689)	59/69
<i>CB02613_orf(+1)</i>	290	UDP pyrophosphate phosphatase	(WP_030588347)	98/99

^a*orf(-1)* and *orf(+1)* are predicted to represent the upstream and downstream boundaries of the *lnm*-type gene cluster.

^bNumber of amino acids. ^cAlso see Fig. 2 for the genetic organization of the *lnm*-type gene cluster.

Table S32. Comparison of the *Inm*-type gene clusters from *Streptomyces* sp. NBRC 109436, *S. hygroscopicus* sp. NBRC 16556, and *S. leeuwenhoekii* DSM 42122 with the cluster from *Streptomyces* sp. TSRI0384-2 (Clade V)

<i>Streptomyces</i> sp. TSRI0384-2 ^a	<i>Streptomyces</i> sp. NBRC 109436 ^b	<i>Streptomyces</i> <i>hygroscopicus</i> sp. NBRC 16556 ^c	<i>S. leeuwenhoekii</i> DSM 42122 ^d
<i>TSRI0384-2_orf(-1)</i>	<i>S109_orf(-1)</i> (78/83)	<i>Shyg_orf(-1)</i> (78/83)	<i>Slee_orf(-1)</i> (82/86)
<i>TSRI0384-2_A</i>	<i>S109_A</i> (82/88)	<i>Shyg_A</i> (82/88)	<i>Slee_A</i> (86/90)
<i>TSRI0384-2_B</i>	<i>S109_B</i> (89/93)	<i>Shyg_B</i> (89/93)	<i>Slee_B</i> (88/93)
<i>TSRI0384-2_C</i>	<i>S109_C</i> (90/95)	<i>Shyg_C</i> (90/95)	<i>Slee_C</i> (90/95)
<i>TSRI0384-2_D</i>	<i>S109_D</i> (92/95)	<i>Shyg_D</i> (92/95)	<i>Slee_D</i> (92/95)
<i>TSRI0384-2_E</i>	<i>S109_E</i> (86/88)	<i>Shyg_E</i> (86/88)	<i>Slee_E</i> (85/88)
<i>TSRI0384-2_F</i>	<i>S109_F</i> (86/90)	<i>Shyg_F</i> (86/90)	<i>Slee_F</i> (78/83)
<i>TSRI0384-2_G</i>	<i>S109_G</i> (87/92)	<i>Shyg_G</i> (87/92)	<i>Slee_G</i> (90/94)
<i>TSRI0384-2_H</i>	<i>S109_H</i> (79/85)	<i>Shyg_H</i> (79/85)	<i>Slee_H</i> (80/85)
<i>TSRI0384-2_I</i>	<i>S109_I</i> (92/95)	<i>Shyg_I</i> (91/95)	<i>Slee_I</i> (91/95)
<i>TSRI0384-2_J</i>	<i>S109_J</i> (77/83)	<i>Shyg_J</i> (76/82)	<i>Slee_J</i> (76/82)
<i>TSRI0384-2_K</i>	<i>S109_K</i> (78/82)	<i>Shyg_K</i> (78/82)	<i>Slee_K</i> (78/82)
<i>TSRI0384-2_L</i>	<i>S109_L</i> (76/80)	<i>Shyg_L</i> (76/80)	<i>Slee_L</i> (76/81)
<i>TSRI0384-2_M</i>	<i>S109_M</i> (85/91)	<i>Shyg_M</i> (85/91)	<i>Slee_M</i> (87/92)
<i>TSRI0384-2_N</i>	<i>S109_N</i> (81/89)	<i>Shyg_N</i> (81/89)	<i>Slee_N</i> (80/90)
<i>TSRI0384-2_O</i>	<i>S109_O</i> (91/94)	<i>Shyg_O</i> (91/95)	<i>Slee_O</i> (91/94)
<i>TSRI0384-2_P</i>	<i>S109_P</i> (79/90)	<i>Shyg_P</i> (80/90)	<i>Slee_P</i> (79/91)
<i>TSRI0384-2_Q</i>	<i>S109_Q</i> (82/86)	<i>Shyg_Q</i> (82/86)	<i>Slee_Q</i> (81/86)
<i>TSRI0384-2_R</i>	<i>S109_R</i> (84/88)	<i>Shyg_R</i> (84/88)	<i>Slee_R</i> (84/88)
<i>TSRI0384-2_S</i>	<i>S109_S</i> (88/93)	<i>Shyg_S</i> (88/93)	<i>Slee_S</i> (88/93)
<i>TSRI0384-2_T</i>	<i>S109_T</i> (88/93)	<i>Shyg_T</i> (87/93)	<i>Slee_T</i> (89/94)
<i>TSRI0384-2_U</i>	<i>S109_U</i> (86/92)	<i>Shyg_U</i> (86/92)	<i>Slee_U</i> (85/91)
<i>TSRI0384-2_V</i>	<i>S109_V</i> (90/94)	<i>Shyg_V</i> (90/93)	<i>Slee_V</i> (93/96)
<i>TSRI0384-2_W</i>	<i>S109_W</i> (89/95)	<i>Shyg_W</i> (89/95)	<i>Slee_W</i> (86/94)
<i>TSRI0384-2_X</i>	<i>S109_X</i> (92/94)	<i>Shyg_X</i> (92/94)	<i>Slee_X</i> (92/94)
<i>TSRI0384-2_Y</i>	<i>S109_Y</i> (85/91)	<i>Shyg_Y</i> (85/91)	<i>Slee_Y</i> (86/92)
<i>TSRI0384-2_Z1</i>	<i>S109_Z1</i> (84/90)	<i>Shyg_Z1</i> (84/90)	<i>Slee_Z1</i> (86/93)
<i>TSRI0384-2_Z2</i>	<i>S109_Z2</i> (82/87)	<i>Shyg_Z2</i> (82/87)	<i>Slee_Z2</i> (84/88)
<i>TSRI0384-2_Z3</i>	<i>S109_Z3</i> (88/94)	<i>Shyg_Z3</i> (88/94)	<i>Slee_Z3</i> (88/94)
<i>TSRI0384-2_orf(+1)</i>	<i>S109_orf(+1)</i> (86/91)	<i>Shyg_orf(+1)</i> (86/91)	<i>Slee_orf(+1)</i> (87/93)

^{a,b,c,d}Genes within the *Inm*-type gene clusters, *orf(-1)* and *orf(+1)* are predicted to represent the upstream and downstream boundaries of the *Inm*-type gene clusters. Numbers inside brackets correspond to the protein sequence similarity/identity to those of *Streptomyces* sp. TSRI0384-2. Also see Fig. 2 for the genetic organization of the *Inm*-type gene clusters.

Table S33. Comparison of the *Inm*-type gene clusters from *Streptomyces* sp. CB01373 and *S. canus* ATCC 12647 (Clade VII)

CB01373 ^a	putative function ^b	<i>S. canus</i> ATCC 12647 ^c	% identity/ % similarity
<i>CB01373_orf(-1)</i>	hypothetical protein		
<i>CB01373_A</i>	antibiotic efflux protein		
<i>CB01373_B</i>	TetR family transcriptional regulator	<i>Scan_orf(-1)</i>	91/94
<i>CB01373_C</i>	hypothetical protein	<i>Scan_Z2</i>	44/47
<i>CB01373_D</i>	Ydel-like protein	<i>Scan_A</i>	91/95
<i>CB01373_E</i>	cytochrome P450 oxygenase	<i>Scan_B</i>	91/94
<i>CB01373_F</i>	hypothetical protein		
<i>CB01373_G</i>	Crp/Fnr family transcriptional regulator	<i>Scan_C</i>	91/93
<i>CB01373_H</i>	phosphopantetheinyl transferase	<i>Scan_D</i>	87/88
<i>CB01373_I</i>	cytochrome P450 oxygenase	<i>Scan_E</i>	97/98
<i>CB01373_J</i>	Crp/Fnr family transcriptional regulator	<i>Scan_F</i>	92/93
<i>CB01373_K</i>	sodium:proton exchanger	<i>Scan_G</i>	92/95
<i>CB01373_L</i>	unknown	<i>Scan_H</i>	93/96
<i>CB01373_M</i>	HMG-CoA-synthase	<i>Scan_I</i>	96/97
<i>CB01373_N</i>	enoyl-CoA hydratase	<i>Scan_J</i>	94/96
<i>CB01373_O</i>	AT-less acyltransferase/oxidoreductase	<i>Scan_K</i>	84/86
<i>CB01373_P</i>	unknown	<i>Scan_L</i>	96/98
<i>CB01373_Q</i>	NRPS (A-PCP)	<i>Scan_M</i>	94/95
<i>CB01373_R</i>	halogenase	<i>Scan_N</i>	96/97
<i>CB01373_S</i>	alpha/beta hydrolase	<i>Scan_O</i>	91/93
<i>CB01373_T</i>	AT-less type I PKS	<i>Scan_P</i>	89/92
<i>CB01373_U</i>	AT-less type I PKS	<i>Scan_Q</i>	87/90
<i>CB01373_V</i>	acyltransferase/decarboxylase	<i>Scan_R</i>	96/97
<i>CB01373_W</i>	acyl carrier protein	<i>Scan_S</i>	94/96
<i>CB01373_X</i>	HMG-CoA synthase	<i>Scan_T</i>	93/95
<i>CB01373_Y</i>	acyl carrier protein	<i>Scan_U</i>	98/98
<i>CB01373_Z1</i>	beta-ketoacyl-ACP synthase	<i>Scan_V</i>	91/94
<i>CB01373_Z2</i>	thioesterase type II	<i>Scan_W</i>	92/96
<i>CB01373_Z3</i>	N-acetylglucosaminyl deacetylase	<i>Scan_X</i>	95/98
<i>CB01373_Z4</i>	unknown	<i>Scan_Y</i>	95/96
<i>CB01373_Z5</i>	4-coumarate:CoA ligase	<i>Scan_Z1</i>	93/95
<i>CB01373_Z6</i>	antibiotic efflux protein		
<i>CB01373_Z7</i>	TetR family transcriptional regulator	<i>Scan_orf(-1)</i>	66/81
<i>CB01373_Z8</i>	FAD-dependent oxidoreductase	<i>Scan_Z2</i>	93/95
<i>CB01373_Z9</i>	glyoxalase/bleomycin resistance protein	<i>Scan_Z3</i>	97/99
<i>CB01373_Z10</i>	4-coumarate:CoA ligase	<i>Scan_Z4</i>	95/97
<i>CB01373_Z11</i>	cytochrome P450 oxygenase	<i>Scan_Z5</i>	94/97
<i>CB01373_orf(+1)</i>	hypothetical protein		60/69
	Repeat domain-containing protein	<i>Scan_orf(+1)</i>	

^{a,c}Genes within the *Inm*-type gene clusters, *orf(-1)* and *orf(+1)* are predicted to represent the upstream and downstream boundaries of the *Inm*-type gene clusters. ^bAlso see Fig. 2 for the genetic organization of the *Inm*-type gene clusters.

Table S34. Comparison of the *Inm*-type gene clusters from *Streptomyces* sp. F5630 and *S. aureofaciens* NRRL B-2183 with the *gnm* gene cluster from *Streptomyces* sp. CB01883 (Clade IX)

gene ^a	putative function ^c	Streptomyces sp. F5630	<i>S. aureofaciens</i> NRRL B-2183
	Ydel-like protein	<i>Sf56_orf(-1)</i>	<i>Saur_orf(-1)</i>
<i>gnm_orf(-1)</i>	putative lanthionine synthetase		
<i>gnmA</i>	truncated hemoglobin	<i>Sf56_A</i> (79/84)	<i>Saur_A</i> (82/87)
<i>gnmB</i>	hybrid NRPS/type I PKS	<i>Sf56_B</i> (76/80)	<i>Saur_B</i> (78/82)
<i>gnmC</i>	type II thioesterase	<i>Sf56_C</i> (87/93)	<i>Saur_C</i> (86/92)
<i>gnmD</i>	4'-phosphopantetheinyl transferase	<i>Sf56_D</i> (72/78)	<i>Saur_D</i> (79/80)
<i>gnmE</i>	HMG-CoA synthase	<i>Sf56_E</i> (87/90)	<i>Saur_E</i> (90/94)
<i>gnmF</i>	enoyl-CoA hydratase	<i>Sf56_F</i> (77/85)	<i>Saur_F</i> (81/86)
<i>gnmG</i>	acyltransferase/oxidoreductase	<i>Sf56_G</i> (67/71)	<i>Saur_G</i> (70/75)
<i>gnmH</i>	AT-less type I PKS	<i>Sf56_H</i> (72/77)	<i>Saur_H</i> (71/76)
<i>gnmI</i>	antibiotic efflux protein	<i>Sf56_I</i> (91/94)	<i>Saur_I</i> (91/94)
<i>gnmJ</i>	unknown	<i>Sf56_J</i> (91/94)	<i>Saur_J</i> (90/96)
<i>gnmK</i>	AT-less acyltransferase/oxidoreductase	<i>Sf56_K</i> (81/86)	<i>Saur_K</i> (90/93)
<i>gnmL</i>	unknown	<i>Sf56_L</i> (88/93)	<i>Saur_L</i> (90/94)
<i>gnmM</i>	glyoxalase/bleomycin resistance protein	<i>Sf56_M</i> (88/95)	<i>Saur_M</i> (91/98)
<i>gnmN</i>	unknown	<i>Sf56_N</i> (86/92)	<i>Saur_N</i> (88/95)
<i>gnmO</i>	N-acetylglucosaminyl deacetylase	<i>Sf56_O</i> (89/93)	<i>Saur_O</i> (95/98)
<i>gnmP</i>	methyltransferase	<i>Sf56_P</i> (87/91)	<i>Saur_P</i> (86/90)
<i>gnmQ</i>	putative alpha/beta hydrolase	<i>Sf56_Q</i> (69/75)	<i>Saur_Q</i> (71/76)
<i>gnmR</i>	peptidyl carrier protein	<i>Sf56_R</i> (86/92)	<i>Saur_R</i> (90/95)
<i>gnmS</i>	discrete adenylation protein	<i>Sf56_S</i> (83/88)	<i>Saur_S</i> (83/86)
<i>gnmT</i>	AT-less type I PKS	<i>Sf56_T</i> (70/75)	<i>Saur_T</i> (71/76)
<i>gnmU</i>	HMG-CoA-synthase	<i>Sf56_U</i> (90/94)	<i>Saur_U</i> (91/94)
<i>gnmV</i>	acyl carrier protein	<i>Sf56_V</i> (85/94)	<i>Saur_V</i> (79/91)
<i>gnmW</i>	beta-ketoacyl-ACP synthase	<i>Sf56_W</i> (78/85)	<i>Saur_W</i> (78/86)
<i>gnmX</i>	cytochrome P450 oxygenase	<i>Sf56_X</i> (89/92)	<i>Saur_X</i> (90/93)
<i>gnmY</i>	aminotransferase	<i>Sf56_Y</i> (85/90)	<i>Saur_Y</i> (89/94)
<i>gnmZ</i>	Crp/Fnr family transcriptional regulator	<i>Sf56_Z</i> (84/92)	<i>Saur_Z</i> (92/96)
<i>gnm_orf(+1)</i>	AfsR-like regulatory protein		
	LysR family transcriptional regulator	<i>Sf56_orf(+1)</i>	
	transposase		<i>Saur_orf(+1)</i>

^{a,b,c,d}Genes within the *Inm*-type gene clusters, *orf(-1)* and *orf(+1)* are predicted to represent the upstream and downstream boundaries of the *Inm*-type gene clusters. Numbers inside brackets correspond to the protein sequence similarity/identity to that of *gnm* gene cluster. Also see **Fig. 2** for the genetic organization of the *Inm*-type gene clusters.

Table S35. Comparison of the *lmm*-type gene clusters from *Streptomyces* sp. NBRC 110035 with the *wsm* gene cluster from *Streptomyces* sp. CB02120-2 (Clade XII)

CB02120-2 ^a	putative function ^b	<i>Streptomyces</i> sp. NBRC 110035 ^c	% identity/ % similarity
	transposase	<i>S110_orf(-1)</i>	
<i>wsm_orf(-1)</i>	SAM-dependent methyltransferase		
<i>wsmA</i>	Crp/Fnr/Fnr family transcriptional regulator	<i>S110_A</i>	81/88
<i>wsmB</i>	Ydel-like protein	<i>S110_B</i>	81/89
<i>wsmC</i>	phosphopantetheinyl transferase	<i>S110_C</i>	73/78
<i>wsmD</i>	HMG-CoA-synthase	<i>S110_D</i>	89/94
<i>wsmE</i>	enoyl-CoA hydratase	<i>S110_E</i>	81/88
<i>wsmF</i>	acyltransferase	<i>S110_F</i>	83/86
<i>wsmG</i>	AT-less type I PKS	<i>S110_G</i>	77/81
	transposase	<i>S110_H</i>	
	glyoxalase/bleomycin resistance protein	<i>S110_I</i>	
<i>wsmH</i>	antibiotic efflux protein	<i>S110_J</i>	84/89
<i>wsmI</i>	unknown	<i>S110_K</i>	91/95
<i>wsmJ</i>	AT-less acyltransferase/oxidoreductase	<i>S110_L</i>	81/87
<i>wsmK</i>	unknown	<i>S110_M</i>	86/91
<i>wsmL</i>	glyoxalase/bleomycin resistance protein	<i>S110_N</i>	81/91
<i>wsmM</i>	N-acetylglucosaminyl deacetylase	<i>S110_O</i>	83/90
<i>wsmN</i>	methyltransferase	<i>S110_P</i>	88/93
<i>wsmO</i>	putative alpha/beta hydrolase	<i>S110_Q</i>	69/76
<i>wsmP</i>	peptidyl carrier protein	<i>S110_R</i>	78/87
<i>wsmQ</i>	discrete adenylation protein	<i>S110_S</i>	80/85
<i>wsmR</i>	AT-less type I PKS	<i>S110_T</i>	74/79
<i>wsmS</i>	HMG-CoA-synthase	<i>S110_U</i>	84/88
<i>wsmT</i>	acyl carrier protein	<i>S110_V</i>	91/93
<i>wsmU</i>	beta-ketoacyl-ACP synthase	<i>S110_W</i>	78/84
<i>wsmV</i>	type II thioesterase	<i>S110_X</i>	81/88
<i>wsmW</i>	hybrid NRPS/type I PKS	<i>S110_Y</i>	70/76
<i>wsmX</i>	truncated hemoglobin	<i>S110_Z1</i>	82/89
<i>wsmY</i>	cytochrome P450 oxygenase	<i>S110_Z2</i>	89/94
<i>wsmZ1</i>	ferredoxin	<i>S110_Z3</i>	78/83
<i>wsmZ2</i>	crotonyl-CoA carboxylase/reductase	<i>S110_Z4</i>	86/93
<i>wsmZ3</i>	ketoacyl-acyl carrier protein synthase III (KASIII)	<i>S110_Z5</i>	82/91
<i>wsmZ4</i>	3-hydroxyacyl-CoA dehydrogenase	<i>S110_Z6</i>	77/86
<i>wsm_orf(+1)</i>	peptidase M1		
	transposase	<i>S110_orf(+1)</i>	

^{a,c}*orf(-1)* and *orf(+1)* are predicted to represent the upstream and downstream boundaries of the *lmm*-type gene clusters.

^bAlso see **Fig. 2** for the genetic organization of the *lmm*-type gene cluster.

Table S36. Comparison of the *Inm*-type gene clusters from *Micromonospora globosa* NRRL B-2673, *Micromonospora marina* DSM 45555, *Micromonospora* sp. CNB394 and *Micromonospora* sp. L5 with the cluster from *Micromonospora aurantiaca* ATCC 27029 (Clade XV)

<i>M. aurantiaca</i> ATCC 27029 ^a	<i>M. globosa</i> NRRL B-2673 ^b	<i>M. marina</i> DSM 45555 ^c	<i>Micromonospora</i> sp. CNB394 ^d	<i>Micromonospora</i> sp. L5 ^e
<i>Maur_orf(-1)</i>	<i>Mglo_orf(-1)</i> (99/99)	<i>Mmar_orf(-1)</i> (99/99)	<i>Mcnb_orf(-1)</i> (94/95)	<i>MI5_orf(-1)</i> (94/95)
<i>Maur_A</i>	<i>Mglo_A</i> (100/100)	<i>Mmar_A</i> (98/99)	<i>Mcnb_A</i> (98/98)	<i>MI5_A</i> (99/99)
<i>Maur_B</i>	<i>Mglo_B</i> (100/100)	<i>Mmar_B</i> (98/98)	<i>Mcnb_B</i> (98/98)	<i>MI5_B</i> (99/100)
<i>Maur_C</i>	<i>Mglo_C</i> (100/100)	<i>Mmar_C</i> (96/98)	<i>Mcnb_C</i> (97/98)	<i>MI5_C</i> (100/100)
<i>Maur_D</i>	<i>Mglo_D</i> (100/100)	<i>Mmar_D</i> (95/96)	<i>Mcnb_D</i> (96/96)	<i>MI5_D</i> (99/99)
<i>Maur_E</i>	<i>Mglo_E</i> (100/100)	<i>Mmar_E</i> (99/99)	<i>Mcnb_E</i> (98/99)	<i>MI5_E</i> (100/100)
<i>Maur_F</i>	<i>Mglo_F</i> (100/100)	<i>Mmar_F</i> (95/97)	<i>Mcnb_F</i> (95/96)	<i>MI5_F</i> (96/96)
<i>Maur_G</i>	<i>Mglo_G</i> (100/100)	<i>Mmar_G</i> (98/100)	<i>Mcnb_G</i> (98/100)	<i>MI5_G</i> (100/100)
<i>Maur_H</i>	<i>Mglo_H</i> (100/100)	<i>Mmar_H</i> (98/97)	<i>Mcnb_H</i> (98/97)	<i>MI5_H</i> (100/100)
<i>Maur_I</i>	<i>Mglo_I</i> (98/97)	<i>Mmar_I</i> (89/90)	<i>Mcnb_I</i> (93/94)	<i>MI5_I</i> (98/98)
<i>Maur_J</i>	<i>Mglo_J</i> (99/99)	<i>Mmar_J</i> (91/93)	<i>Mcnb_J</i> (91/92)	<i>MI5_J</i> (98/98)
<i>Maur_K</i>	<i>Mglo_K</i> (99/100)	<i>Mmar_K</i> (97/98)	<i>Mcnb_K</i> (97/98)	<i>MI5_K</i> (98/98)
<i>Maur_L</i>	<i>Mglo_L</i> (100/100)	<i>Mmar_L</i> (92/93)	<i>Mcnb_L</i> (91/92)	<i>MI5_L</i> (95/96)
<i>Maur_M</i>	<i>Mglo_M</i> (100/100)	<i>Mmar_M</i> (98/98)	<i>Mcnb_M</i> (98/98)	<i>MI5_M</i> (99/99)
<i>Maur_N</i>	<i>Mglo_N</i> (100/100)	<i>Mmar_N</i> (95/96)	<i>Mcnb_N</i> (95/96)	<i>MI5_N</i> (99/98)
<i>Maur_O</i>	<i>Mglo_O</i> (99/99)	<i>Mmar_O</i> (96/97)	<i>Mcnb_O</i> (96/97)	<i>MI5_O</i> (99/99)
<i>Maur_P</i>	<i>Mglo_P</i> (100/100)	<i>Mmar_P</i> (99/99)	<i>Mcnb_P</i> (99/99)	<i>MI5_P</i> (99/99)
<i>Maur_Q</i>	<i>Mglo_Q</i> (100/100)	<i>Mmar_Q</i> (97/98)	<i>Mcnb_Q</i> (97/97)	<i>MI5_Q</i> (98/98)
<i>Maur_R</i>	<i>Mglo_R</i> (100/100)	<i>Mmar_R</i> (98/99)	<i>Mcnb_R</i> (98/99)	<i>MI5_R</i> (98/99)
<i>Maur_S</i>	<i>Mglo_S</i> (100/100)	<i>Mmar_S</i> (99/99)	<i>Mcnb_S</i> (99/99)	<i>MI5_S</i> (100/100)
<i>Maur_T</i>	<i>Mglo_T</i> (100/100)	<i>Mmar_T</i> (97/96)	<i>Mcnb_T</i> (96/96)	<i>MI5_T</i> (100/100)
<i>Maur_U</i>	<i>Mglo_U</i> (99/98)	<i>Mmar_U</i> (93/94)	<i>Mcnb_U</i> (93/94)	<i>MI5_U</i> (99/99)
<i>Maur_V</i>	<i>Mglo_V</i> (99/99)	<i>Mmar_V</i> (96/97)	<i>Mcnb_V</i> (96/96)	<i>MI5_V</i> (99/99)
<i>Maur_W</i>	<i>Mglo_W</i> (99/100)	<i>Mmar_W</i> (98/99)	<i>Mcnb_W</i> (98/99)	<i>MI5_W</i> (99/100)
<i>Maur_X</i>	<i>Mglo_X</i> (98/98)	<i>Mmar_X</i> (92/93)	<i>Mcnb_X</i> (93/94)	<i>MI5_X</i> (99/99)
<i>Maur_Y</i>	<i>Mglo_Y</i> (99/100)	<i>Mmar_Y</i> (98/98)	<i>Mcnb_Y</i> (98/98)	<i>MI5_Y</i> (99/100)
<i>Maur_Z1</i>	<i>Mglo_Z1</i> (100/100)	<i>Mmar_Z1</i> (100/100)	<i>Mcnb_Z1</i> (100/100)	<i>MI5_Z1</i> (100/100)
<i>Maur_Z2</i>	<i>Mglo_Z2</i> (99/99)	<i>Mmar_Z2</i> (97/98)	<i>Mcnb_Z2</i> (98/99)	<i>MI5_Z2</i> (99/99)
<i>Maur_Z3</i>	<i>Mglo_Z3</i> (99/99)	<i>Mmar_Z3</i> (96/98)	<i>Mcnb_Z3</i> (97/98)	<i>MI5_Z3</i> (100/100)
<i>Maur_Z4</i>	<i>Mglo_Z4</i> (99/100)	<i>Mmar_Z4</i> (99/99)	<i>Mcnb_Z4</i> (99/99)	<i>MI5_Z4</i> (99/100)
<i>Maur_Z5</i>	<i>Mglo_Z5</i> (100/100)	<i>Mmar_Z5</i> (99/99)	<i>Mcnb_Z5</i> (99/99)	<i>MI5_Z5</i> (100/100)
<i>Maur_Z6</i>	<i>Mglo_Z6</i> (100/100)	<i>Mmar_Z6</i> (98/98)	<i>Mcnb_Z6</i> (98/98)	<i>MI5_Z6</i> (100/100)
<i>Maur_Z7</i>	<i>Mglo_Z7</i> (99/99)	<i>Mmar_Z7</i> (99/99)	<i>Mcnb_Z7</i> (98/98)	<i>MI5_Z7</i> (99/99)
<i>Maur_Z8</i>	<i>Mglo_Z8</i> (99/100)	<i>Mmar_Z8</i> (98/100)	<i>Mcnb_Z8</i> (99/100)	<i>MI5_Z8</i> (100/100)

<i>Maur_Z9</i>	<i>Mglo_Z9</i> (100/100)	<i>Mmar_Z9</i> (99/100)	<i>Mcnb_Z9</i> (99/100)	<i>MI5_Z9</i> (100/100)
<i>Maur_Z10</i>	<i>Mglo_Z10</i> (100/100)	<i>Mmar_Z10</i> (99/100)	<i>Mcnb_Z10</i> (100/100)	<i>MI5_Z10</i> (100/100)
<i>Maur_Z11</i>	<i>Mglo_Z11</i> (99/100)	<i>Mmar_Z11</i> (97/98)	<i>Mcnb_Z11</i> (97/98)	<i>MI5_Z11</i> (99/100)
<i>Maur_orf(+1)</i>	<i>Mglo_orf(+1)</i> (97/98)	<i>Mmar_orf(+1)</i> (91/92)	<i>Mcnb_orf(+1)</i> (91/92)	<i>MI5_orf(+1)</i> (97/97)

^{a,b,c,d,e} Genes within the *Inm*-type gene clusters, *orf(-1)* and *orf(+1)* are predicted to represent the upstream and downstream boundaries of the *Inm*-type gene clusters. Numbers inside brackets correspond to the protein sequence similarity/identity. Also see Fig. 2 for the genetic organization of the *Inm*-type gene clusters.

Table S37. Substrate specificity-conferring codes and predicted substrates of the adenylation proteins/domains from LNM-type biosynthetic pathways.

Adenylation protein/domain ^a	8 angstrom signature ^b	Stachelhaus code ^c	Predicted substrates
Group I			
WsmQ	FTAYFDLSMSELHAVFCGEDNLYGPTEASVACTG	DLSHVCLVAK	D-Ala ^d
S110_S	FTAYFDLSMSELHAIFCGEDNLYGPTEASVACTG	DLSHICLVAK	Unknown
LnmQ	FASYFDLSMFECTSVFCGEDNLYGPTELTIACTA	DLFTVCLI AK	D-Ala ^d
CB01635_Q	FASYFDLSMFECTSVFCGEDNLYGPTELTIACTA	DLFTVCLI AK	D-Ala ^d
CB02959_Q	FATYFDLSMFEATSVCFCGEDNLYGPTELTVACTG	DLFTVCLVAK	Unknown
CB02891_F	FAVYFDLSMFEATSVCFCGEDNLYGPTELAVACTG	DLFTMCLVAK	Unknown
Sast_X	FAAYFDLAMFDMHTVFCGEDNIYGPTELTIACTA	DLFHVCIIAK	Unknown
CB01201_S	FSSHFDLALADPHSVFAGEDNIYGPTELTIACSA	DLAHVAAI AK	Unknown
GnmS	FTSHFDLAMCDPHSVFAGEDNIYGPTELTIACTA	DLCHVAAI AK	ACC ^d
Sf56_S	FASHFDLALCDPHSVFAGEDNIYGPTELTIACTA	DLCHVAAI AK	ACC ^d
Saur_S	FASHFDLAMCDPHSVFAGEDNIYGPTELTIACTA	DLCHVAAI AK	ACC ^d
Group II			
S109_H	LSSHFDHSVWEQSQVFGGEVNMYGITETCVHVTH	DFWSVGMVHK	L-Thr
Shyg_H	LSSHFDHSVWEQSQVFGGEVNMYGITETCVHVTH	DFWSVGMVHK	L-Thr
Slee_H	LSSHFDHSVWEQSQVFGGEVNMYGITETCVHVTH	DFWSVGMVHK	L-Thr
TSRI0384-2_H	LSSHFDHSVWEQSQVLGGEVNMYGITETCVHVTH	DFWSVGMVHK	L-Thr
Mtul_C	LQLHFDFSVWEQSQVLGGEINMYGITETTVHVTH	DFWSVGMVHK	L-Thr
Caci_L	LQTHFDFSVWEQSQVFGGEVNMYGITETTVHVTH	DFWSVGMVHK	L-Thr
Saes_Y	LRAHFDFSVWEQSQVFGGEVNMYGITEITVHATH	DFWSVGMVHK	L-Thr
Mcnb_X	LHGHFDFSVWEQNQVFGGEVNMYGITEVTVHATA	DFWNVGMVHK	L-Thr
Mmar_X	LHGHFDFSVWEQNQVFGGEVNMYGITEVTVHATA	DFWNVGMVHK	L-Thr
Maur_X	LHGHFDFSVWEQNQVFGGEVNMYGITEVTVHATE	DFWNVGMVHK	L-Thr
Mglo_X	LHGHFDFSVWEQNQVFGGEVNMYGITEVTVHATA	DFWNVGMVHK	L-Thr
MI5_X	LHGHFDFSVWEQNQVFGGEVNMYGITEVTVHATA	DFWNVGMVHK	L-Thr
CB01373_Q	LQTHFDFSVWEQNQVFGGEVNMYGITETTVHVTA	DFWNVGMVHK	L-Thr
Scan_M	LQTHFDFSVWEQNQVFGGEVNMYGITETTVHVTA	DFWNVGMVHK	L-Thr
Bubo_N	LASHFDFSVWEGLVMGGEVNMYGITETTVHVTH	DFWSVGMVHK	L-Thr
others			
CB02613_Z17	NDISFDMSVYEGNSLCGGDIALGGATEASVHSTV	DMYNLGLVHK	Unknown
Sal964_D	NDLSFDMSVYEGNTLGGDISLGGVTEASIHS TV	DMYNLGLIHK	Unknown
CB02613_M	HAKAFDISLWQAQISVTGEVNAYGATEVSDDTMH	DIWQSTADDK	Unknown
Sal964_T	HIKAFDISLWQAQISVTGEVNAYGATEVSDDTMH	DIWQSTADDK	Unknown
Snov_N	AAILFDYGLYQLPLNTGAVSMFGLTECKRVTIA	DYYPTTMRVK	Unknown

^aAdenylation proteins/domains from the LNM and 28 LNM-type pathways. The analysis was performed with NRPSpredictor2 (18).

^bThe extracted 8 angstrom signature (19).

^cThe extracted Stachelhaus code (20).

^dThe adenylation proteins/domains whose substrates have been identified experimentally.

Table S38. ^1H NMR (700 MHz) and ^{13}C NMR (175 MHz) data of GNM A in DMSO- d_6

No.	Major rotamer		Minor rotamer	
	δ_{C}	δ_{H}	δ_{C}	δ_{H}
1	169.9		174.4	
2	40.4	2.89 (1H, d, 14.6) 2.39 (1H, d, 14.6)	39.0	3.13 (1H, d, 15.2) 3.00 (1H, d, 15.2)
3	53.6		53.9	
4	34.3	1.62 (1H, m) 1.46 (1H, m)	36.2	1.53 (1H, m) 0.48 (1H, m)
5	33.2	1.84 (2H, m)	33.5	1.87 (1H, m) 1.74 (1H, m)
6	134.9		134.8	
7	122.8	4.96 (1H, t, 6.4)	124.1	4.81 (1H, d, 6.5)
8	32.68	2.97 (1H, m) 2.90 (1H, m)	32.73	3.22 (1H, dd, 8.3, 15.2) 2.81 (1H, d, 15.6)
9	145.9		146.0	
10	132.1	6.38 (1H, d, 16.2)	132.0	6.40 (1H, d, 16.0)
11	128.1	7.00 (1H, d, 16.1)	128.5	7.10 (1H, d, 15.1)
12	136.2		136.1	
13^a	124.2	6.36 (1H, s)	124.2	6.36 (1H, s)
14	150.4		150.0	
15	117.9	7.40 (1H, s)	118.1	7.51 (1H, s)
16	170.8		173.4	
17	33.1		35.9	
18^b	15.0	1.39 (1H, m) 1.19 (1H, m)	19.2	1.36 (1H, m) 1.14 (1H, m)
19^b	14.6	1.19 (1H, m) 1.13 (1H, m)	17.4	2.06 (1H, m) 1.36 (1H, m)
20	19.8	1.96 (3H, s)	19.6	1.99 (3H, s)
21	118.5	5.10 (2H, m)	118.5	5.11 (2H, m)
22	16.25	1.57 (3H, s)	16.31	1.58 (3H, s)
23	41.0	2.96 (1H, d, 15.5) 2.58 (1H, d, 15.5)	38.6	3.20 (1H, d, 15.5) 2.33 (1H, d, 15.5)
24	171.5		171.4	
25	24.2	2.37 (3H, s)	24.0	2.16 (3H, s)
CO₂H^a		12.12 (1H, br s)		12.12 (1H, br s)
NH		8.92 (1H, br s)		8.78 (1H, br s)

^aoverlapped. ^binterchangeable.

Table S39. ^1H NMR (700 MHz) and ^{13}C NMR (175 MHz) data of GNM B and GNM B3 in $\text{DMSO}-d_6$

No.	GNM B ^a		GNM B3	
	δ_{C}	δ_{H}	δ_{C}	δ_{H}
1	170.8		170.4	
2	50.1	2.55 (1H, d, 13.1) 2.21 (1H, d, 13.0)	43.6	2.76 (1H, d, 11.8) 2.18 (1H, d, 12.0)
3	46.6		53.4	
4	41.6	1.09 (1H, m) 1.00 (1H, m)	39.0	1.41 (1H, m) 0.62 (1H, t, 12.9)
5	33.5	1.94 (1H, m) 1.69 (1H, dt, 4.1, 12.4)	33.4	1.81 (1H, m) 1.62 (1H, m)
6	135.9		135.8	
7	122.0	4.73 (1H, t, 5.3)	122.3	4.71 (1H, t, 5.0)
8	32.62	2.96 (1H, dd, 7.2, 15.9) 2.84 (1H, dd, 5.8, 15.8)	32.5 ^c	3.00 (1H, dd, 6.5, 15.8) 2.79 (1H, d, 14.6)
9	145.9		146.0	
10	131.8	6.38 (1H, d, 16.0)	131.7	6.37 (1H, d, 16.0)
11	128.1	6.73 (1H, d, 16.0)	128.3	6.72 (1H, d, 16.0)
12	136.5		136.4	
13	124.9	6.37 (1H, s)	124.9	6.36 (1H, s)
14	149.7		149.7	
15	117.6	7.29 (1H, s)	118.0	7.29 (1H, s)
16	170.1		169.8	
17	32.56		32.5 ^c	
18 ^b	14.4	1.33 (1H, m) 1.04 (1H, m)	15.4	1.26 (1H, m) 1.08 (1H, m)
19 ^b	13.9	1.08 (1H, m) 1.06 (1H, m)	12.7	1.12 (1H, m) 1.07 (1H, m)
20	19.6	1.96 (3H, s)	19.7	1.95 (3H, d, 1.1)
21	118.4	5.09 (1H, d, 2.1) 5.08 (1H, d, 2.1)	118.4	5.08 (1H, s) 5.07 (1H, s)
22	16.4	1.49 (3H, s)	16.0	1.45 (3H, s)
23	50.8	2.37 (1H, d, 13.1) 2.10 (1H, d, 13.0)	46.4	2.25 (1H, d, 12.7) 2.09 (1H, d, 13.5)
24	174.4		174.2	
CO₂H				11.32 (1H, br s)
NH		10.70 (1H, br s)		

^aOnly the major rotamer is shown. ^bInterchangeable. ^coverlapped

Table S40. ^1H NMR (700 MHz) and ^{13}C NMR (175 MHz) data of (*S*)- and (*R*)-PGME-GNM B2 in $\text{DMSO}-d_6$

No.	(<i>S</i>)-PGME-GNM B2		(<i>R</i>)-PGME-GNM B2	
	δ_{C}	δ_{H}	δ_{C}	δ_{H}
1	170.4		171.3 ^e	
2	38.4	2.96 (1H, d, 15.3) 2.26 (1H, d, 15.3)	38.1	3.14 (1H, d, 14.8) 2.72 (1H, d, 14.8)
3	44.6		44.7	
4	37.0	1.93 (1H, td, 3.5, 14.4) 1.79 (1H, dt, 4.3, 13.9)	37.4	1.81 (1H, td, 4.3, 15.0) 1.78 (1H, dt, 3.5, 14.4)
5	32.8	1.64-1.61 (1H, m) 1.62-1.58 (1H, m)	33.0	1.68 (1H, td, 3.7, 13.6) 1.61 (1H, dt, 3.9, 13.0)
6	76.4		76.6	
7	42.6	3.64 (1H, dd, 2.8, 9.0)	43.2	3.74 (1H, d, 6.9)
8	31.3	2.59 (1H, br s) 2.50 ^b (1H, m)	30.4	2.73 (1H, br s) 2.54 (1H, dd, 8.6, 13.9)
9	144.4		144.5	
10	133.6	6.37 (1H, d, 16.2)	133.7	6.36 (1H, d, 16.2)
11	128.3 ^a	8.05 (1H, d, 16.1)	128.9 ^f	8.16 (1H, d, 13.6)
12	133.5		133.5	
13	121.8	6.27 (1H, s)	121.8	6.26 (1H, s)
14	153.1		153.2	
15	117.1	7.33 (1H, s)	117.0	7.32 (1H, s)
16	173.3		173.0	
17	34.8		35.1	
18 ^d	19.5 ^c	1.43-1.41 (2H, m)	19.7	1.58-1.55 (1H, m) 1.21-1.18 (1H, m)
19 ^d	19.5 ^c	1.29-1.27 (1H, m) 1.21-1.18 (1H, m)	19.5	1.51 (1H, br s) 1.38 ^g (1H, m)
20	21.1	1.96 (3H, s)	21.1	1.95 (3H, s)
21	120.9	5.20 (1H, d, 1.1) 5.11 (1H, d, 1.1)	121.3	5.24 (1H, s) 5.12 (1H, s)
22	16.7	1.38 (3H, s)	16.8	1.38 (3H, s)
23	44.0	2.85 (1H, d, 13.4) 2.20 (1H, d, 13.4)	45.1	2.83 (1H, d, 12.5) 2.04 (1H, d, 12.4)
24	168.6		168.7	
25	48.3	3.12 (3H, s)	48.4	3.19 (3H, s)
1'	170.9		171.3 ^e	
2'	56.1	5.36 (1H, d, 7.1)	56.7	5.27 (1H, d, 6.7)
3'	136.2		135.6	
4'	127.6	7.35-7.33 (2H, m)	127.6	7.35-7.33 (2H, m)
5'	128.7	7.39-7.37 (2H, m)	128.9 ^f	7.41-7.38 (2H, m)
6'	128.3 ^a	7.36-7.34 (1H, m)	128.5	7.38-7.36 (1H, m)
7'	52.2	3.61 (3H, s)	52.5	3.58 (3H, s)
1-NH		8.98 (1H, s)		9.14 (1H, s)
24-NH		8.81 (1H, d, 7.1)		9.04 (1H, d, 6.4)

^{a,c,e,f}overlapped. ^boverlapped with solvent. ^dinterchangeable. ^goverlapped by 22-CH₃.

Table S41. ^1H NMR (700 MHz) and ^{13}C NMR (175 MHz) data of (*S*)- and (*R*)-PGME-LNM E2 in DMSO- d_6

No.	<i>(S)</i> -PGME-LNM E2		<i>(R)</i> -PGME-LNM E2	
	δ_{C}	δ_{H}	δ_{C}	δ_{H}
1	169.0		169.0	
2	38.2	3.16 (1H, d, 14.8) 2.32 (1H, d, 14.9)	38.2	3.14 (1H, d, 14.8) 2.37 (1H, d, 14.9)
3	48.2		48.2	
4	30.5	2.58 (1H, dt, 3.4, 14.4) 1.39 (1H, td, 3.5, 14.4)	31.0	2.61 (1H, dt, 3.2, 14.3) 1.45 (1H, td, 3.4, 14.3)
5	37.9	1.78 (1H, dt, 2.5, 14.0) 1.36 (1H, td, 3.7, 13.7)	38.0	1.82 (1H, dt, 2.5, 14.2) 1.40 (1H, td, 3.5, 13.8)
6	71.0		71.1	
7	45.2	3.75 (1H, dd, 3.7, 12.5)	45.4	3.79 (1H, dd, 3.9, 12.5)
8	40.9	2.69 (1H, dd, 3.6, 12.7) 2.03 (1H, t, 12.7)	41.2	2.78 (1H, dd, 3.9, 12.7) 2.12 (1H, t, 12.6)
9	198.9		198.9	
10	133.7	6.02 (1H, d, 16.1)	133.8	6.04 (1H, d, 16.1)
11	140.4	8.55 (1H, dd, 11.3, 16.3)	140.4	8.61 (1H, dd, 11.3, 16.7)
12	128.24	6.35 (1H, t, 11.5)	128.3 ^a	6.36 (1H, t, 11.3)
13	127.6	6.71 (1H, d, 11.5)	127.6	6.72 (1H, d, 11.6)
14	152.5		152.6	
15	122.5	7.85 (1H, s)	122.5	7.86 (1H, s)
16	172.9		173.0	
17	47.4	5.16 (1H, quintet, 6.4)	47.4	5.20 (1H, quintet, 6.5)
18	21.4	1.57 (3H, d, 6.7)	21.4	1.59 (3H, d, 6.7)
19	18.8	1.14 (3H, s)	18.8	1.26 (3H, s)
20	44.1	3.45 (1H, q, 7.0)	44.5	3.41 (1H, q, 7.0)
21	173.5		173.5	
22	12.7	1.11 (3H, d, 7.0)	13.0	1.06 (3H, d, 7.0)
1'	171.1		170.8	
2'	56.3	5.40 (1H, d, 7.1)	56.1	5.40 (1H, d, 7.4)
3'	136.2		137.0	
4'	128.21	7.41-7.39 (2H, m)	127.8 ^b	7.43-7.42 (2H, m)
5'	128.1	7.34-7.32 (2H, m)	128.3 ^a	7.35-7.33 (2H, m)
6'	127.9	7.32-7.30 (1H, m)	127.8 ^b	7.31-7.30 (1H, m)
7'	52.1	3.62 (3H, s)	52.0	3.60 (3H, s)
1-NH		8.51 (1H, d, 6.3)		8.54 (1H, d, 6.4)
21-NH		8.57 (1H, d, 6.9)		8.67 (1H, d, 7.3)
6-OH		4.18 (1H, br s)		4.24 (1H, br s)

^{a,b}overlapped

Table S42. ^1H NMR (700 MHz) and ^{13}C NMR (175 MHz) data of WSM A1, WSM A2 and WSM A3 in $\text{DMSO}-d_6$

No.	WSM A1		WSM A2		WSM A3	
	δ_{C}	δ_{H}	δ_{C}	δ_{H}	δ_{C}	δ_{H}
1	169.1		169.2		168.8	
2	40.5	3.04 (1H, d, 13.9) 2.40 (1H, d, 13.9)	41.2	3.25 (1H, d, 14.4) 2.47 (1H, d, 14.5)	40.7	3.08 (1H, d, 14.4) 2.64 (1H, d, 13.9)
3	44.9		46.4		46.2	
4	36.6 ^b	2.02 (1H, td, 3.5, 14.1) 1.94 (1H, dt, 2.5, 14.1)	42.0	2.27 (1H, m) 1.92 (1H, dt, 5.1, 14.1)	35.2	2.09 (1H, d, 14.4) 2.00 (1H, t, 12.7)
5	38.0	1.77 (1H, dt, 2.3, 13.8) 1.42 (1H, td, 3.4, 14.1)	32.6	2.26-2.20 (2H, m)	35.3	1.72 (1H, dt, 2.9, 12.7) 1.68 (1H, td, 3.5, 12.8)
6	71.2		147.5		81.2	
7	44.7	3.47 (1H, dd, 5.4, 9.2)	38.9	4.05 (1H, dd, 2.2, 11.4)	45.0	3.13 (1H, dd, 6.2, 13.5)
8	33.9	2.54-2.50 (1H, m) 2.25 (1H, dd, 4.7, 13.7)	34.4	2.75 (1H, dd, 12.0, 13.7) 2.53 (1H, dd, 2.1, 12.4)	32.6	2.15 (1H, dd, 6.1, 12.1) 1.86 (1H, t, 12.8)
9	144.9		142.6		83.6	
10	132.9	6.38 (1H, d, 16.5)	132.7	6.46 (1H, d, 16.6)	133.6	5.93 (1H, d, 16.5)
11	126.7	7.78 (1H, d, 13.2)	125.9	7.96 (1H, d, 16.6)	125.9	7.50 (1H, d, 16.4)
12	138.8		138.0		139.1	
13	120.2 ^a	6.35 (1H, s)	120.9	6.36 (1H, s)	119.9	6.34 (1H, s)
14	152.7		152.7		151.9	
15	118.4	7.48 (1H, s)	118.9	7.50 (1H, s)	118.1	7.51 (1H, s)
16	170.5		171.2		170.1	
17	47.5	5.16-5.13 (1H, m)	47.4	5.21 (1H, quintet, 6.9)	48.1	5.06 (1H, quintet, 5.9)
18	23.0	1.50 (3H, d, 6.5)	22.9	1.54 (3H, d, 6.7)	23.2	1.52 (3H, d, 6.5)
19	36.6 ^b	2.37-2.33 (1H, m) 2.31-2.28 (1H, m)	36.2	2.36-2.31 (2H, m)	36.3	2.37 (1H, ddd, 6.2, 8.3, 14.3) 2.25 (1H, ddd, 6.8, 8.3, 14.7)
20	22.3	1.53-1.50 (2H, m)	22.4	1.54-1.50 (2H, m)	21.6	1.55-1.49 (2H, m)
21	14.0	0.94 (3H, t, 7.3)	14.0	0.94 (3H, t, 7.4)	14.0	0.92 (3H, t, 7.3)
22	120.2 ^a	5.16 (1H, s) 5.11 (1H, s)	123.0	5.35 (1H, s) 5.31 (1H, s)	69.0	3.42 (2H, s)
23	19.2	1.32 (3H, s)	107.8	5.09 (1H, s) 4.88 (1H, s)	19.9	1.23 (3H, s)
24	43.1	2.64 (1H, d, 15.4) 2.39 (1H, d, 15.4)	43.2	2.63 (1H, d, 15.3) 2.40 (1H, d, 15.3)	44.9	2.73 (1H, d, 14.7) 2.54 (1H, d, 13.9)
25	170.9		170.6		171.6	
<u>CO₂H</u>				12.27 (1H, br s)		12.46 (1H, br s)
<u>NH</u>		7.89 (1H, d, 6.6)		8.21 (1H, d, 7.2)		7.80 (1H, d, 5.0)
<u>OH</u>		3.81 (1H, br s)				4.87 (1H, br s)

^{a,b}overlapped

Table S43. ^1H NMR (700 MHz) and ^{13}C NMR (175 MHz) data of (*S*)- and (*R*)-PGME-WSM A2 in $\text{DMSO}-d_6$

No.	(<i>S</i>)-PGME-WSM A2		(<i>R</i>)-PGME-WSM A2	
	δ_{C}	δ_{H}	δ_{C}	δ_{H}
1	169.8		170.7	
2	40.7	3.26 (1H, d, 14.3) 2.31 (1H, d, 14.4)	40.3	3.49 (1H, d, 13.9) 2.80 (1H, d, 14.0)
3	47.1		47.4	
4	42.4	2.02 (1H, td, 3.6, 13.6) 1.88 (1H, ddd, 6.0, 11.3, 13.5)	43.0	1.96 (1H, td, 3.8, 13.5) 1.88 (1H, dt, 4.1, 13.1)
5	32.7	2.21-2.19 (2H, m)	32.7	2.27 (1H, dt, 2.7, 13.2) 2.23 (1H, td, 4.1, 13.7)
6	147.8		148.0	
7	38.8	4.07 (1H, dd, 2.3, 11.5)	38.8	4.15 (1H, dd, 2.3, 11.4)
8	34.4	2.74 (1H, dd, 12.0, 13.7) 2.52 (1H, dd, 2.2, 13.9)	34.3	2.74 (1H, dd, 12.0, 13.7) 2.51-2.49 ^b (1H, m)
9	142.6		142.6	
10	132.7	6.47 (1H, d, 16.7)	133.0	6.49 (1H, d, 16.6)
11	125.9	7.99 (1H, d, 16.6)	125.9	8.00 (1H, d, 16.6)
12	138.0		138.2	
13	120.8	6.36 (1H, s)	120.7	6.38 (1H, s)
14	152.8		152.8	
15	118.8	7.50 (1H, s)	118.8	7.52 (1H, s)
16	170.89 ^a		170.2	
17	47.6	5.19 (1H, quintet, 9.6)	48.0	5.21 (1H, quintet, 7.0)
18	22.8	1.55 (3H, d, 6.6)	22.9	1.54 (3H, d, 6.6)
19	36.2	2.36 (1H, td, 6.8, 14.1) 2.32 (1H, td, 6.8, 14.1)	36.3	2.37 (1H, td, 7.3, 14.2) 2.34 (1H, td, 7.4, 14.2)
20	22.4	1.54 (2H, m)	22.5	1.55-1.51 (2H, m)
21	14.0	0.94 (3H, t, 7.4)	14.1	0.95 (3H, t, 7.4)
22	123.1	5.35 (1H, s) 5.32 (1H, s)	123.4	5.37 (1H, s) 5.33 (1H, s)
23	107.7	5.10 (1H, s) 4.88 (1H, s)	107.8	5.12 (1H, s) 4.90 (1H, s)
24	44.5	2.71 (1H, d, 13.3) 2.27 (1H, d, 13.2)	45.5	2.68 (1H, d, 12.5) 2.12 (1H, d, 12.5)
25	168.0		168.2	
1'	170.91 ^a		171.4	
2'	56.4	5.39 (1H, d, 6.8)	56.8	5.35 (1H, d, 7.0)
3'	136.1		135.5	
4'	127.7	7.39-7.38 (2H, m)	127.6	7.42-7.39 (2H, m)
5'	128.8	7.39-7.38 (2H, m)	129.0	7.43-7.40 (2H, m)
6'	128.3	7.36-7.33 (1H, m)	128.5	7.40-7.37 (1H, m)
7'	52.2	3.62 (3H, s)	52.3	3.60 (3H, s)
1-NH		8.21 (1H, d, 6.9)		8.11 (1H, d, 6.4)
25-NH		9.01 (1H, d, 6.8)		9.29 (1H, d, 7.1)

^ainterchangeable. ^boverlapped with solvent.

Table S44. ^1H NMR (700 MHz) and ^{13}C NMR (175 MHz) data of GNM B1 and GNM B2 in DMSO- d_6

No.	GNM B1		GNM B2	
	δ_{C}	δ_{H}	δ_{C}	δ_{H}
1	170.2		170.9	
2	38.6	3.03 (1H, d, 15.4) 2.43 (1H, d, 15.5)	39.3 ^b	2.88 (1H, d, 16.4) 2.76 (1H, d, 15.8)
3	43.9		44.9	
4	37.5	1.98 (1H, m) 1.79 (1H, dt, 2.9, 13.9)	37.4	2.23 (1H, d, 14.1) 1.73 (1H, m)
5	38.8	1.69 (1H, t, 13.9) 1.42 (1H, m)	32.7	1.66 (1H, m) 1.56 (1H, m)
6	71.4		76.4	
7	45.0	3.51 (1H, dd, 3.3, 8.8)	41.6	3.53 ^c (1H, m)
8	31.7	2.64 (1H, d, 13.7) 2.57 (1H, dd, 9.0, 13.7)	33.5	2.45 (1H, dd, 10.6, 13.8) 2.32 (1H, d, 13.6)
9	145.0		144.8	
10	133.4	6.36 (1H, d, 16.2)	133.5 ^d	6.38 (1H, d, 16.2)
11	128.6	8.09 (1H, d, 16.2)	127.2	7.96 (1H, d, 16.5)
12	133.6		133.5 ^d	
13	121.7	6.27 (1H, s)	121.7	6.28 (1H, s)
14	153.1		153.1	
15	117.0	7.32 (1H, s)	117.2	7.33 (1H, s)
16	173.4		173.9	
17	34.7		34.4	
18 ^a	19.5	1.42 (1H, m) 1.24 (1H, m)	19.4	1.45 (1H, m) 1.09 (1H, m)
19 ^a	19.2	1.47 (1H, m) 1.42 (1H, m)	19.0	1.41 (2H, m)
20	21.1	1.97 (3H, s)	21.3	1.98 (3H, s)
21	120.9	5.20 (2H, s)	119.6	5.12 (1H, s) 5.07 (1H, s)
22	20.1	1.33 (3H, s)	16.8	1.37 (3H, s)
23	43.3	2.77 (1H, d, 15.1) 2.27 (1H, d, 15.1)	47.0	2.50 ^b (1H, m) 1.98 (1H, m)
24	171.1		172.3	
25			48.1	3.01 (3H, s)
CO₂H		12.10 (1H, br s)		
NH		8.97 (1H, br s)		9.31 (1H, br s)
OH		4.33 (1H, br s)		

^ainterchangeable. ^boverlapped with the solvent. ^coverlapped with water peak. ^doverlapped.

Fig. S1. Proposed biosynthetic pathway of leinamycin (LNM) in *S. atroolivaceus* S-140 and the modes of action for LNM and LNM E1 as DNA damaging antitumor antibiotics. **(A)** Genetic organization of *lnm* gene cluster. **(B)** The biosynthetic machinery of LNM featuring a hybrid NRPS-AT-less type I PKS (LnmQPIJ) with a discrete acyl transferase (AT, LnmG) loading malonyl-CoA as the extender unit to all six PKS modules, and a set of enzymes consisting of LnmKLMF responsible for the installation of the β -alkyl branch at C3 position. The DUF-SH didomain in PKS module-8 was proposed to be involved in the incorporation of 3-thiol group during LNM biosynthesis. After off-loaded from the PKS by TE domain, the nascent product LNM E1 was modified by tailoring enzymes to afford the natural product LNM. Colored structural moieties indicate their biosynthetic origin installed by NRPS (blue), PKS (red), β -alkyl branching cassette (green), and other tailoring enzymes (black). A, adenylation protein; Cy, condensation/cyclization domain; DH, dehydratase domain; DUF, domain of unknown function; KR, ketoreductase domain; KS, ketosynthase domain; KS⁰, nonelongating KS domain; MT, methyltransferase domain; Ox, oxidation domain; SH, cysteine lyase domain; TE, thioesterase domain; solid blue circle, peptidyl carrier protein (PCP); solid red circle, acyl carrier protein (ACP). Gaps between domains denote protein boundaries, and solid line-connect domains are in the same protein. **(C)** LNM can be activated by cellular thiols to form a hydrodisulfide derivative, causing oxidative DNA damage, and an episulfonium ion intermediate that can alkylate DNA, thus leading to cell death. LNM E1 can be oxidatively activated by reactive oxygen species (ROS) to give a similar episulfonium ion intermediate, thereby alkylating DNA and leading to eventual cell death.

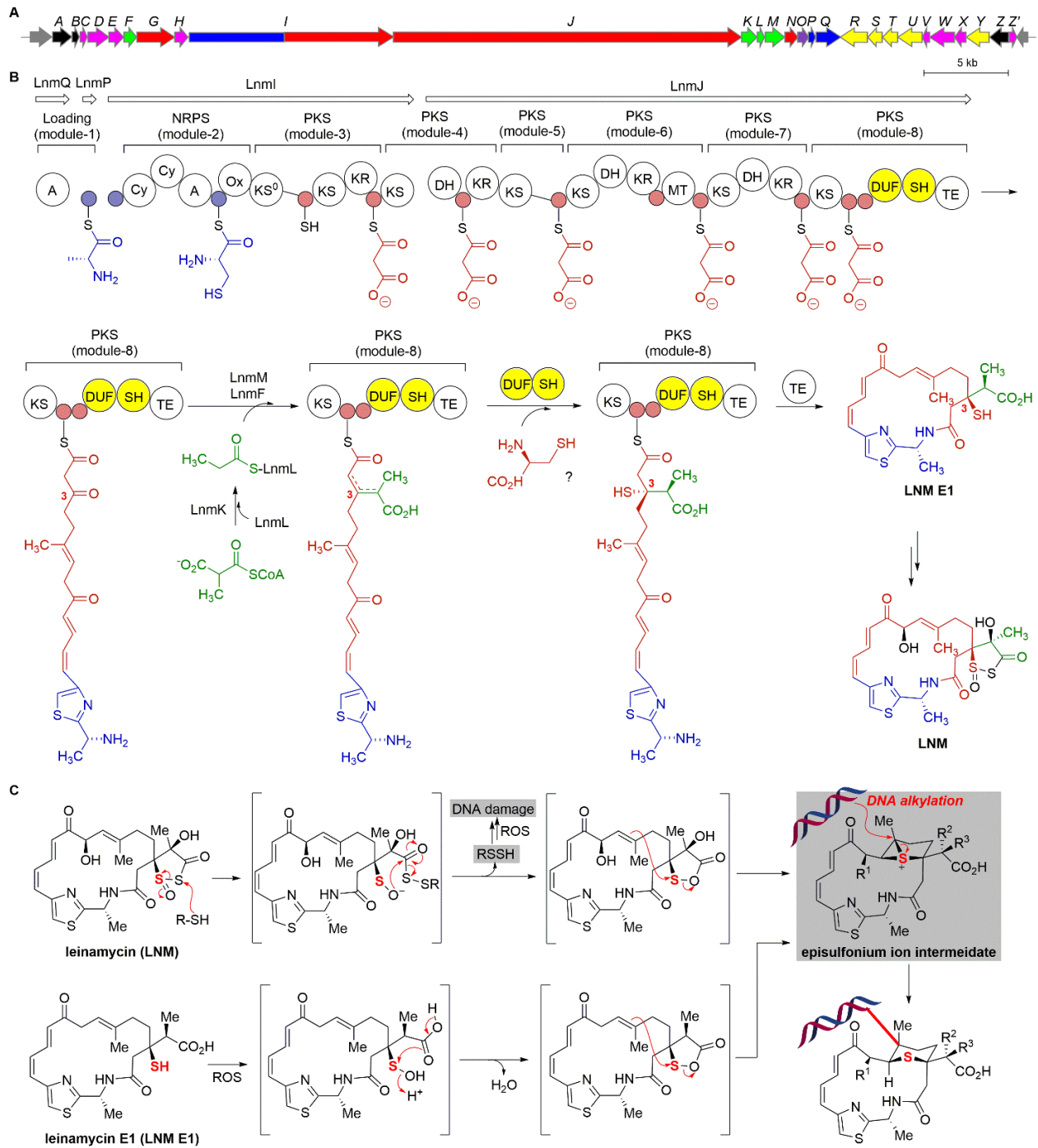


Fig. S2. Discovery-based approach to combinatorial biosynthesis for the LNM family of natural products by genome mining for the *lhm*-type gene clusters. **(A)** Identification of 19 *lhm*-type gene clusters from public databases including ~12,000 actinobacterial genomes using DUF-SH didomain as a probe. **(B)** A high-throughput method for the identification of *lhm*-type gene clusters from 5,000 strains of the actinomycetes collection at TSRI (including ~100 from the Naicons' collection and ~500 from Myongji University). Real-time PCR with degenerate primers targeting the 0.6-kb internal fragment of DUF-SH didomain-coding sequence afforded 51 hits based on the analysis of melting curves and gel electrophoresis of the corresponding PCR products. All the 72 hits were further confirmed to be true by sequencing a 1.2-kb PCR-amplified internal fragment of DUF-SH didomain-coding sequence. The 72 hits were subsequently dereplicated to 30 based on the analysis of the 1.2-kb DNA sequences, taxonomy and geographic locations of the hit strains. **(C)** Representative melting curve analysis in real-time PCR. Each peak represents a specific PCR product. Solid line with open circles represents the positive control with gDNA of *S. atroolivaceus* S-140 (LNM producer) as the template, and dashed line represents the negative control without a template. An inset shows PCR products of the representative hits that were analyzed by agarose gel electrophoresis. **(D)** Pie chart representing the taxonomic distribution of the 49 newly identified potential producers, and the original LNM producer *S. atroolivaceus* S-140. Approximately 74% of the hit strains belong to the *Streptomyces* genus. **(E)** Geographic distribution of the hit strains showing *lhm*-type gene clusters are found worldwide.

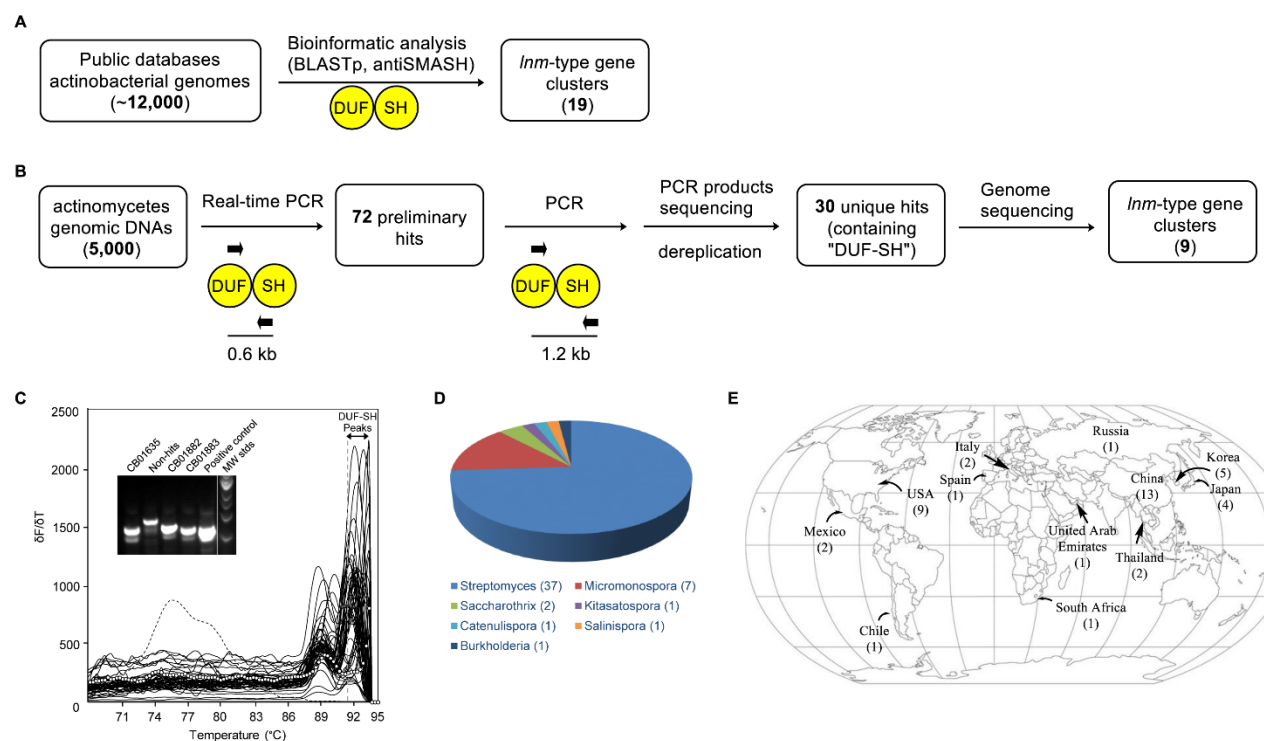
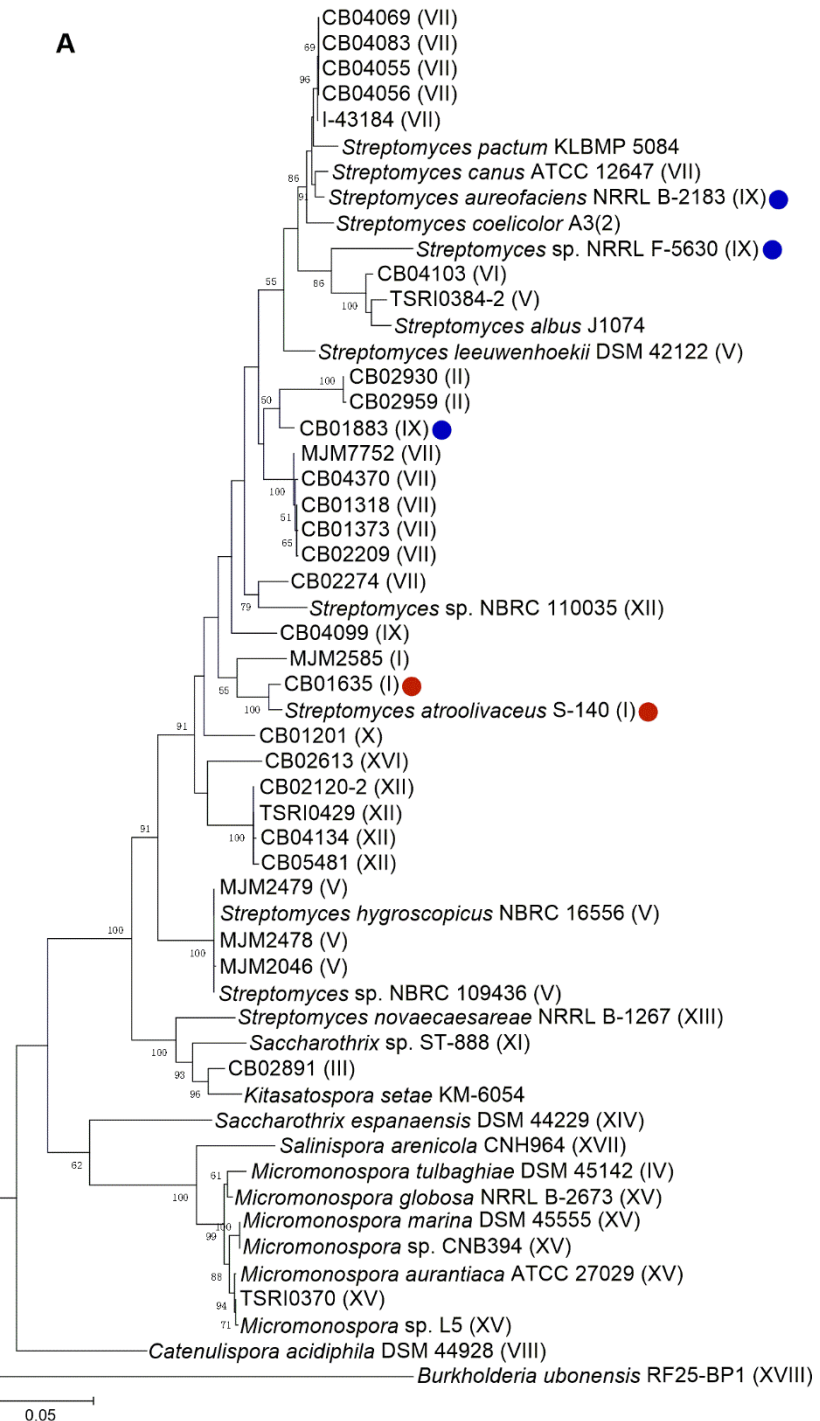
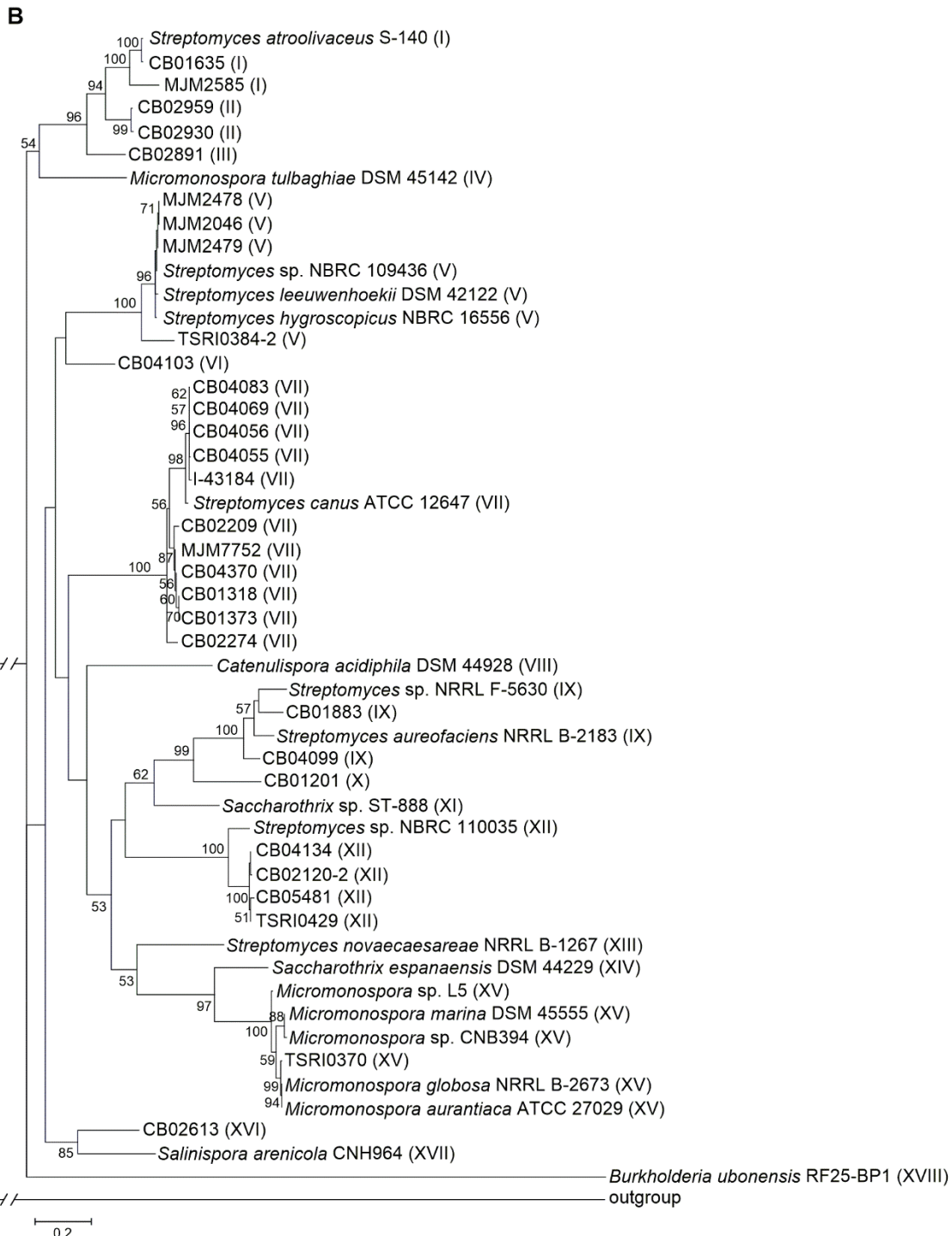
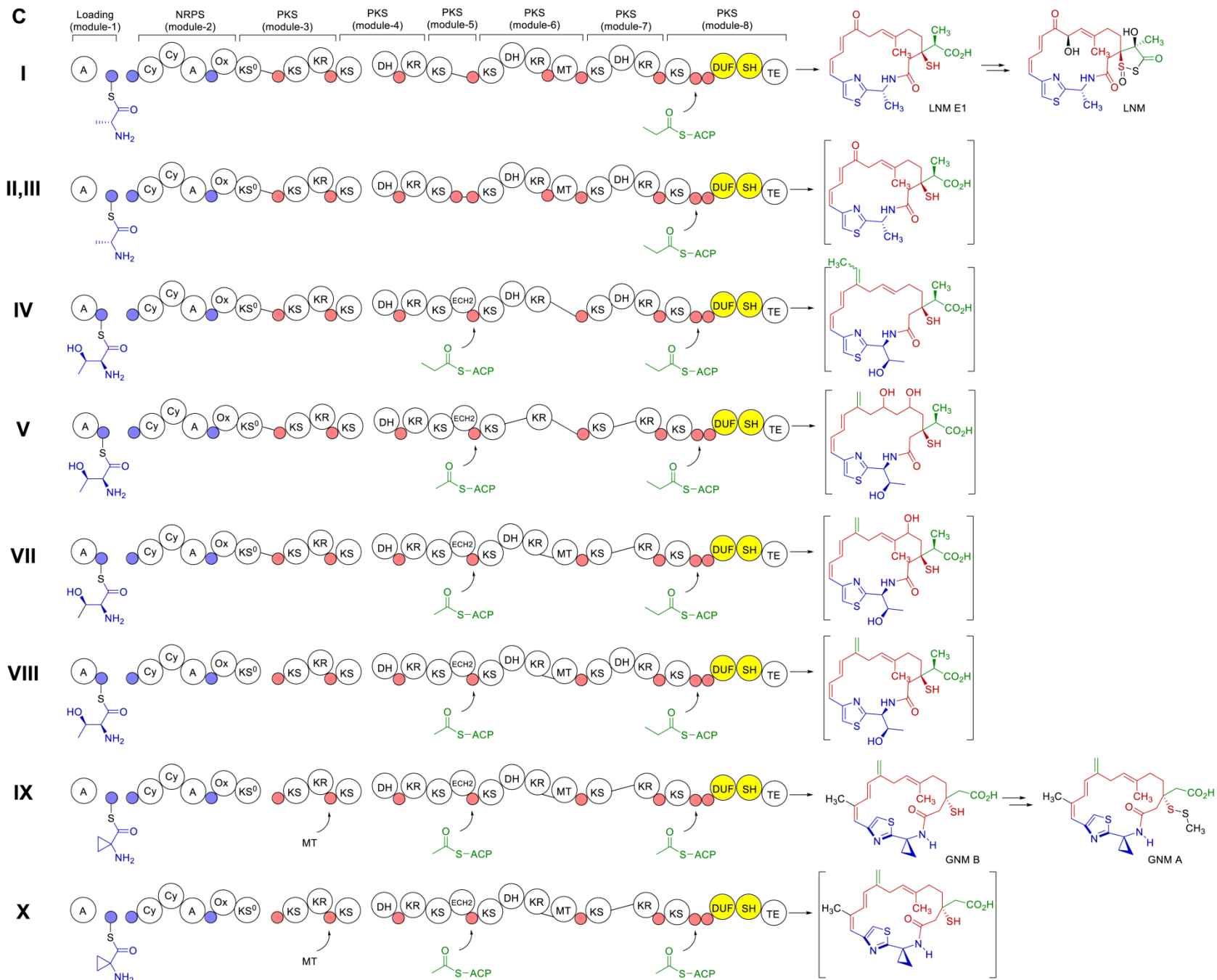


Fig. S3. Phylogenetic analysis of the hit strains, and domain organization and the proposed/identified nascent products of the hybrid NRPS-PKS biosynthetic machineries of LNM-type natural products from different clades. **(A)** Phylogenetic analysis of the taxonomy of the 49 hit strains, as well as the known LNM producer *S. atroolivacues* S-140, based on the concatenated partial sequences of the three housekeeping genes including 16S rRNA, *recA* and *trpB* (**Table S1**), in comparison with several known strains from databases. Selected strains included *Streptomyces pactum* KLBMP 5084 (NZ_CP016795); *Streptomyces coelicolor* A3(2) (NC_003888); *Streptomyces albus* J1074 (NC_020990); *Kitasatospora setae* KM-6054 (NC_016109). LNM E1 producers are highlighted with red dots. GNMs producers are highlighted with blue dots. The Roman numerals in the parentheses denote the different clades of the *Inm*-type gene clusters (see **Figs. 2** and **S3B** for detailed information). **(B)** Phylogenetic analysis of the 49 *Inm*-type gene cluster harboring strains based on the translated 1.2-kb internal fragment of DUF-SH didomain with *S. atroolivaceus* S-140 as a reference. CalE6 (AAM94792), methionine γ-lyase from *Micromonospora echiospora*, was used as an outgroup reference. Also see **Fig. 2** in main text for detailed information of *Inm*-type gene clusters. The accession number of LnmJ homologues of hit strains from public databases are as follows: clade IV, *Micromonospora tulbaghiae* DSM 45142 (SCE73393); clade V, *Streptomyces* sp. NBRC 109436 (WP_064455881); *S. hygroscopicus* NBRC 16556 (WP_063816964); *S. leeuwenhoekii* DSM 42122 (CQR60407); clade VII, *S. canus* ATCC 12647 (WP_059300321); clade VIII, *Catenulispura acidiphila* DSM 44928 (ACU71516.1); clade IX, *Streptomyces* sp. NRRL F-5630 (WP_037826198); *S. aureofaciens* NRRL B-2183 (WP_052841990); clade XI, *Saccharothrix* sp. ST-888 (KJK59202.1); clade XII, *Streptomyces* sp. NBRC 110035 (WP_042163782); clade XIII, *S. novaecaesareae* NRRL B-1267 (WP_033331212); clade XIV, *Saccharothrix espanaensis* DSM 44229 (WP_015102008); clade XV, *Micromonospora* sp. L5 (WP_013476297); *Micromonospora* sp. CNB394 (WP_026267551); *M. marina* DSM 45555 (SCE83186); *M. aurantiaca* ATCC 27029 (WP_013287043); *M. globosa* NRRL B-2673 (WP_030268223); clade XVII, *Salinispora arenicola* CNH964 (not available); clade XVIII, *Burkholderia ubonensis* RF25-BP1 (WP_059615564). **(C)** Compared to LNM pathway, variations at module-1 (different priming amino acids), module-3 (incorporation of unusual extender unit and/or trans-acting modification), module-5 (β-alkylation), module-6 and -7 (α-/β-modifications) and module-8 (β-alkylation and C3-stereochemistry) are identified in the newly discovered pathways. Gaps between domains denote protein boundaries; solid lines connect domains in the same protein; “X” denotes the amino acids whose structures are not bioinformatically predicted.







C (continued)

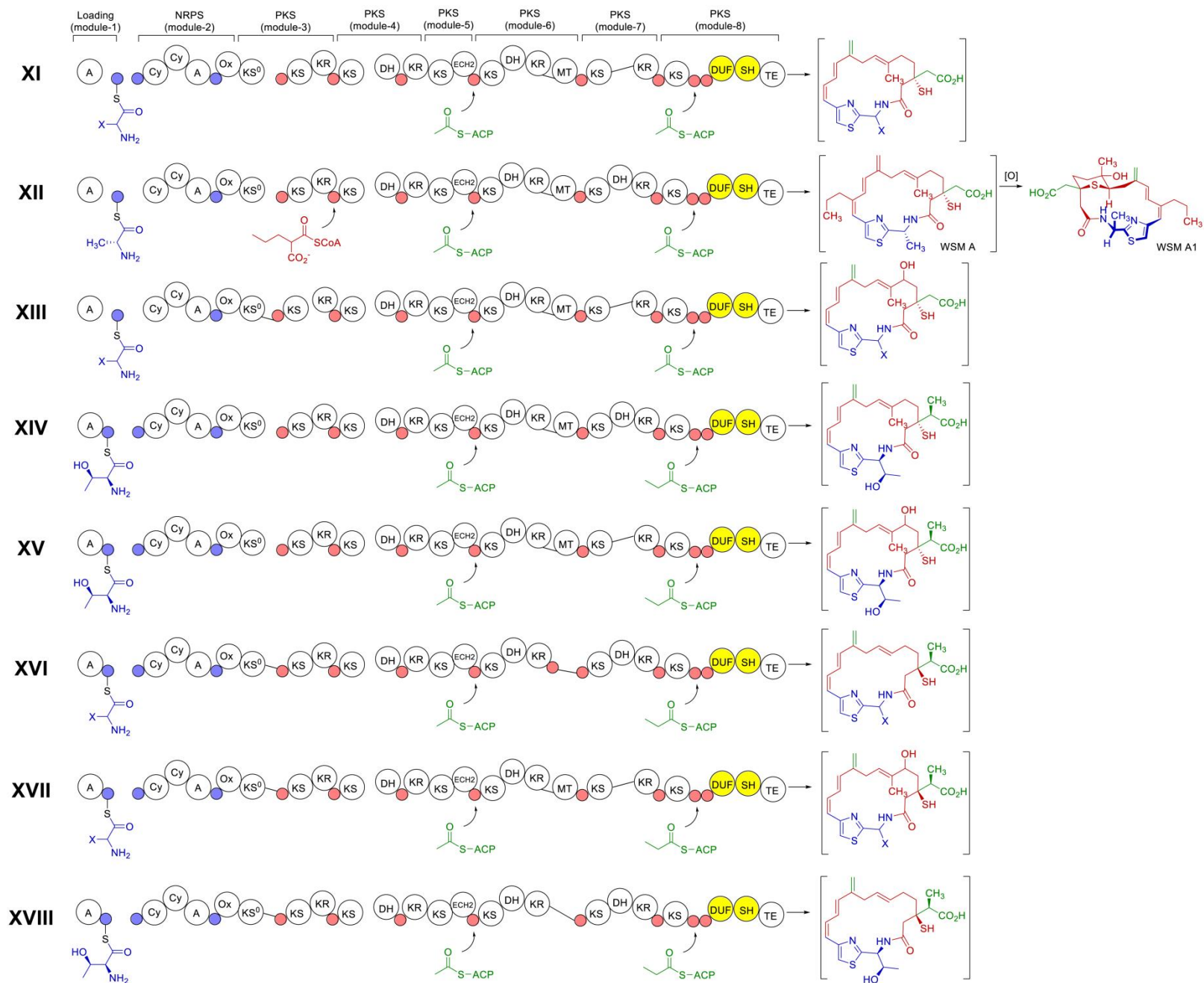
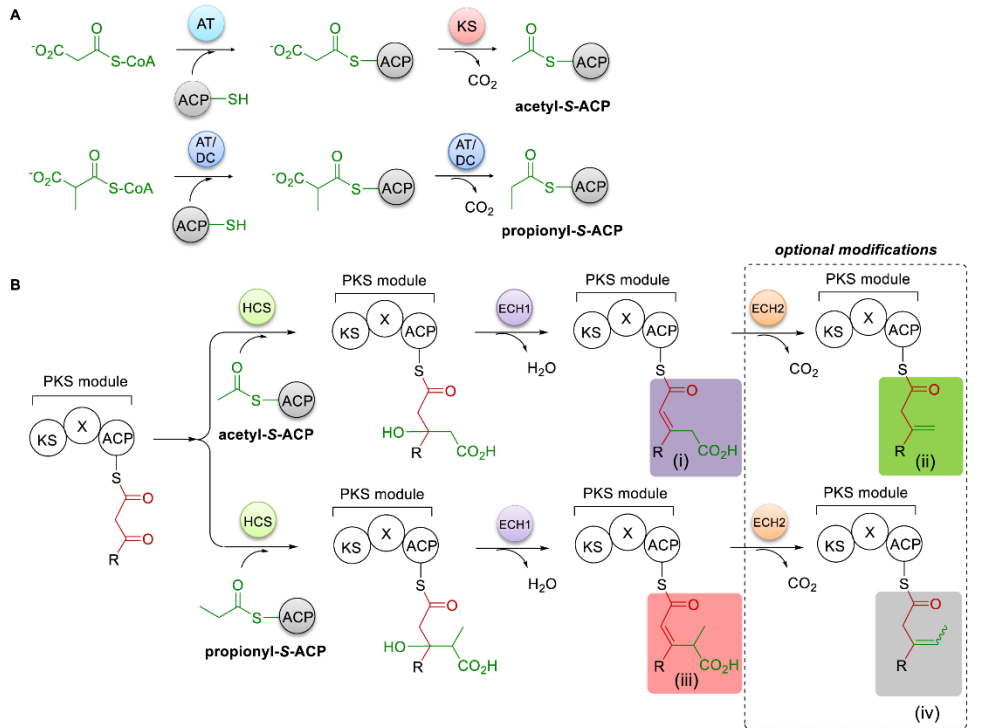


Fig. S4. The variations of β-branch pathway in the biosynthesis of LNM-type natural products. **(A)** Biosynthetic pathways of acetyl-S-ACP and propionyl-S-ACP. **(B)** Installation of different structural moieties by β-alkyl branching processes during polyketide biosynthesis. HCS, hydroxymethylglutaryl-CoA synthase; ECH1: enoyl-CoA hydratase 1; ECH2: enoyl-CoA hydratase 2. “X” denotes the potential accessory domains in PKS module. **(C)** β-alkylation related enzymes from the 17 representative LNM-type pathways (one representative pathway from each clade, except clade VI, was shown) and the corresponding structural outcomes at C-3 and/or C-9 of the final products. “#” denotes the trans-acting AT that was proposed to be responsible for loading malonyl-CoA to each ACP of the six PKS modules. The “star” mark indicates that ECH2 was integrated into the PKS as a domain. The Roman numerals in the first column denote the different clades of the *Inm*-type gene clusters (see **Fig. S3B** and **Fig. 2** in main text for detailed information).



C	AT	KS	AT/DC	ACP	HCS	ECH1	ECH2*	Structural outcome
I	-	-	LnmK	LnmL	LnmM	LnmF	-	C-3 (iii)
II	-	-	CB02959_J	CB02959_K	CB02959_L	CB02959_E	-	C-3 (iii)
III	-	-	CB02891_Q	CB02891_R	CB02891_S	CB02891_L	-	C-3 (iii)
IV	-	-	Mtu1_M	Mtu1_N	Mtu1_O	Mtu1_H	-	C-3 (iii)
	-	-	Mtu1_M	Mtu1_N	Mtu1_O	Mtu1_H	Mtu1_L	C-9 (iv)
V	-	-	TSRI0384-2_M	TSRI0384-2_N	TSRI0384-2_O	TSRI0384-2_E	-	C-3 (iii)
	TSRI0384-2_F#	TSRI0384-2_Q	-	TSRI0384-2_P	TSRI0384-2_D	TSRI0384-2_E	TSRI0384-2_L	C-9 (ii)
VII	-	-	CB01373_V	CB01373_W	CB01373_X	CB01373_N	-	C-3 (iii)
	CB01373_O#	CB01373_Z	-	CB01373_Y	CB01373_M	CB01373_N	CB01373_U	C-9 (ii)
VIII	-	-	Caci_W	Caci_X	Caci_Y	Caci_T	-	C-3 (iii)
	Caci_K#	Caci_Z2	-	Caci_Z1	Caci_S	Caci_T	Caci_V	C-9 (ii)
IX	GnmG	GnmW	-	GnmV	GnmU	GnmF	-	C-3 (i)
	GnmG	GnmW	-	GnmV	GnmE	GnmF	GnmT	C-9 (ii)
X	CB01201_G	CB01201_W	-	CB01201_V	CB01201_U	CB01201_F	-	C-3 (i)
	CB01201_G	CB01201_W	-	CB01201_V	CB01201_E	CB01201_F	CB01201_T	C-9 (ii)
XI	Sast_J	Sast_Z3	-	Sast_Z2	Sast_Z1	Sast_I	-	C-3 (i)
	Sast_J	Sast_Z3	-	Sast_Z2	Sast_H	Sast_I	Sast_Y	C-9 (ii)
XII	WsmF	WsmU	-	WsmT	WsmS	WsmE	-	C-3 (i)
	WsmF	WsmU	-	WsmT	WsmD	WsmE	WsmR	C-9 (ii)
XIII	Snov_C	Snov_Z3	-	Snov_Z2	Snov_Z1	Snov_B	-	C-3 (i)
	Snov_C	Snov_Z3	-	Snov_Z2	Snov_A	Snov_B	Snov_Y	C-9 (ii)
XIV	-	-	Saes_L	Saes_M	Saes_N	Saes_G	-	C-3 (iii)
	Saes_F	Saes_Z3	-	Saes_Z2	Saes_H	Saes_G	Saes_K	C-9 (ii)
XV	-	-	Maur_K	Maur_L	Maur_M	Maur_G	-	C-3 (iii)
	Maur_F	Maur_Z2	-	Maur_Z1	Maur_B	Maur_G	Maur_J	C-9 (ii)
XVI	-	-	CB02613_U	CB02613_V	CB02613_W	CB02613_Z4	-	C-3 (iii)
	CB02613_I#	CB02613_Y	-	CB02613_X	CB02613_Z5	CB02613_Z4	CB02613_T	C-9 (ii)
XVII	-	-	Sal964_Y	Sal964_Z1	Sal964_Z2	Sal964_O	-	C-3 (iii)
	Sal964_P#	Sal964_Z4	-	Sal964_Z3	Sal964_N	Sal964_O	Sal964_X	C-9 (ii)
XVIII	-	-	Bubo_S	Bubo_T	Bubo_U	Bubo_K	-	C-3 (iii)
	Bubo_L	Bubo_W	-	Bubo_V	Bubo_J	Bubo_K	Bubo_R	C-9 (ii)

Fig. S5. Phylogenetic analysis of the hydroxymethylglutaryl-CoA synthases (HCSs) from LNM and 28 newly discovered LNM-type biosynthetic pathways. The analysis revealed two major groups of HCSs, which are proposed for the installation of the β -alkyl branches at C3 and C9, respectively. The group of HCSs responsible for the installation of β -alkyl branch at C3 tends to be clustered into two subgroups that using propionyl-S-ACP and acetyl-S-ACP as substrates, respectively. The second group of HCSs responsible for the installation of β -alkyl branch at C9 is predicted to use acetyl-S-ACP as the substrate. The HCS from *Staphylococcus aureus* (AAG02422) was used as an outgroup reference. HCSs from the pathways with their corresponding natural products being discovered are highlighted in red. The Roman numerals in parentheses denote the different clades of the *Inm*-type gene clusters (see **Fig. S3B** and **Fig.2** in main text for detailed information).

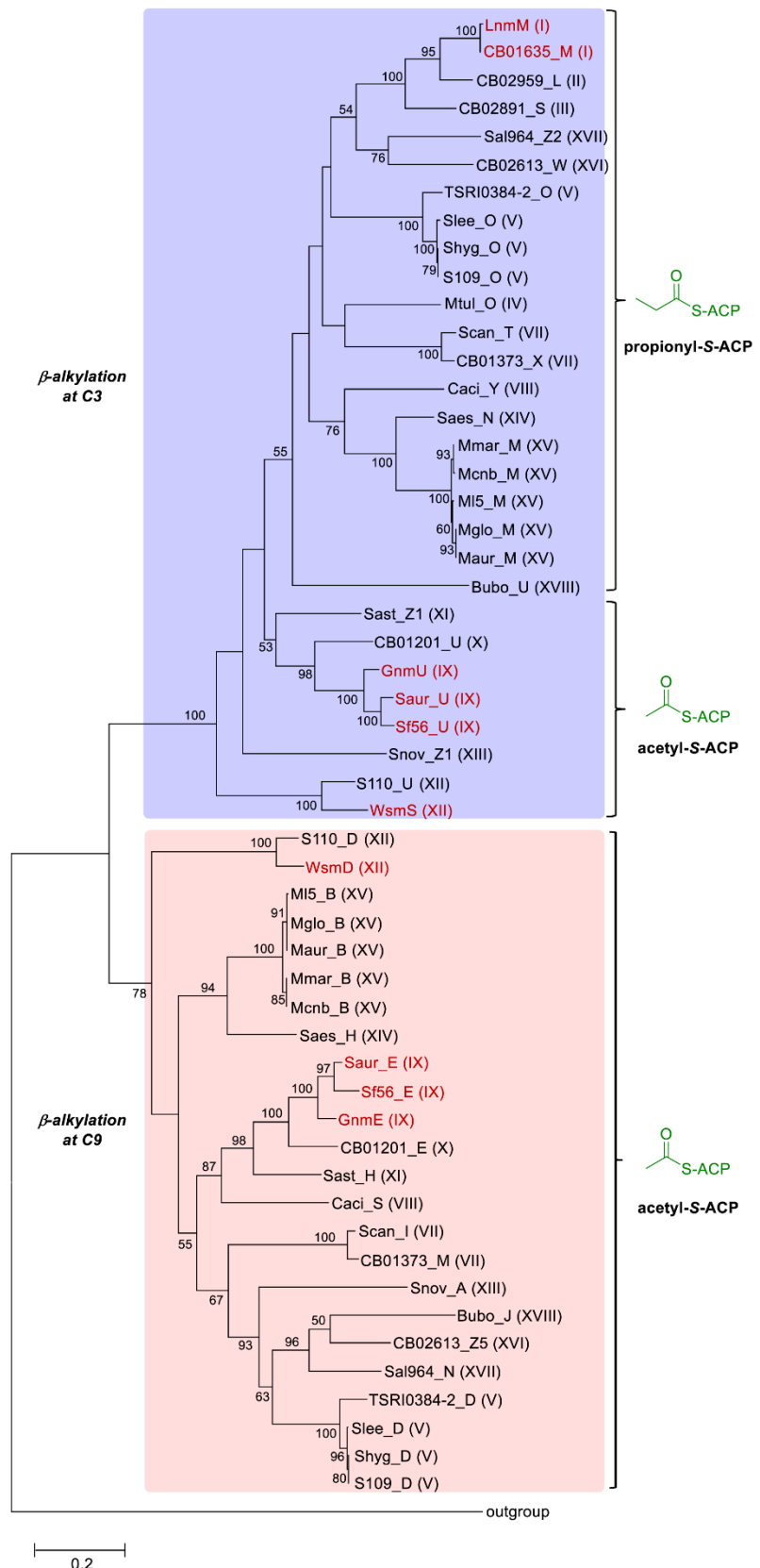


Fig. S6. Phylogenetic analysis of domain of unknown function (DUF domain), and cysteine lyase (SH) domains from LNM and 28 LNM-type biosynthetic pathways. **(A)** The analysis revealed that DUF domains tend to cluster into two groups (highlighted with light blue and light red, respectively). One group of DUF domains are from pathways with C3 β -alkylation using propionyl-S-ACP as the predicted substrate, and the other group are from pathways with C3 β -alkylation using acetyl-S-ACP as the predicted substrate. MprF (EWS52466), the phosphatidylglycerol lysyltransferase from *Methylibium* sp. T29, was used as an outgroup reference. **(B)** The analysis revealed that the SH domains tend to cluster into two groups (highlighted with light red and light blue, respectively). One group of SH domains are from pathways with C3 β -alkylation using acetyl-S-ACP as the predicted substrate, and the other group are from pathways with C3 β -alkylation using propionyl-S-ACP as the predicted substrate. TPL-1 (ABI75028), the tyrosine phenol-lyase from *Citrobacter freundii*, was used as an outgroup reference. The DUF domains/SH domains from the pathways with their corresponding natural products being discovered are highlighted in red. The Roman numerals in parentheses denote the different clades of the *Inm*-type gene clusters (see **Fig. S3B** and **Fig. 2** in main text for detailed information). It should be noted that the configurations at C3 of LNM-type natural products discovered from clade I (LNM) are opposite to those discovered from clades IX (GNM) and XII (WSM).

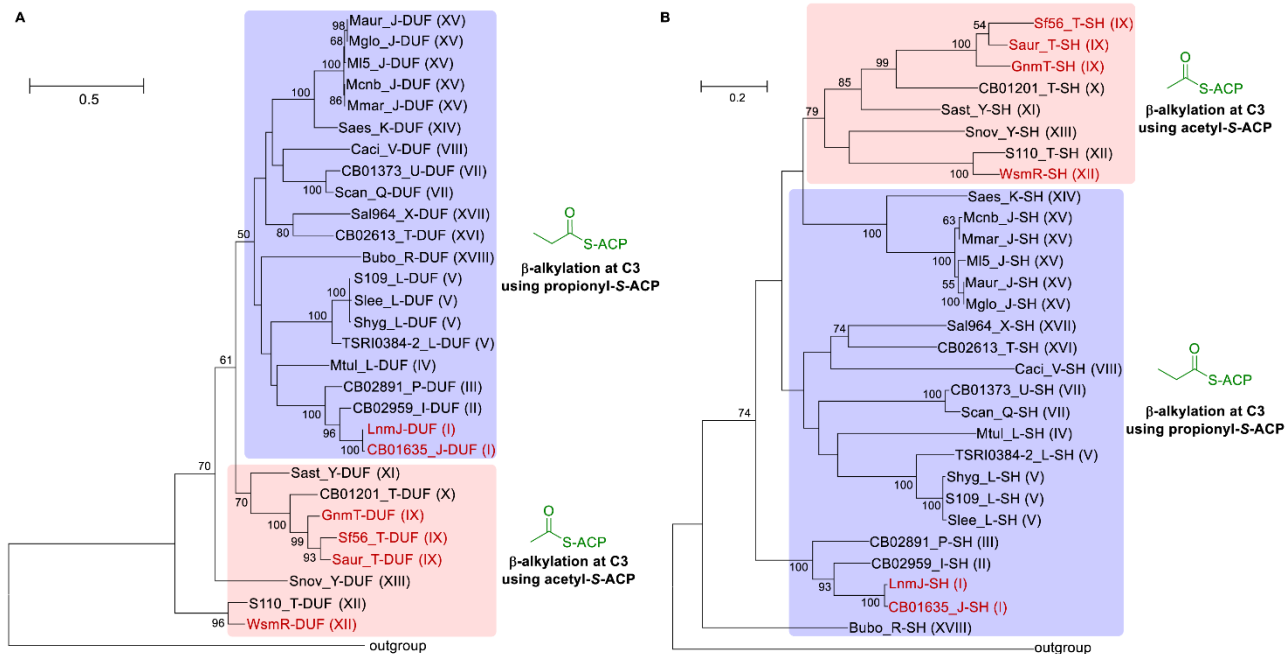


Fig. S7. Genome neighborhood network (GNN) analysis (E value of 10^{-6}) of *Inm* and other 28 new discovered *Inm*-type gene clusters (see Fig. 2 in main text for detailed information) shows that both conserved and diverse proteins are involved in the biosynthesis of LNM-type natural products. The enzymes from the LNM, GNM and WSM biosynthetic pathways are highlighted with red, yellow, and green dots, respectively. The relatively conserved enzymes with unknown functions marked with “1” are proposed to be involved in the post-assembly-line modification steps. In comparison with the LNM pathway, the newly discovered pathways feature various new enzymes, e.g. **2**: discrete methyltransferases; **5**: truncated hemoglobin; **8**: halogenases; **9**: FAD-dependant oxidoreductases; **14**: class-III aminotransferases; **15**: radical SAM superfamily proteins; **19**: aminotransferases; **11** and **12**: unknown functions. Other distinct families of enzymes in the newly discovered pathways include **3** and **18**: glyoxalase/bleomycin resistance protein; **4**: phosphopantetheinyl transferases; **6**: Ydel-like protein; **7**: ferredoxin; **10**: sodium:proton exchanger; **13**: ABC transporter; **16**: TetR family transcriptional regulator; **17**: dTDP-4-dehydrorhamnose 3,5-epimerase.

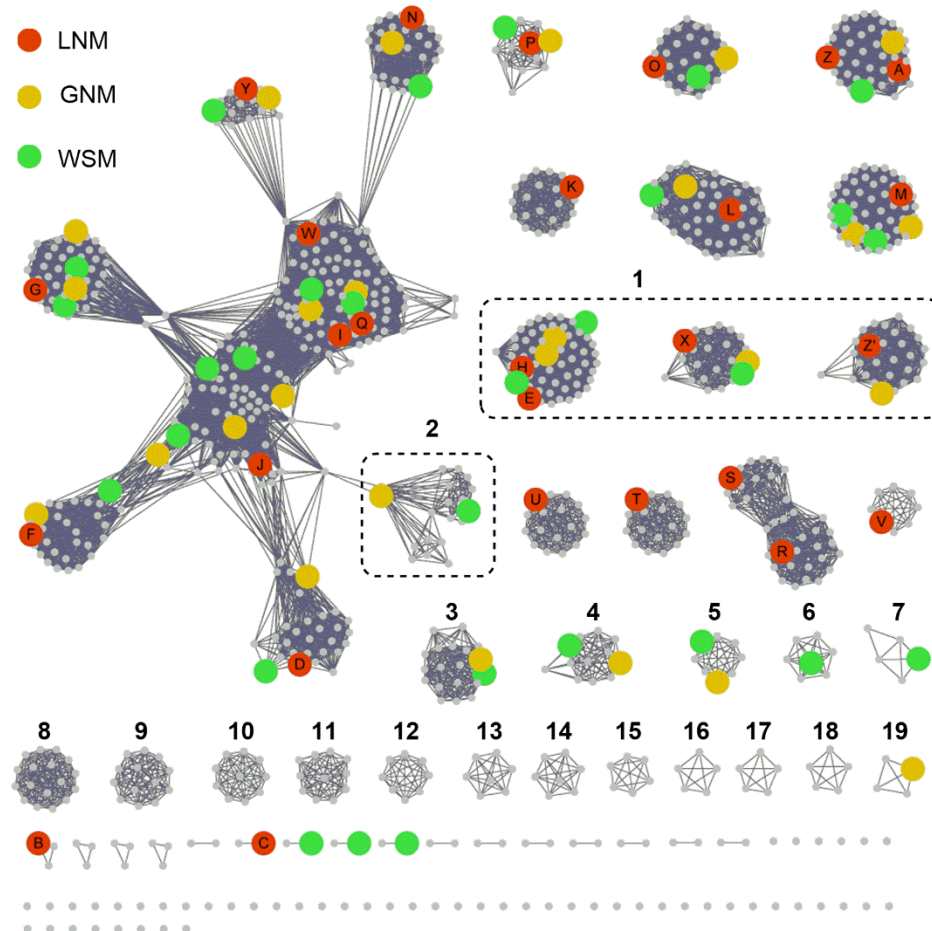


Fig. S8. Construction of the in-frame deletion mutant strain SB21001 (i.e. $\Delta gnmB$) and confirmation of its genotype by Southern analysis. **(A)** Schematic representation for the deletion of *gnmB* in strain CB01883 by homologous recombination. The probe (517 bp) for Southern blot was amplified with primers orf155-SBlot-5n and orf155-SBlot-3n using genomic DNA of strain CB01883 as the template. Apr^S, apramycin sensitive; Apr^R, apramycin resistance; acc(3)/IV, apramycin resistance gene. **(B)** Southern blot verification of strain CB01883 wild-type (4.8 kb) and SB21001 (2.7 kb). Genomic DNAs were digested with *Eco*NI and then used for Southern analysis. Lane 1, DNA marker VII, DIG-labeled (Roche); lane 2, strain CB01883 wild type; lane 3, SB21001.

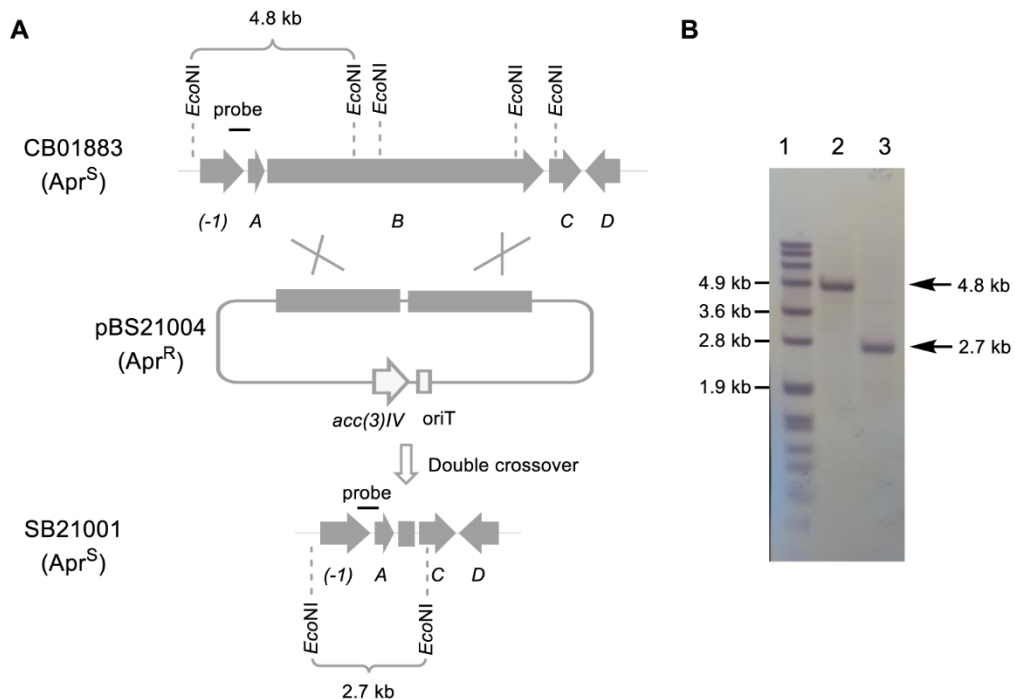


Fig. S9. Proposed biosynthetic pathway of guangnanmycin (GNM) in *S. sp.* CB01883. **(A)** Genetic organization of *gnm* gene cluster, together with two cosmids pBS21001 (1C4) and pBS21002 (1B9) covering the whole gene cluster. **(B)** The biosynthetic machinery of GNM featuring a similar hybrid NRPS-AT-less type I PKS to that of LNM consisting of GnmSRBHT and a discrete AT GnmK, producing GNM B as the nascent product, which was further converted to GNM by tailoring enzymes. **(C)** A set of enzymes including GnmWGVEF and ECH2 domain in PKS module-5 are proposed to be responsible for the installation of the β -alkyl branch at module-5, leading to the formation of a terminal double bond at C9. **(D)** A set of enzymes including GnmWGVUF are proposed to be responsible for the installation of the β -alkyl branch at module-8, leading to the formation of carboxymethyl moiety at C3. Also, the DUF-SH didomain was proposed to be responsible for the installation of 3-thiol group.

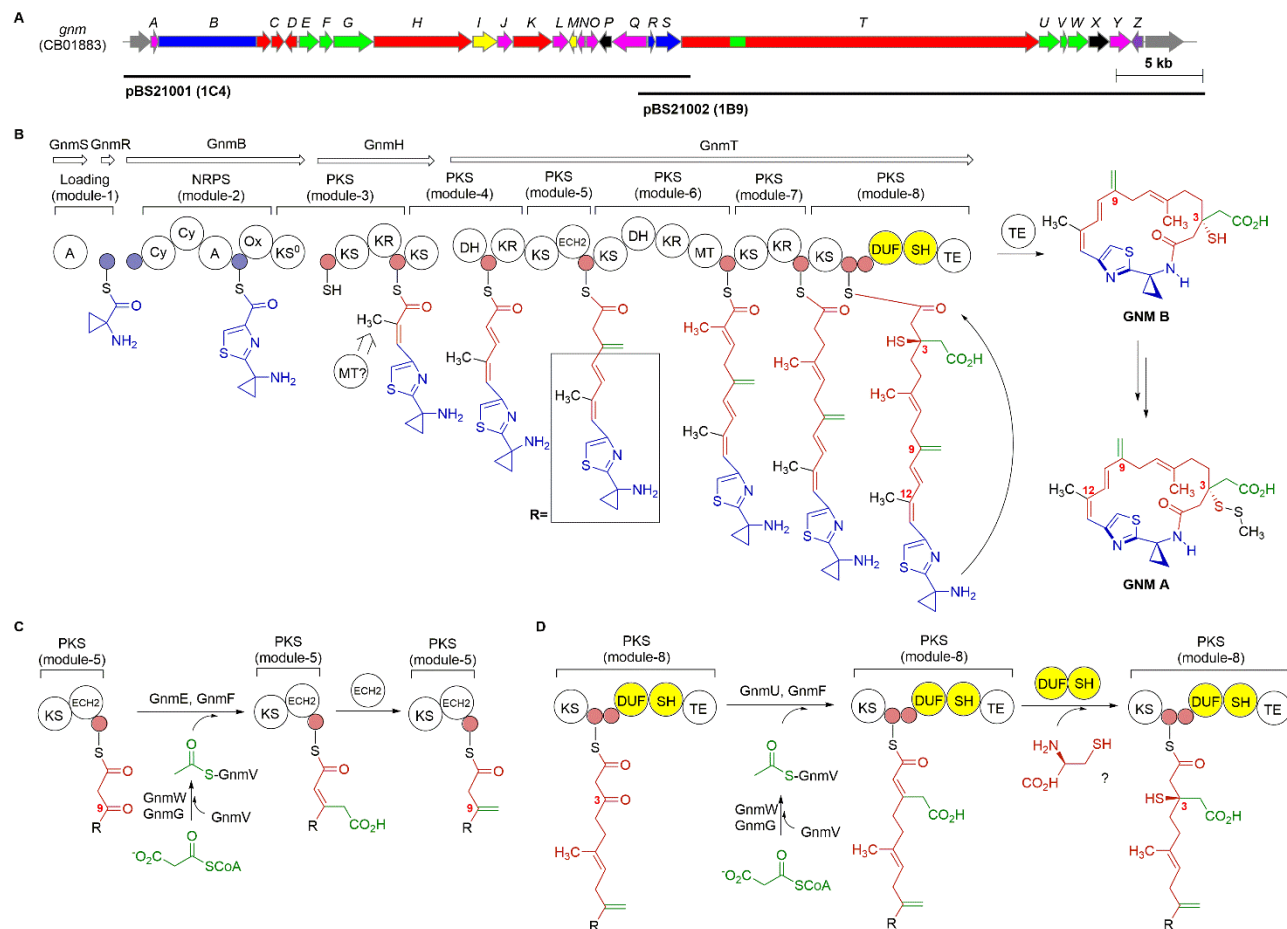


Fig. S10. Elucidation of new metabolites isolated from strain CB01883 wild type and mutant strain SB21003 (i.e. $\Delta gnmO$). Key ^1H - ^1H COSY, HMBC and ROESY correlations are shown.

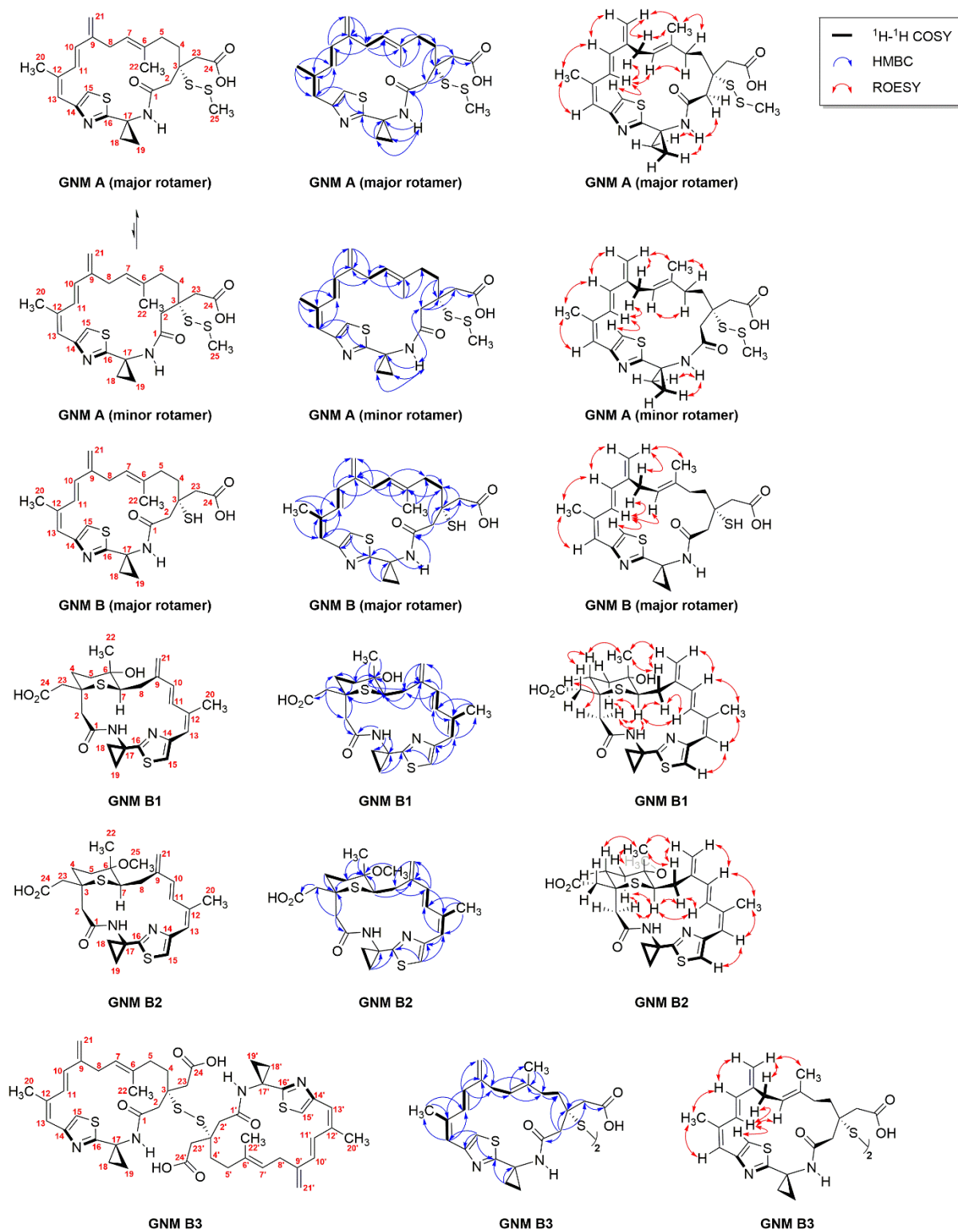


Fig. S11A. ^1H NMR spectra of GNM A (700 MHz, DMSO- d_6)

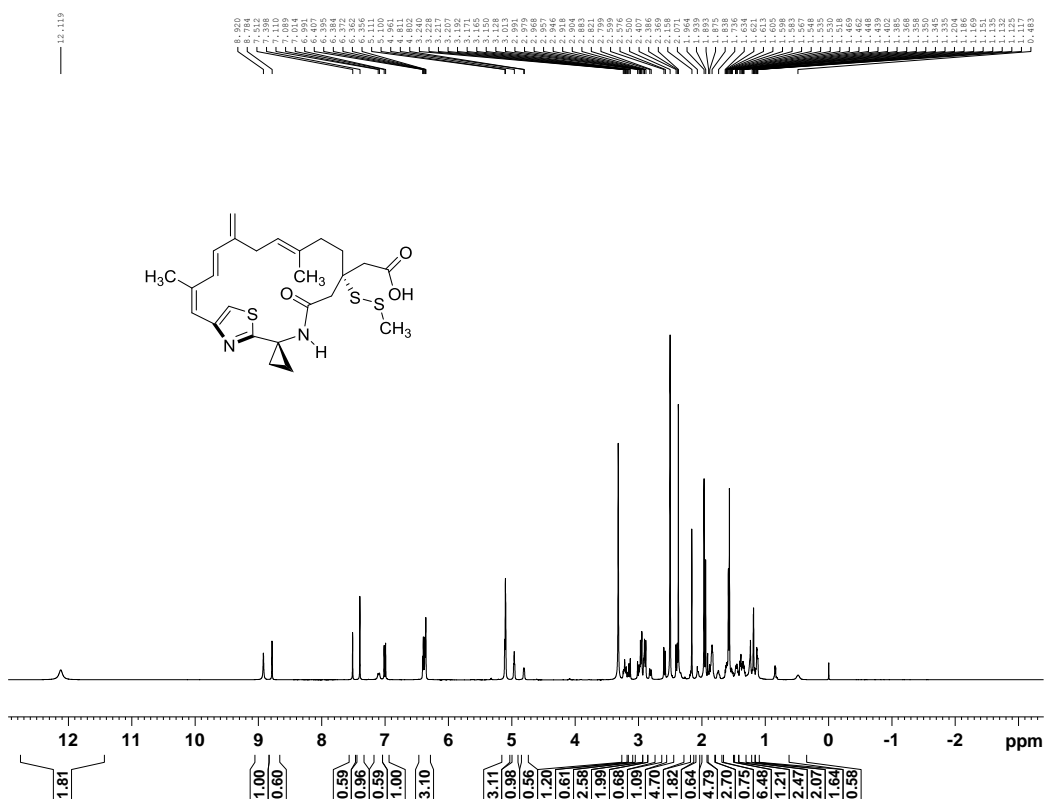


Fig. S11B. ^{13}C NMR spectra of GNM A (175 MHz, DMSO- d_6)

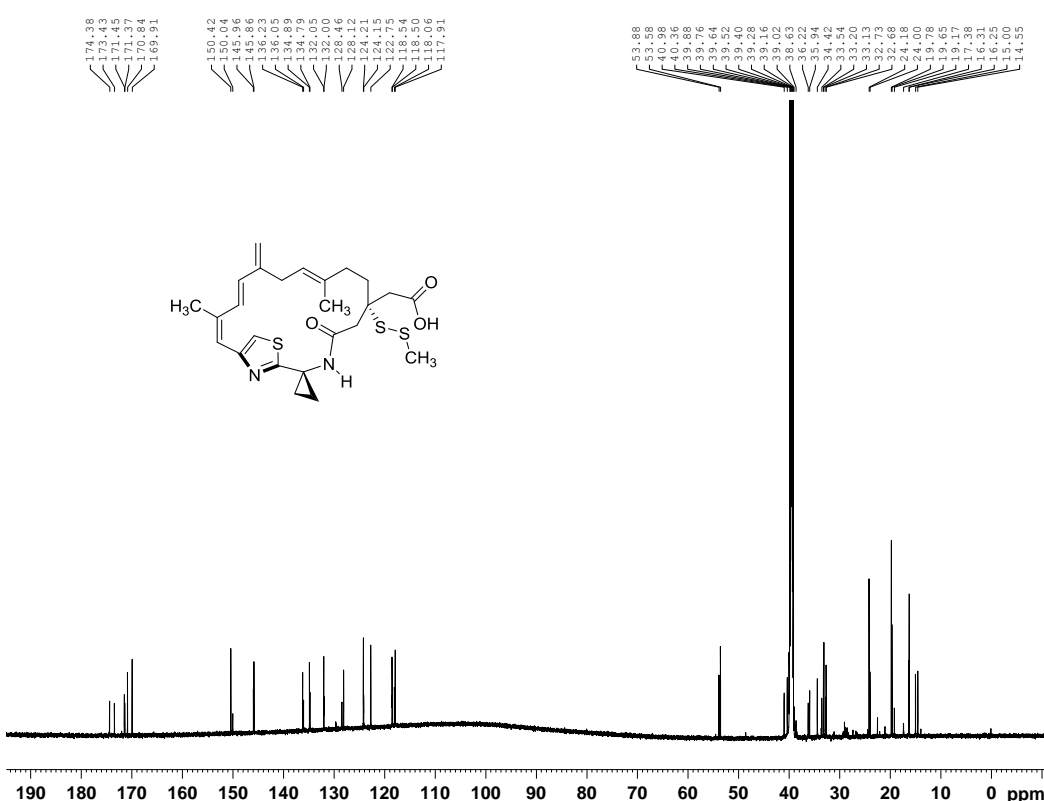


Fig. S11C. DEPT-135 spectra of GNM A (DMSO-*d*₆)

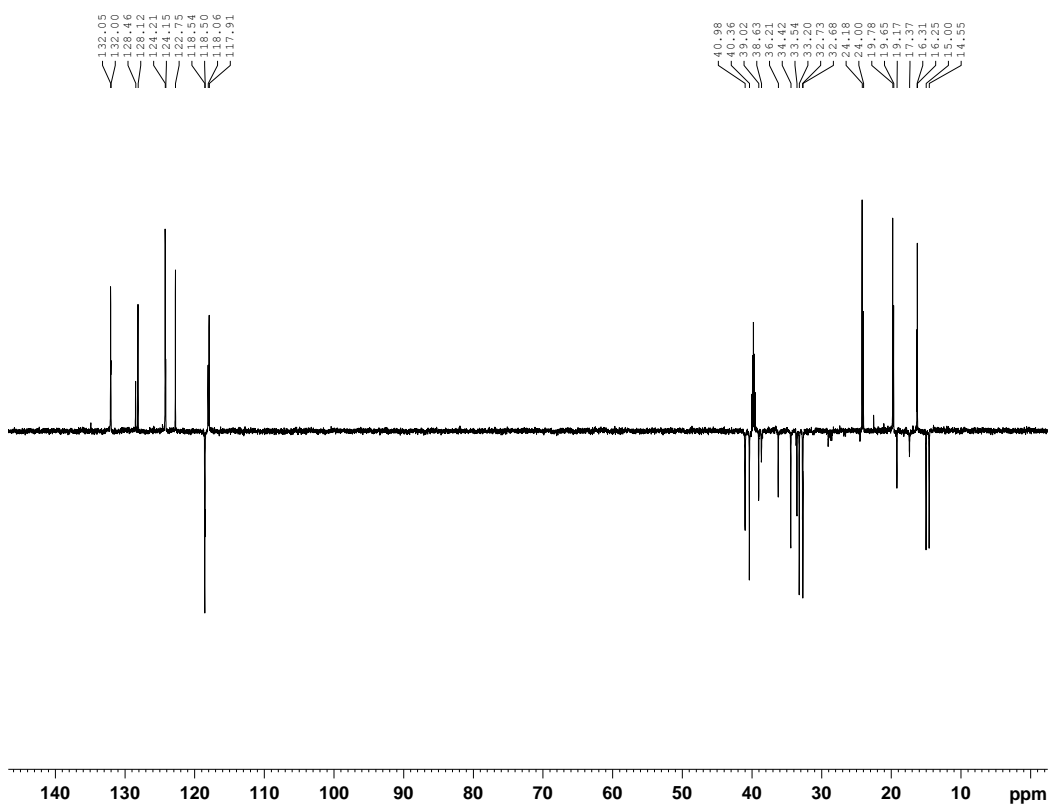


Fig. S11D. HSQC spectra of GNM A (DMSO-*d*₆)

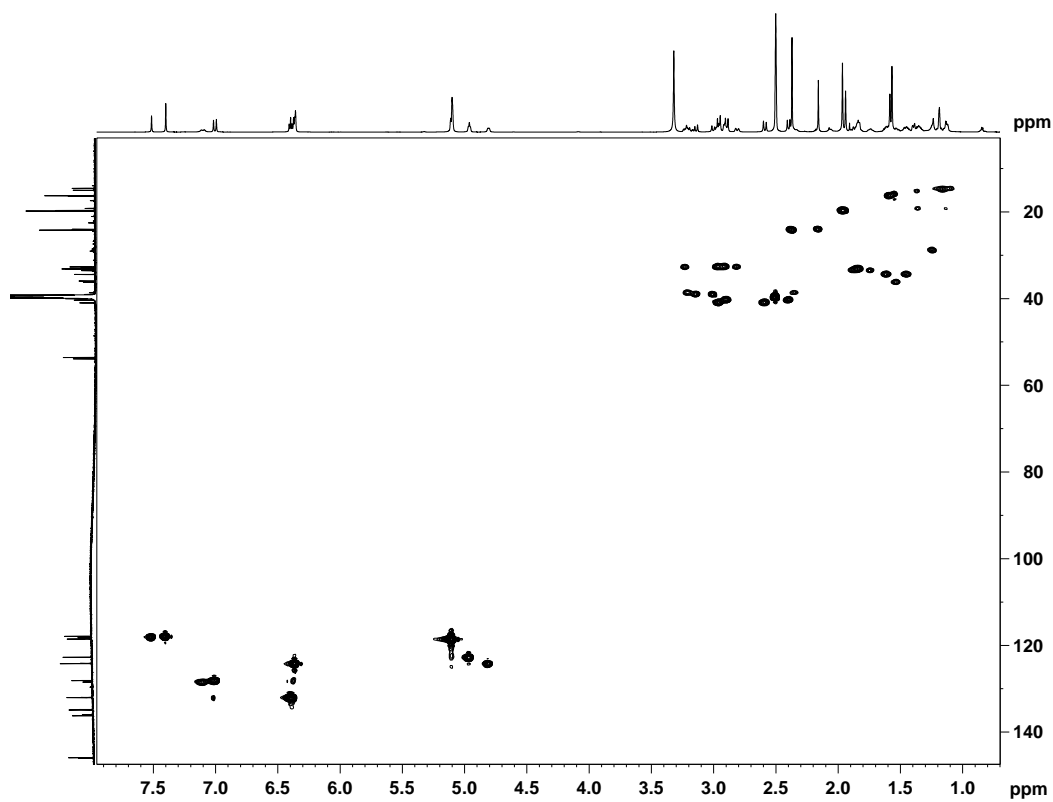


Fig. S11E. ^1H - ^1H COSY spectra of GNM A (DMSO- d_6)

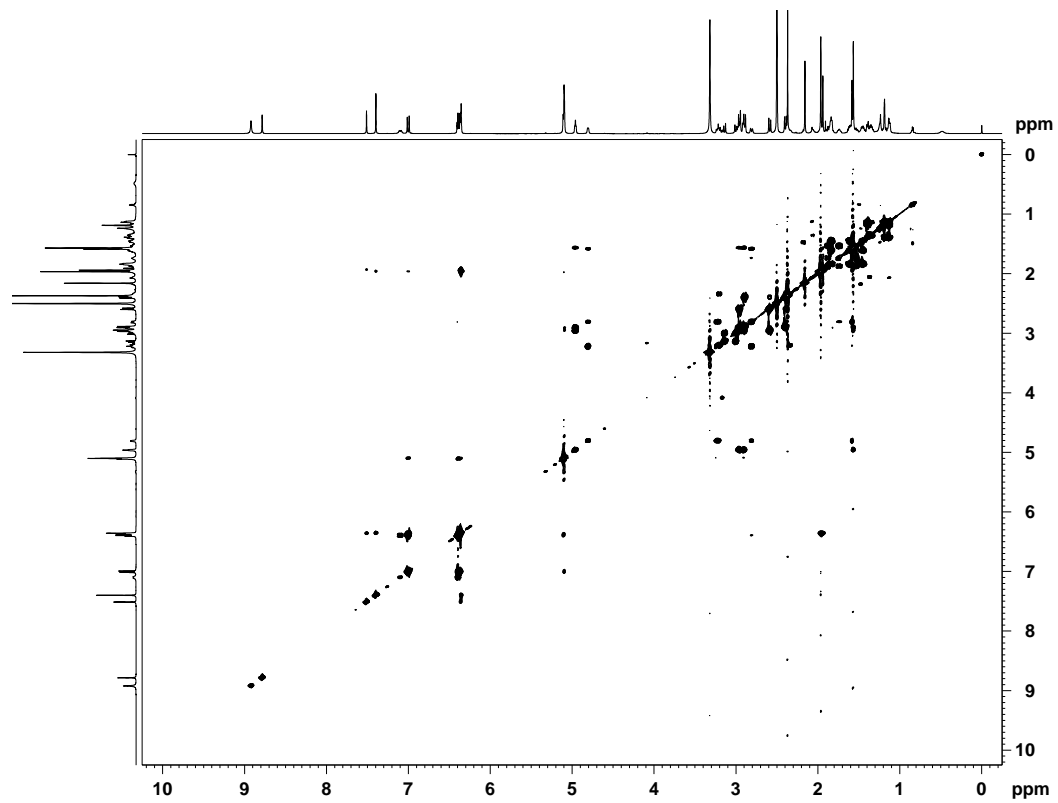


Fig. S11F. HMBC spectra of GNM A (DMSO- d_6)

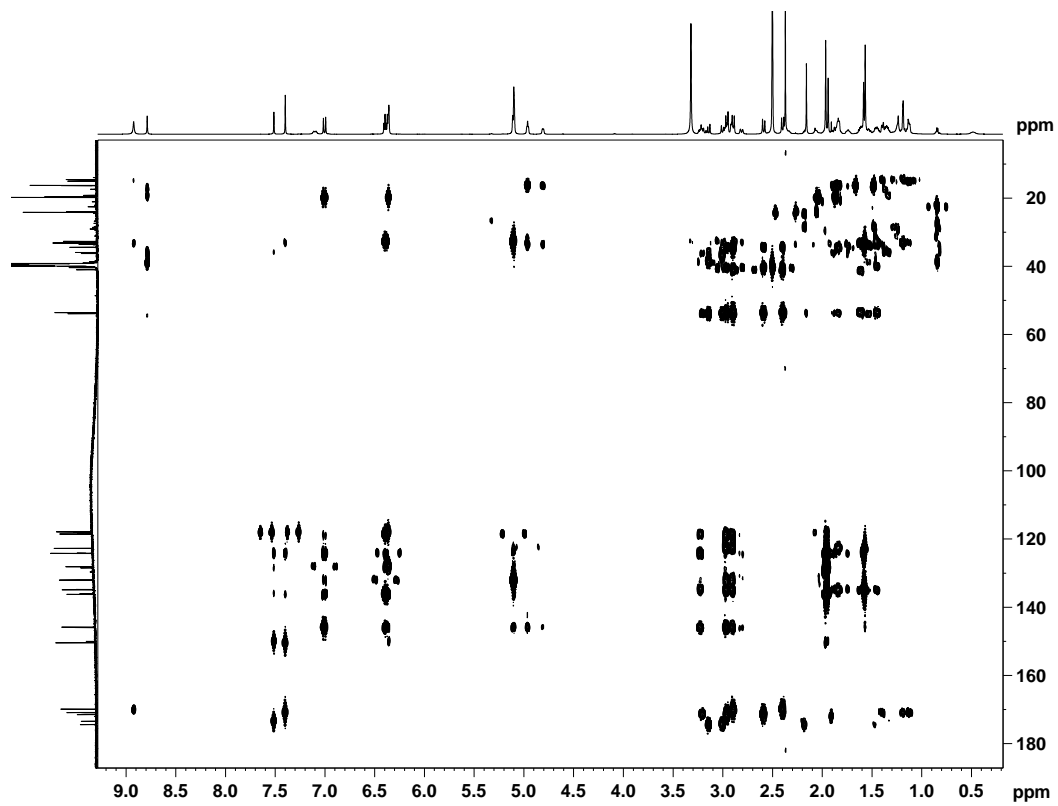


Fig. S11G. ROESY spectra of GNM A (DMSO- d_6)

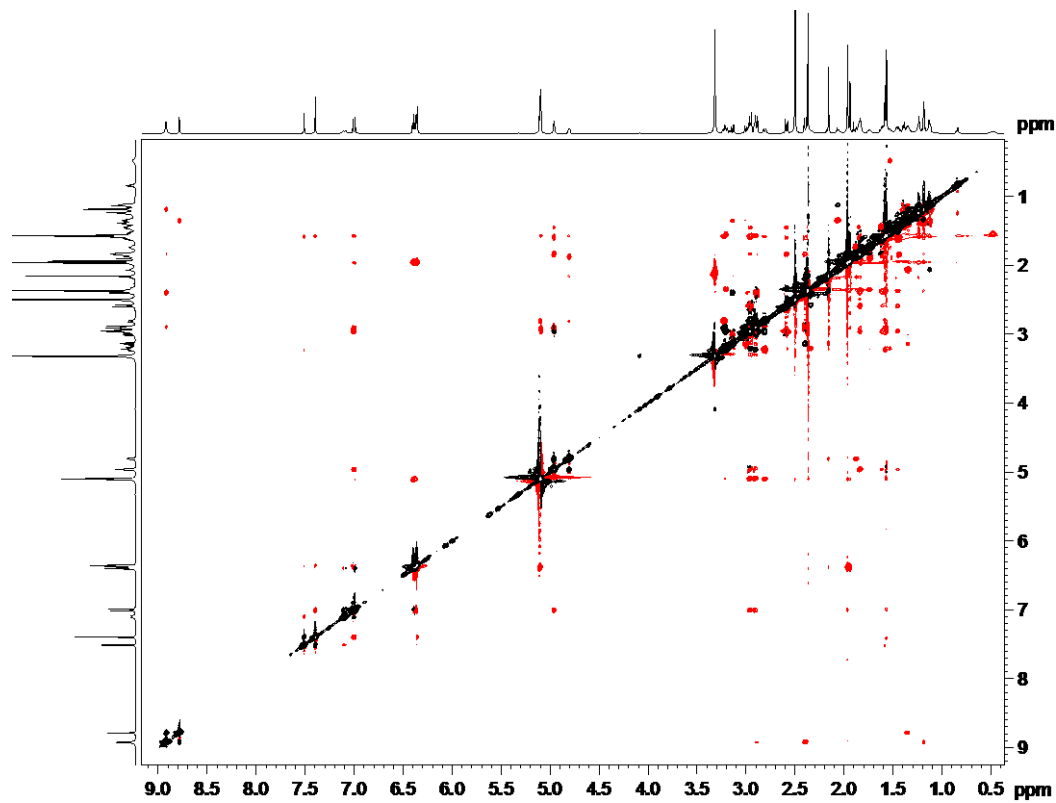


Fig. S11H. 2D-EXSY (21) signals (black) on ROESY spectra (red) of GNM A ($\text{DMSO}-d_6$)

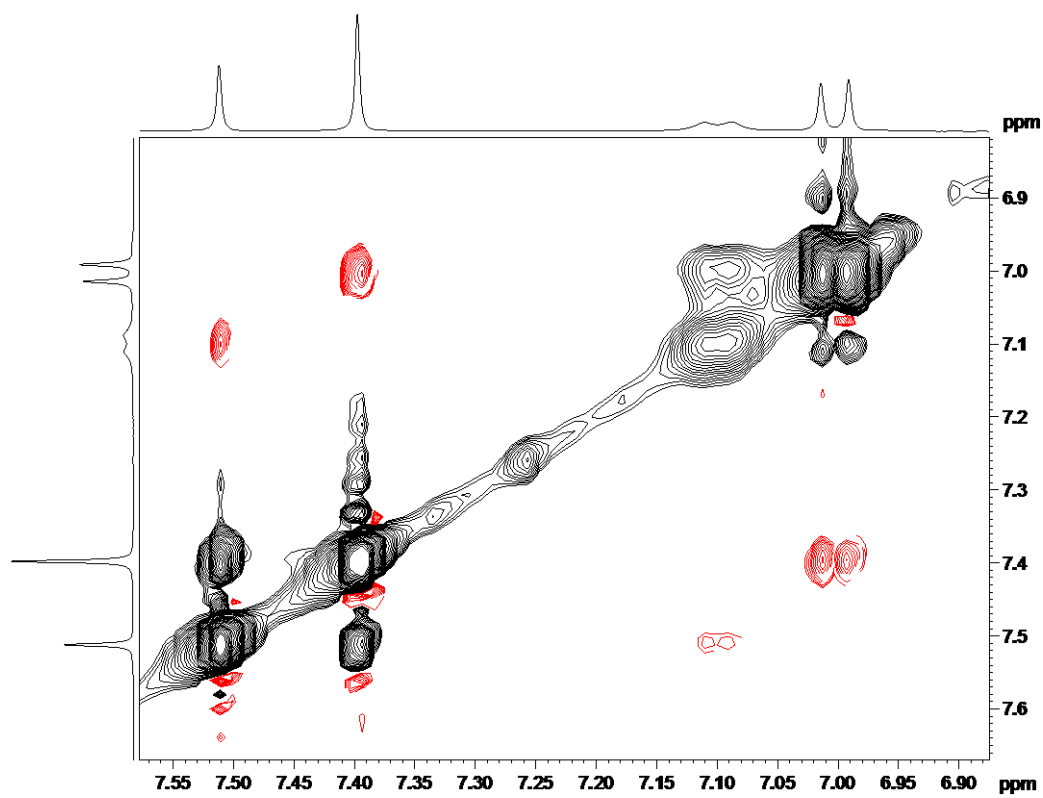


Fig. S11I. 2D-EXSY signals (black) on ROESY spectra (red) of GNM A (DMSO-d_6)

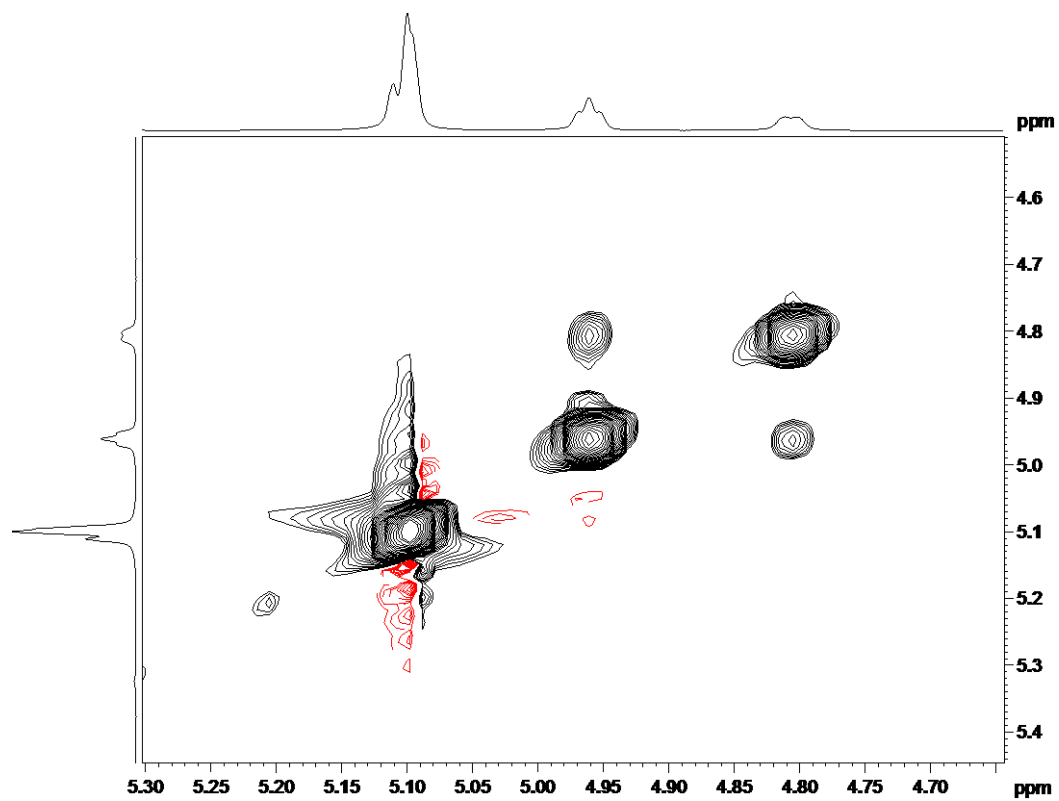


Fig. S11J. 2D-EXSY signals (black) on ROESY spectra (red) of GNM A (DMSO-d_6)

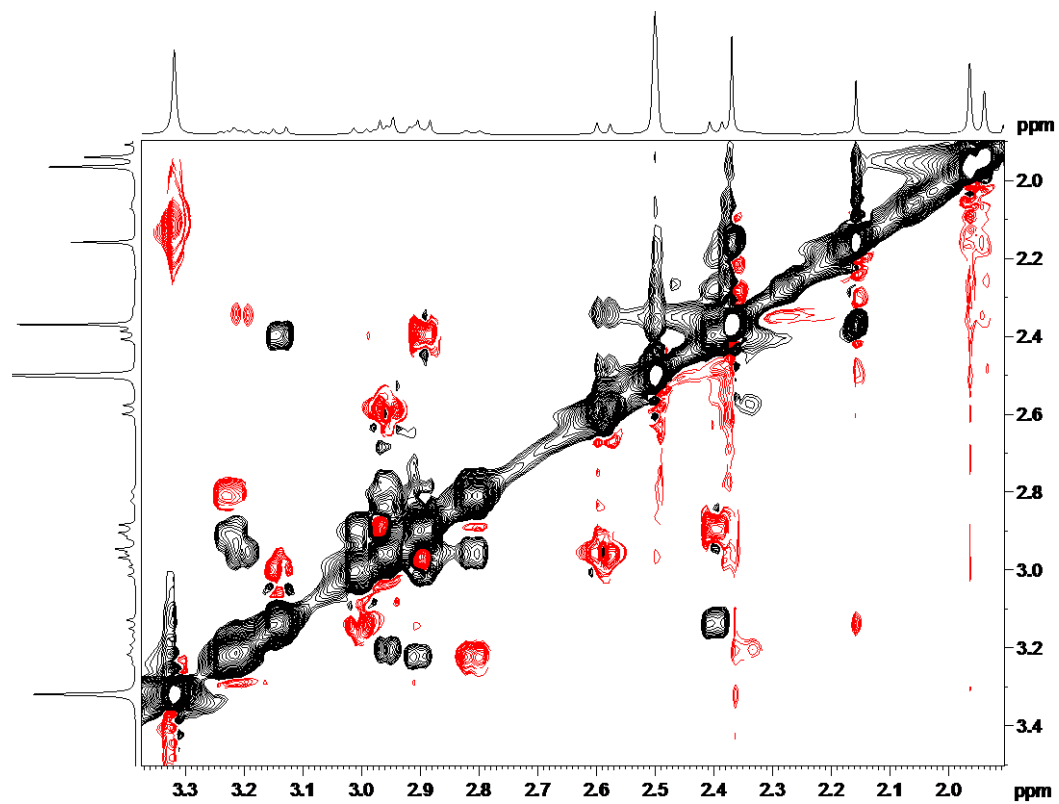


Fig. S11K. 1D-EXSY signals on 1D-NOE spectra (22) of GNM A (DMSO- d_6 , 400 MHz)
(red arrow showing the irradiated proton)

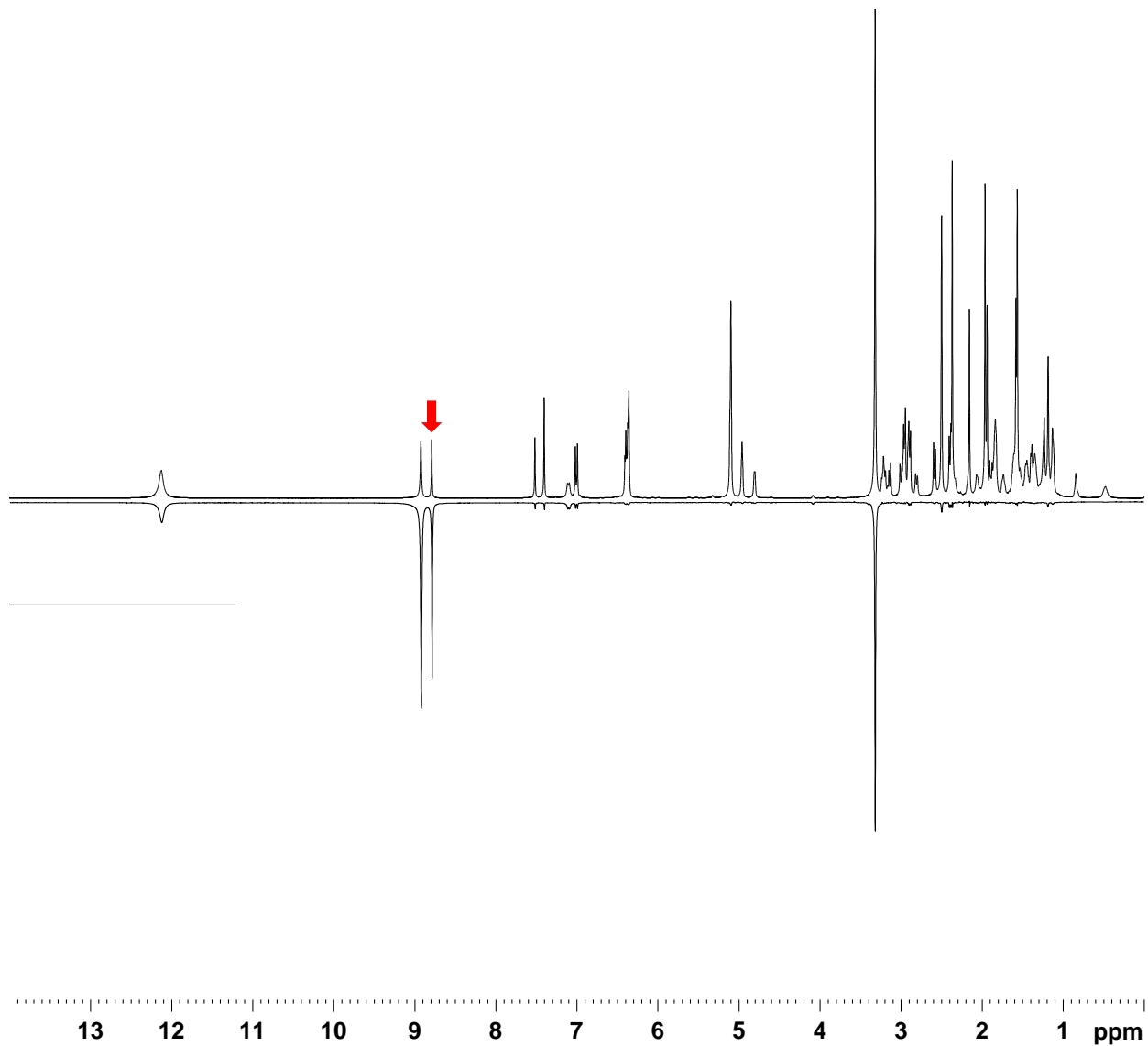


Fig. S11L. 1D-EXSY signals on 1D-NOE spectra of GNM A (DMSO-*d*₆, 400 MHz)
(red arrow showing the irradiated proton)

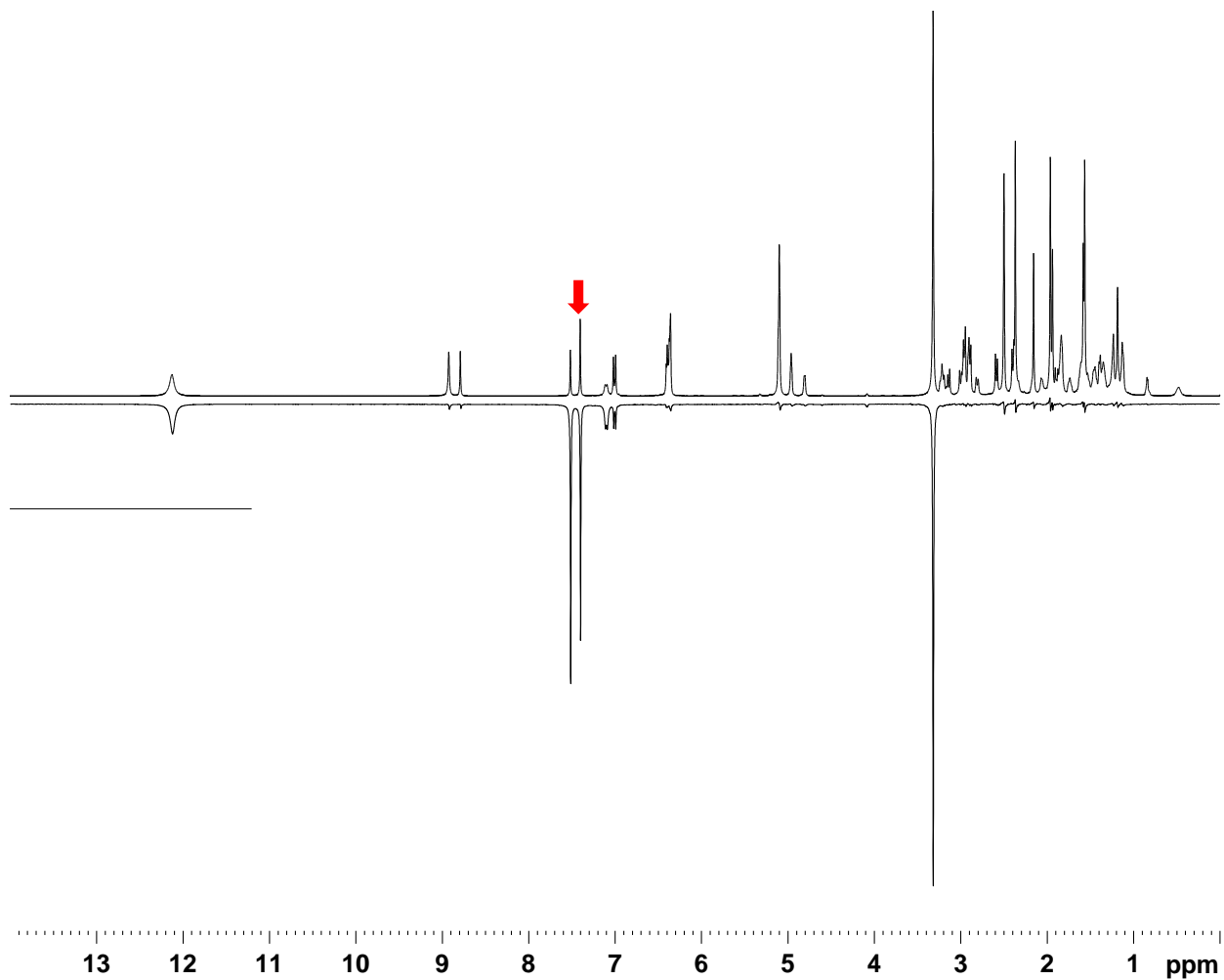


Fig. S11M. ^1H NMR spectra of GNM A at varied temperatures (400 MHz, $\text{DMSO}-d_6$)

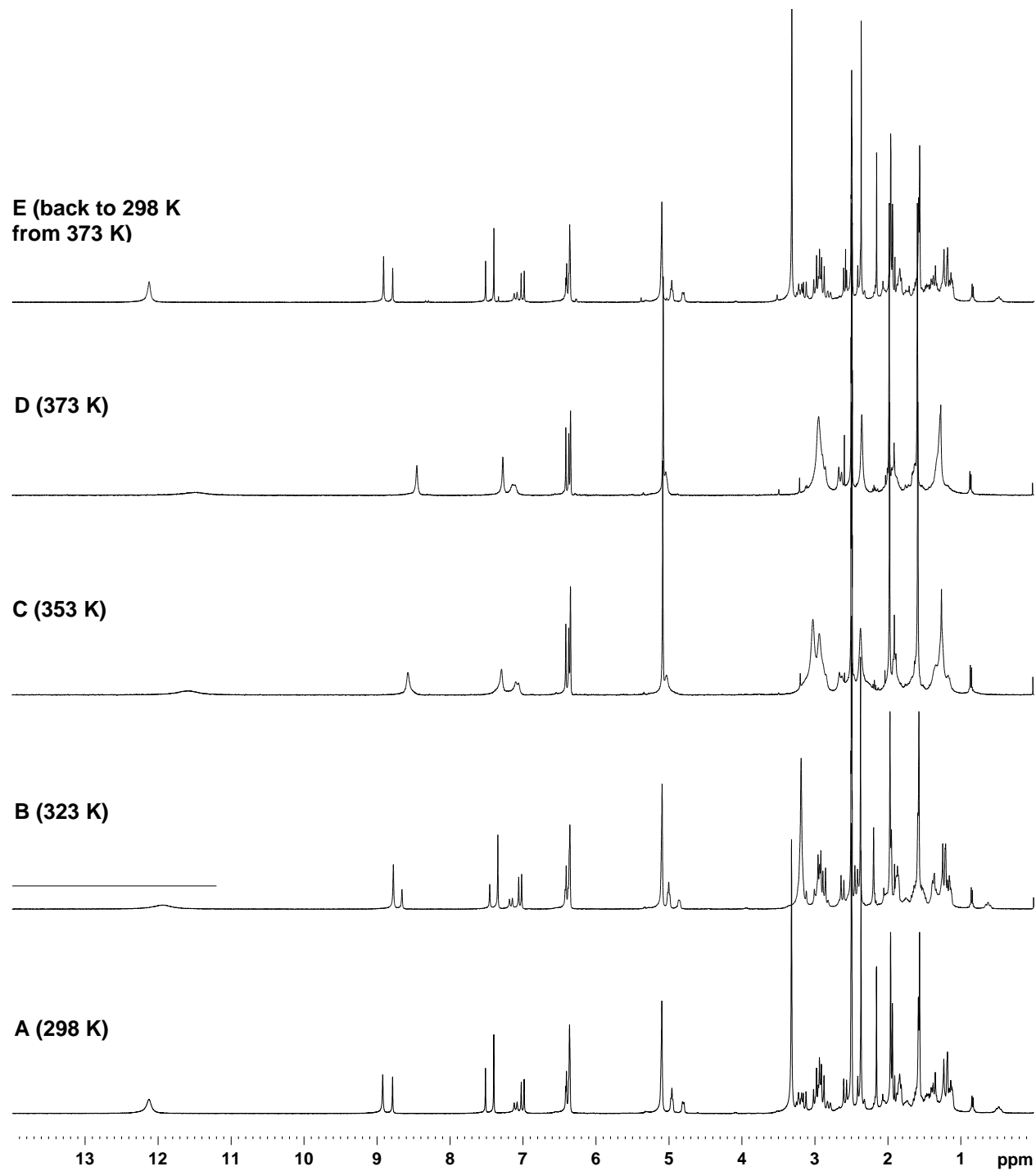


Fig. S11N. HR-MS (ESI) spectra of GNM A

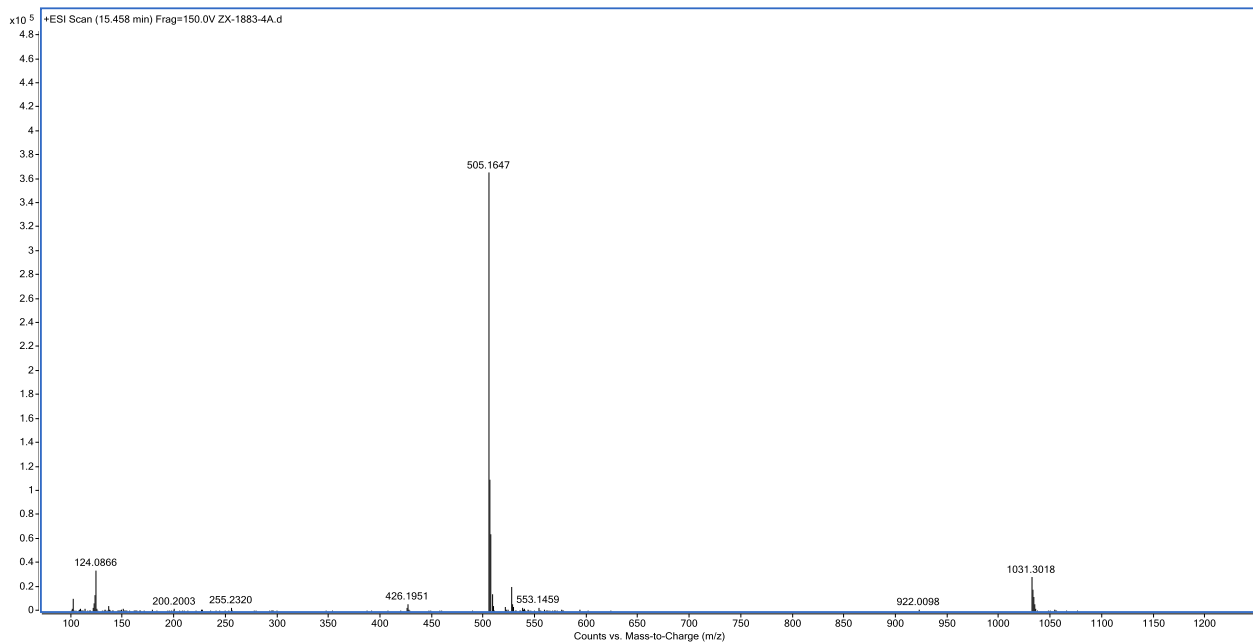


Fig. S12A. ^1H NMR spectra of GNM B (700 MHz, $\text{DMSO}-d_6$)

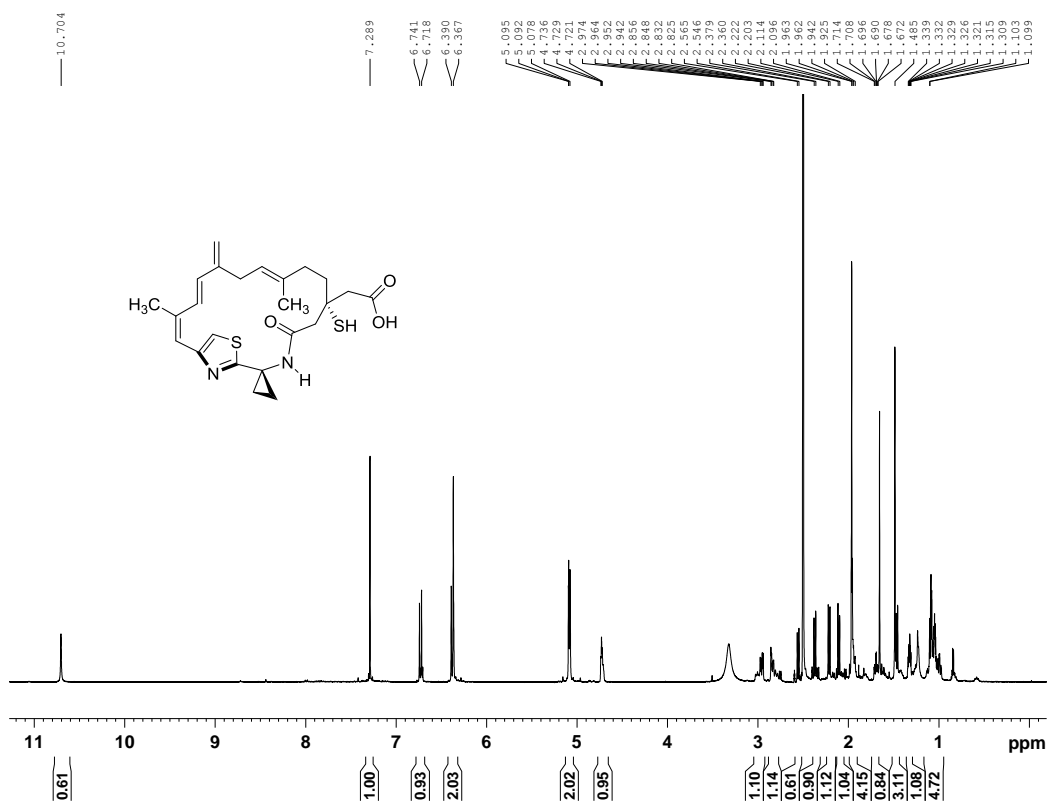


Fig. S12B. ^{13}C NMR spectra of GNM B (175 MHz, $\text{DMSO}-d_6$)

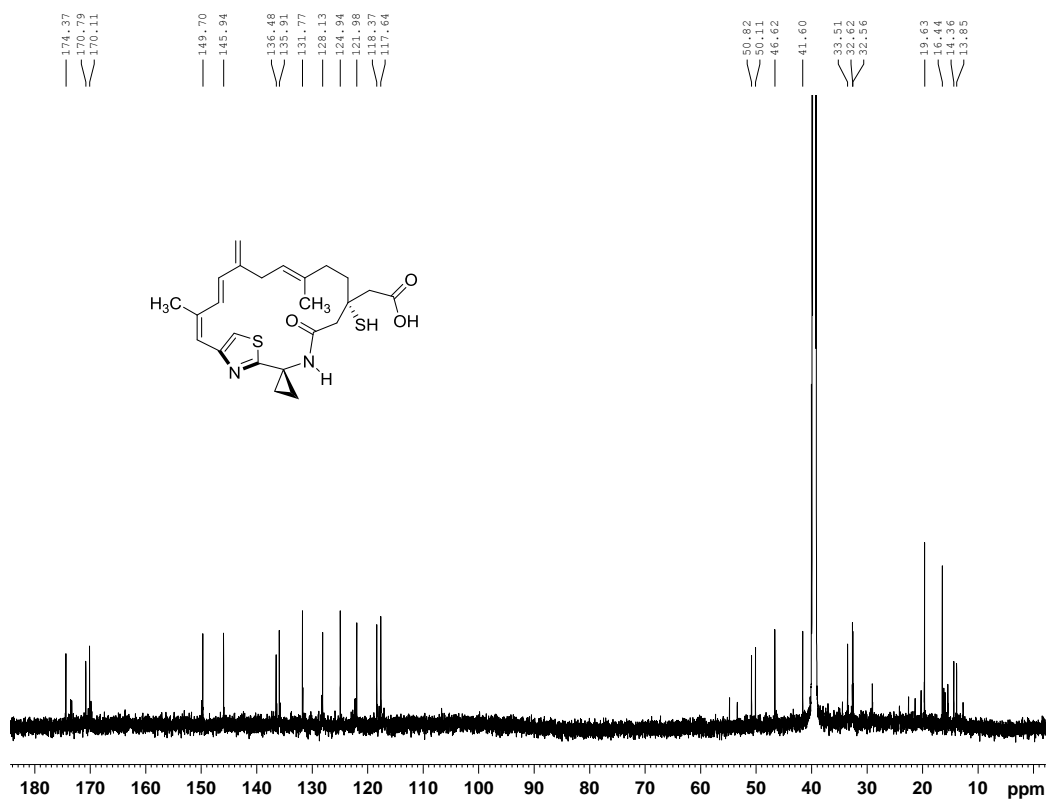


Fig. S12C. DEPT-135 spectra of GNM B (DMSO-*d*₆)

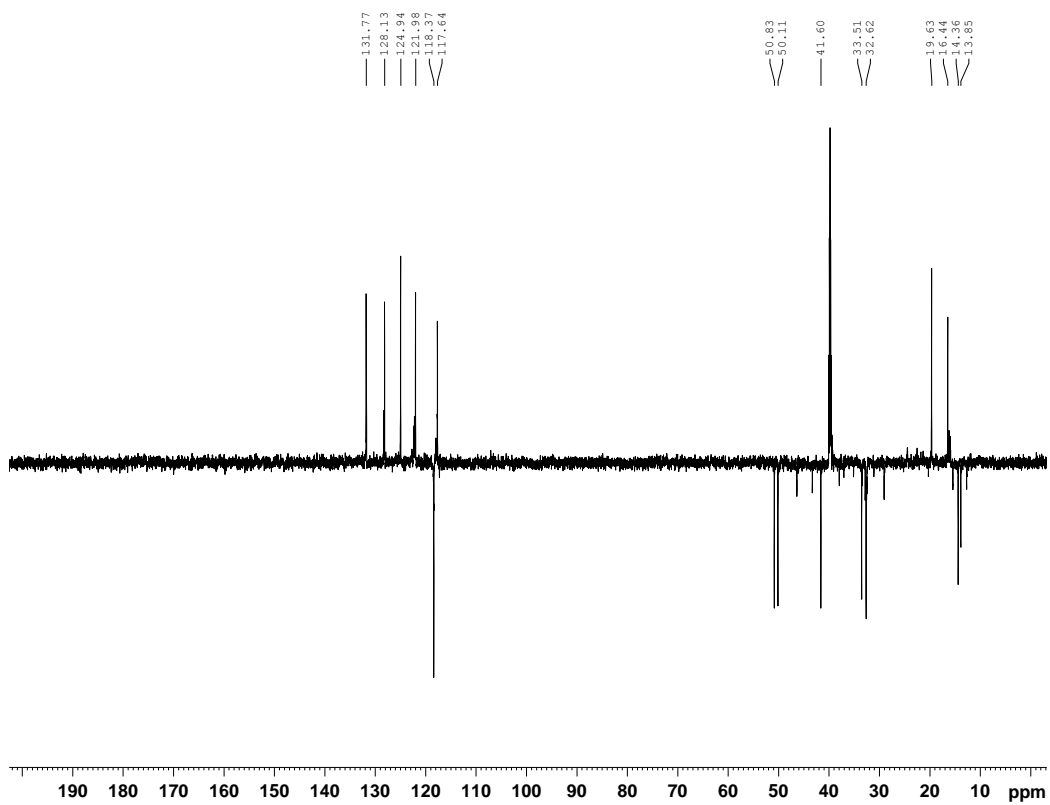


Fig. S12D. HSQC spectra of GNM B (DMSO-*d*₆)

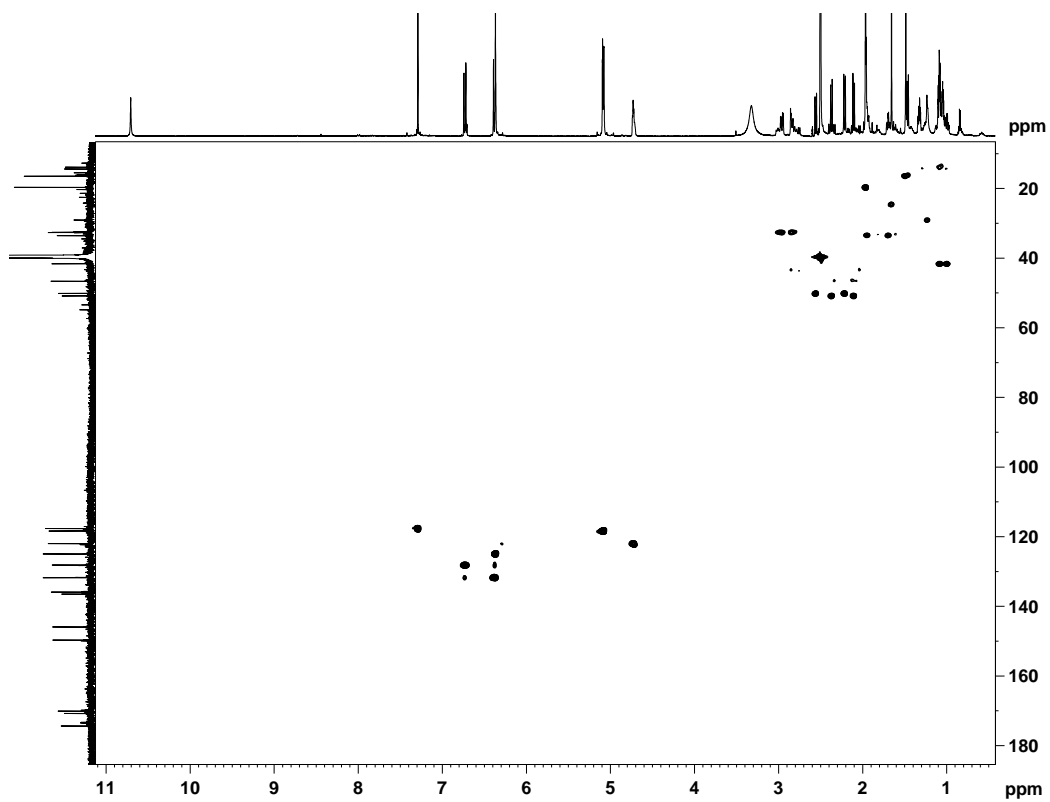


Fig. S12E. ^1H - ^1H COSY spectra of GNM B (DMSO- d_6)

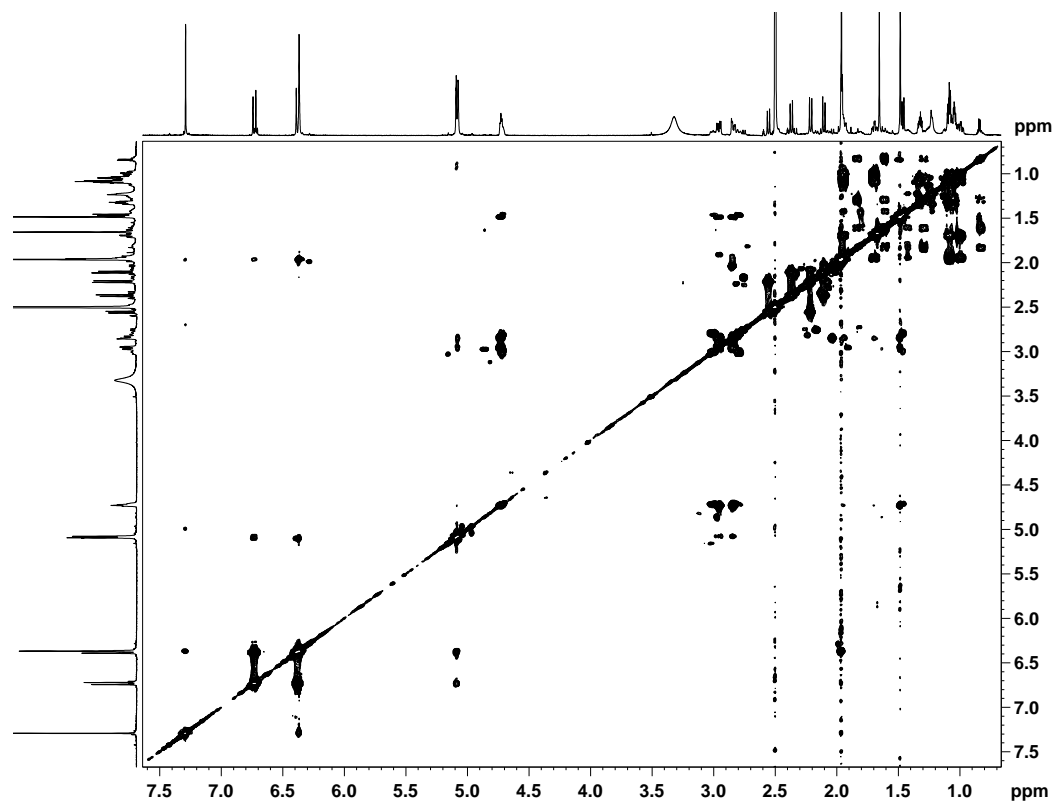


Fig. S12F. HMBC spectra of GNM B (DMSO- d_6)

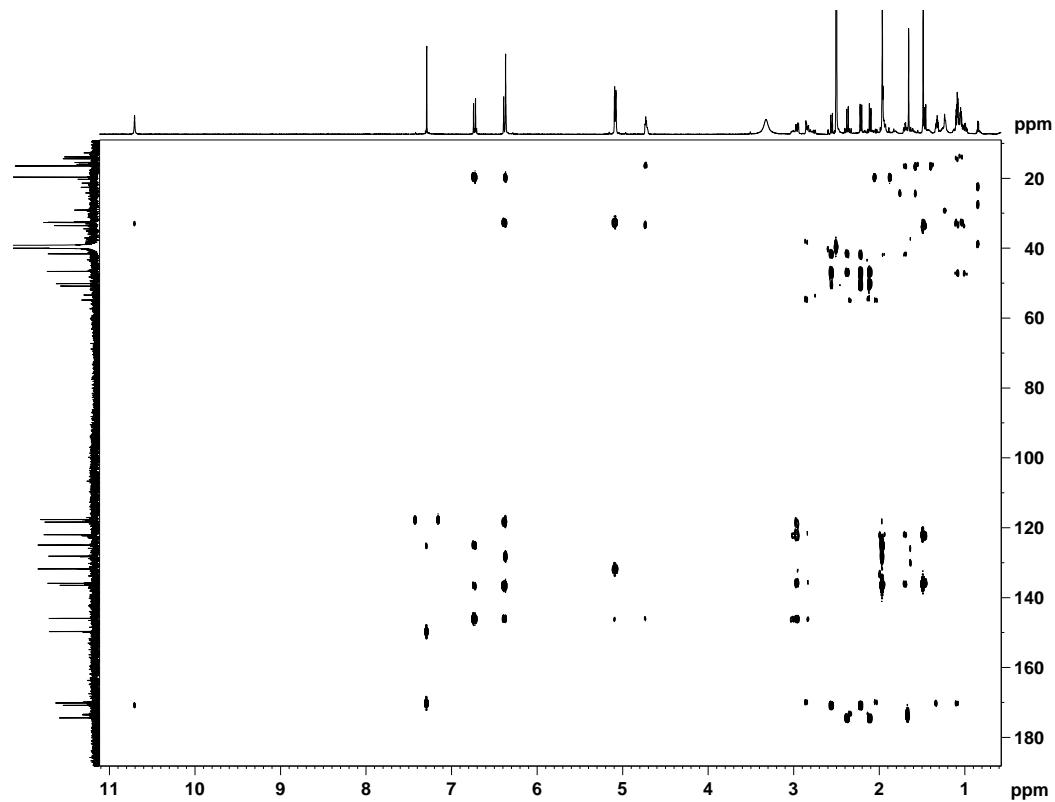


Fig. S12G. ROESY spectra of GNM B (DMSO-d₆)

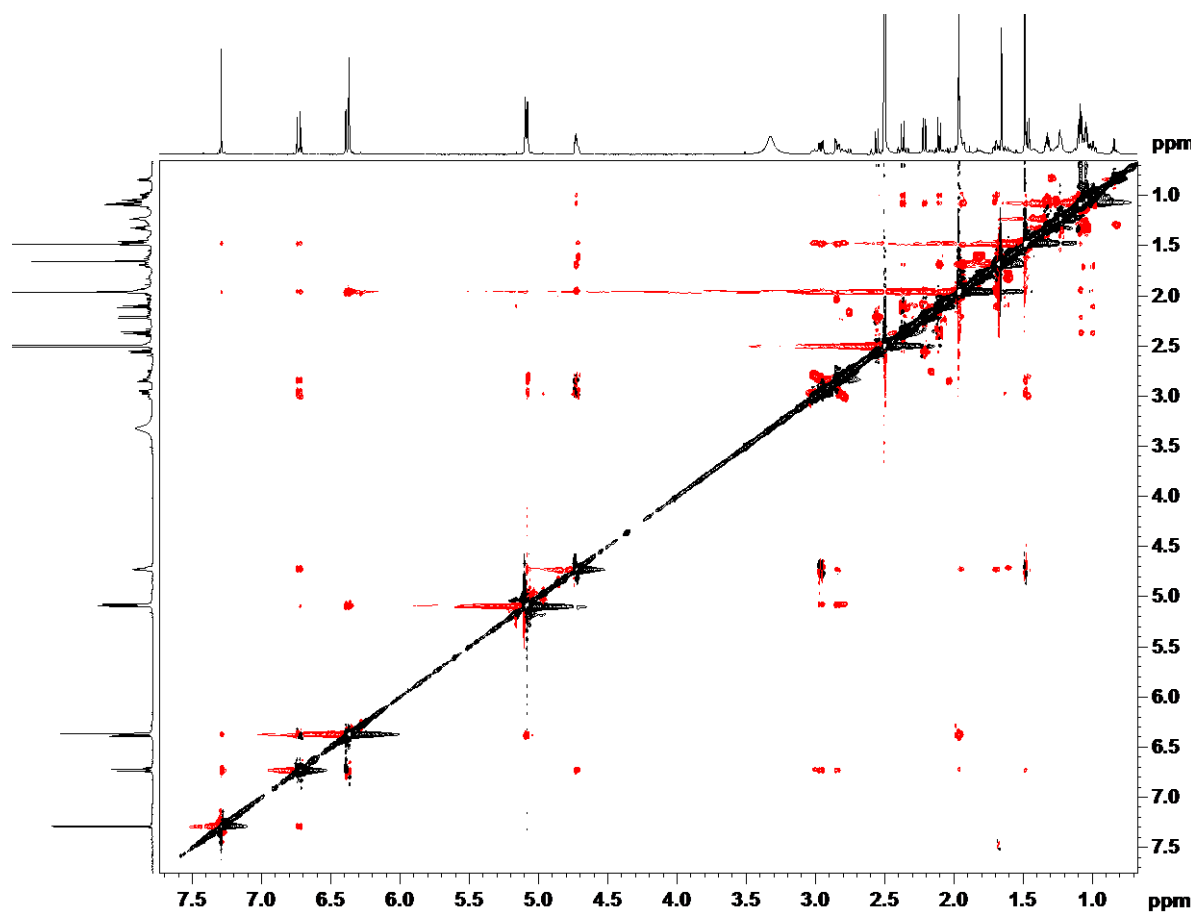


Fig. S12H. HR-MS (ESI) spectra of GNM B

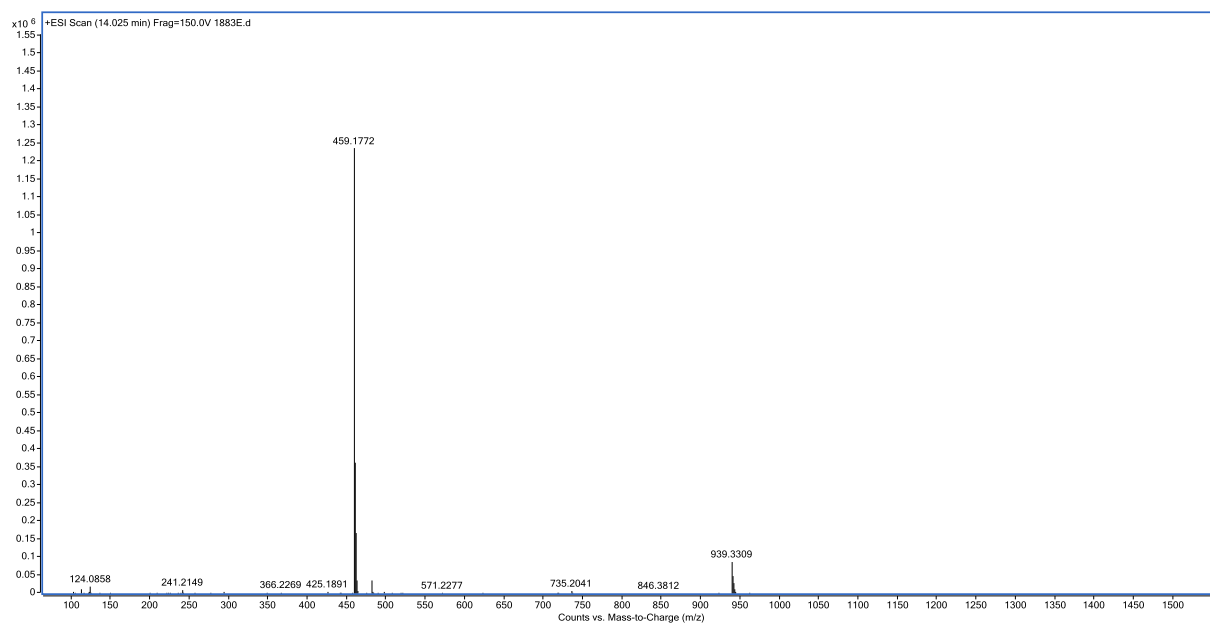


Fig. S13. Elucidation of (*S*)- and (*R*)-PGME derivatives of LNM E2, GNM B2 and WSM A2. Key ^1H - ^1H COSY, HMBC and ROESY correlations are shown.

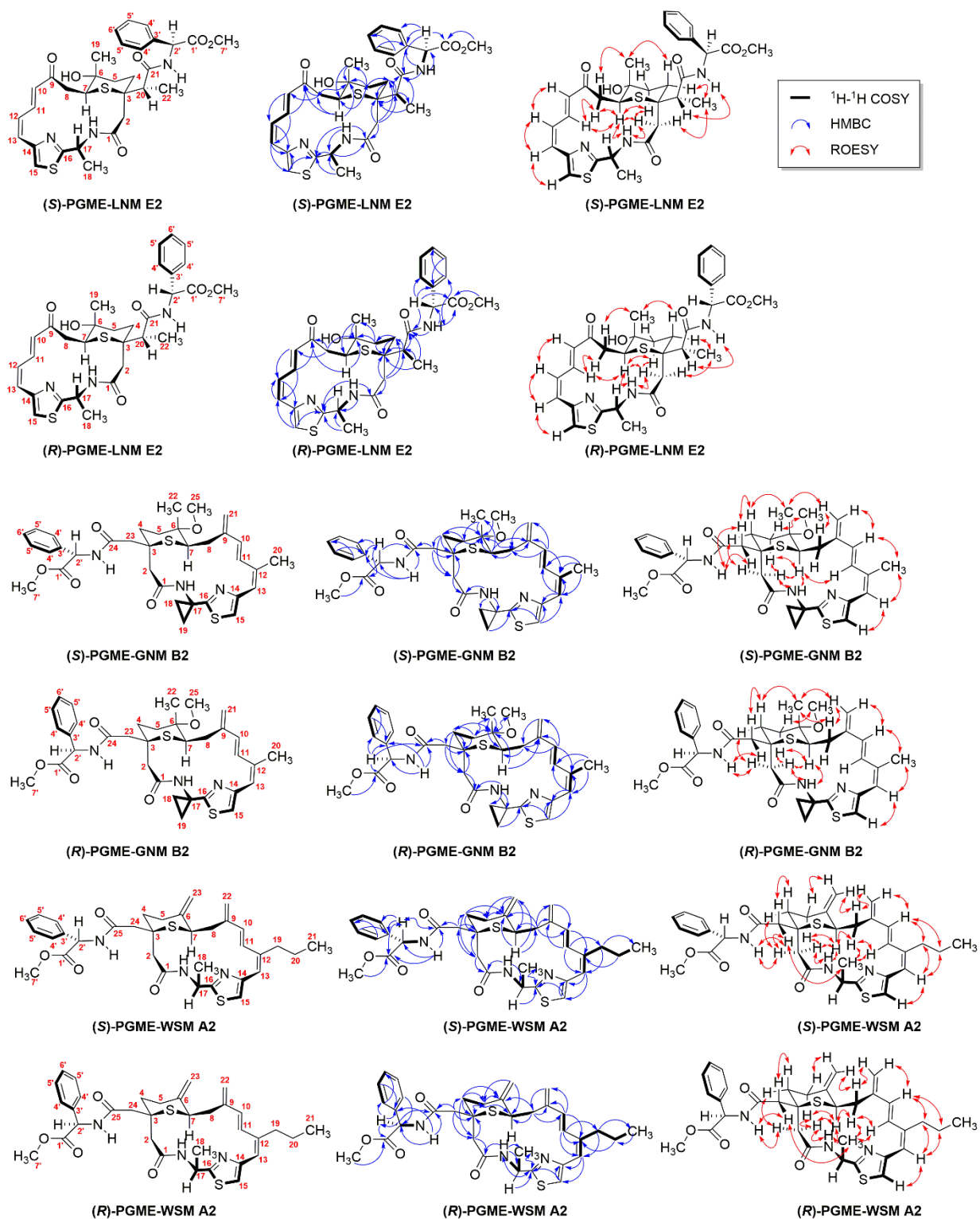


Fig. S14. Determination of the absolute configuration of GNM B2 using its (S)- and (R)-PGME derivatives. Two major conformations of (S)- and (R)-PGME-GNM B2 are shown in **A**, which are different from that of the corresponding derivatives of LNM E2 probably due to the missing methyl group at C23 position. In the ROESY spectra (**B**), the presence of correlations between 23-H_b and 4-H_b, between 2-H_b and 4-H_a, as well as the absent correlations between 23-H_a and 2-H/4-H, support that C23-C24 and C3-S are *anti*-oriented, and 23-H_b takes a pseudo-axial position in the preferred conformation at C23. Two major conformations (**A**, conformations I and II), due to the rotation of C23-C24 single bond, could be observed based on the ROESY correlations between 24-NH and 23-H_a/23-H_b/2-H_b (**C** and **D**). The relatively weak correlation between 24-NH and 23-H_b (**C**) supports that conformation I is the favored conformation of (R)-PGME-GNM B2, while the relatively weak correlation between 24-NH and 2-H_b (**D**) supports that conformation II is the favored conformation of (S)-PGME-GNM B2. Although several hydrogens in the macrolactam backbone are positioned in different sides of PGME plane in two different conformations, 23-H_b and 2-H_a/H_b are always positioned at the two different sides of the PGME plane in both conformations I and II, hence making them diagnostic useful for determination of the absolute configuration. Based on the differences of chemical shift in ¹H NMR between (R)- and (S)-PGME-GNM B2 ($\Delta\delta = \delta_{(R)} - \delta_{(S)}$) as shown in **A**, the absolute configuration of C3 is elucidated to be 3S for GNM B2 [3R for (R)/(S)-PGME-GNM B2]. H_a denotes one of the geminal hydrogens appearing at lower field in ¹H NMR, and H_b denotes one of the geminal hydrogens appearing at higher field in ¹H NMR.

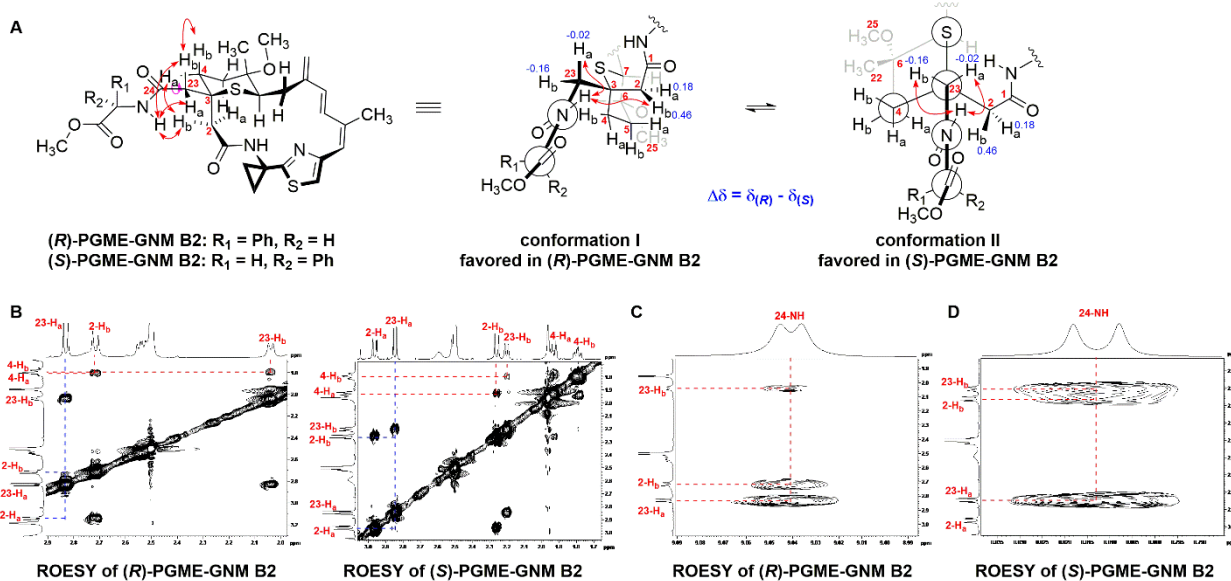


Fig. S15-SA. ^1H NMR spectra of (S)-PGME-GNM B2 (700 MHz, $\text{DMSO}-d_6$)

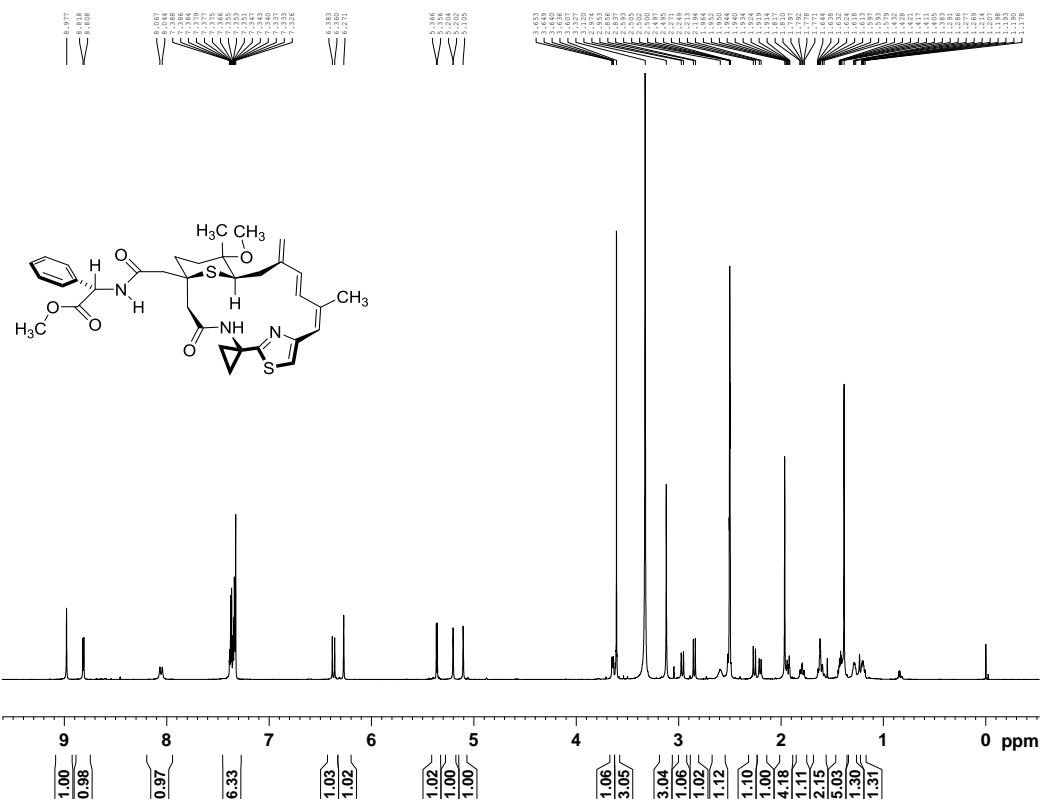


Fig. S15-SB. ^{13}C NMR spectra of (S)-PGME-GNM B2 (175 MHz, $\text{DMSO}-d_6$)

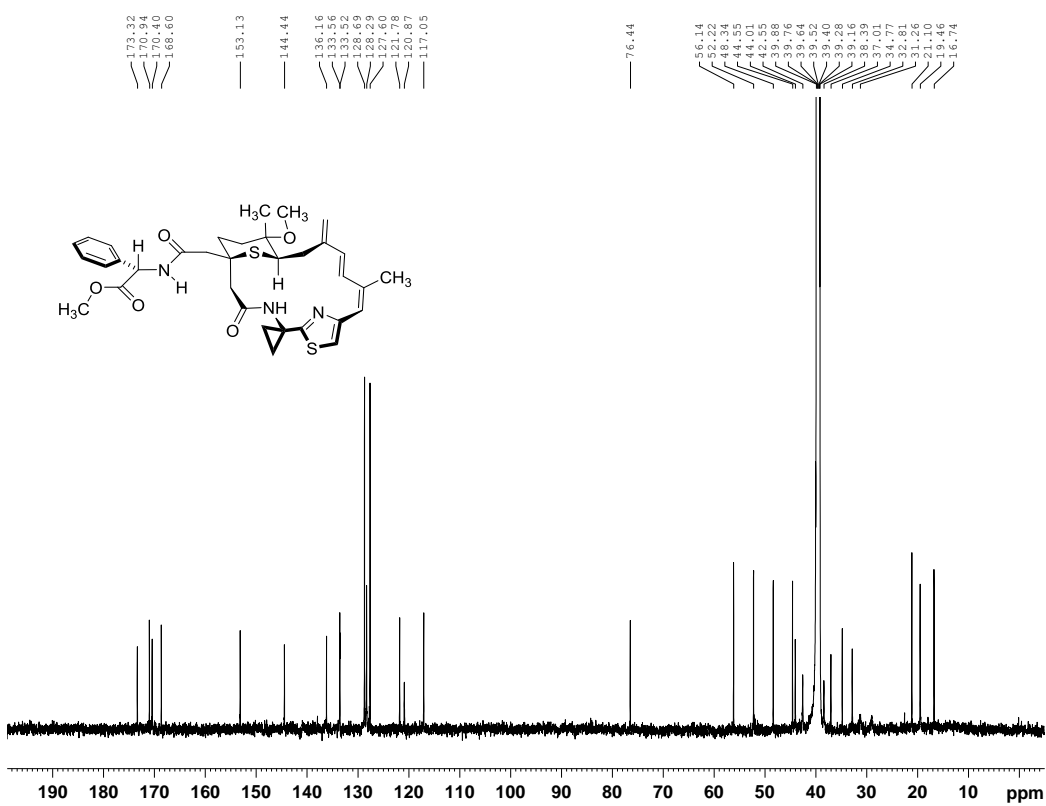


Fig. S15-SC. DEPT-135 spectra of (S)-PGME-GNM B2 (DMSO- d_6)

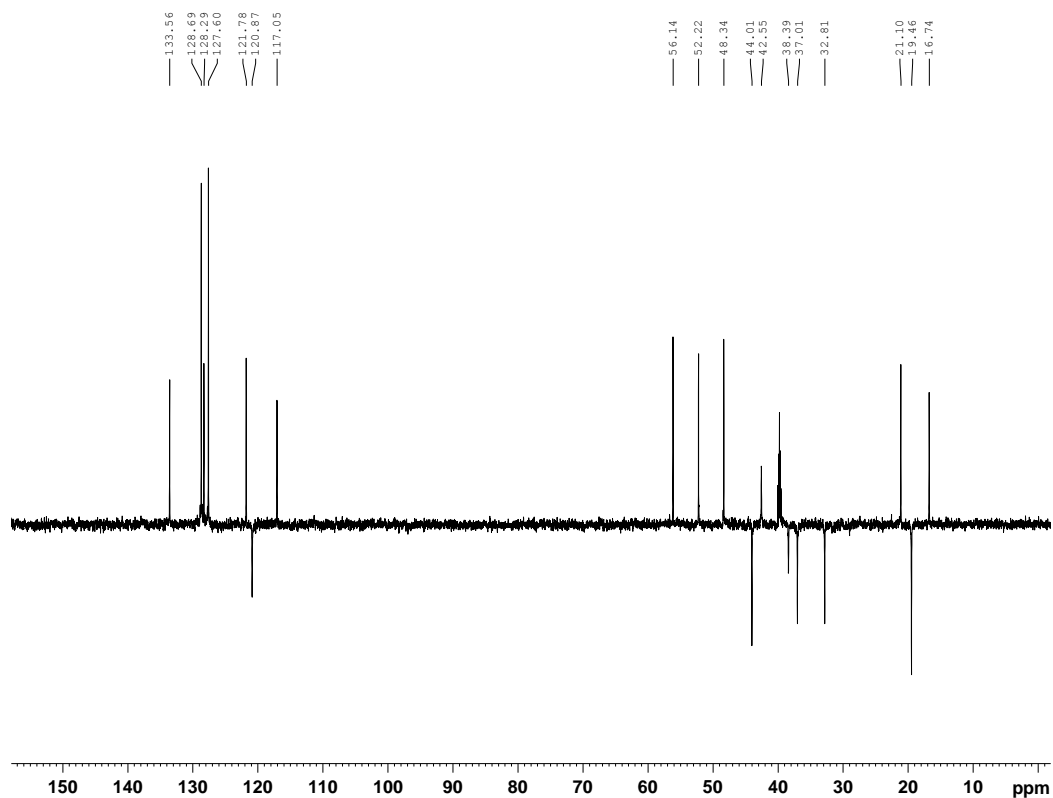


Fig. S15-SD. HSQC spectra of (S)-PGME-GNM B2 (DMSO- d_6)

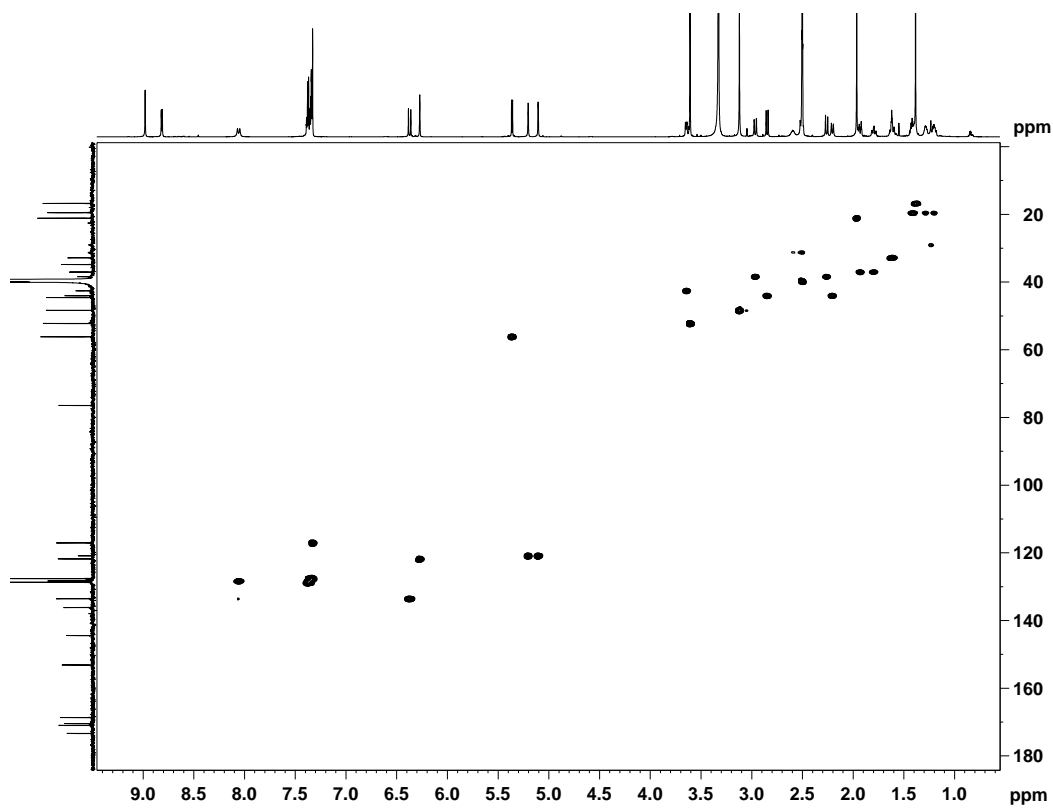


Fig. S15-SE. ^1H - ^1H COSY spectra of (S)-PGME-GNM B2 (DMSO- d_6)

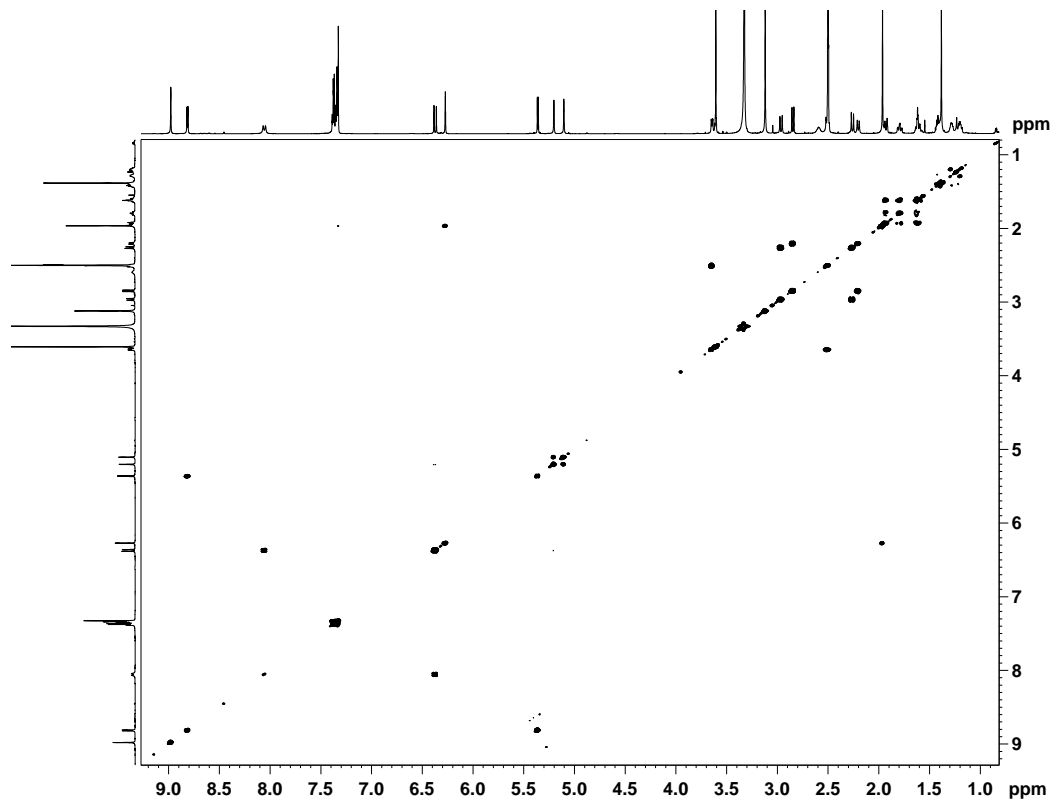


Fig. S15-SF. HMBC spectra of (S)-PGME-GNM B2 (DMSO- d_6)

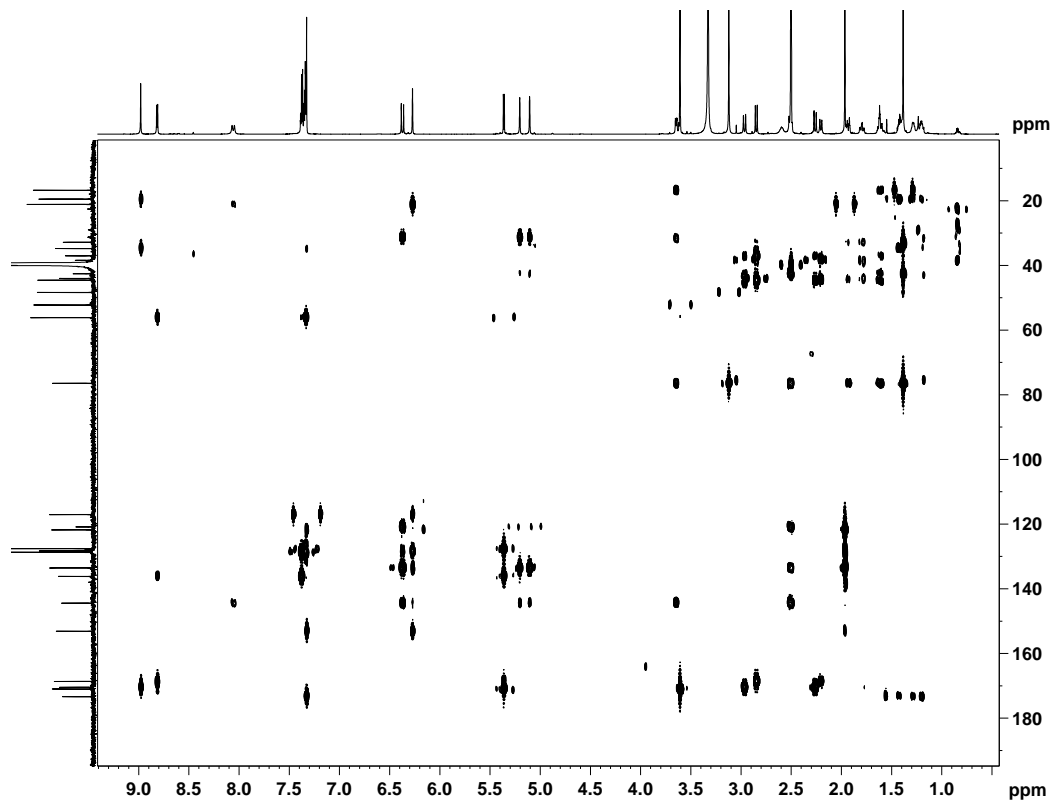


Fig. S15-SG. ROESY spectra of (S)-PGME-GNM B2 (DMSO-*d*₆)

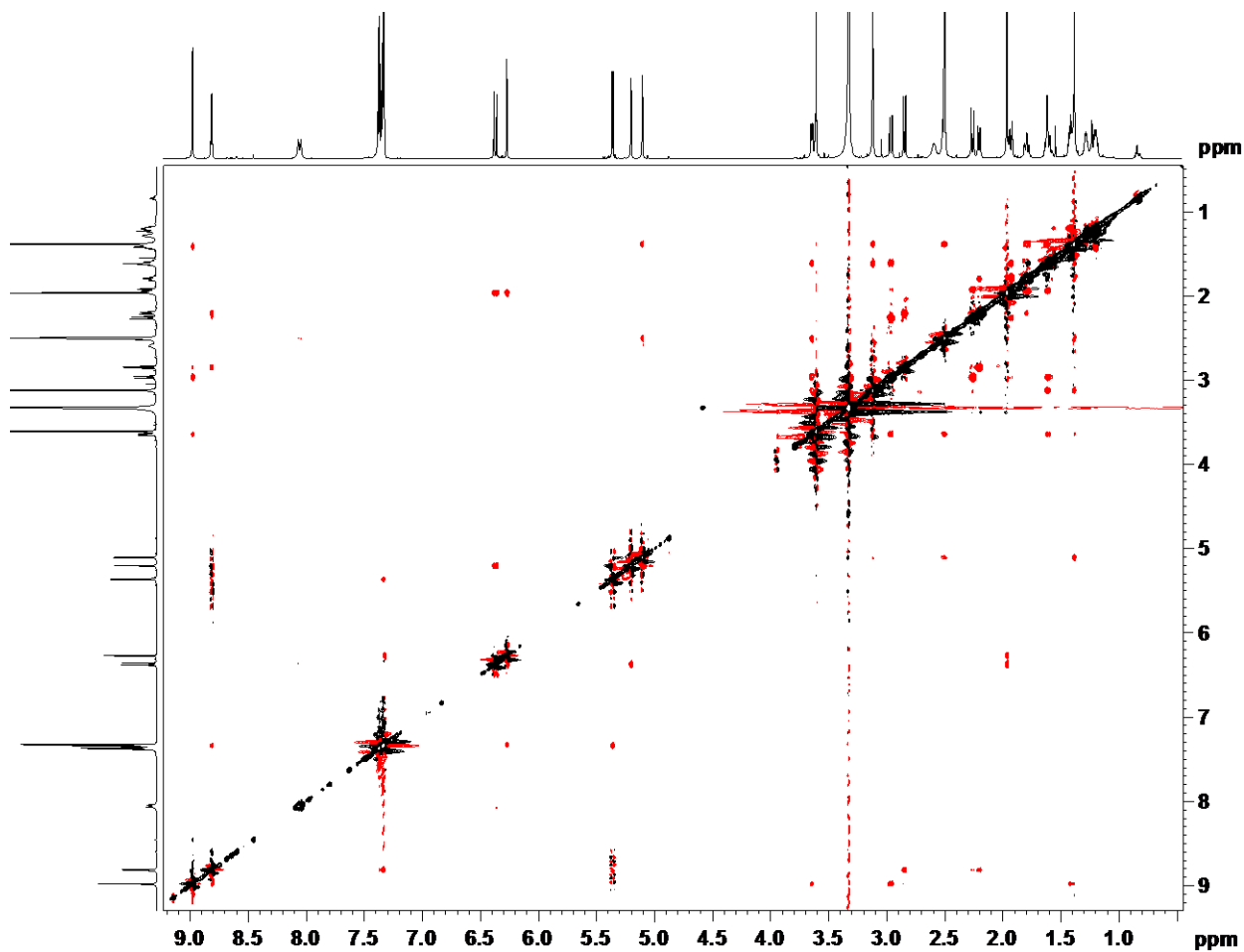


Figure S15-SH. HR-MS (ESI) spectra of (S)-PGME-GNM B2

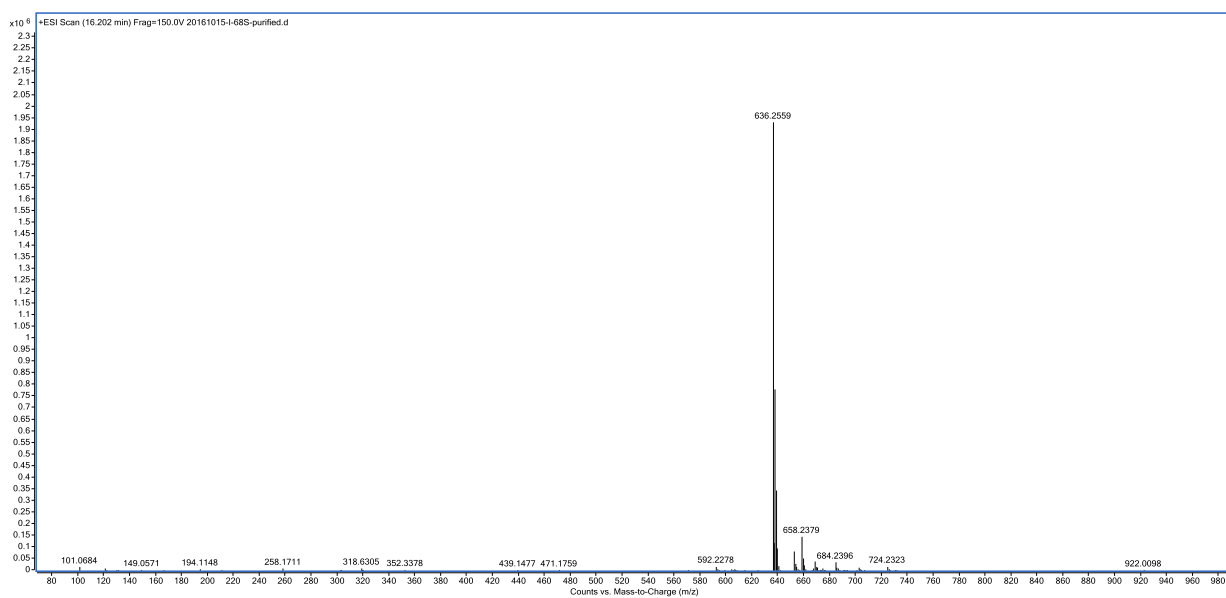


Fig. S15-RA. ^1H NMR spectra of (*R*)-PGME-GNM B2 (700 MHz, DMSO- d_6)

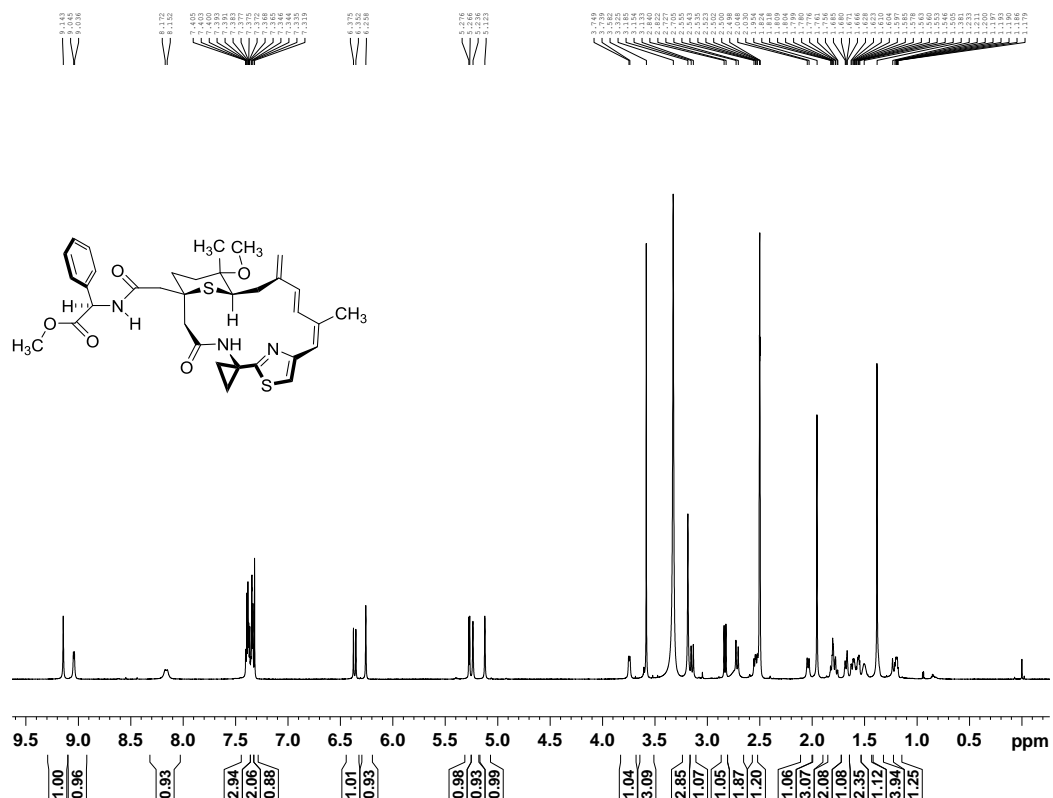


Fig. S15-RB. ^{13}C NMR spectra of (*R*)-PGME-GNM B2 (175 MHz, DMSO- d_6)

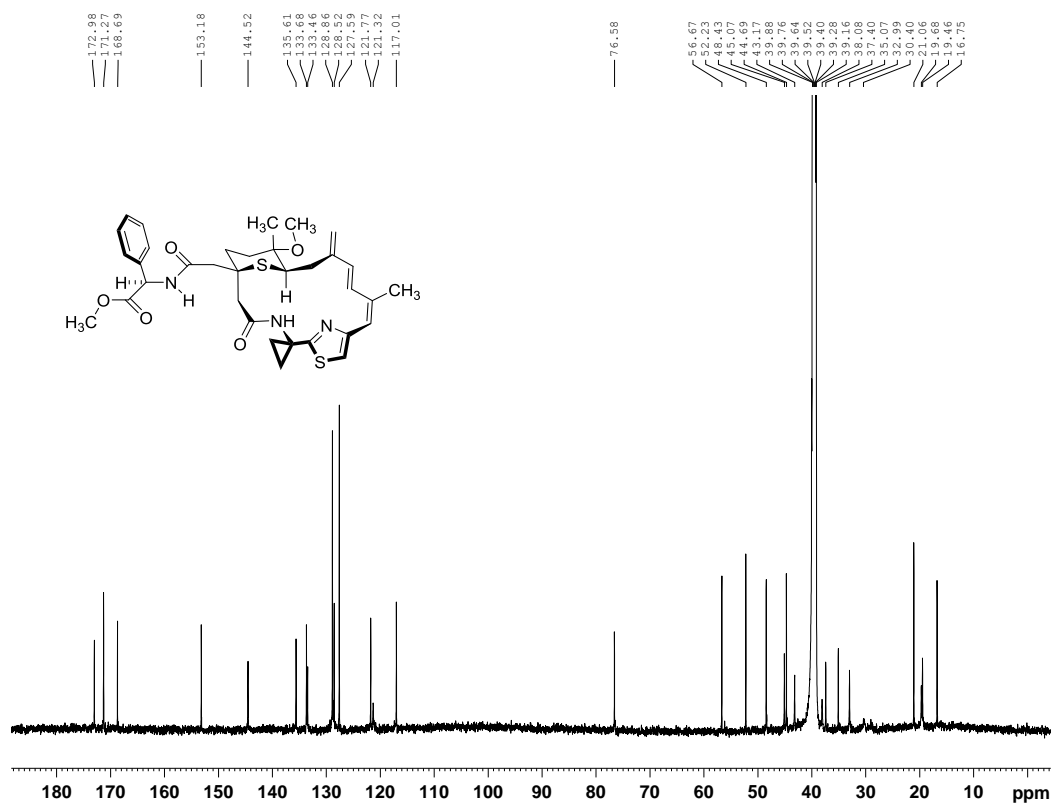


Fig. S15-RC. DEPT-135 spectra of (*R*)-PGME-GNM B2 (DMSO- d_6)

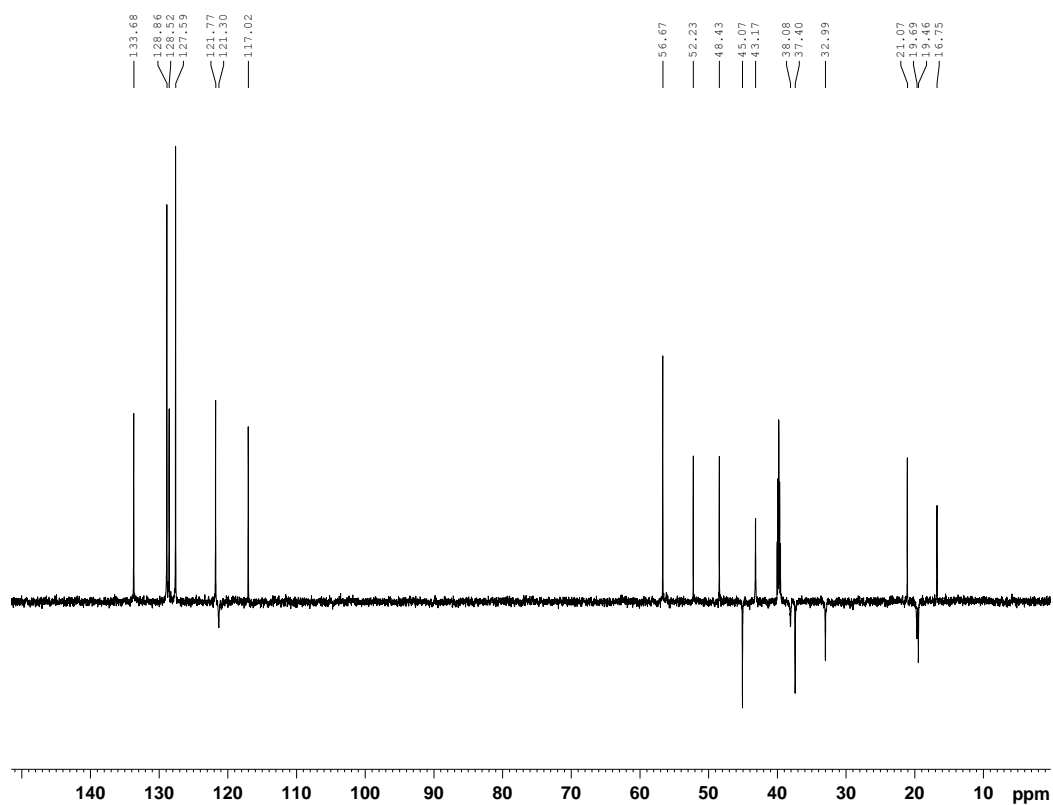


Fig. S15-RD. HSQC spectra of (*R*)-PGME-GNM B2 (DMSO- d_6)

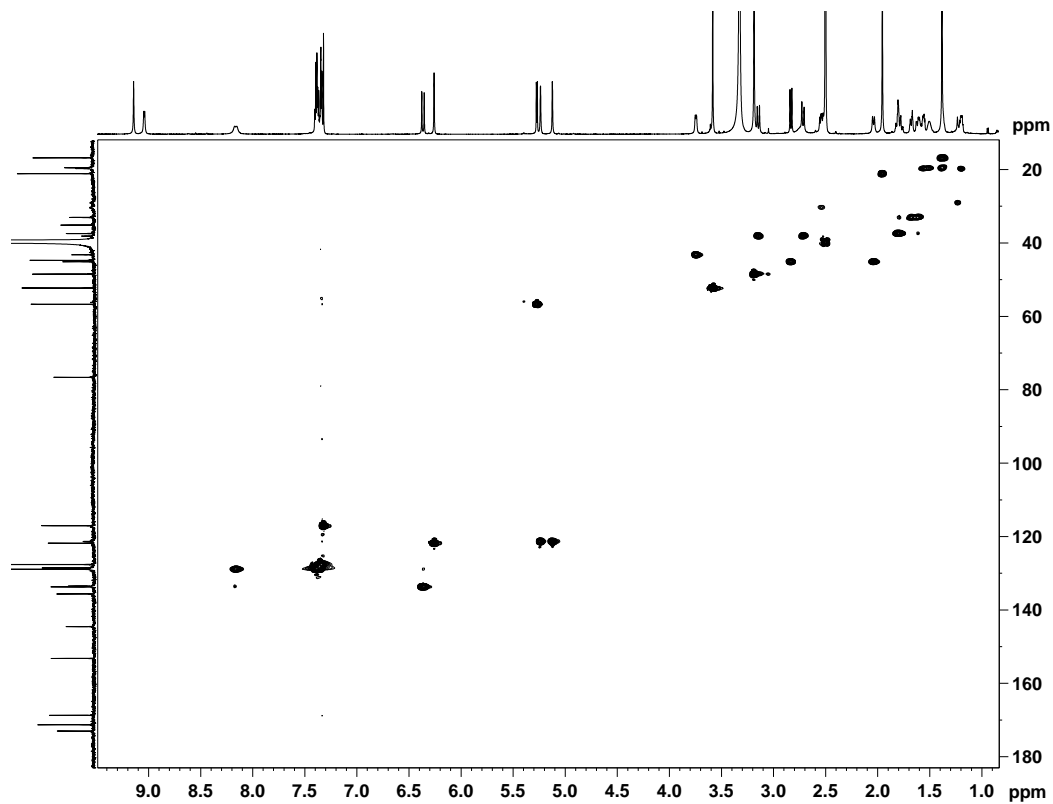


Fig. S15-RE. ^1H - ^1H COSY spectra of (*R*)-PGME-GNM B2 (DMSO- d_6)

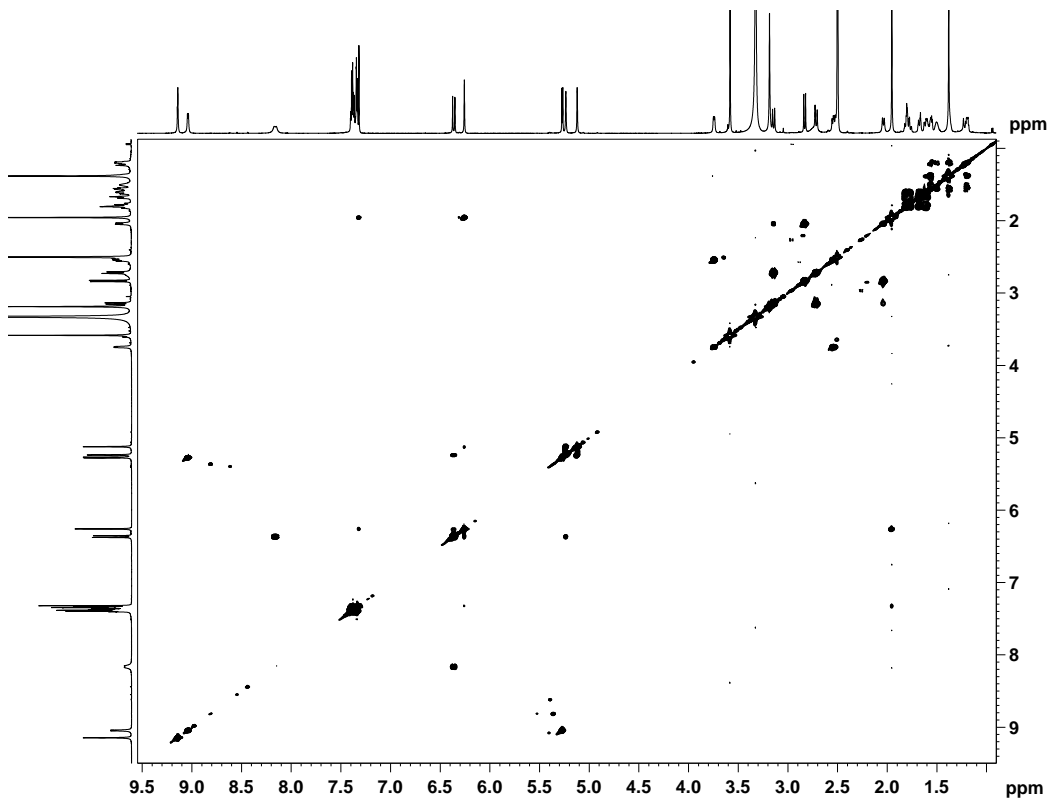


Fig. S15-RF. HMBC spectra of (*R*)-PGME-GNM B2 (DMSO- d_6)

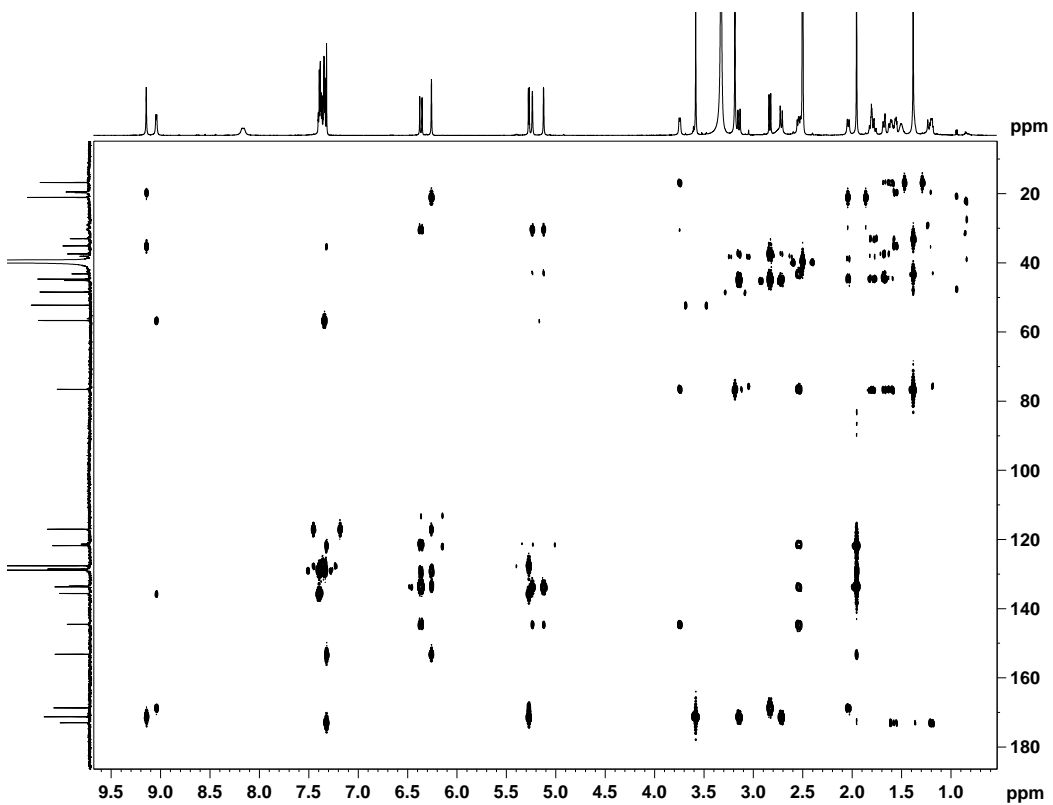


Fig. S15-RG. ROESY spectra of (*R*)-PGME-GNM B2 (DMSO-*d*₆)

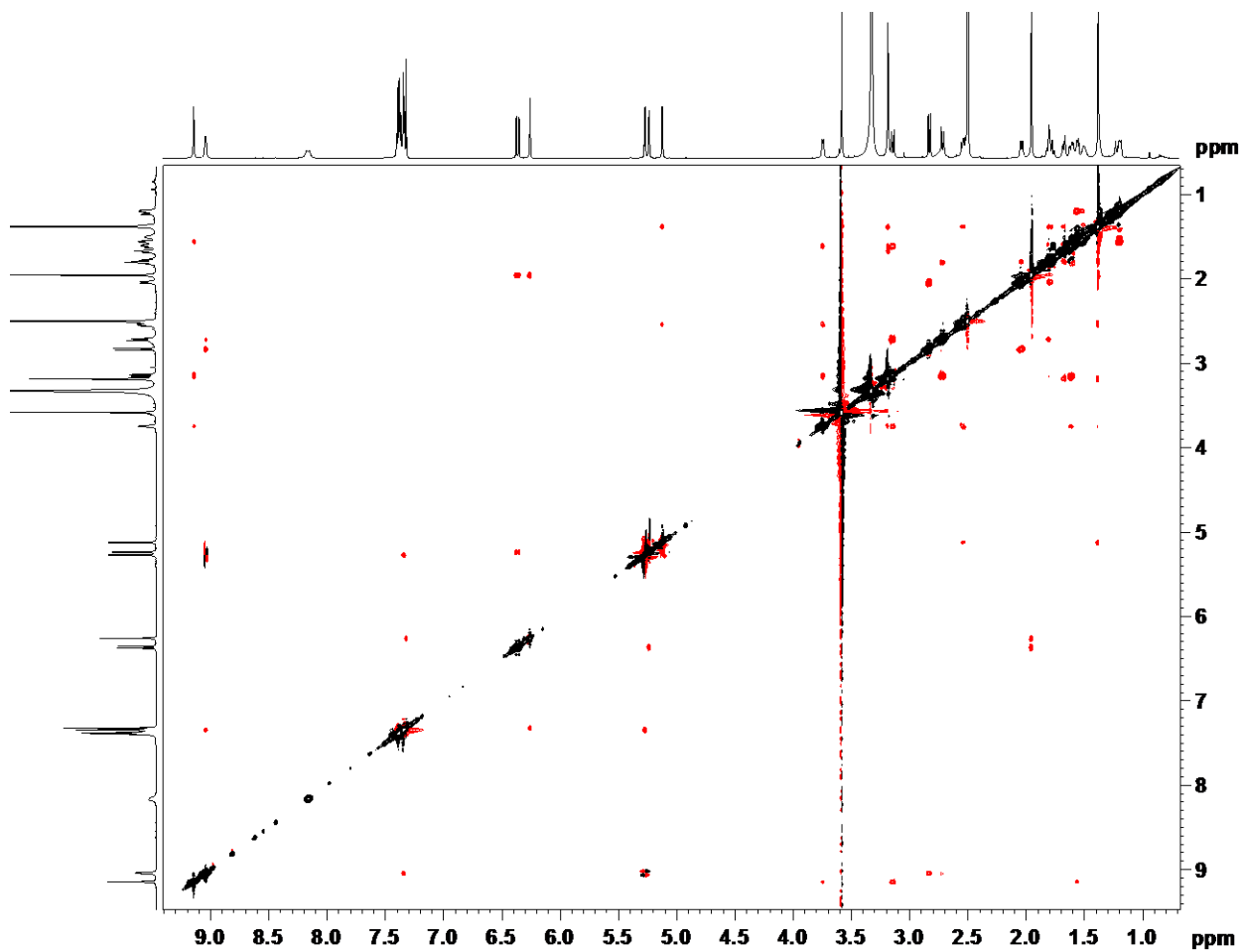


Fig. S15-RH. HR-MS (ESI) spectra of compound (*R*)-PGME-GNM B2

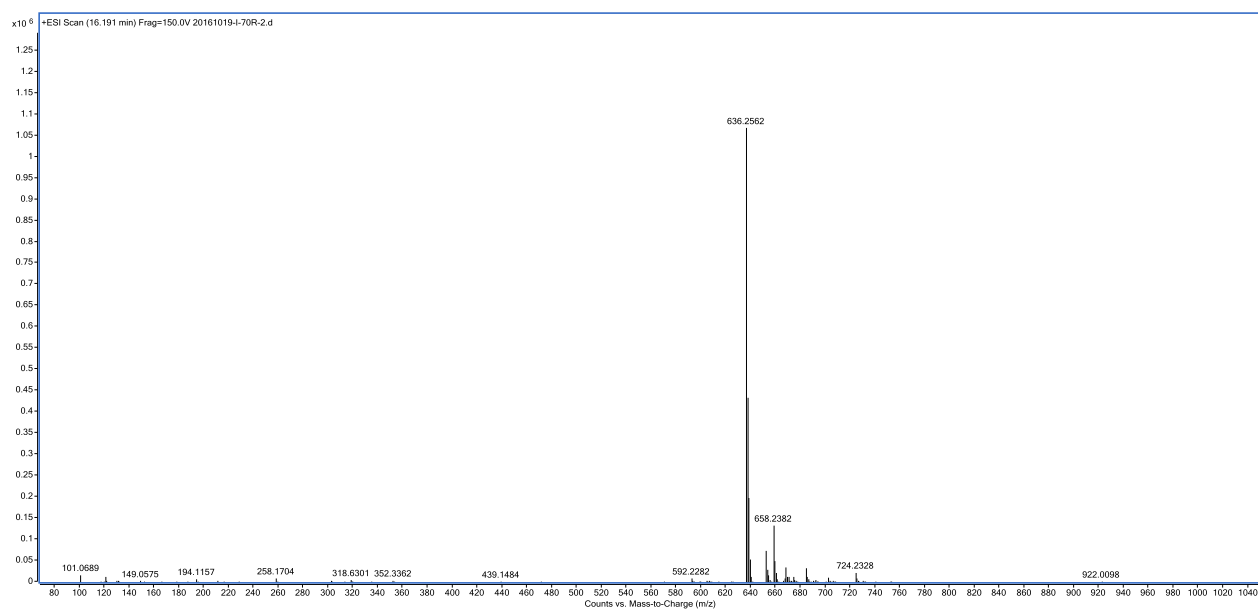


Fig. S16. Using (*S*)- and (*R*)-PGME derivatives of LNM E2 as models for the determination of the absolute configuration of LNM E2 (14, 23). The preferred conformations, especially the conformation of the C3 side chain, of both (*S*)- and (*R*)-PGME-LNM E2 (**A**) resembled that of LNM E2 (**C**) based on detailed analysis of their ROESY correlations. The presence of strong ROESY correlations between 20-H and 21-NH (**D**), as well as the residual correlations between 22-CH₃ and 21-NH (**E**), indicate in the preferred conformation, 20-H and 21-NH are syn-positioned, and 22-CH₃ and the macrolactam skeleton are positioned at the two sides of the plane defined by PGME. Based on the differences of chemical shift in ¹H NMR between (*R*)- and (*S*)-PGME-LNM E2 ($\Delta\delta = \delta_{(R)} - \delta_{(S)}$) as shown in **B**, the absolute configuration at C20 of LNM E2 is elucidated as (20*S*). In this case, $\Delta\delta$ could not be directly applied to determine the absolute configuration of C3, since the macrolactam backbone will be at the same side when C3 takes an opposite configuration as shown in **H**. This problem could be circumvented by correlating 20-H and 22-CH₃ with the hydrogens in the macrolactam backbone. The presence of ROESY correlations between 22-CH₃ and 2-H_b/4-H_b (**F**), support that C20-C22 and C3-S are anti-oriented in the preferred conformation. On the other hand, the absent correlations between 20-H and 2-H/4-H (**G**) is consistent with the 3*R* configurational assignment (**A**). Otherwise, strong correlation between 20-H and 4-H_a should be found in ROESY spectra due to their 1,3-diaxial relation (**H**), which is observed in the cases of GNM B2 (**Fig. S14**) and WSM A2 (**Fig. S24**). Furthermore, since the priming amino acid has been determined to be D-alanine in previous studies, the absent correlations between 18-CH₃ and 8-H_a/11-H (**I**), which is observed in the case of WSM A2 (**Fig. S20**), is supportive for 3*R* configurational assignment rather than 3*S*. Therefore, the absolute configuration of LNM E2 determined by PGME-derivatives is the same as that determined previously by total synthesis and X-ray diffractions. We thus conclude that the process by combination of conformational analysis based on ROESY correlations, and determination of the chirality of the α -carbon with PGME-derivatives, would provide reliable approach for the elucidation of the absolute configurations of other related natural products discovered from strains CB01883 and CB02120-2. H_a denotes one of the geminal hydrogens appearing at lower field in ¹H NMR, and H_b denotes one of the geminal hydrogens appearing at higher field in ¹H NMR.

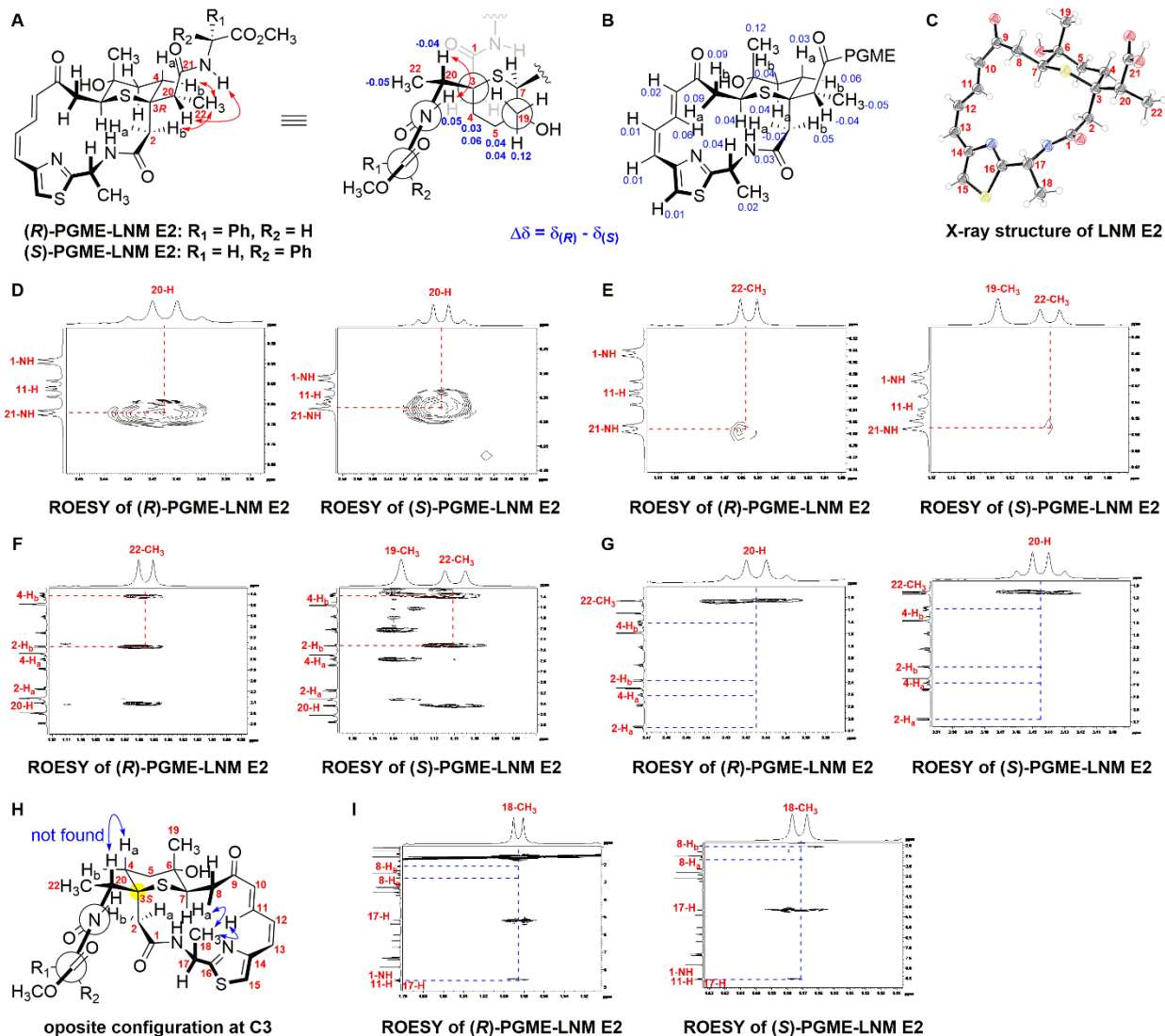


Fig. S17-SA. ^1H NMR spectra of (S)-PGME-LNM E2 (700 MHz, $\text{DMSO}-d_6$)

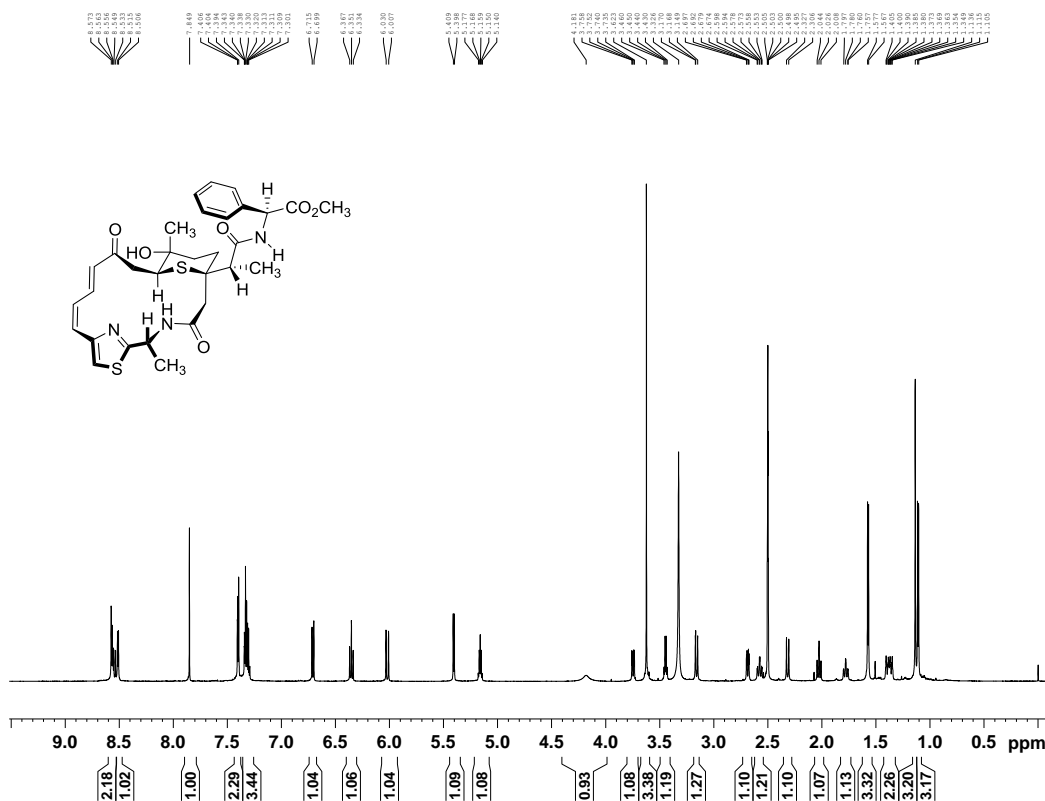


Fig. S17-SB. ^{13}C NMR spectra of (S)-PGME-LNM E2 (175 MHz, $\text{DMSO}-d_6$)

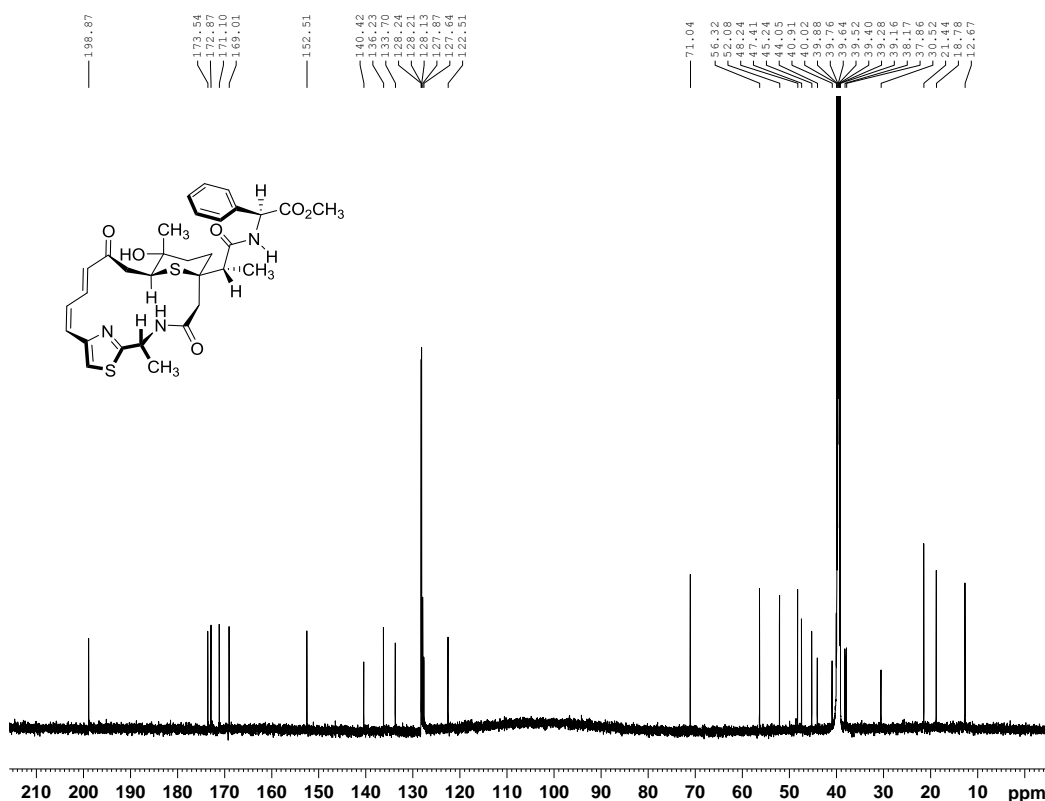


Fig. S17-SC. DEPT-135 spectra of (S)-PGME-LNM E2 (DMSO- d_6)

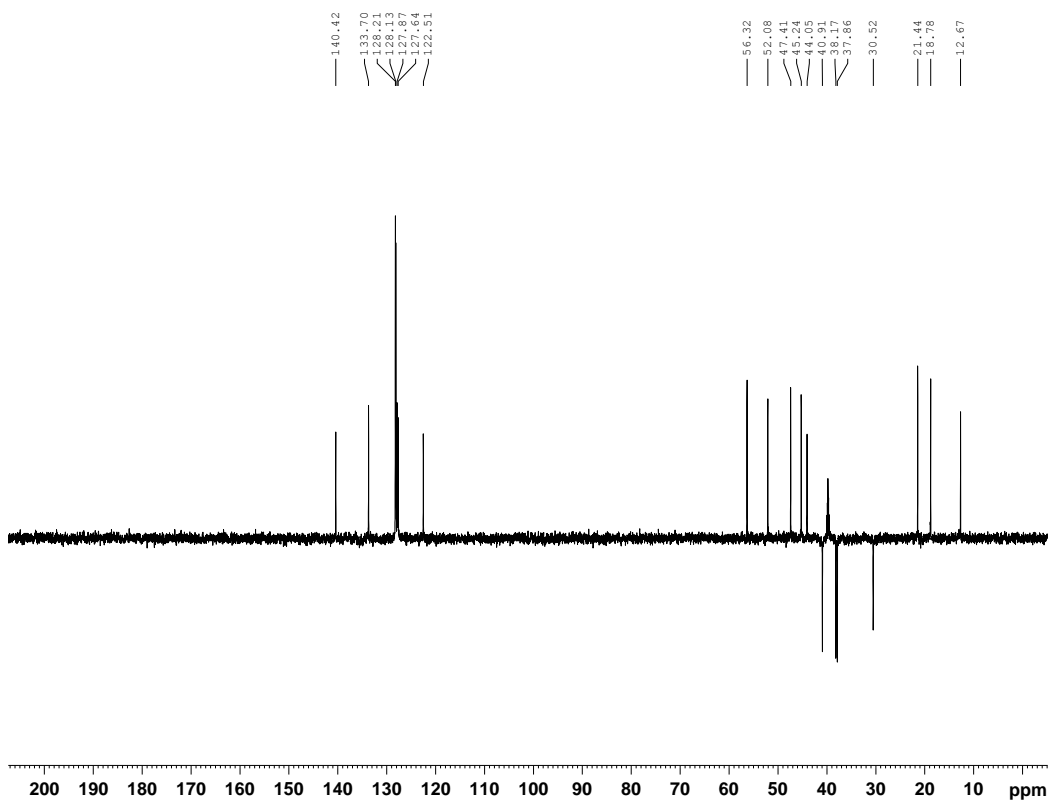


Fig. S17-SD. HSQC spectra of (S)-PGME-LNM E2 (DMSO- d_6)

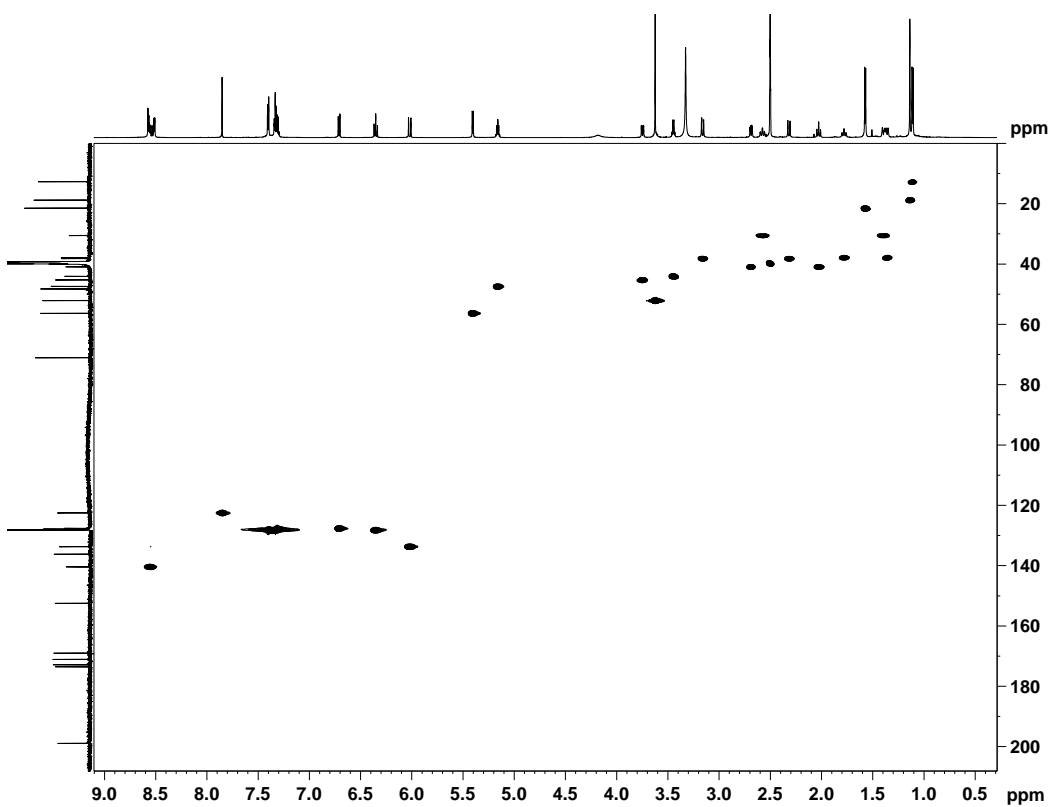


Fig. S17-SE. ^1H - ^1H COSY spectra of (S)-PGME-LNM E2 (DMSO- d_6)

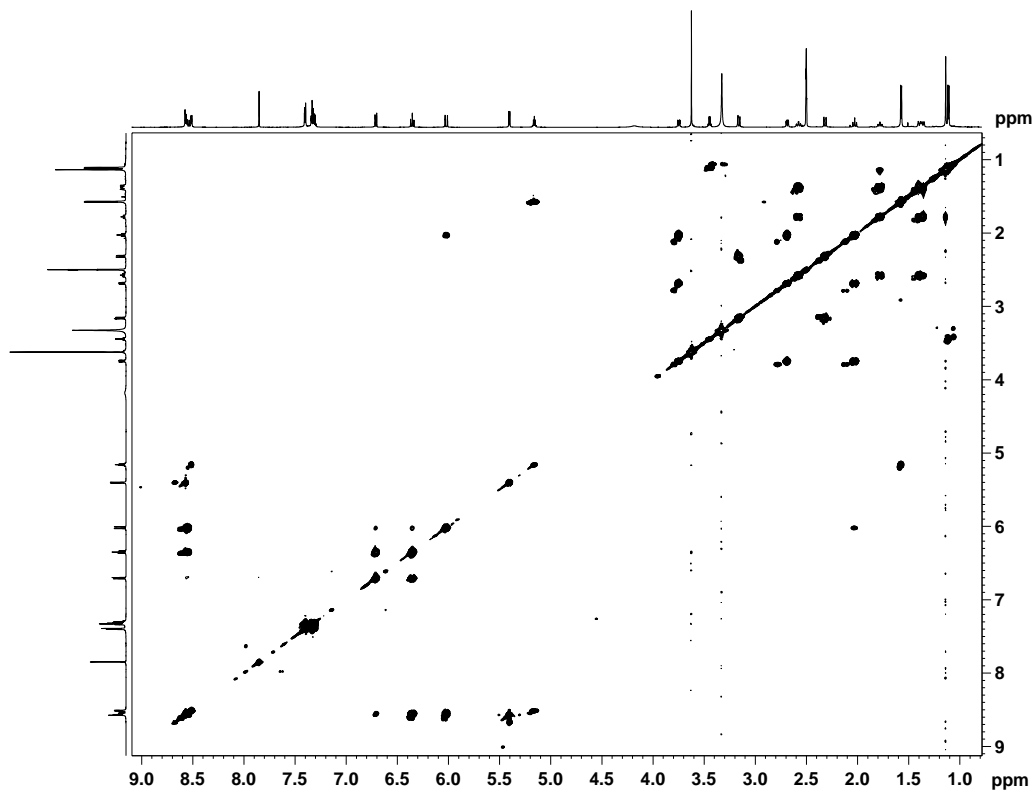


Fig. S11-SF. HMBC spectra of (S)-PGME-LNM E2 (DMSO- d_6)

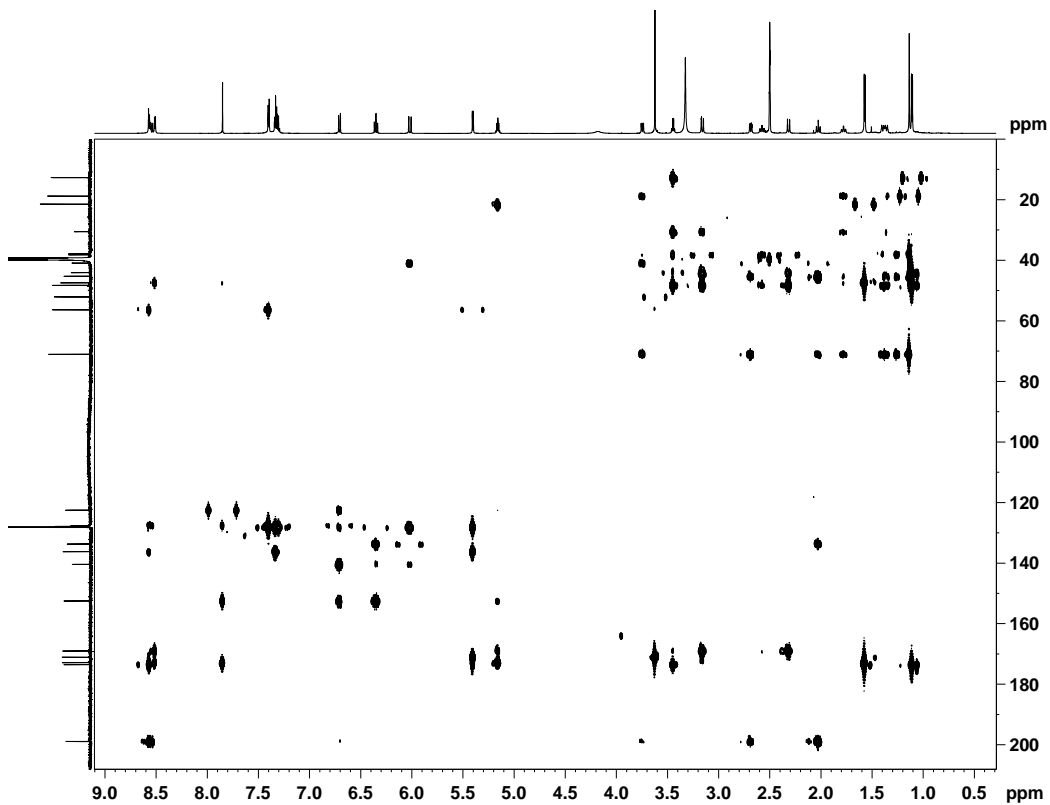


Fig. S17-SG. ROESY spectra of (S)-PGME-LNM E2 (DMSO-*d*₆)

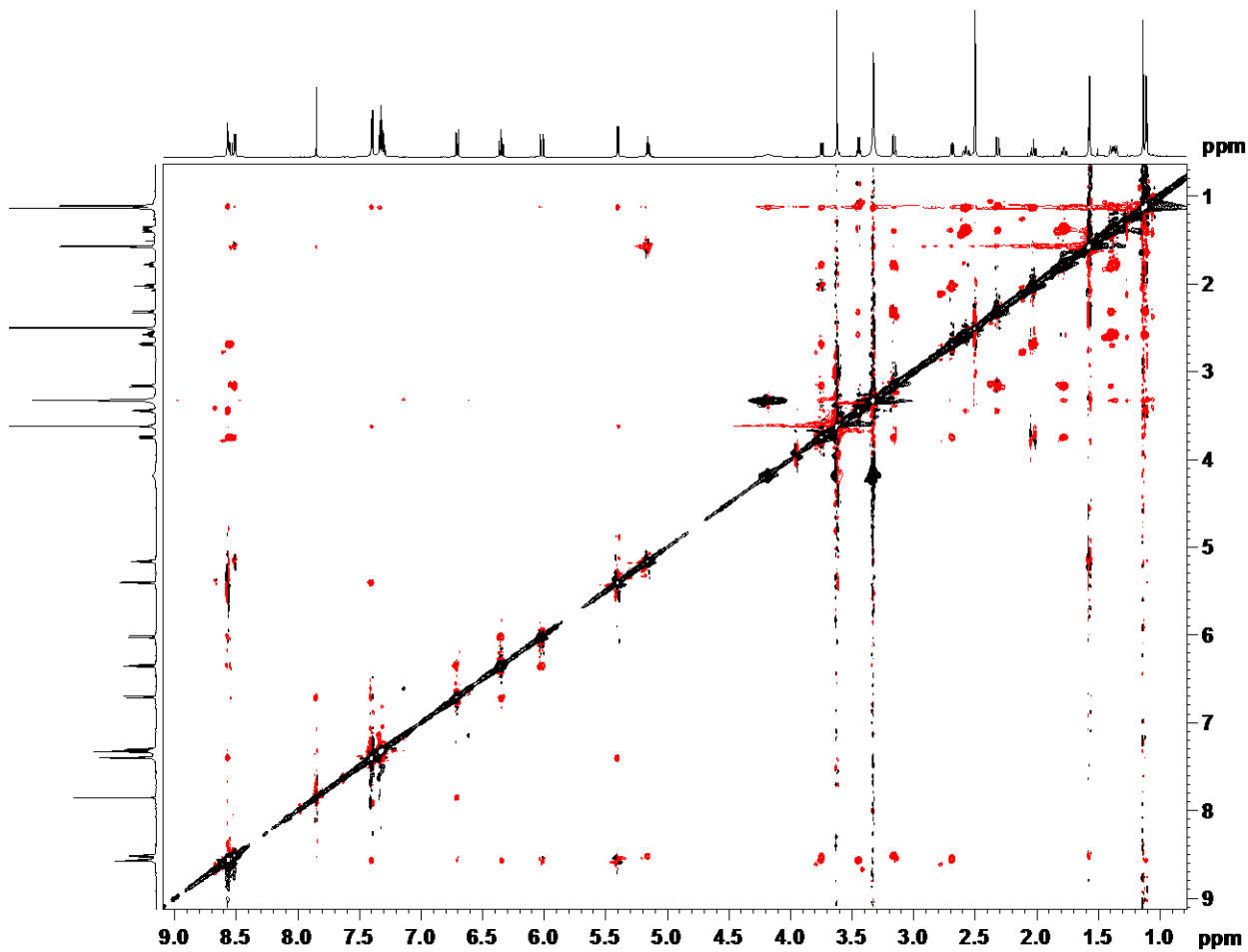


Fig. S17-SH. HR-MS (ESI) spectra of (S)-PGME-LNM E2

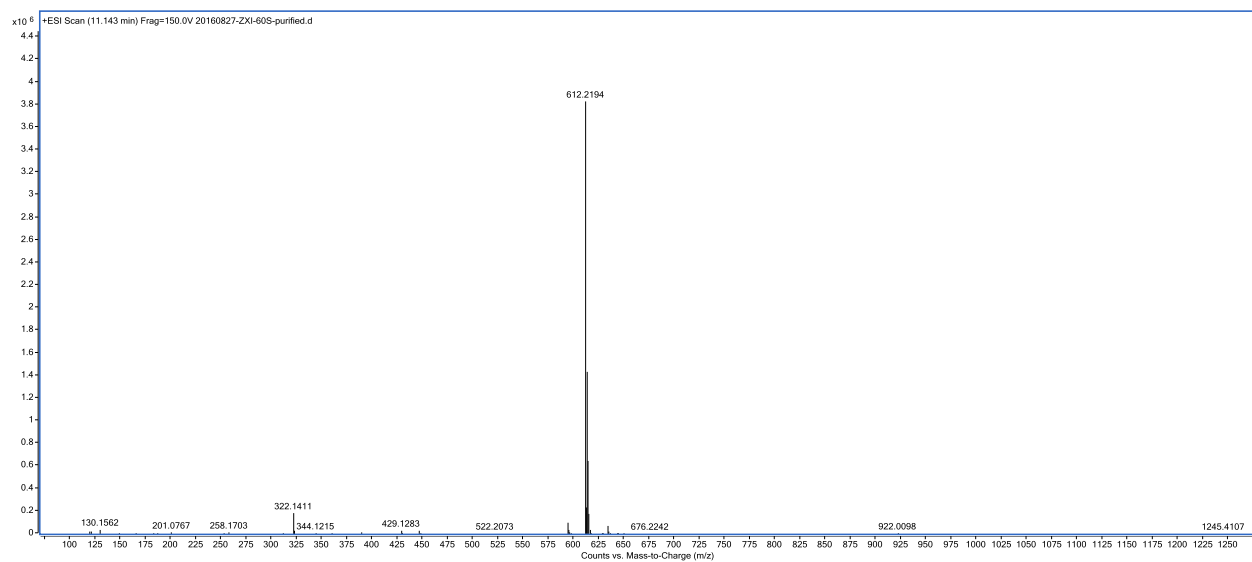


Fig. S17-RA. ^1H NMR spectra of (*R*)-PGME-LNM E2 (700 MHz, DMSO- d_6)

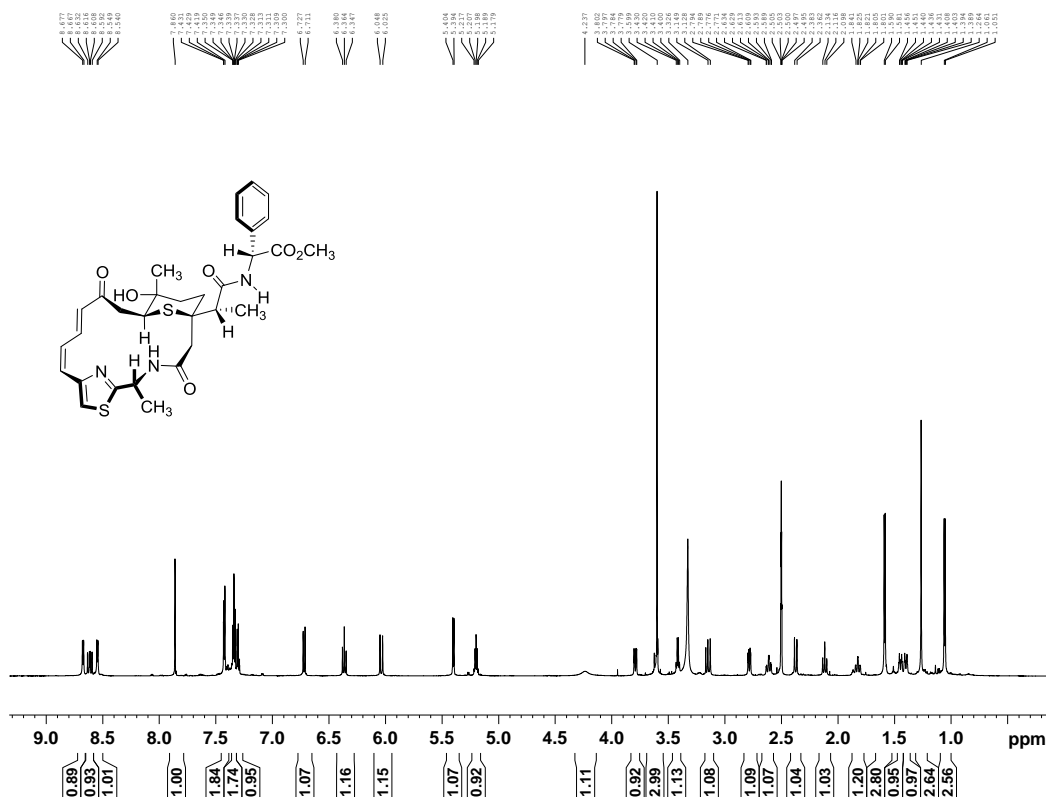


Fig. S17-RB. ^{13}C NMR spectra of (*R*)-PGME-LNM E2 (175 MHz, DMSO- d_6)

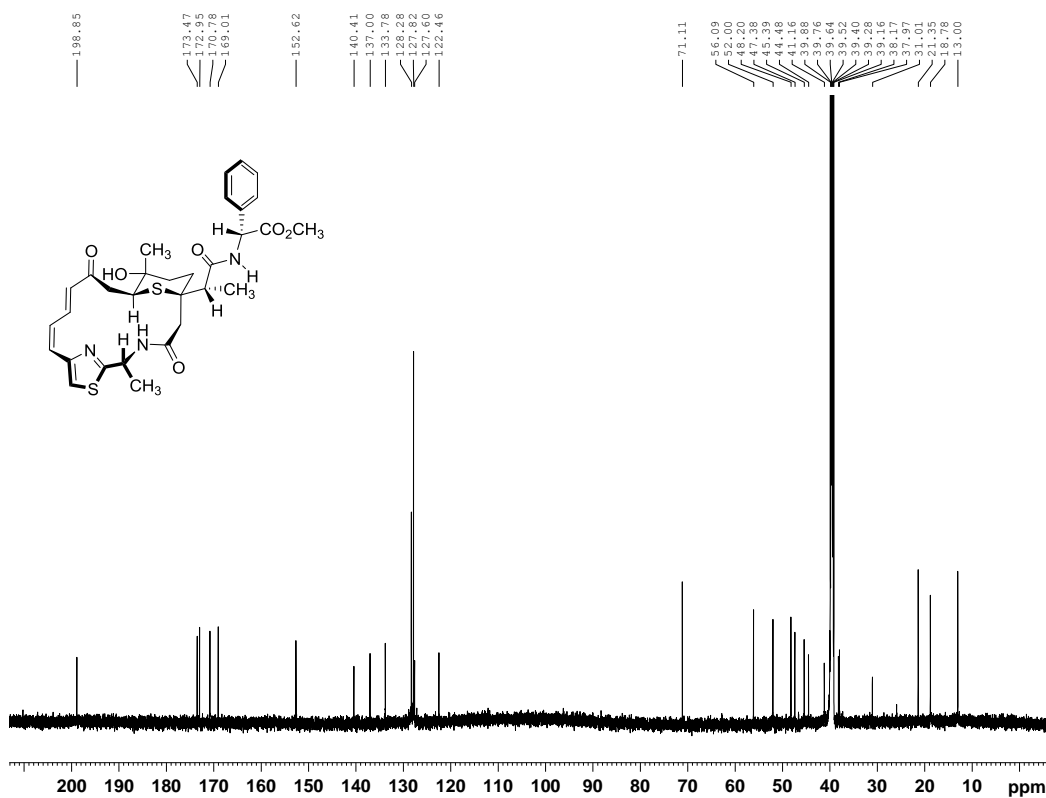


Fig. S17-RC. DEPT-135 spectra of (*R*)-PGME-LNM E2 (DMSO-*d*₆)

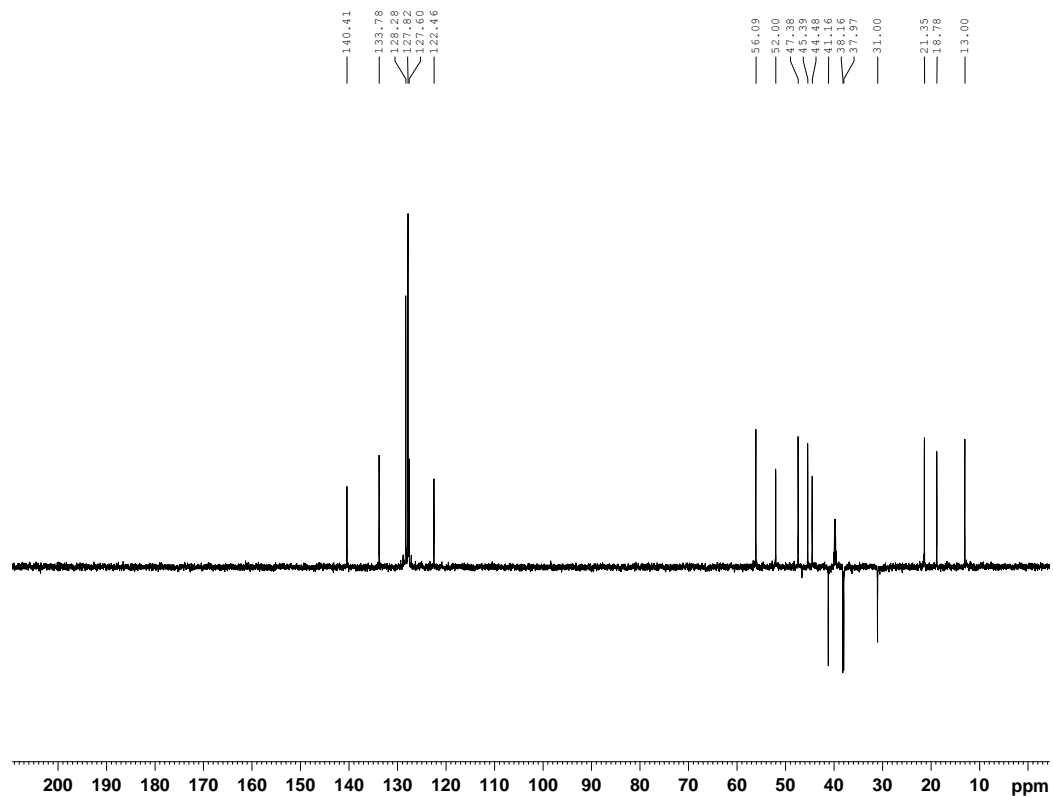


Fig. S17-RD. HSQC spectra of (*R*)-PGME-LNM E2 (DMSO-*d*₆)

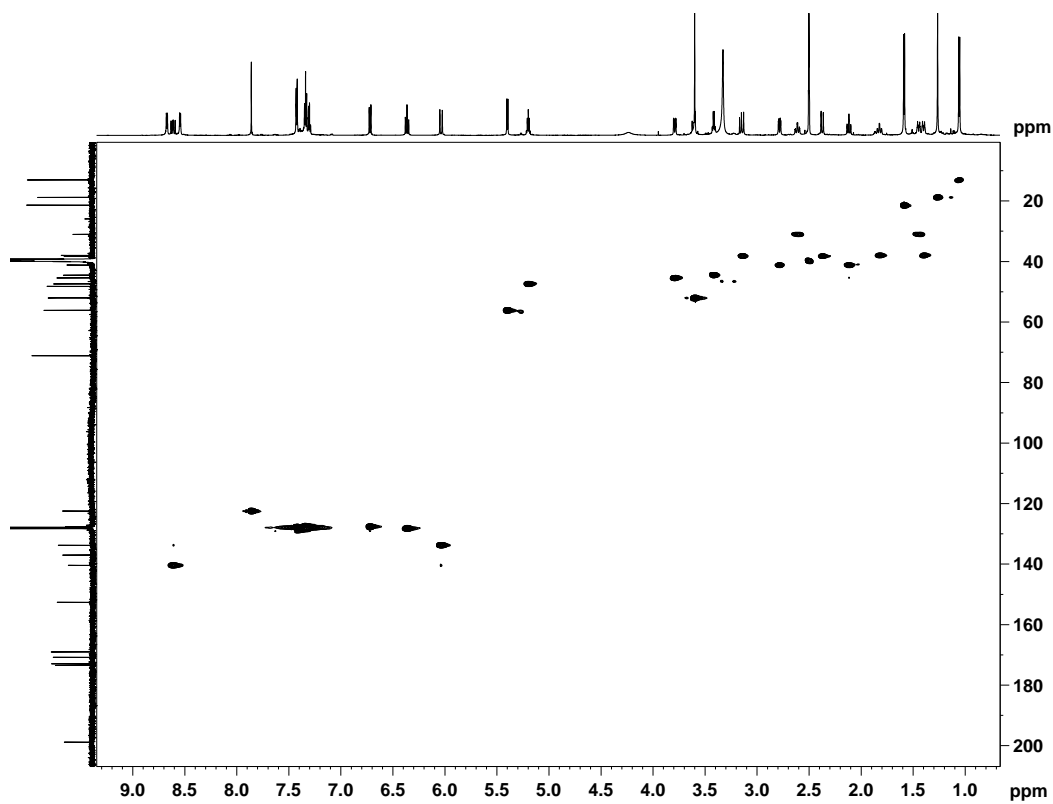


Fig. S17-RE. ^1H - ^1H COSY spectra of (*R*)-PGME-LNM E2 (DMSO- d_6)

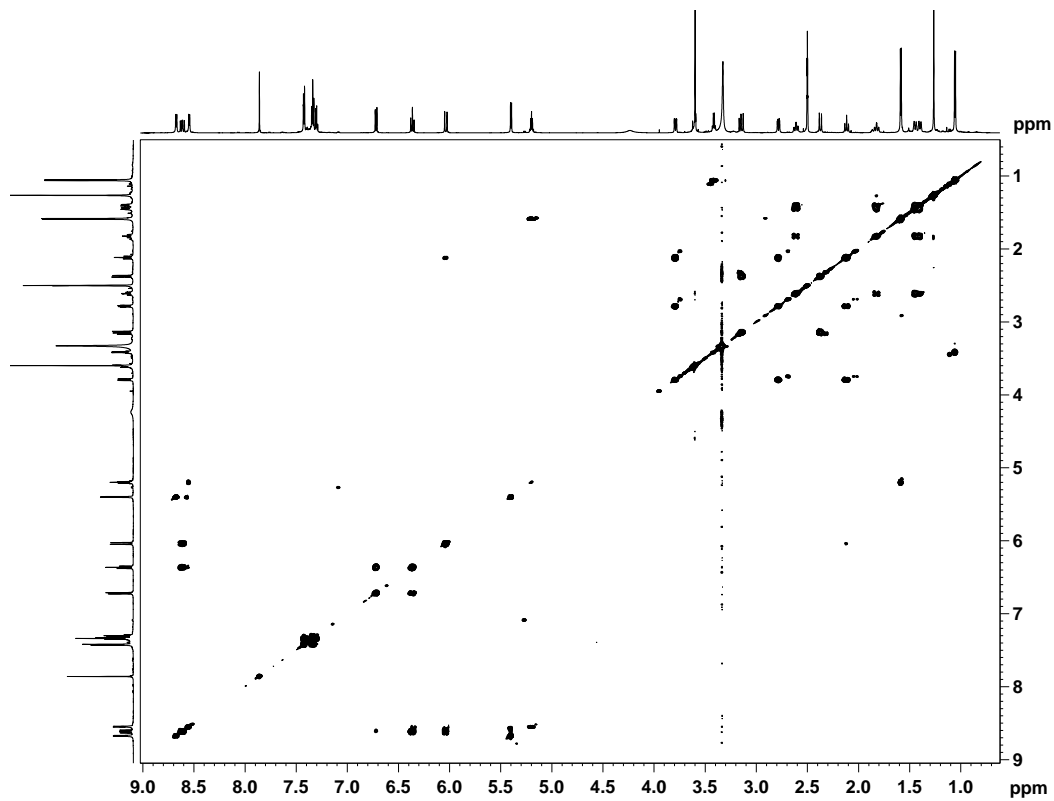


Fig. S17-RF. HMBC spectra of (*R*)-PGME-LNM E2 (DMSO- d_6)

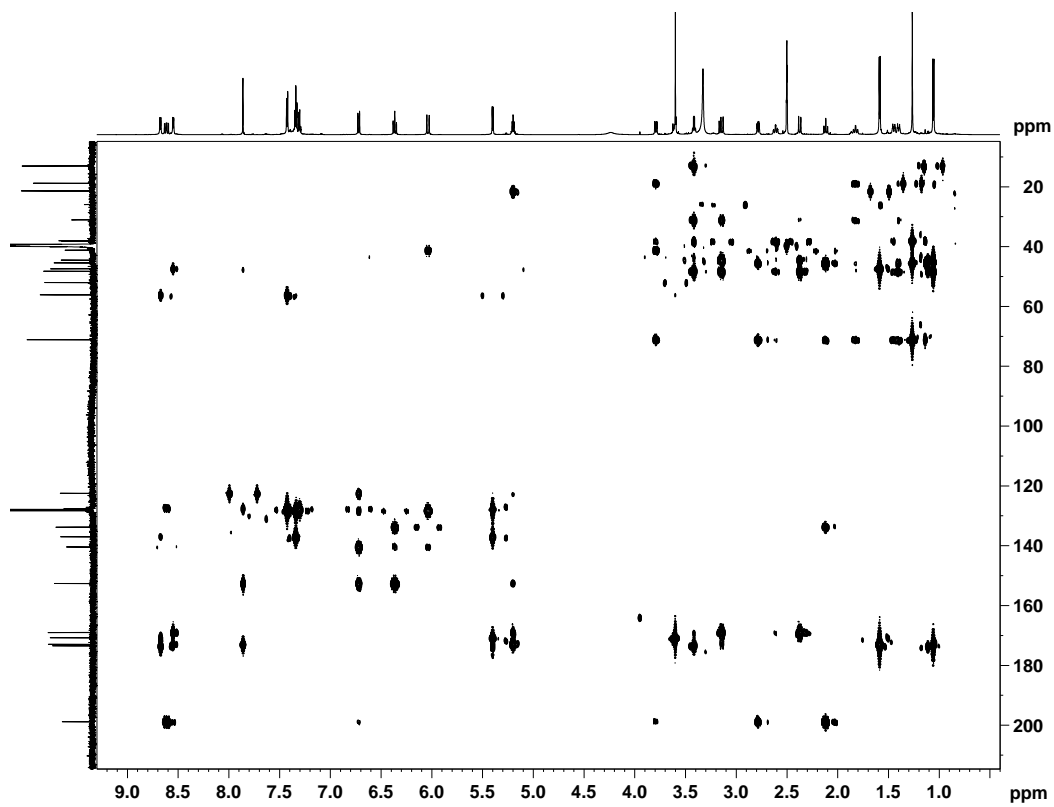


Fig. S17-RG. ROESY spectra of (*R*)-PGME-LNM E2 (DMSO-*d*₆)

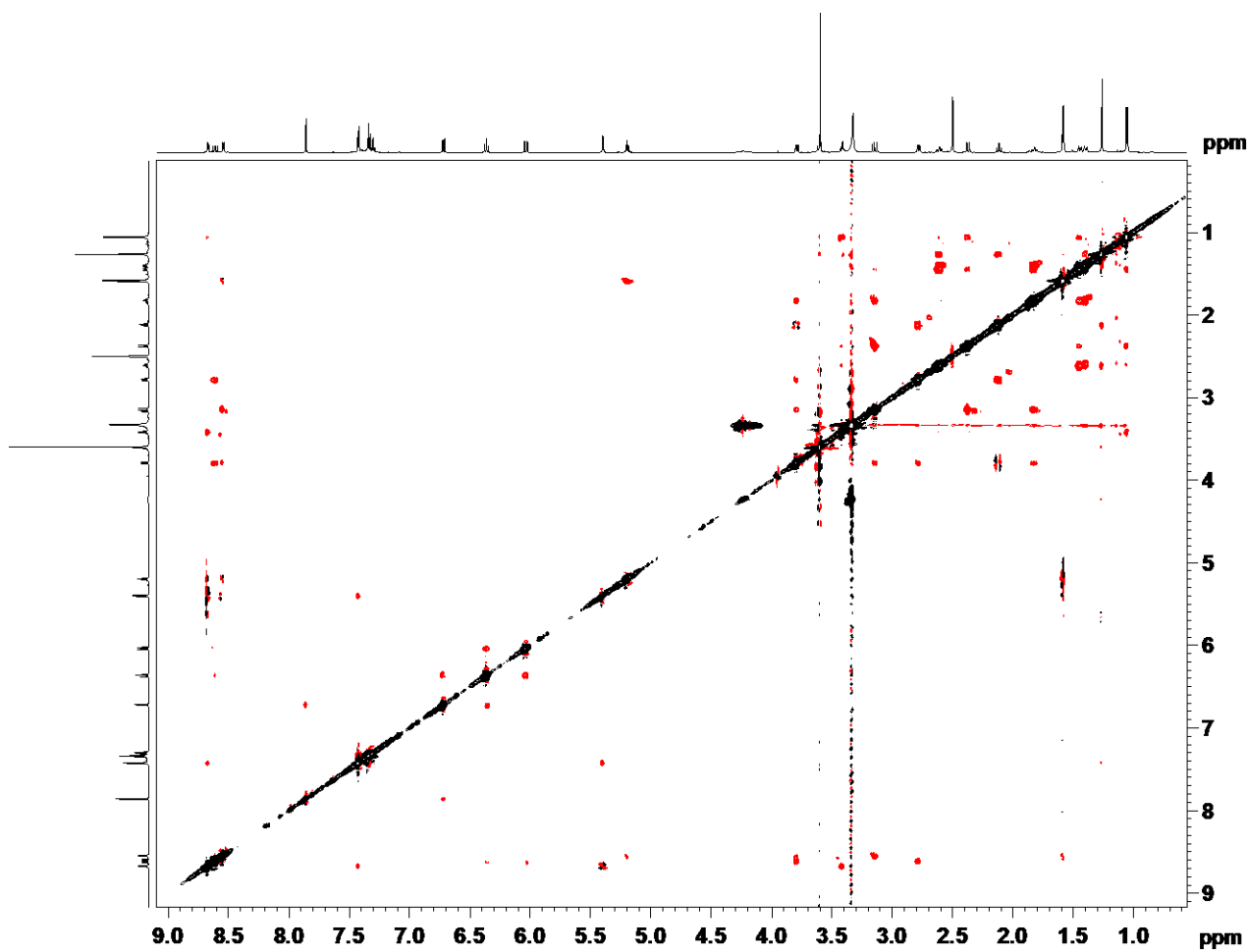


Fig. S17-RH. HR-MS (ESI) spectra of (*R*)-PGME-LNM E2

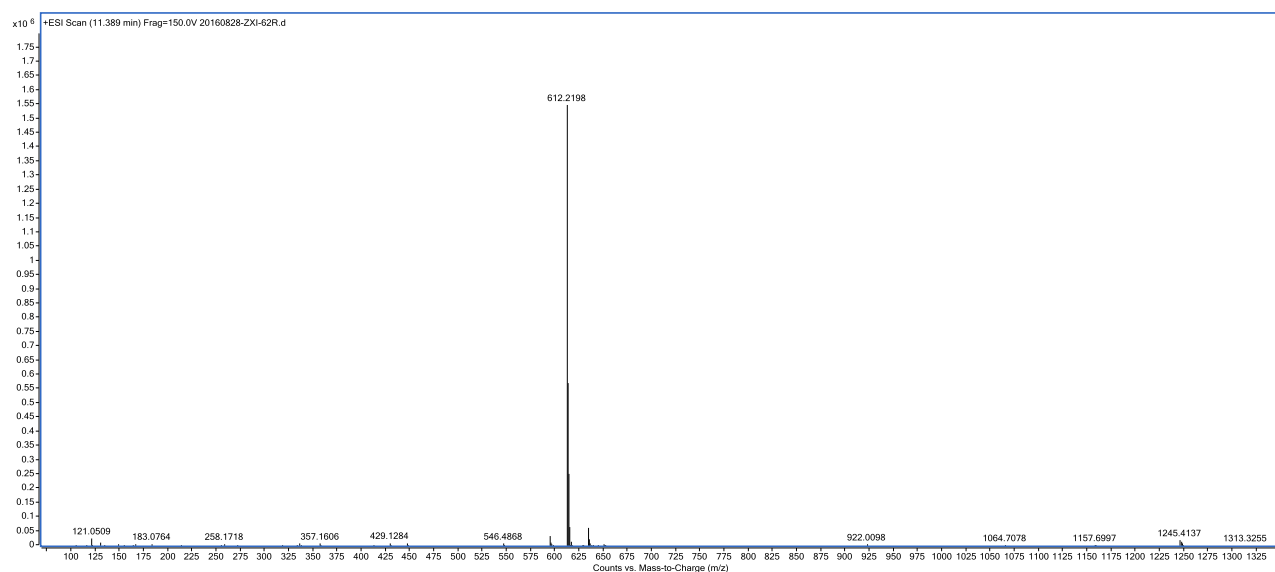


Fig. S18. Construction of the in-frame deletion mutant strain SB22001 (i.e. $\Delta wsmW$) and confirmation of its genotype by Southern analysis. **(A)** Schematic representation for the deletion of *wsmW* in strain CB02120-2 by homologous recombination. The probe (503 bp) for Southern blot was amplified with primers orf25-SBlot-5 and orf25-SBlot-3 using genomic DNA of strain CB02120-2 as the template. Apr^S, apramycin sensitive; Apr^R, apramycin resistance; *acc(3)/V*, apramycin resistance gene. **(B)** Southern blot verification of strain CB02120-2 wild type (3.3 kb) and mutant strain SB22001 (1.3 kb). Genomic DNAs were digested with *Kpn*I and then used for Southern analysis. Lane 1, DNA marker VII, DIG-labeled (Roche); lane 2, strain CB02120-2 wild type; lane 3, SB22001.

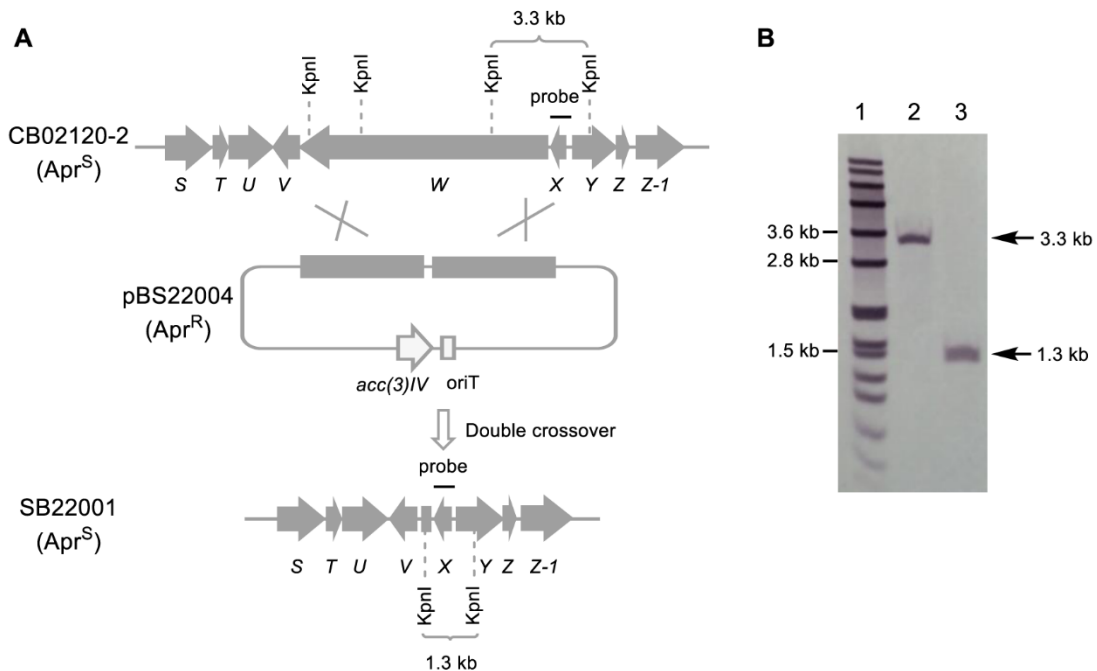


Fig. S19. Proposed biosynthetic pathway of weishanmycins (WSMs) in *S. sp.* CB002120-2. **(A)** Genetic organization of *wsm* gene cluster, together with three cosmids pBS22001 (8E4), pBS22002 (7F6) and pBS22003 (3F12) covering the whole gene cluster. **(B)** The biosynthetic machinery of WSMs featuring a similar hybrid NRPS-AT-less type I PKS to that of LNM consisting of WsmQPWGR and a discrete AT WsmJ, producing the nascent product with 3-thiol group, which was further oxidized to give WSM A1, A2, and A3. **(C)** Two possible pathways for the formation of propylmalonyl-S-ACP as the extender unit during the biosynthesis of WSMs. The propylmalonyl-S-ACP can be formed either by loading propylmalonyl-CoA, which is biosynthesized from malonyl-CoA and propionyl-CoA by WsmZ2Z3Z4, directly to the ACP of PKS module-3 by an unidentified trans-acting AT, or by loading malonyl-CoA to the ACP of PKS module-3 by trans-acting AT WsmJ, followed by modification of the resultant malonyl-S-ACP by WsmZ2Z3Z4 within the PKS before being incorporated into the growing intermediate.

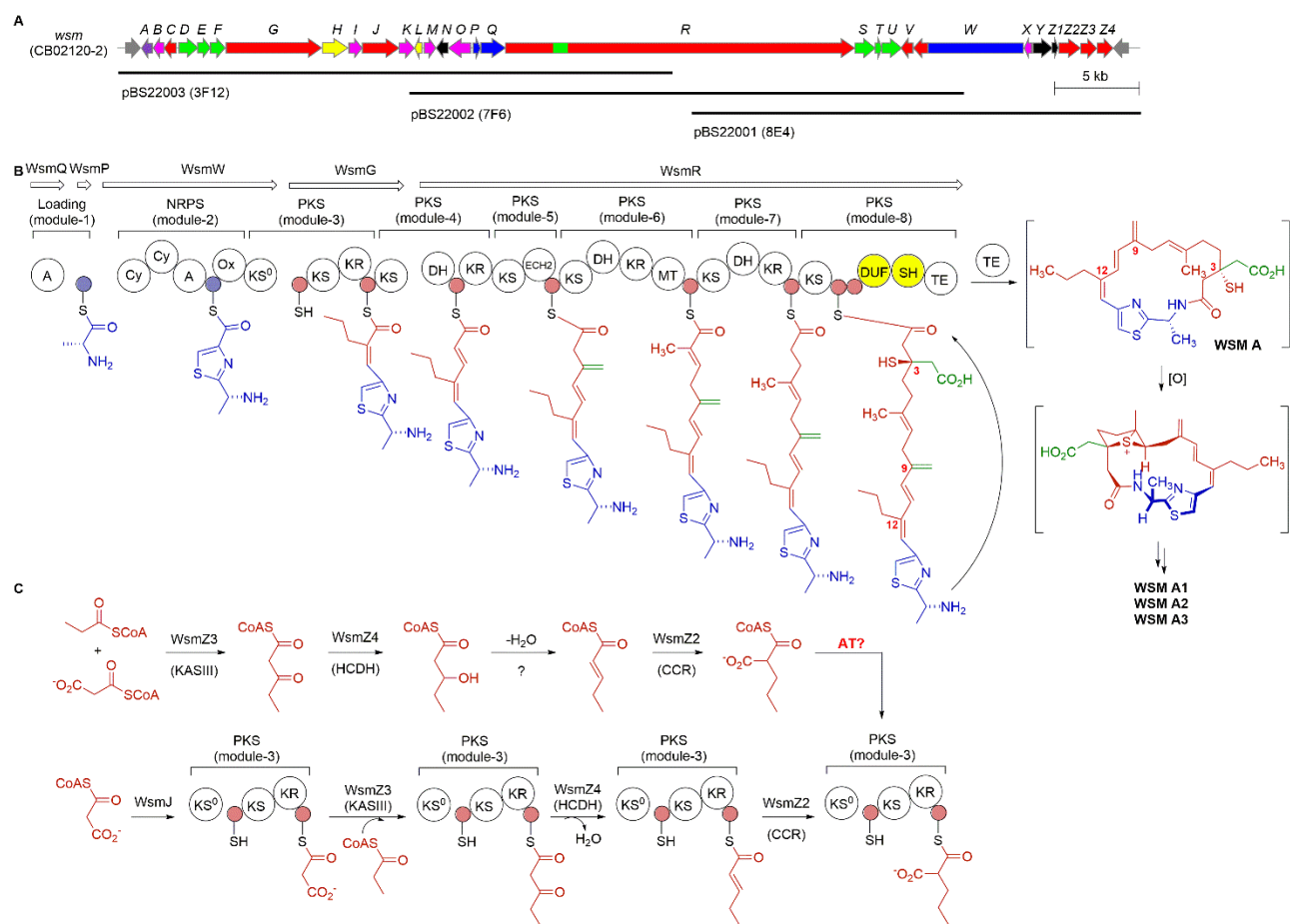


Fig. S20. Elucidation of new metabolites WSM A1, A2, and A3 isolated from strain CB02120-2 wild type. Key ^1H - ^1H COSY, HMBC and ROESY correlations are shown.

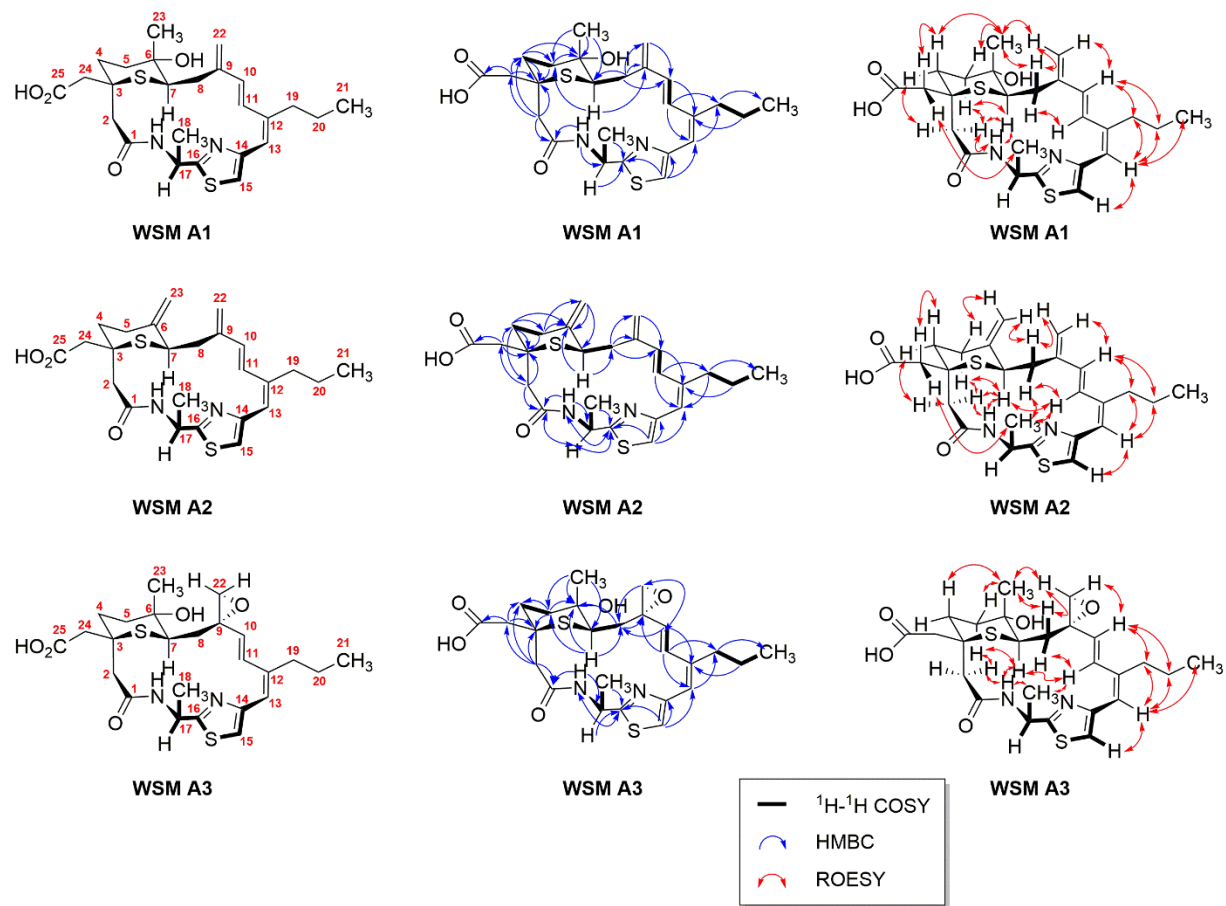


Fig. S21A. ^1H NMR spectra of WSM A1 (700 MHz, $\text{DMSO}-d_6$)

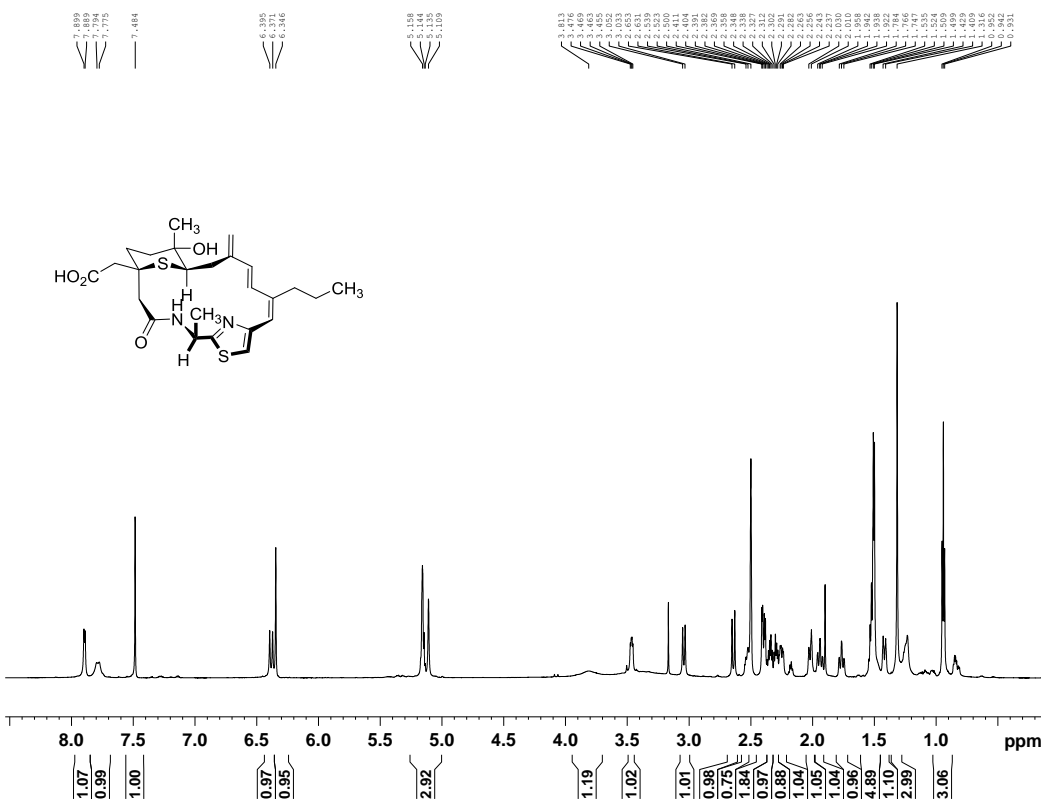


Fig. S21B. ^{13}C NMR spectra of WSM A1 (175 MHz, $\text{DMSO}-d_6$)

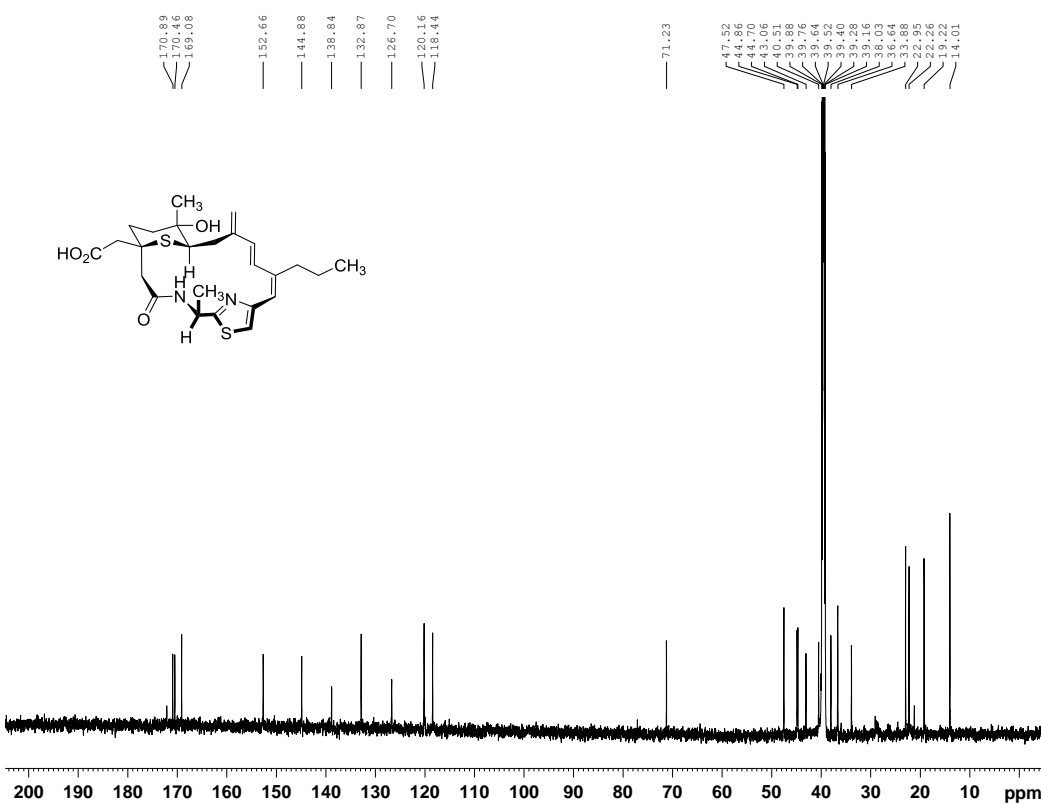


Fig. S21C. DEPT-135 spectra of WSM A1 (DMSO- d_6)

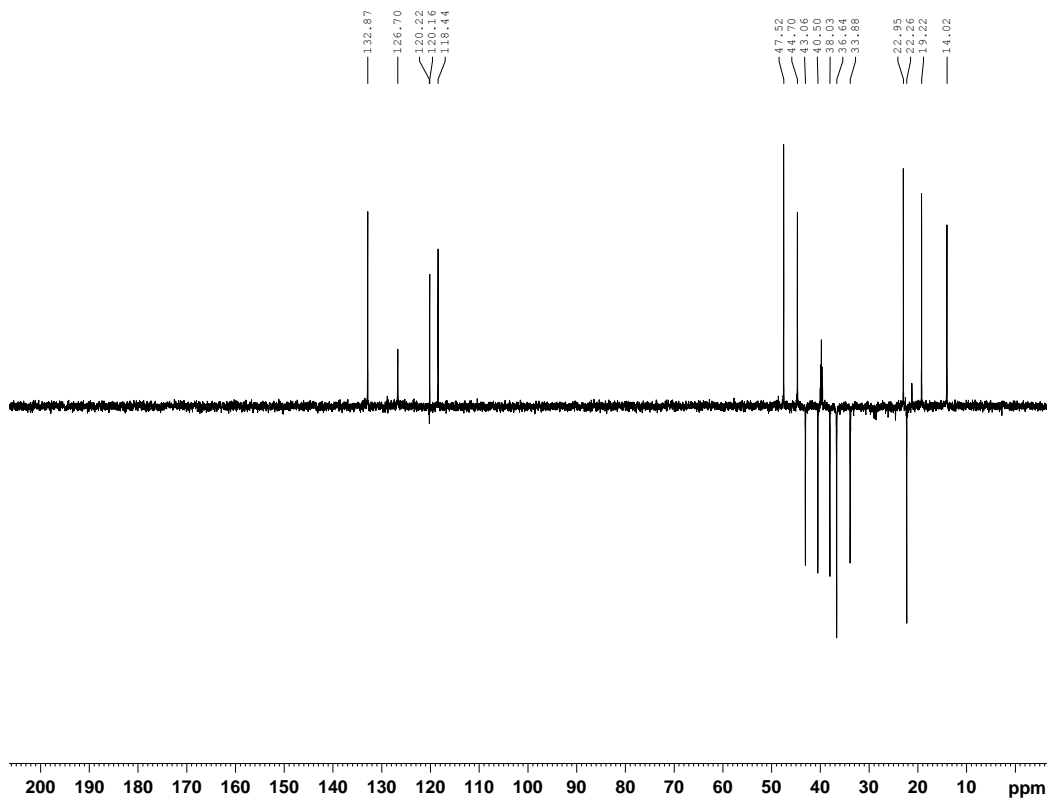


Fig. S21D. HSQC spectra of WSM A1 (DMSO- d_6)

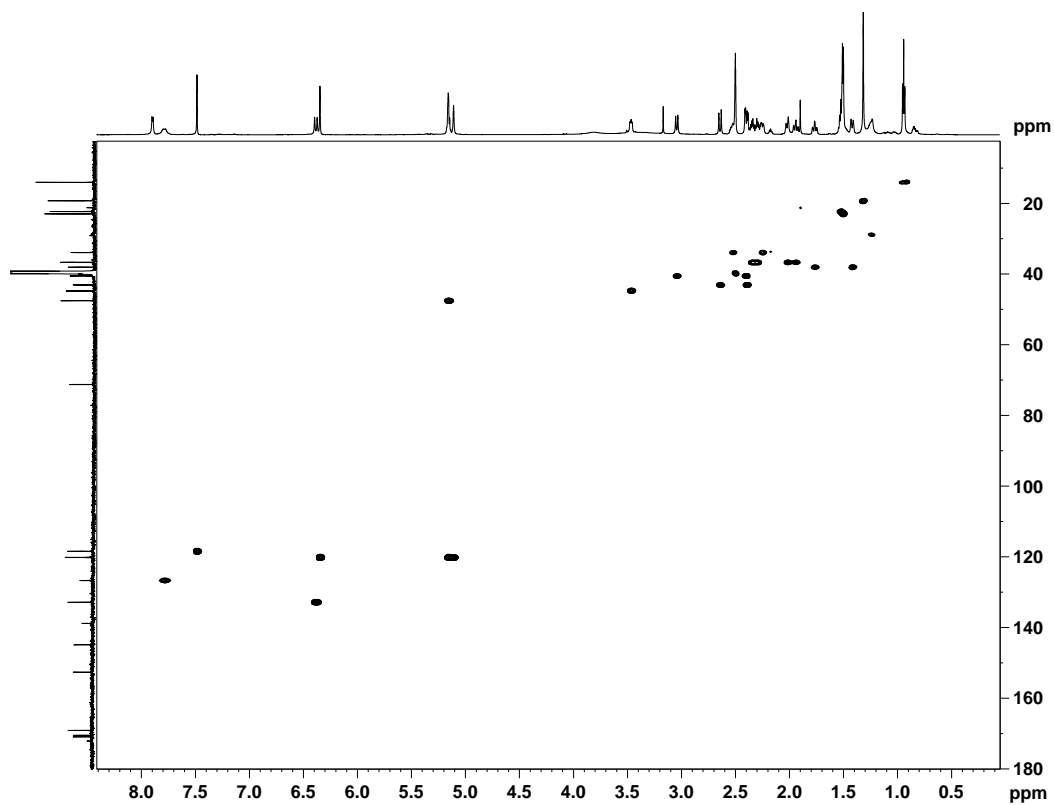


Fig. S21E. ^1H - ^1H COSY spectra of WSM A1 (DMSO- d_6)

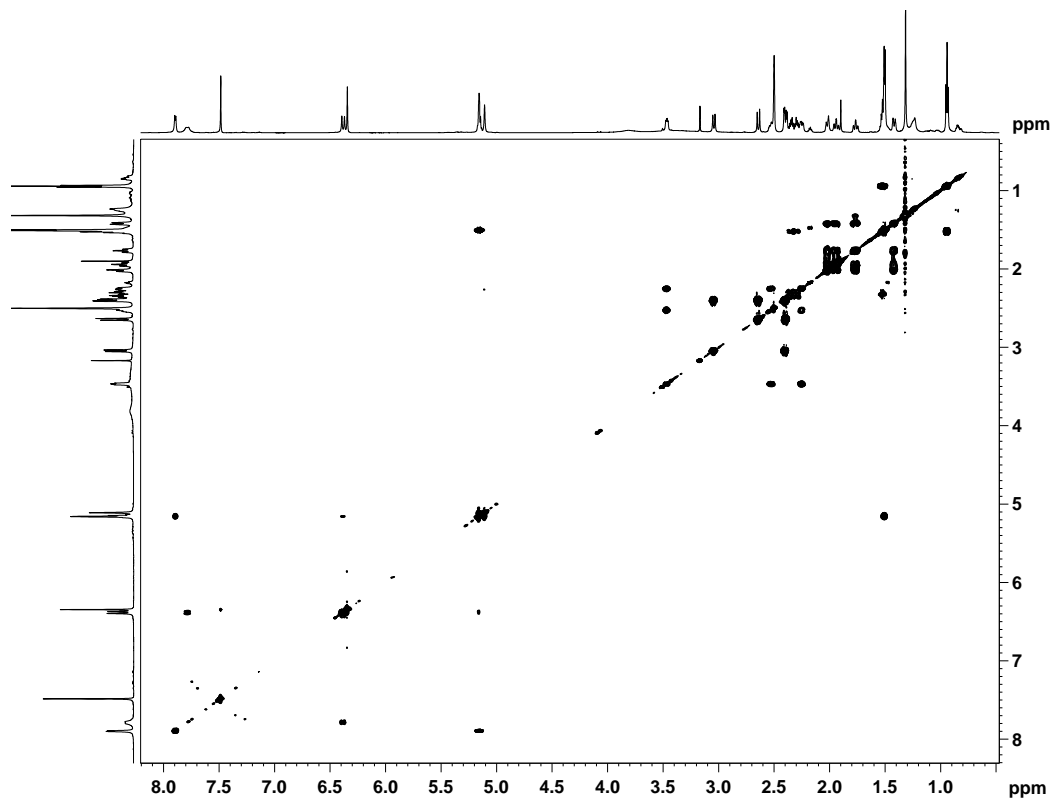


Fig. S21F. HMBC spectra of WSM A1 (DMSO- d_6)

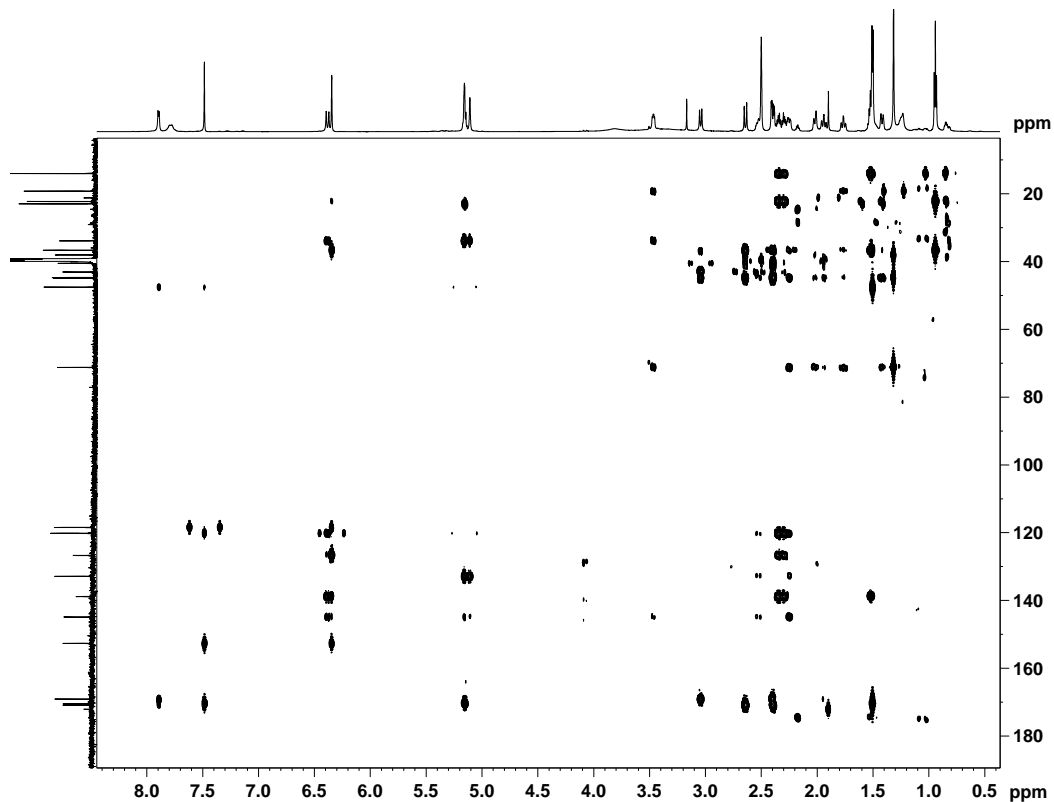


Fig. S21G. ROESY spectra of WSM A1 (DMSO-*d*₆)

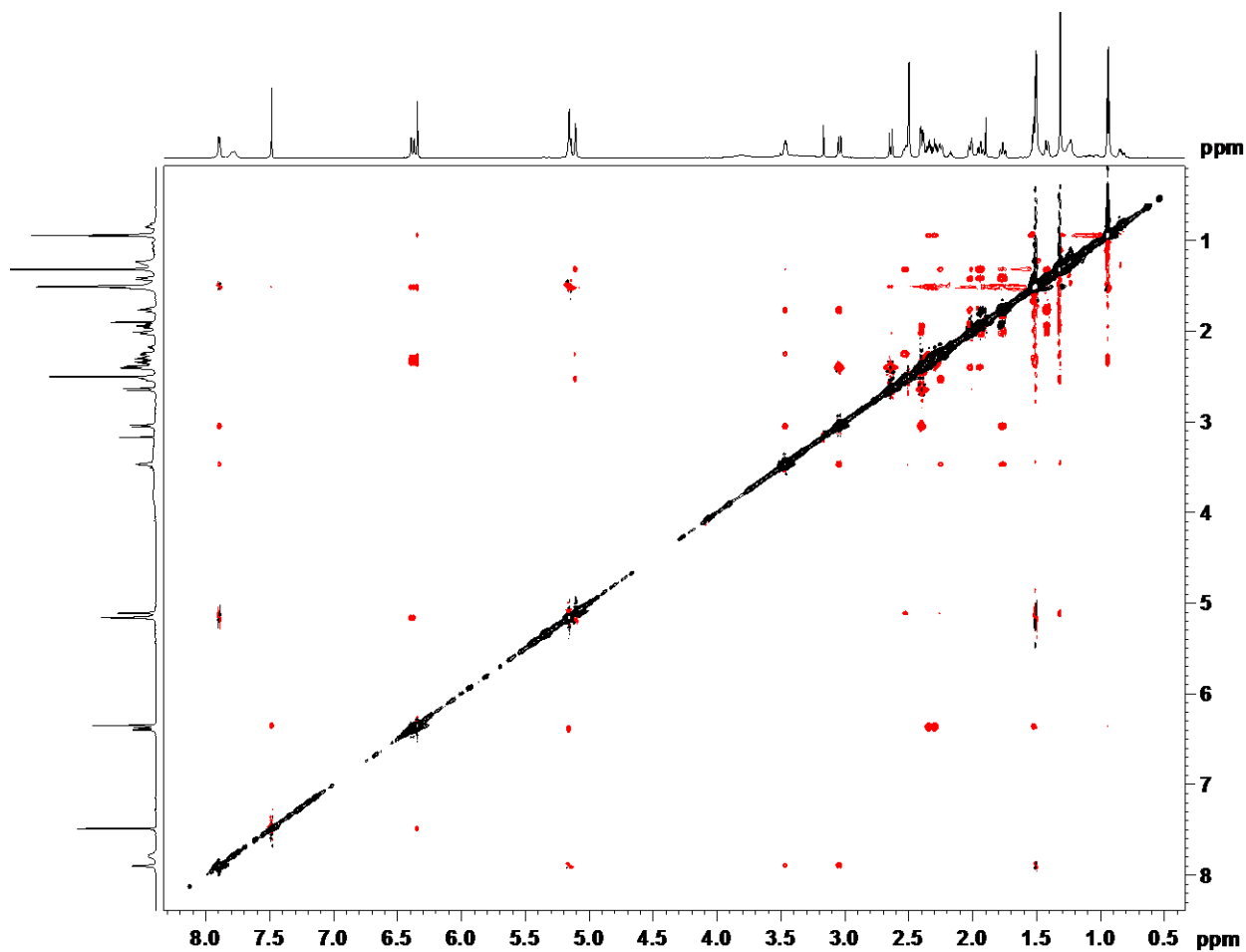


Fig. S21H. HR-MS (ESI) spectra of WSM A1

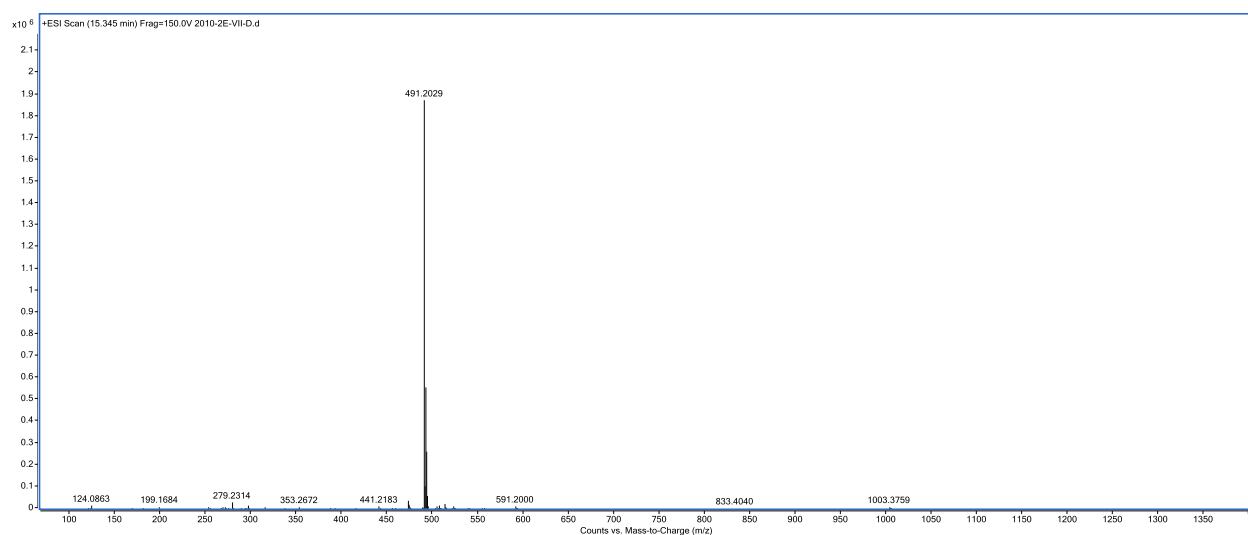


Fig. S22A. ^1H NMR spectra of WSM A2 (700 MHz, $\text{DMSO}-d_6$)

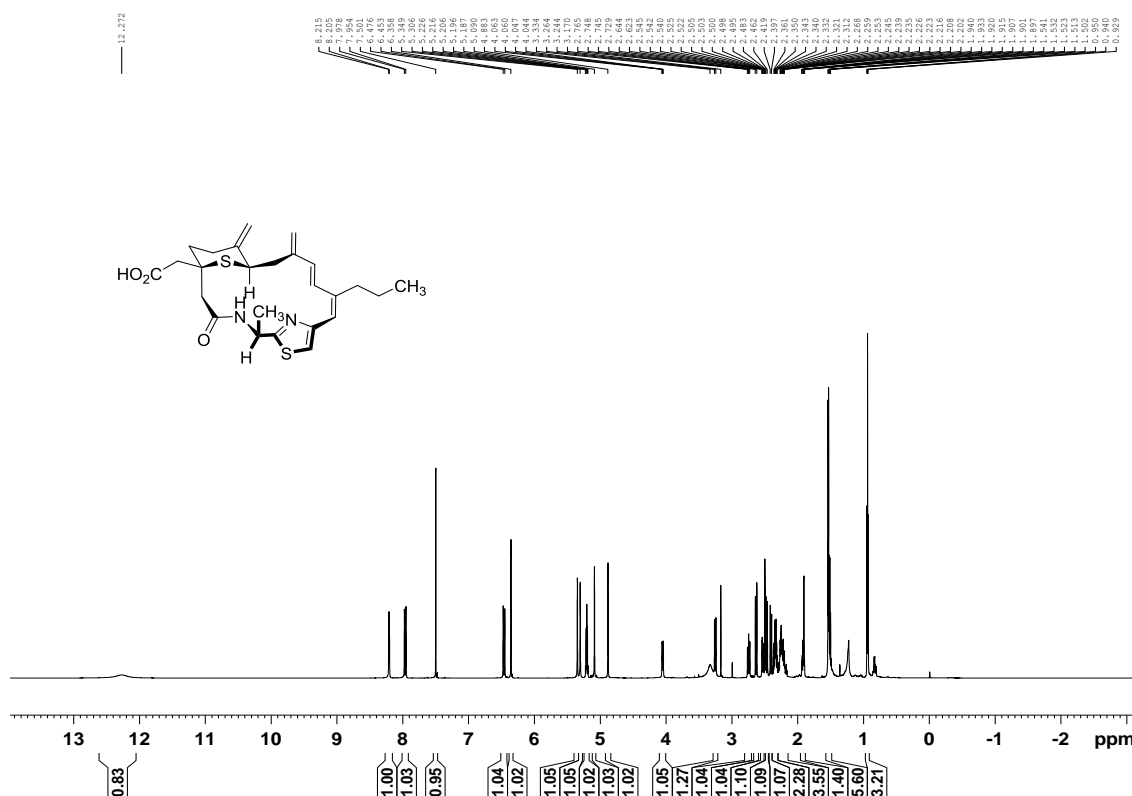


Fig. S22B. ^{13}C NMR spectra of WSM A2 (175 MHz, $\text{DMSO}-d_6$)

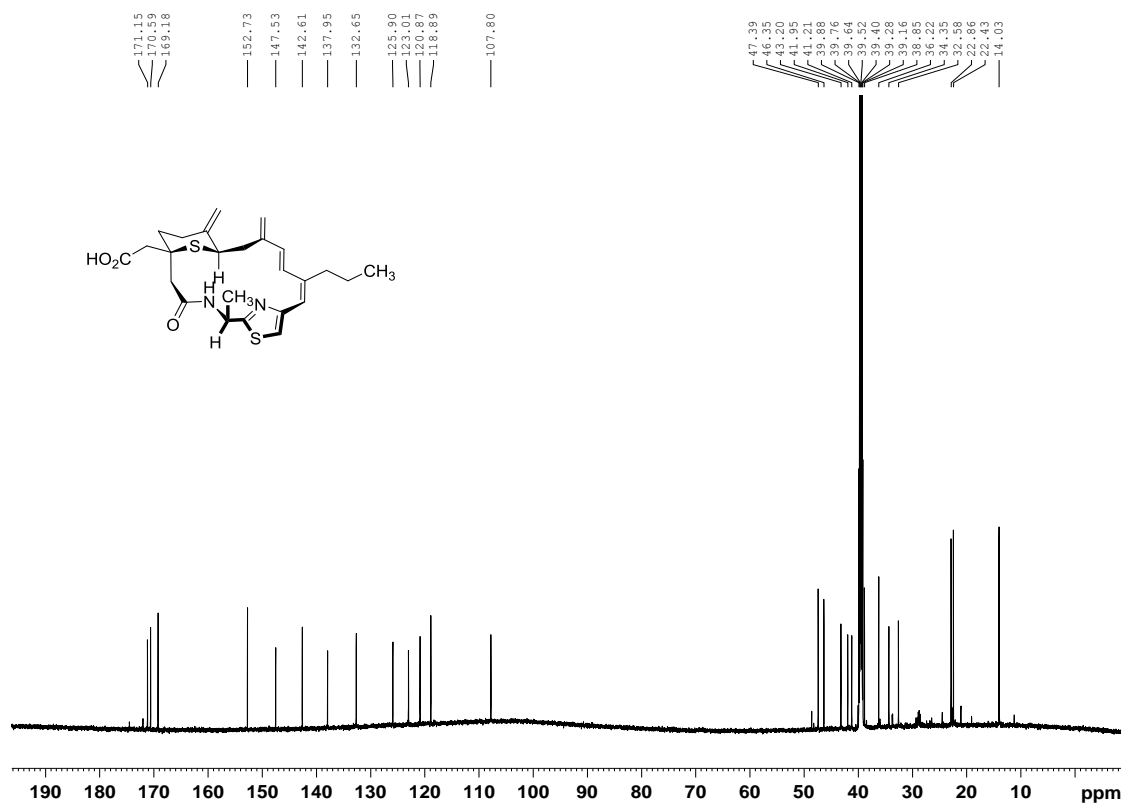


Fig. S22C. DEPT-135 spectra of WSM A2 (DMSO-*d*₆)

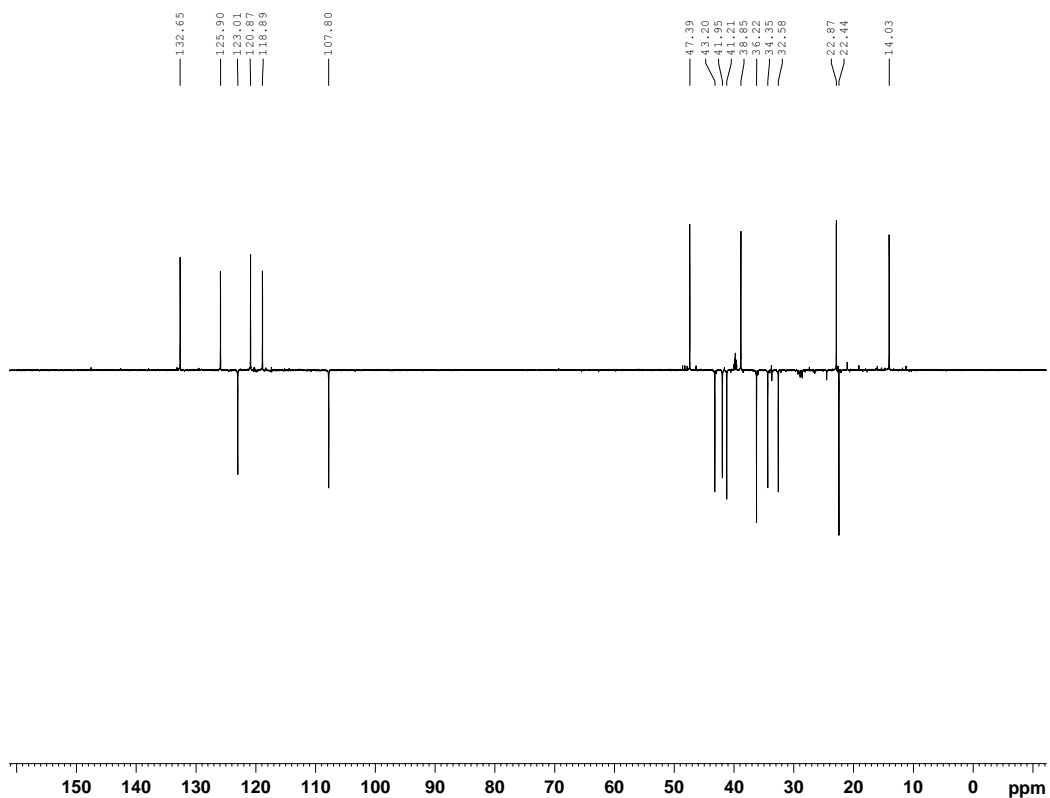


Fig. S22D. HSQC spectra of WSM A2 (DMSO-*d*₆)

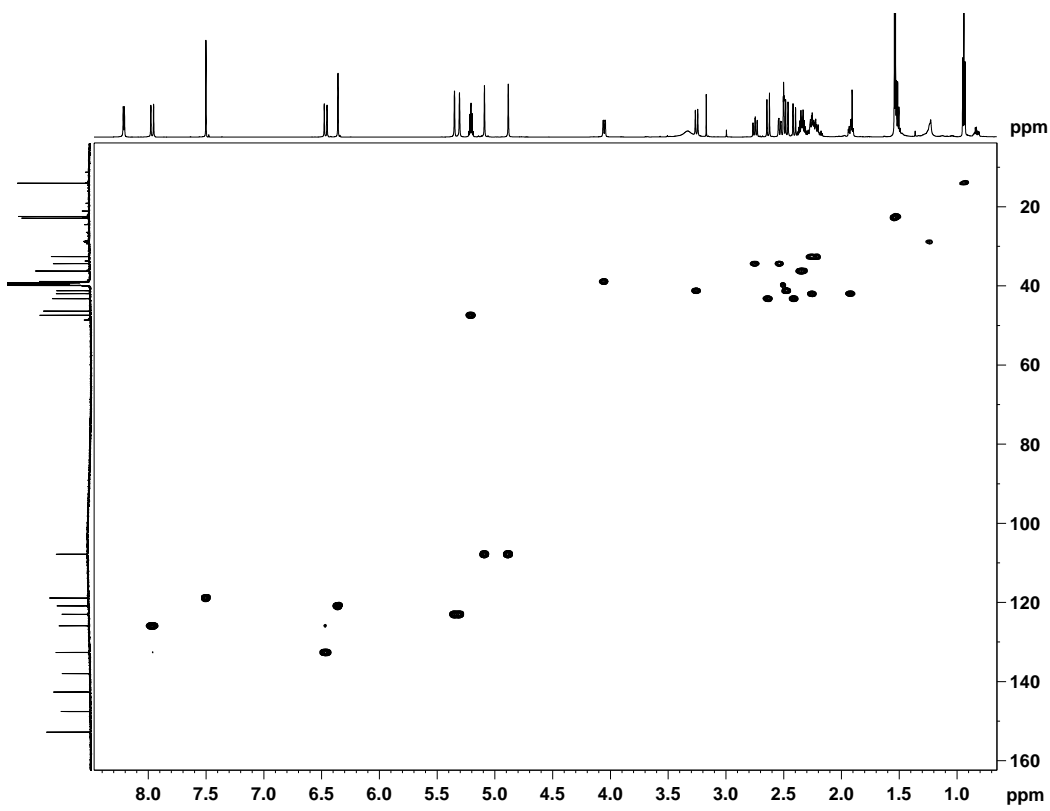


Fig. S22E. ^1H - ^1H COSY spectra of WSM A2 (DMSO- d_6)

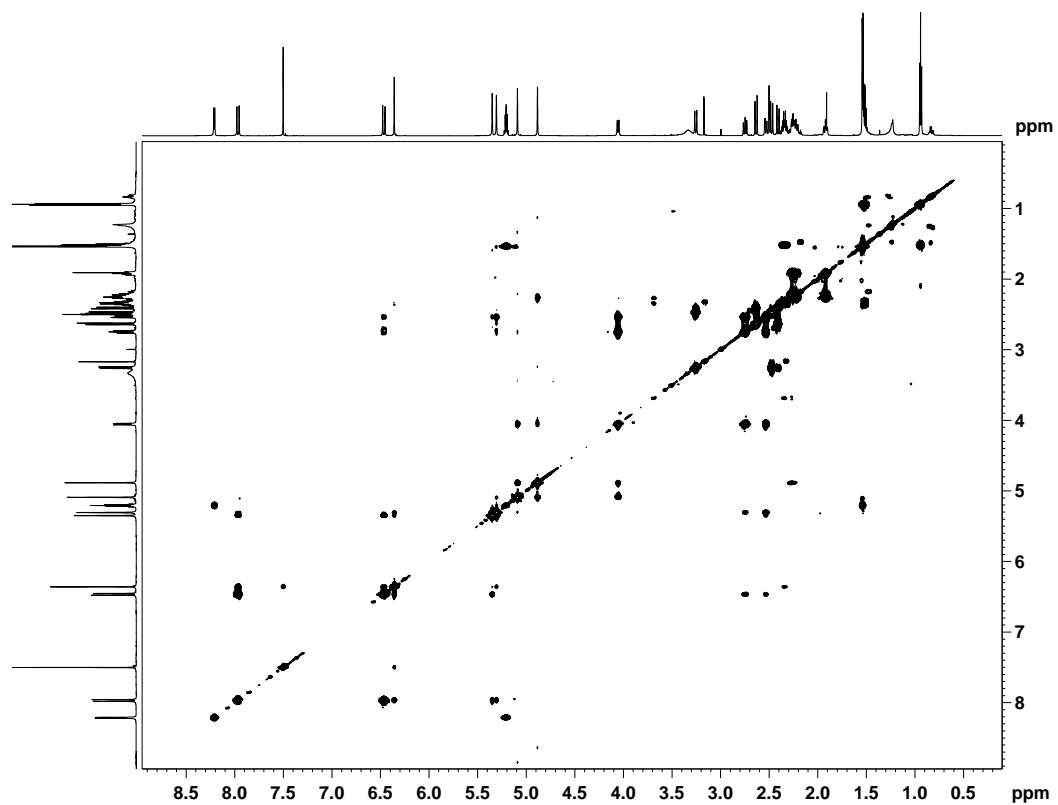


Fig. S22F. HMBC spectra of WSM A2 (DMSO- d_6)

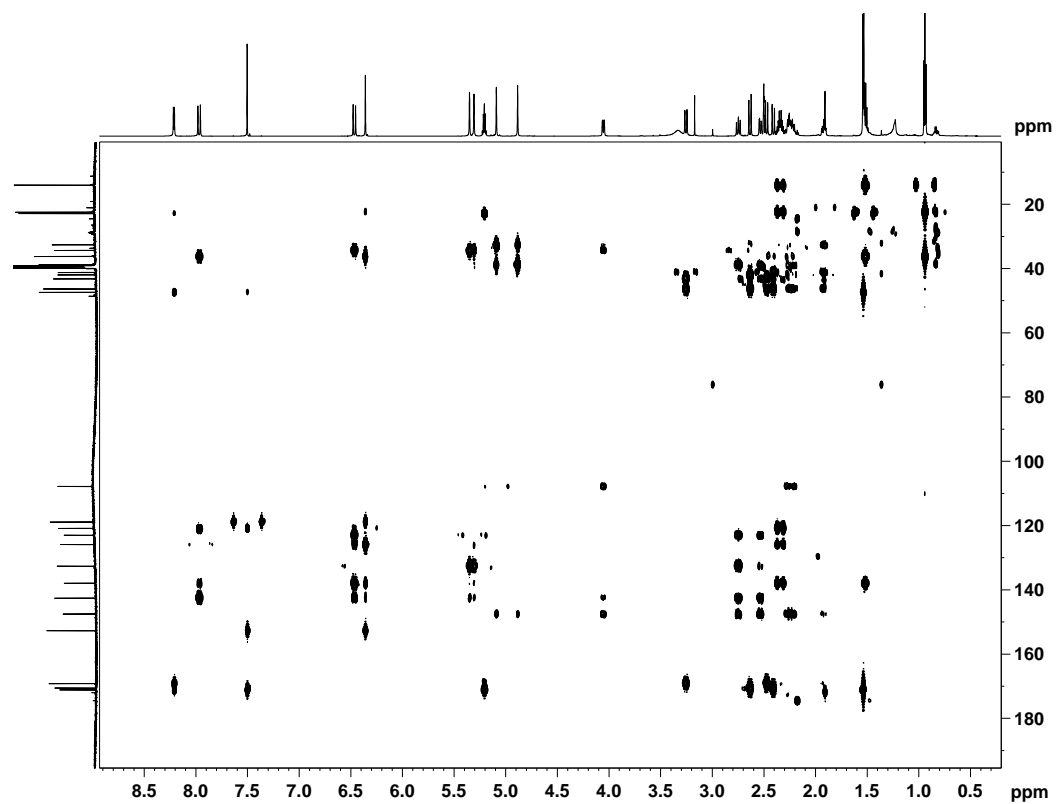


Fig. S22G. ROESY spectra of WSM A2 (DMSO-*d*₆)

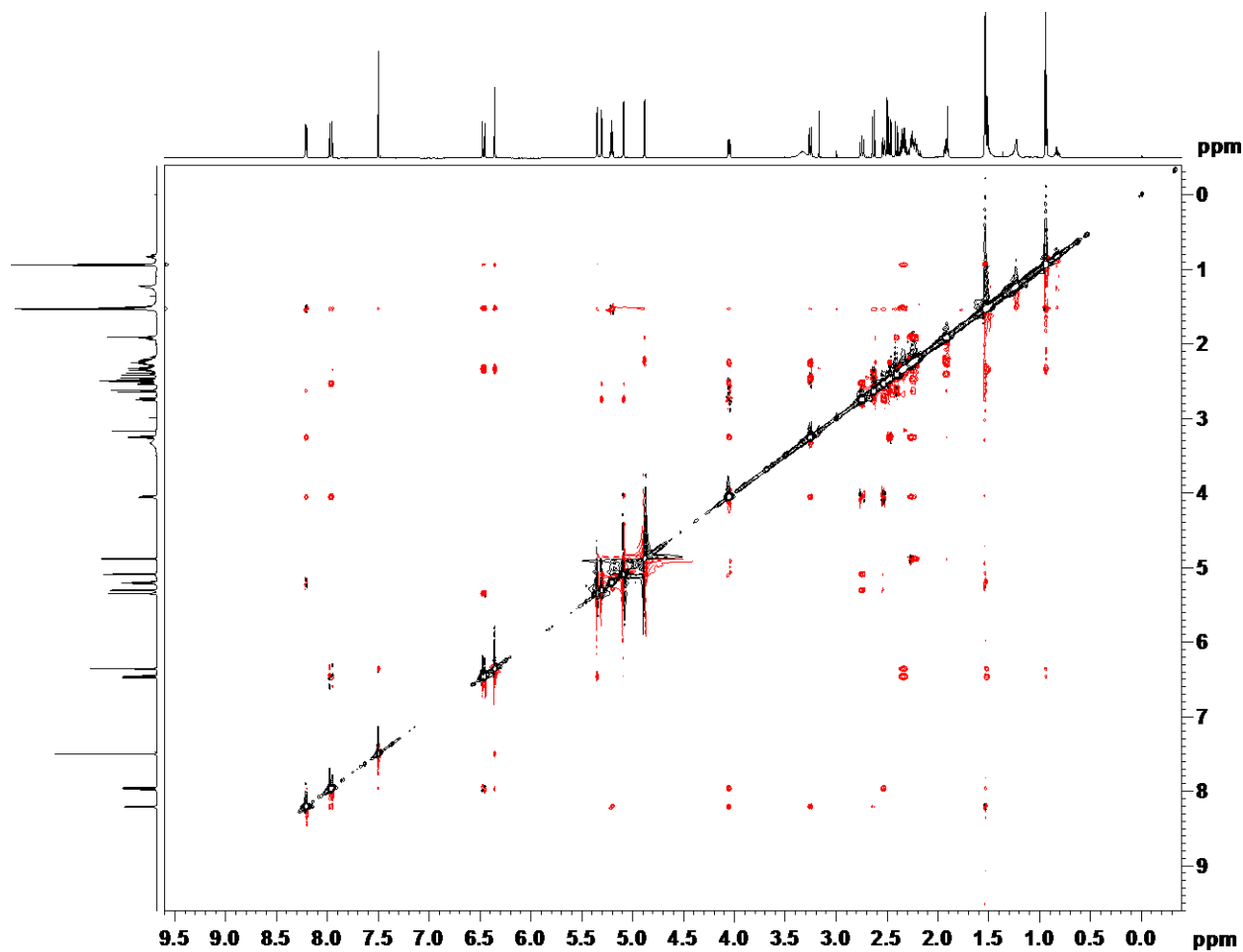


Fig. S22H. HR-MS (ESI) spectra of WSM A2

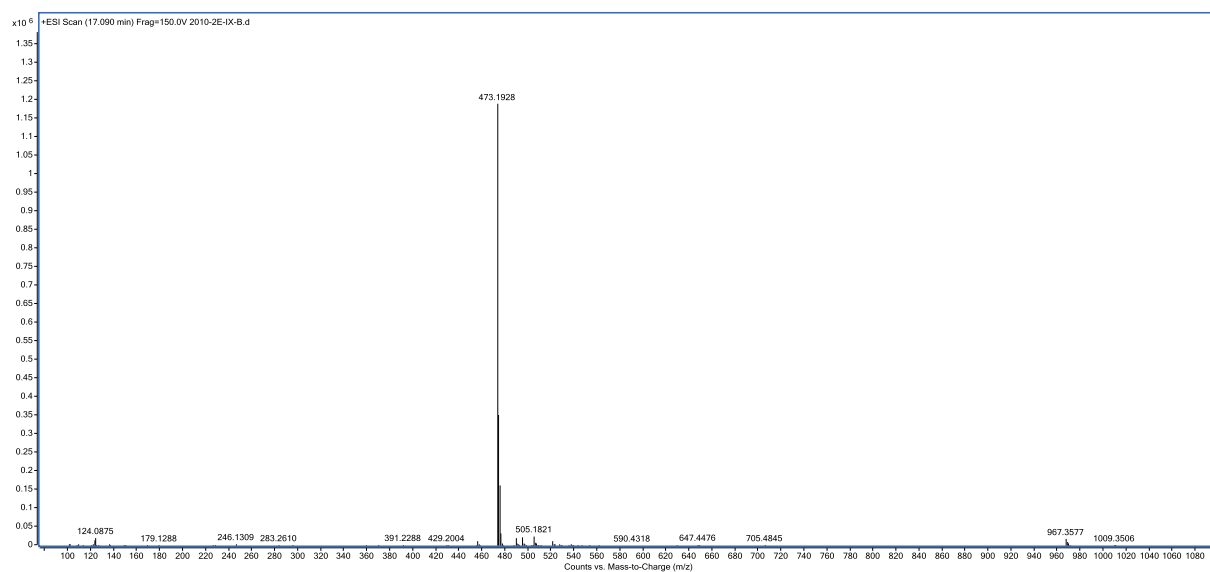


Fig. S23A. ^1H NMR spectra of WSM A3 (700 MHz, CDCl_3)

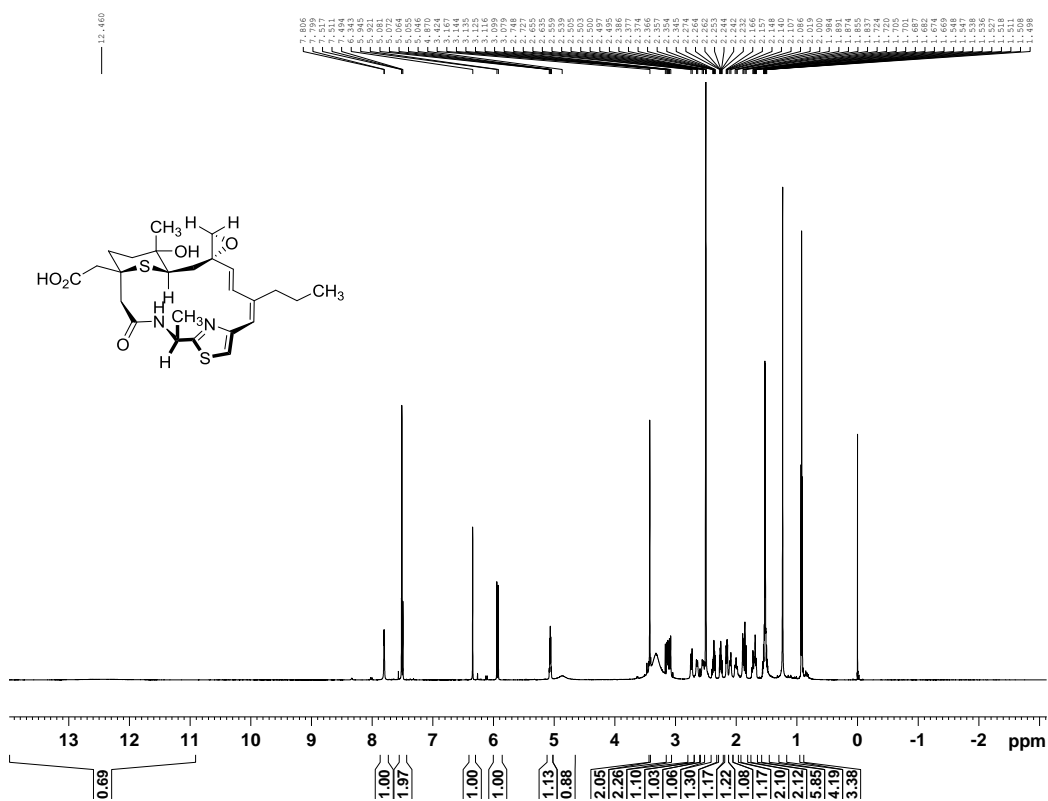


Fig. S23B. ^{13}C NMR spectra of WSM A3 (175 MHz, $\text{DMSO}-d_6$)

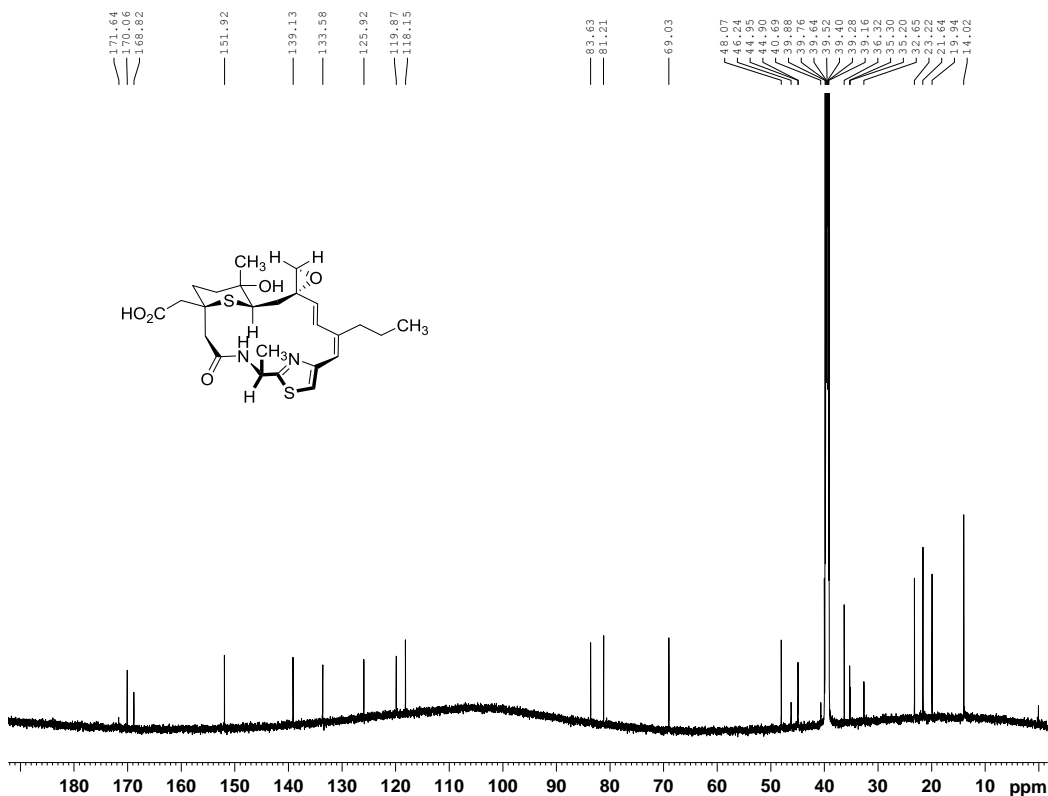


Fig. S23C. DEPT-135 spectra of WSM A3 (DMSO- d_6)

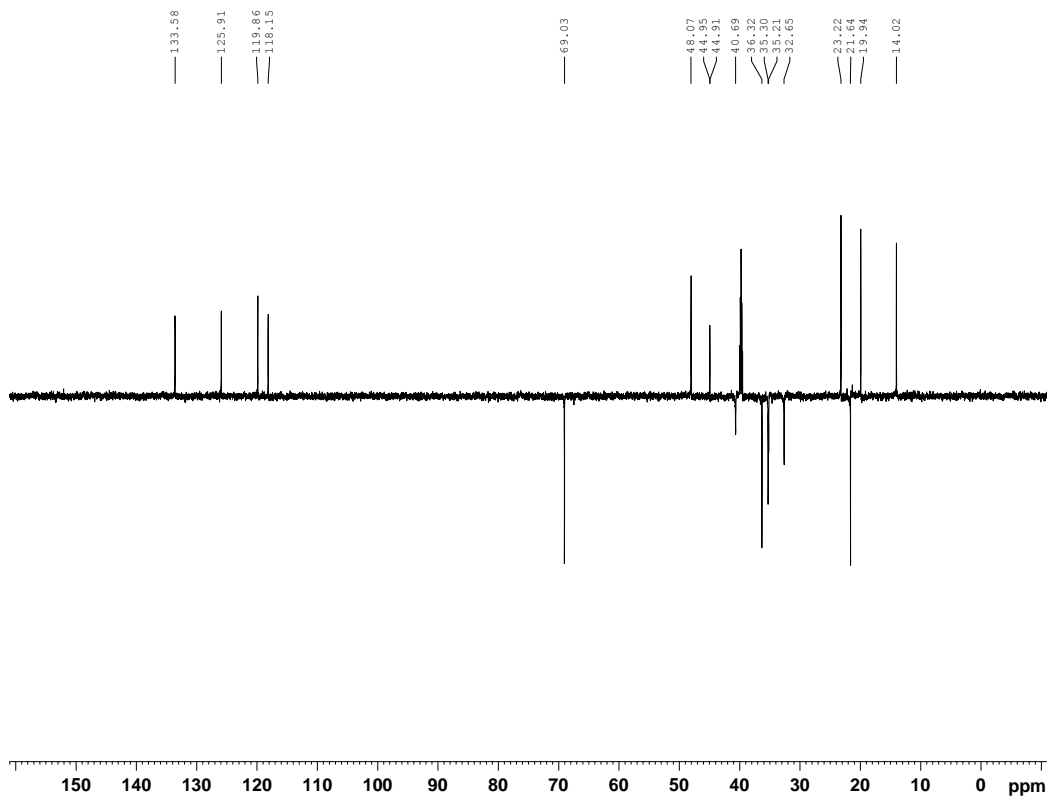


Fig. S23D. HSQC spectra of WSM A3 (DMSO- d_6)

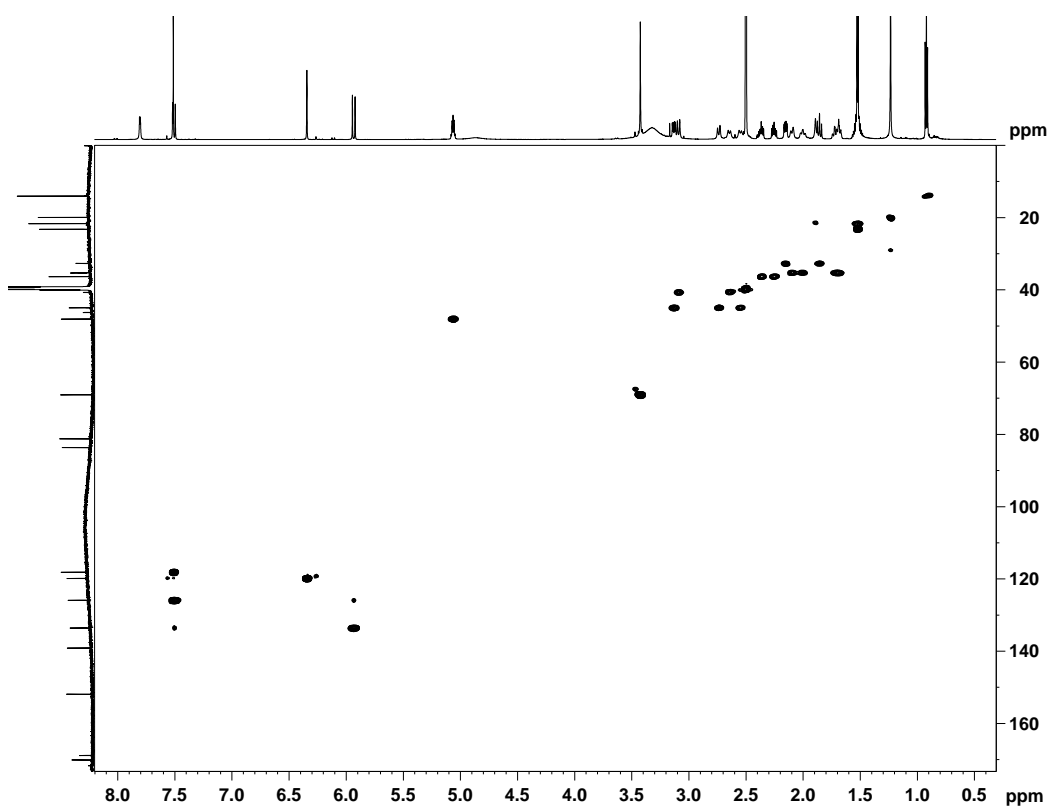


Fig. S23E. ^1H - ^1H COSY spectra of WSM A3 (DMSO- d_6)

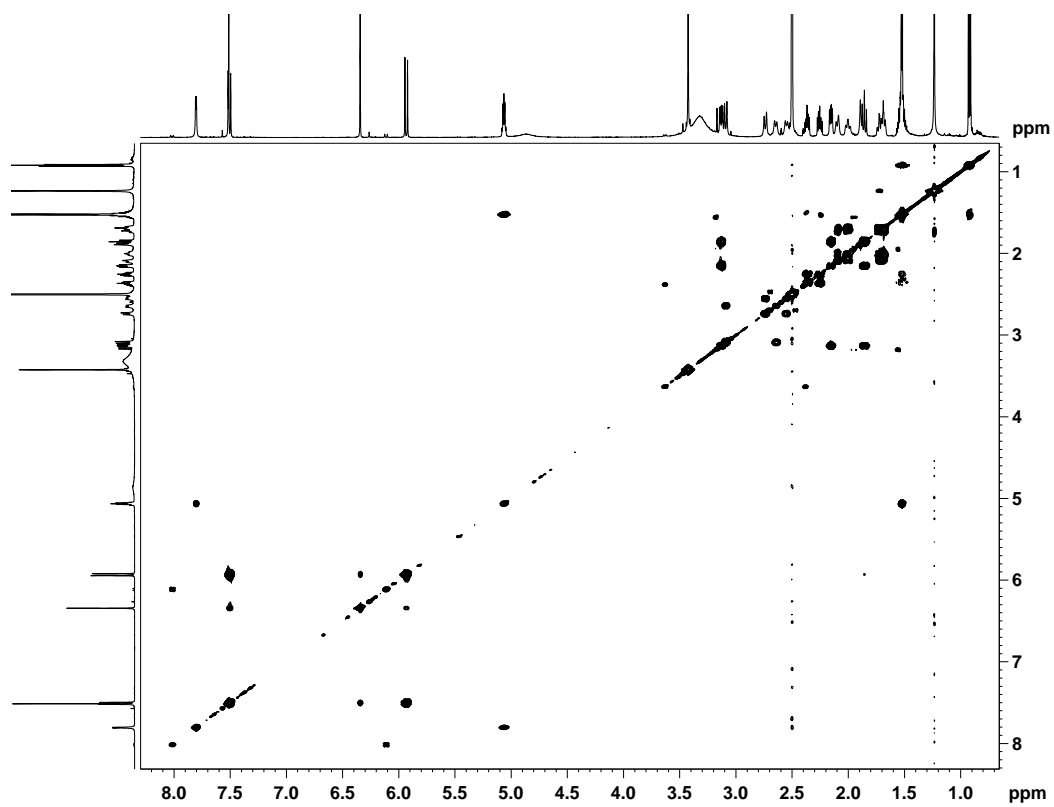


Fig. S23F. HMBC spectra of WSM A3 (DMSO- d_6)

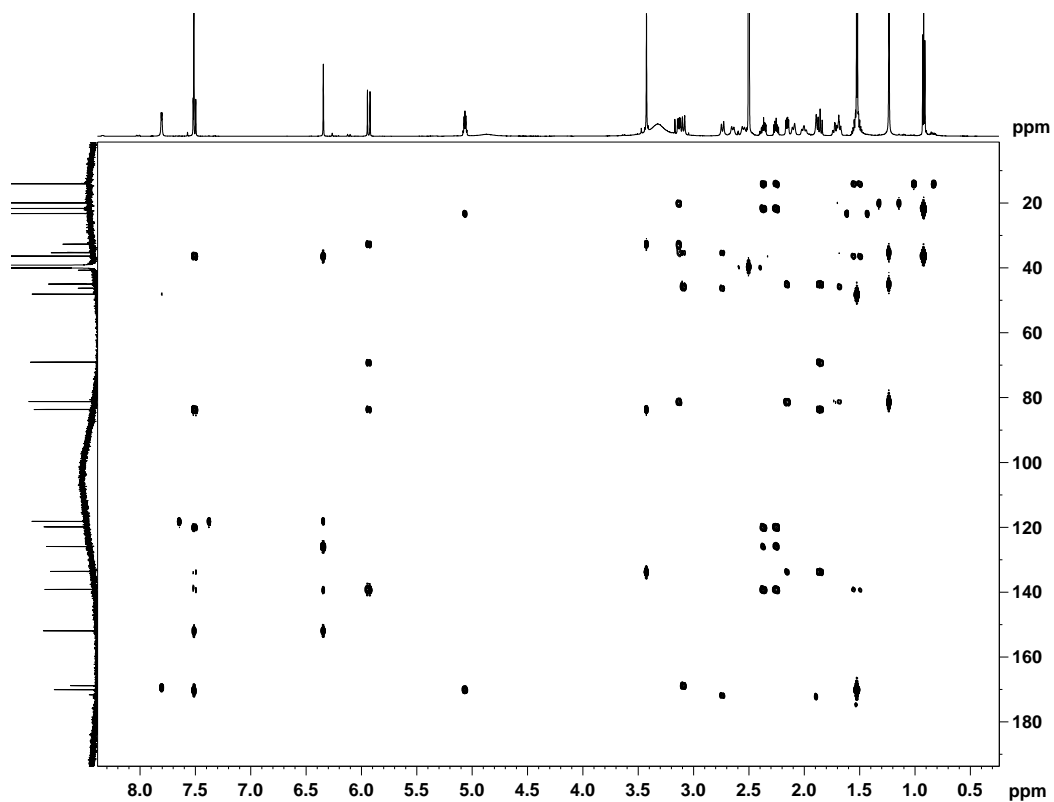


Fig. S23G. ROESY spectra of WSM A3 (DMSO-*d*₆)

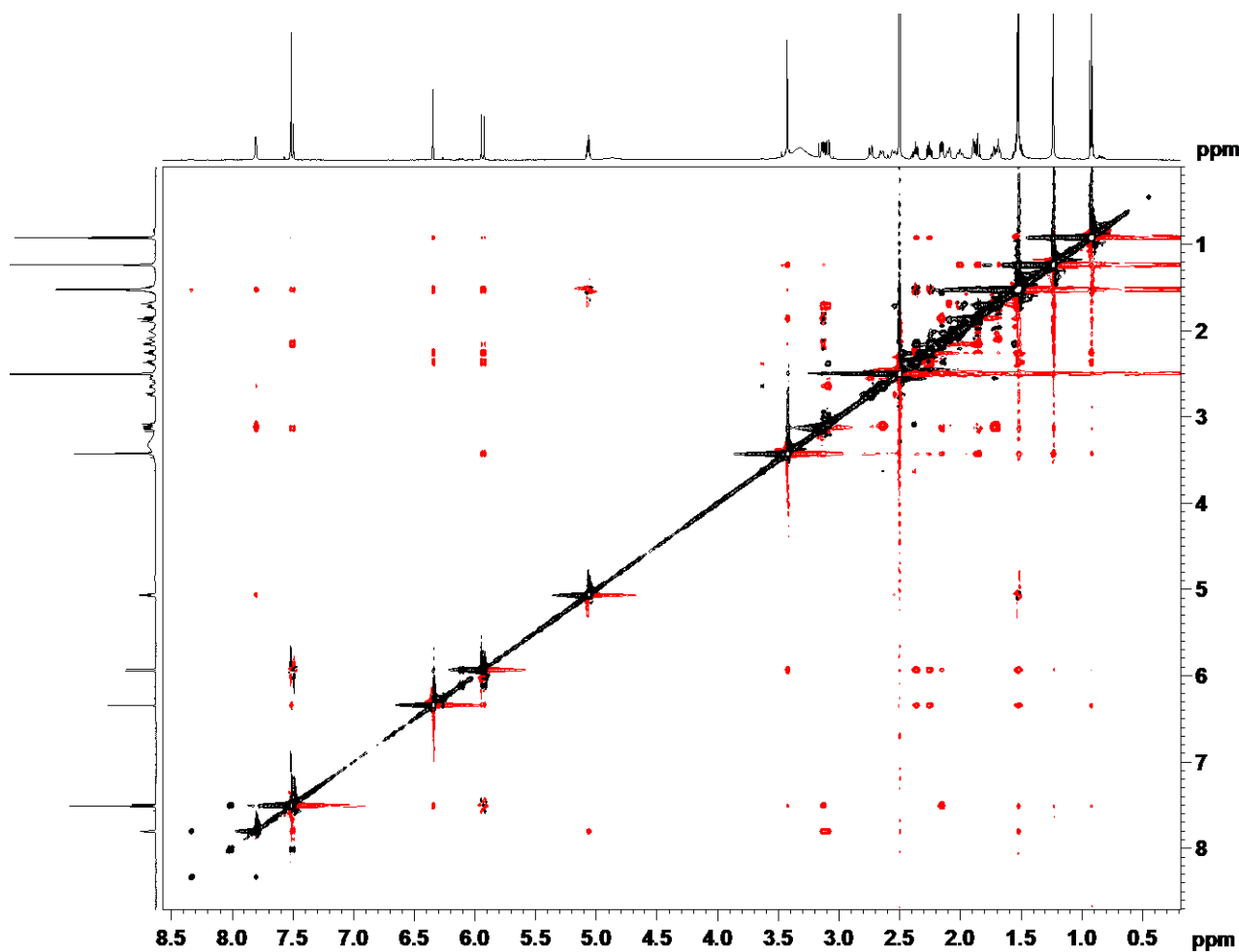


Fig. S23H. HR-MS (ESI) spectra of WSM A3

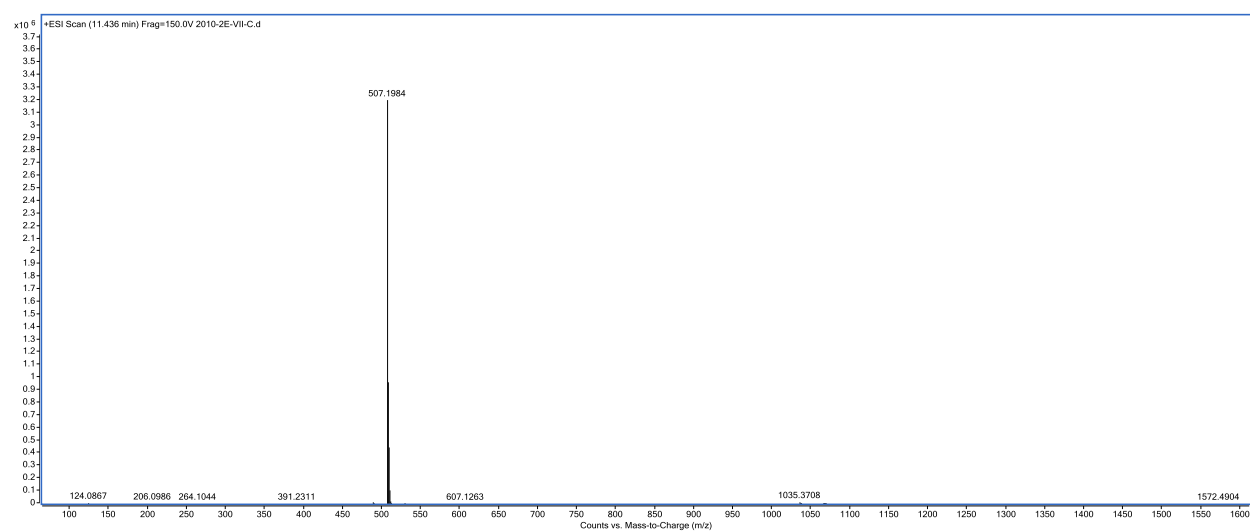


Fig. S24. Determination of the absolute configuration of WSM A2 using its (S)- and (R)-PGME derivatives. The two major conformations of (S)- and (R)-PGME-WSM A2 resembling that of GNM B2 derivatives (**Fig. S14**), which are different from that of the corresponding derivatives of LNM E2 probably due to the missing methyl group at C24 position, are shown in **A**. In the ROESY spectra (**B**), the presence of correlations between 24-H_b and 4-H_b, between 2-H_b and 4-H_a, as well as the absent correlations between 24-H_a and 2-H/4-H, support that C24-C25 and C3-S are *anti*-oriented, and 24-H_b takes a pseudo-axial position in the preferred conformation at C24. Two major conformations (**A**, conformations I and II), due to the rotation of C24-C25 single bond, could be observed based on the ROESY correlations between 25-NH and 24-H_a/24-H_b/2-H_b (**C** and **D**). The relatively weak correlation between 25-NH and 24-H_b (**C**) supports that conformation I is the favored conformation of (R)-PGME-WSM A2, while the relatively weak correlation between 25-NH and 2-H_b (**D**) supports that conformation II is the favored conformation of (S)-PGME-WSM A2. Although several hydrogens in the macrolactam backbone are positioned in opposite sides of PGME plane in two different conformations, 24-H_b and 2-H_a/H_b are always positioned at the two different sides of the PGME plane in both conformations I and II, hence making them diagnostic useful for determination of the absolute configuration. Based on the differences of chemical shift in ¹H NMR between (R)- and (S)-PGME-WSM A2 ($\Delta\delta = \delta_{(R)} - \delta_{(S)}$) as shown in **A**, the absolute configuration of C3 is elucidated to be 3S for WSM A2 [3R for (R)/(S)-PGME-WSM A2]. Additionally, since the priming amino acid during the biosynthesis has been determined biochemically as D-Alanine (**Fig. 3B**), the ROESY correlations between 24-H_a and 18-CH₃ (**B**, **E**), and between 11-H and 18-CH₃ (**F**), further support the determined absolute configuration at C3, which is opposite to that of LNM E2 (**Fig. S16**). H_a denotes one of the geminal hydrogens appearing at lower field in ¹H NMR, and H_b denotes one of the geminal hydrogens appearing at higher field in ¹H NMR.

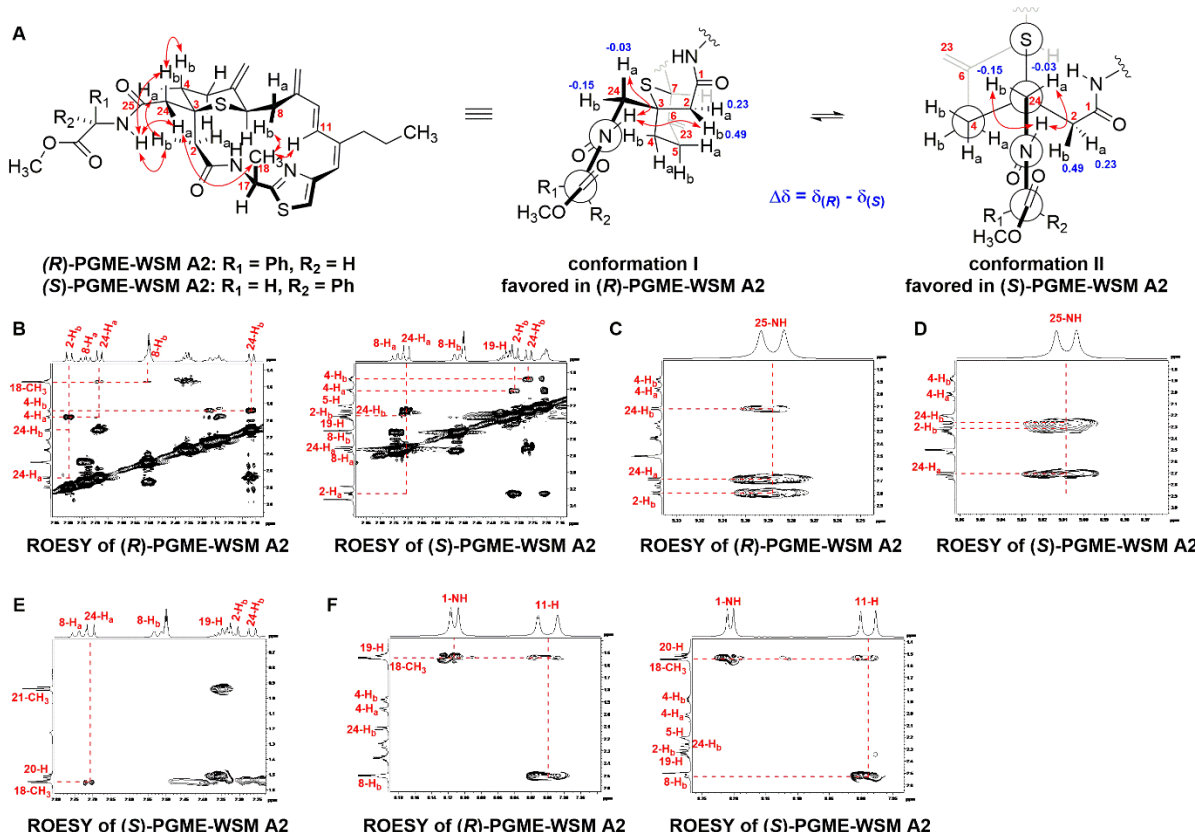


Fig. S25-SA. ^1H NMR spectra of (S)-PGME-WSM A2 (700 MHz, $\text{DMSO}-d_6$)

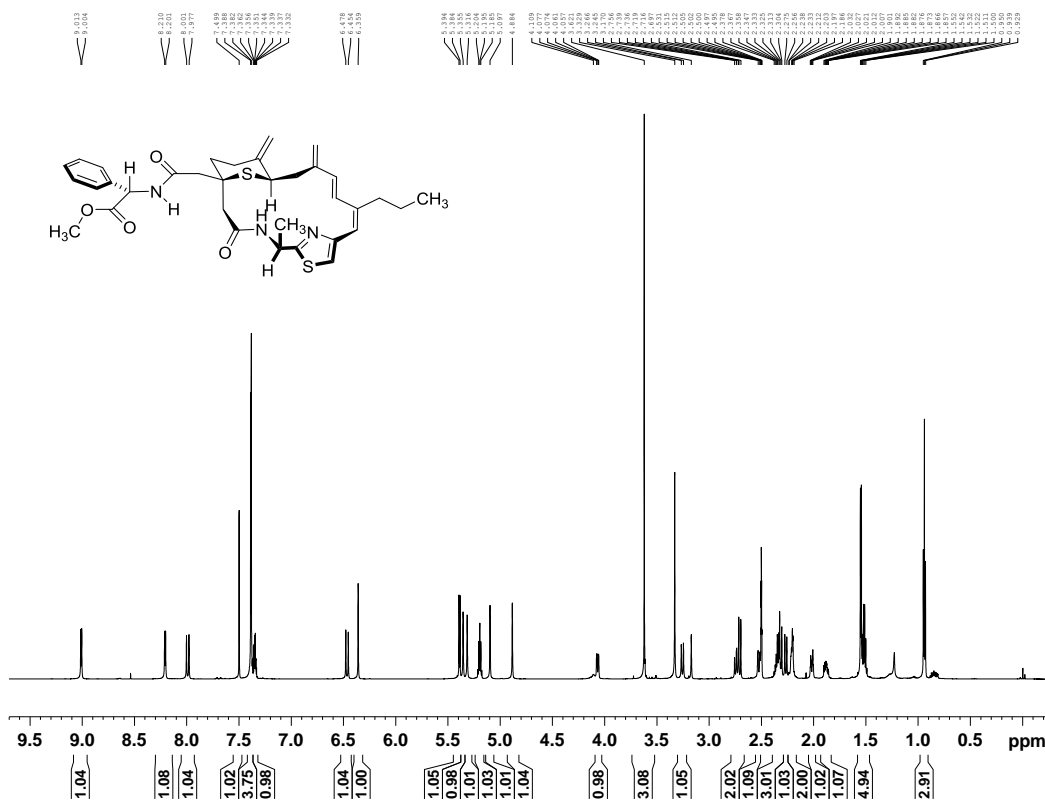


Fig. S25-SB. ^{13}C NMR spectra of (S)-PGME-WSM A2 (175 MHz, $\text{DMSO}-d_6$)

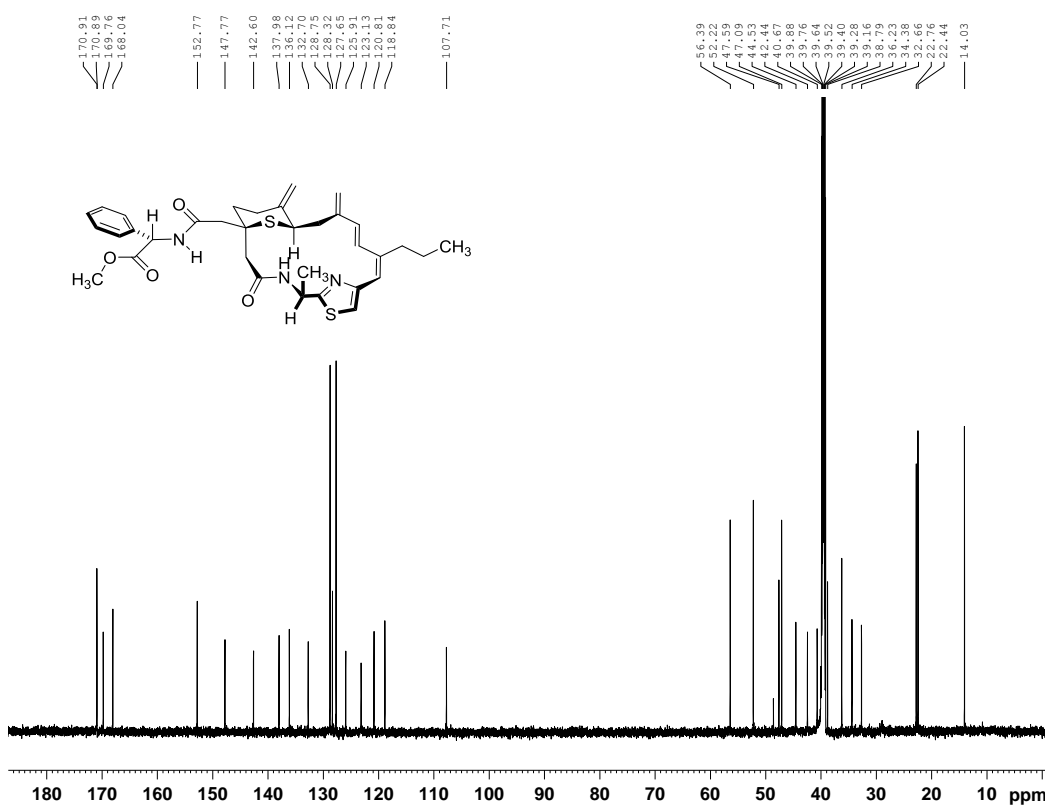


Fig. S25-SC. DEPT-135 spectra of (S)-PGME-WSM A2 (DMSO- d_6)

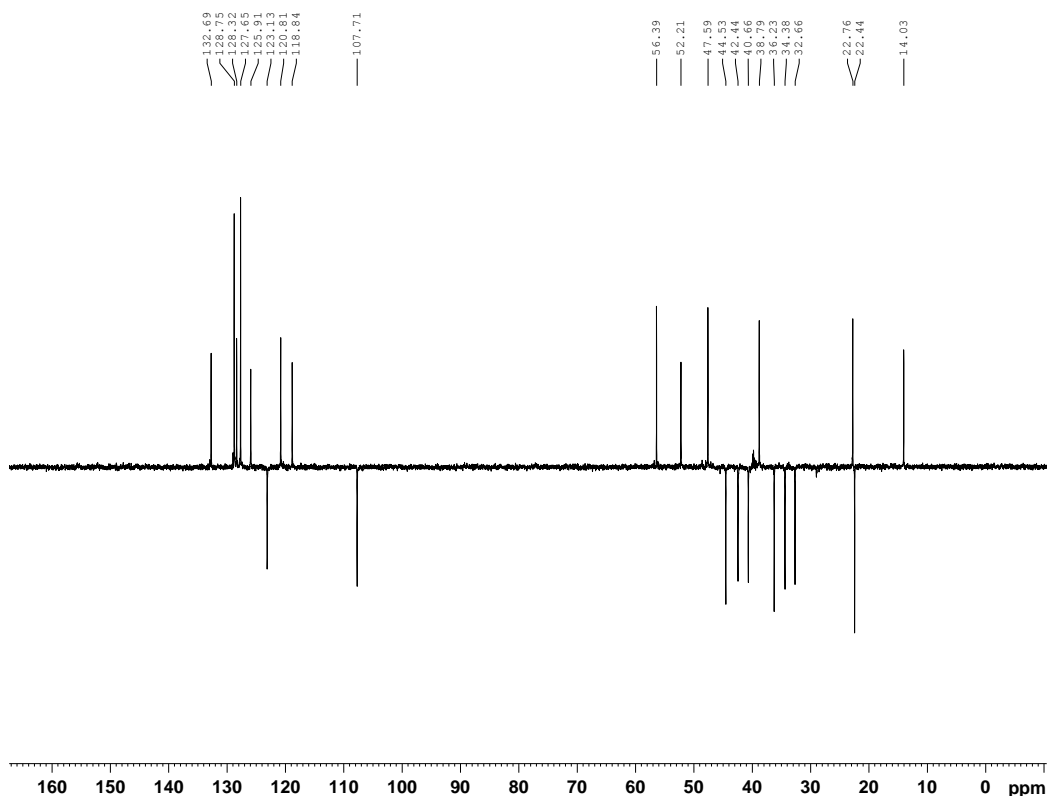


Fig. S25-SD. HSQC spectra of (S)-PGME-WSM A2 (DMSO- d_6)

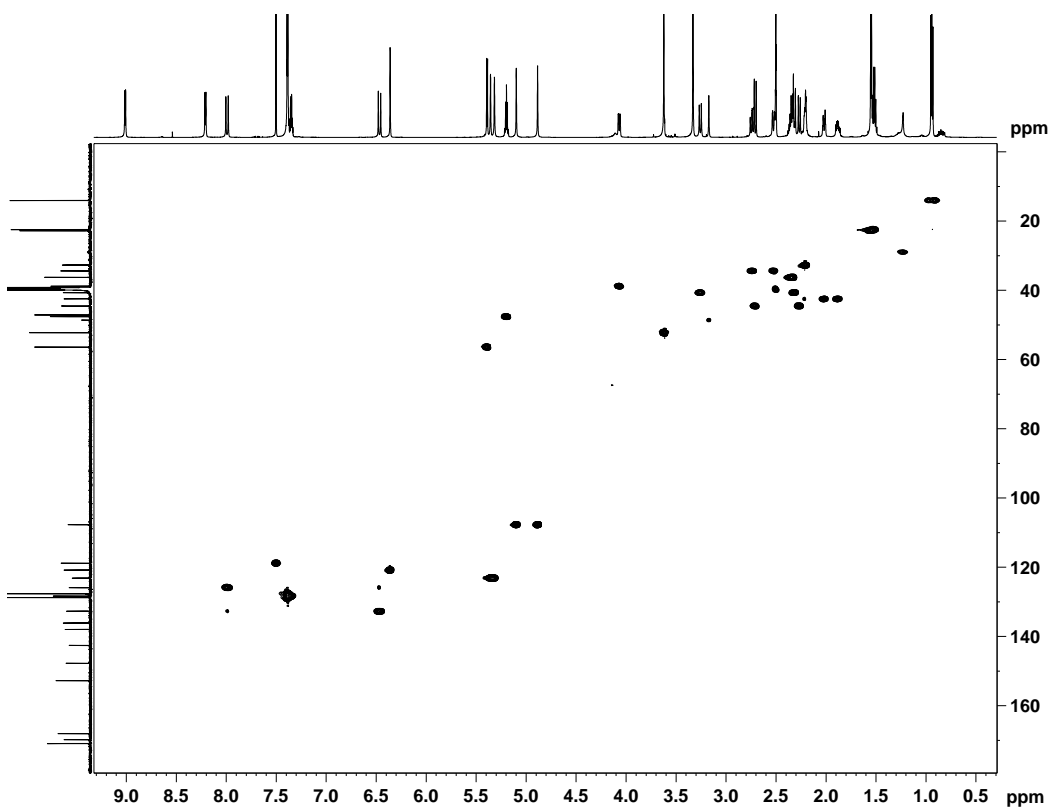


Fig. S25-SE. ^1H - ^1H COSY spectra of (S)-PGME-WSM A2 (DMSO- d_6)

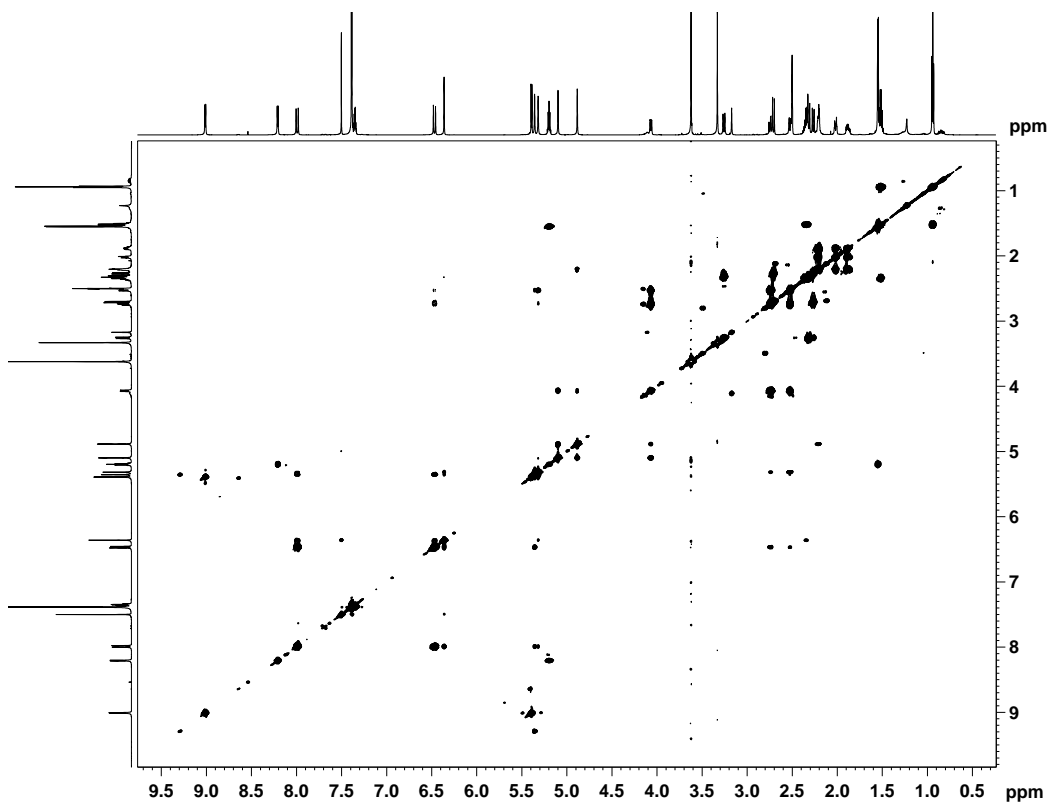


Fig. S25-SF. HMBC spectra of (S)-PGME-WSM A2 (DMSO- d_6)

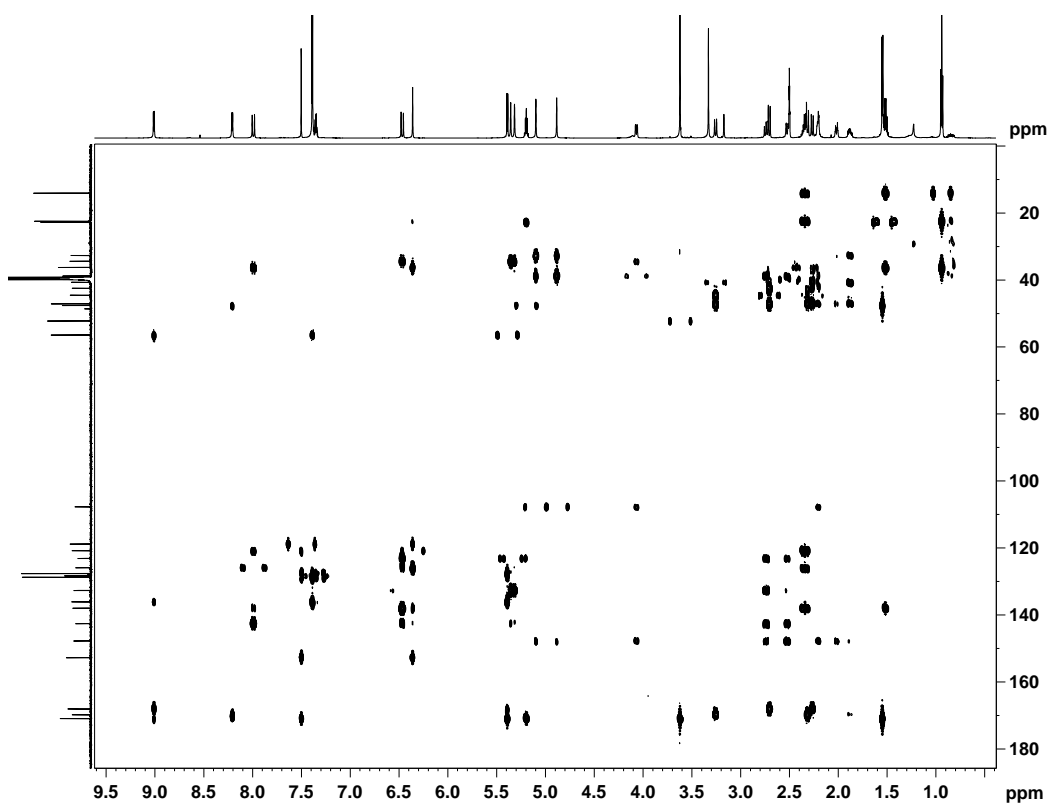


Fig. S25-SG. ROESY spectra of (S)-PGME-WSM A2 (DMSO-*d*₆)

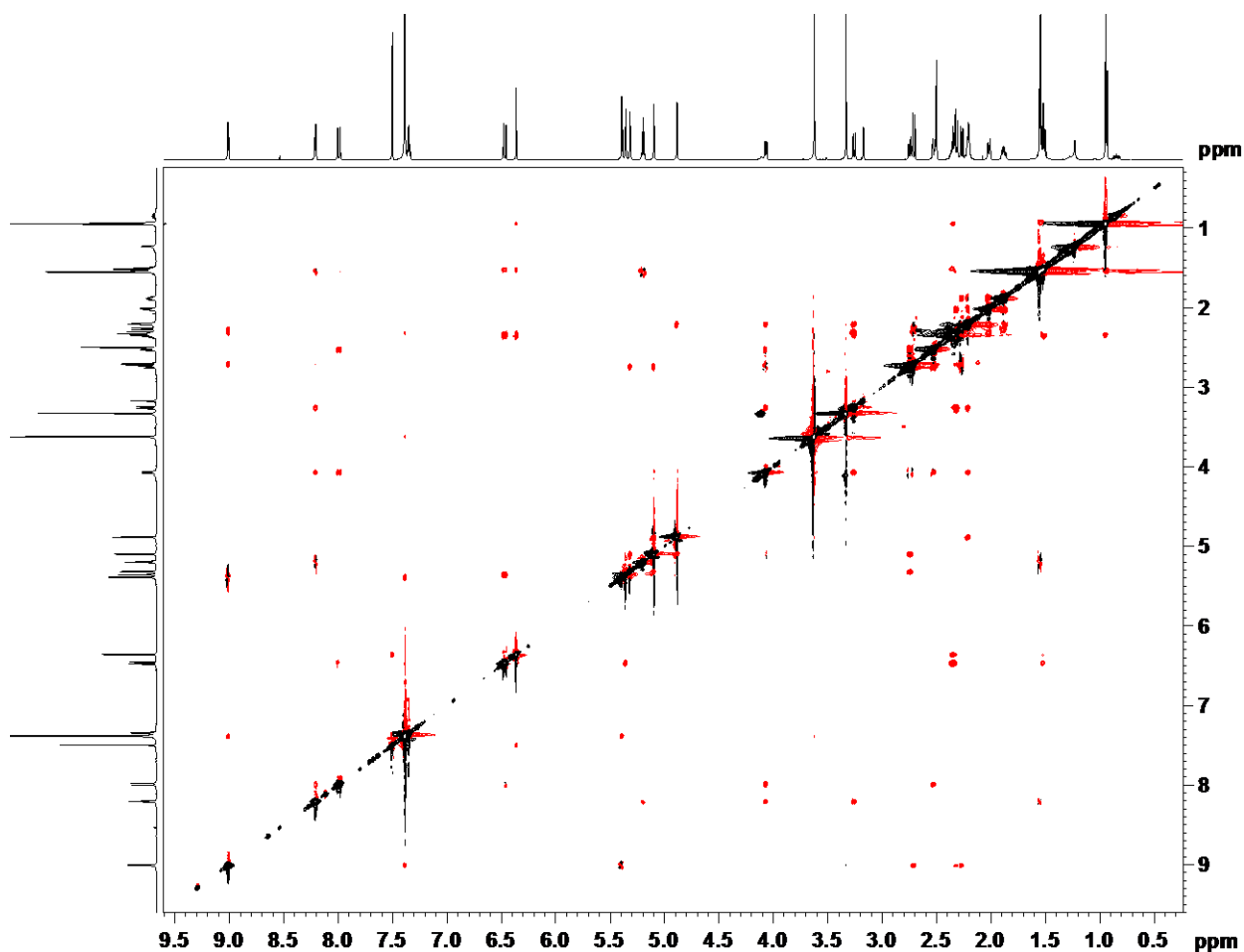


Fig. S25-SH. HR-MS (ESI) spectra of (S)-PGME-WSM A2

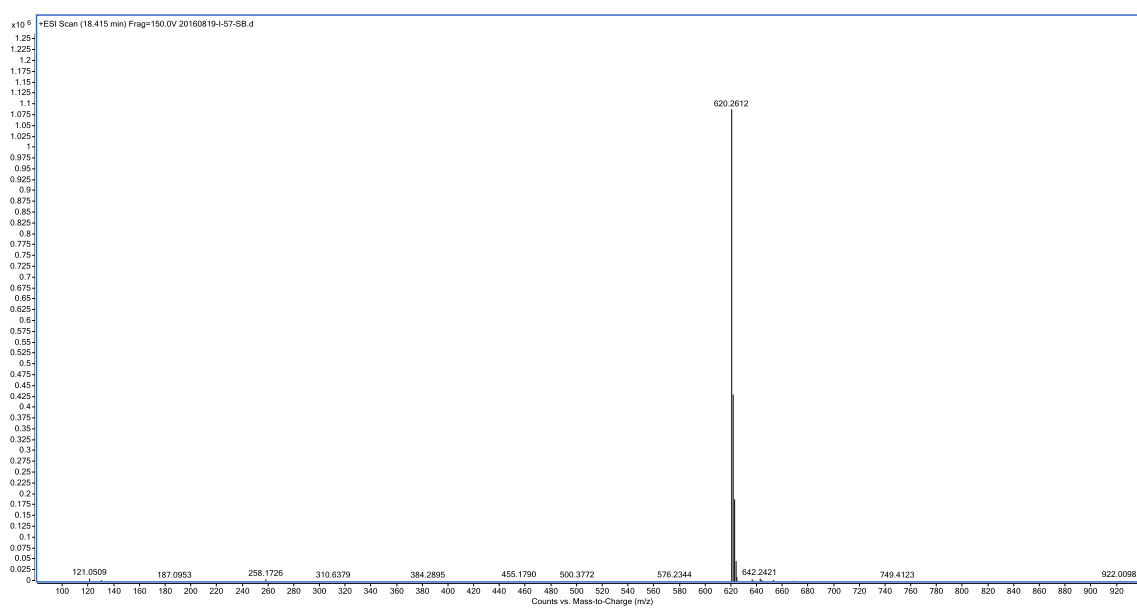


Fig. S25-RA. ^1H NMR spectra of (*R*)-PGME-WSM A2 (700 MHz, DMSO- d_6)

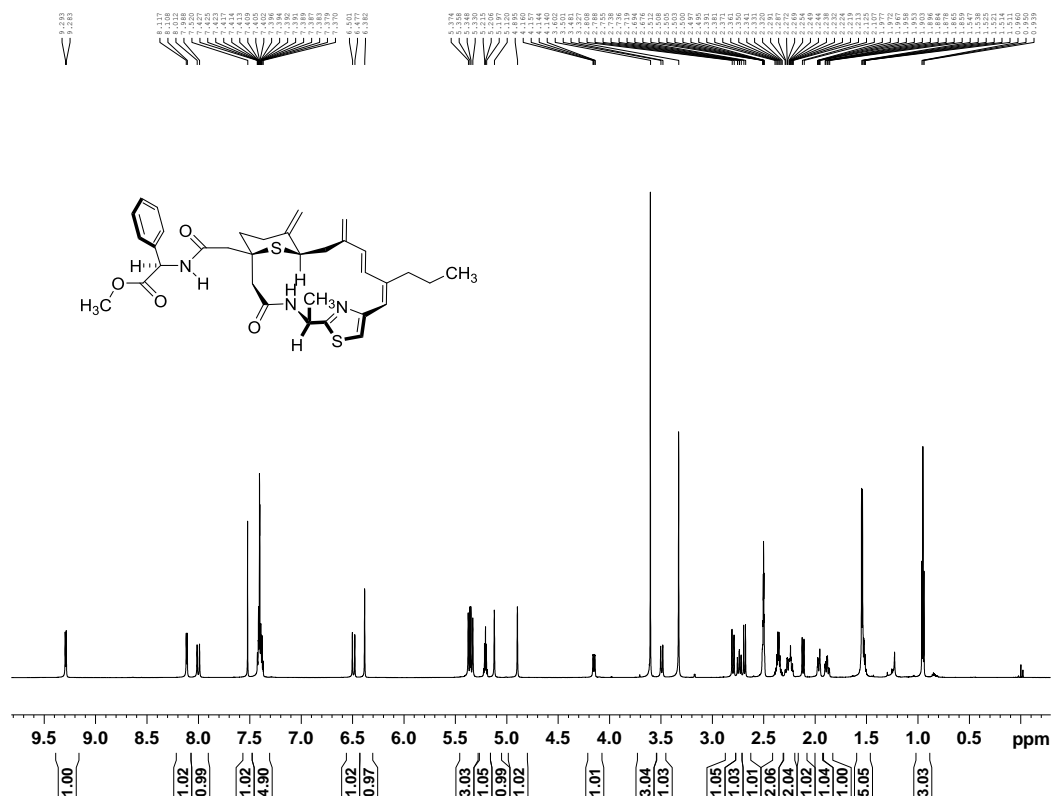


Fig. S25-RB. ^{13}C NMR spectra of (R)-PGME-WSM A2 (175 MHz, DMSO-d_6)

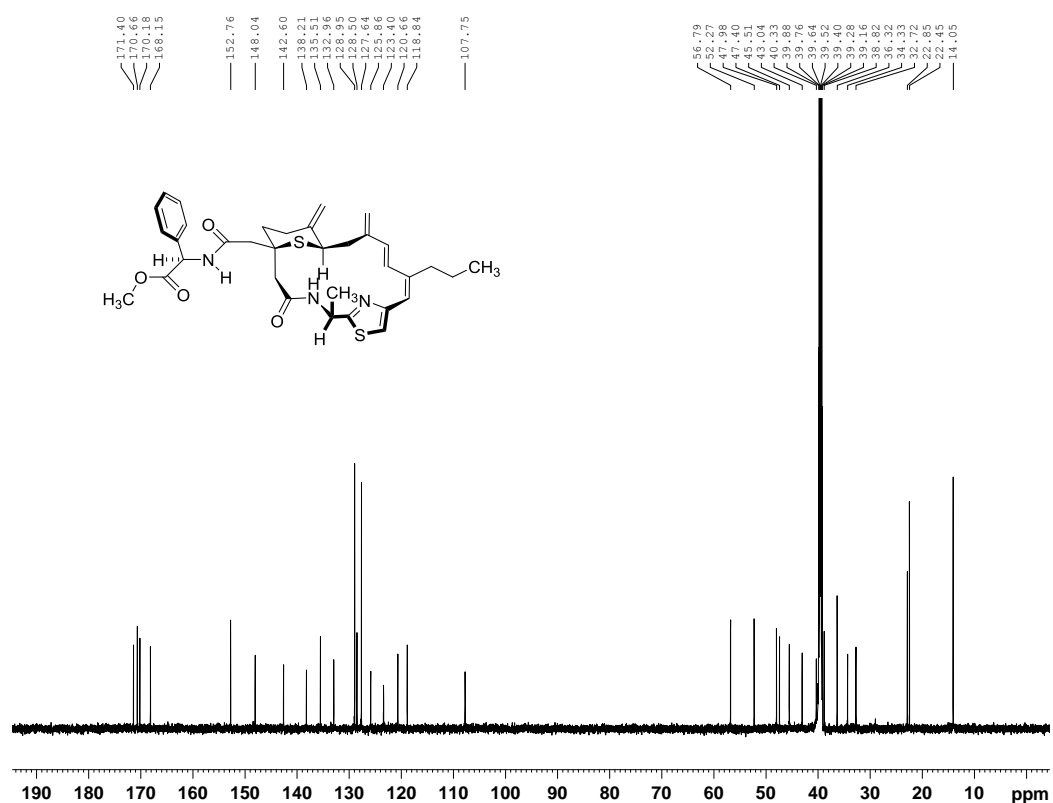


Fig. S25-RC. DEPT-135 spectra of (*R*)-PGME-WSM A2 (DMSO-*d*₆)

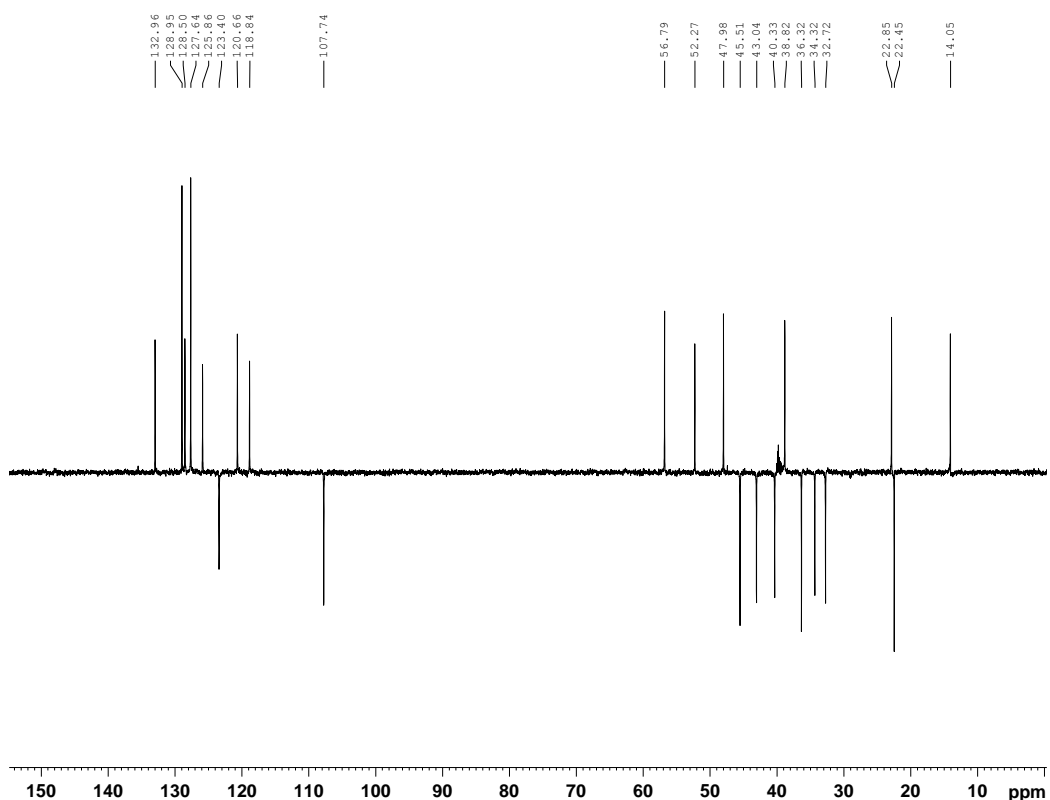


Fig. S25-RD. HSQC spectra of (*R*)-PGME-WSM A2 (DMSO-*d*₆)

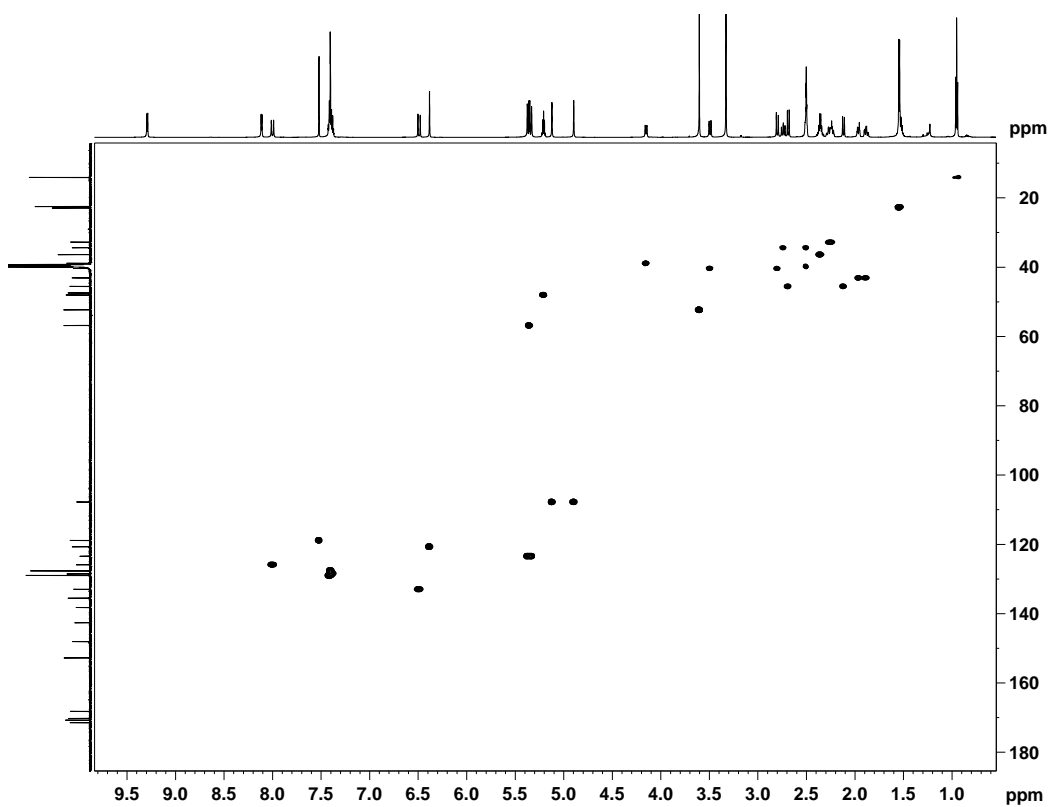


Fig. S25-RE. ^1H - ^1H COSY spectra of (*R*)-PGME-WSM A2 (DMSO- d_6)

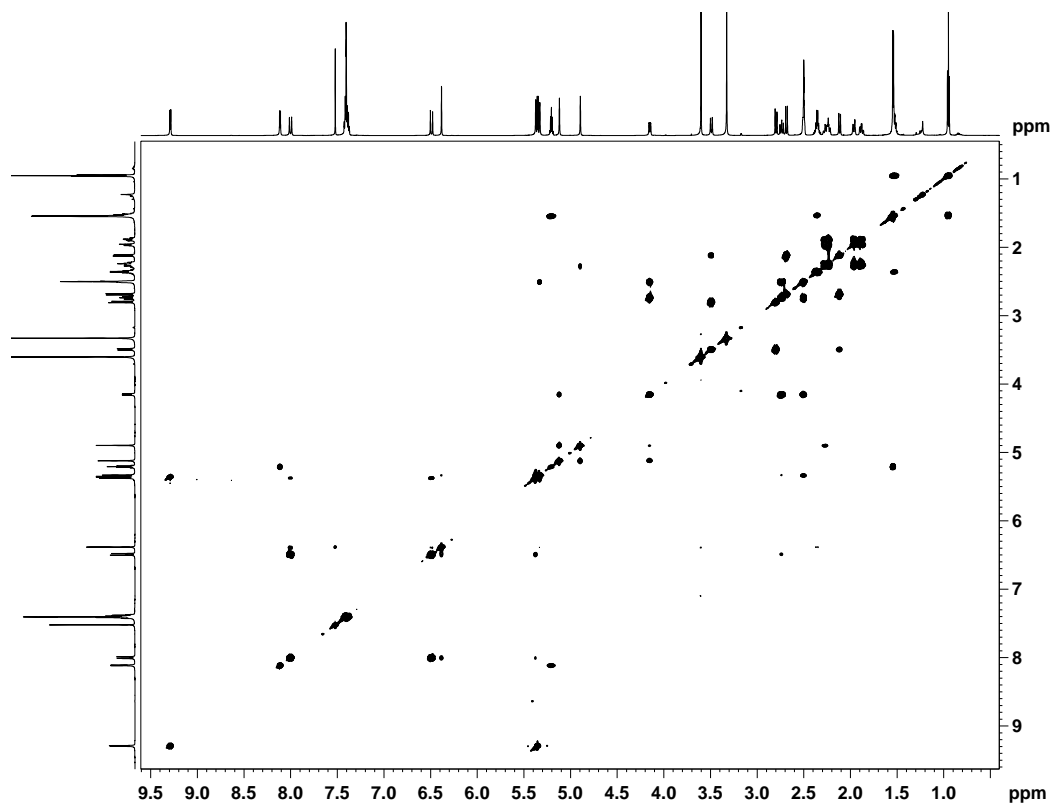


Fig. S25-RF. HMBC spectra of (*R*)-PGME-WSM A2 (DMSO- d_6)

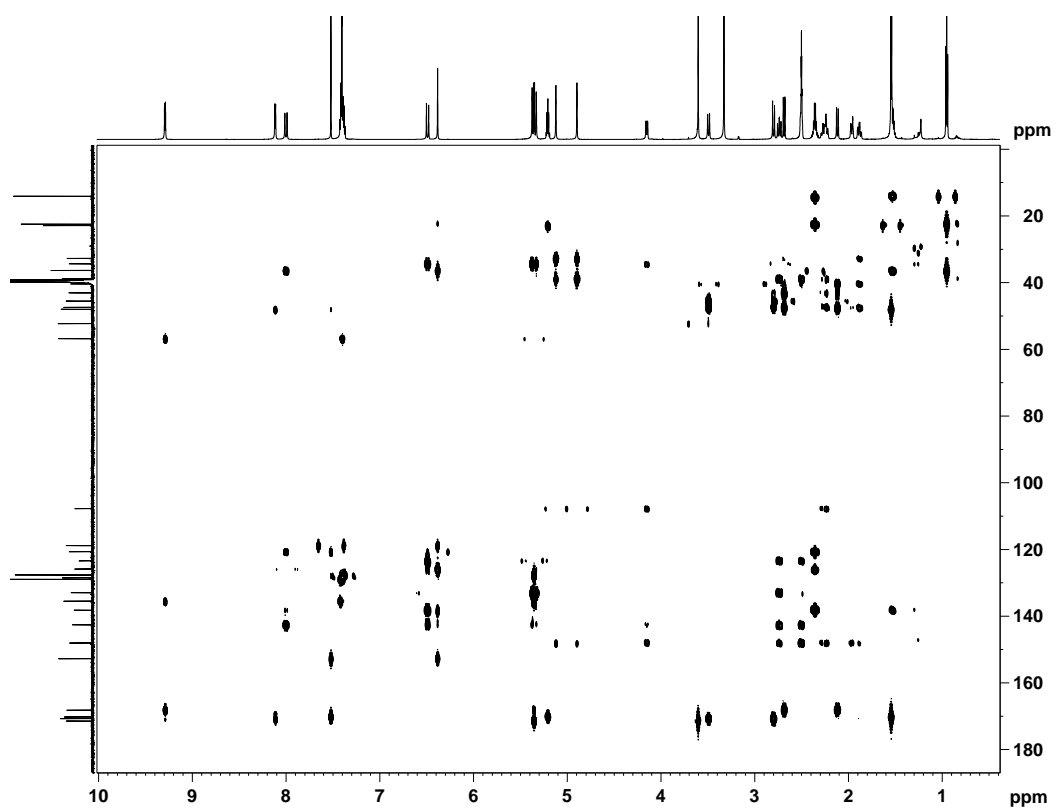


Fig. S25-RG. ROESY spectra of *R*)-PGME-WSM A2 (DMSO-*d*₆)

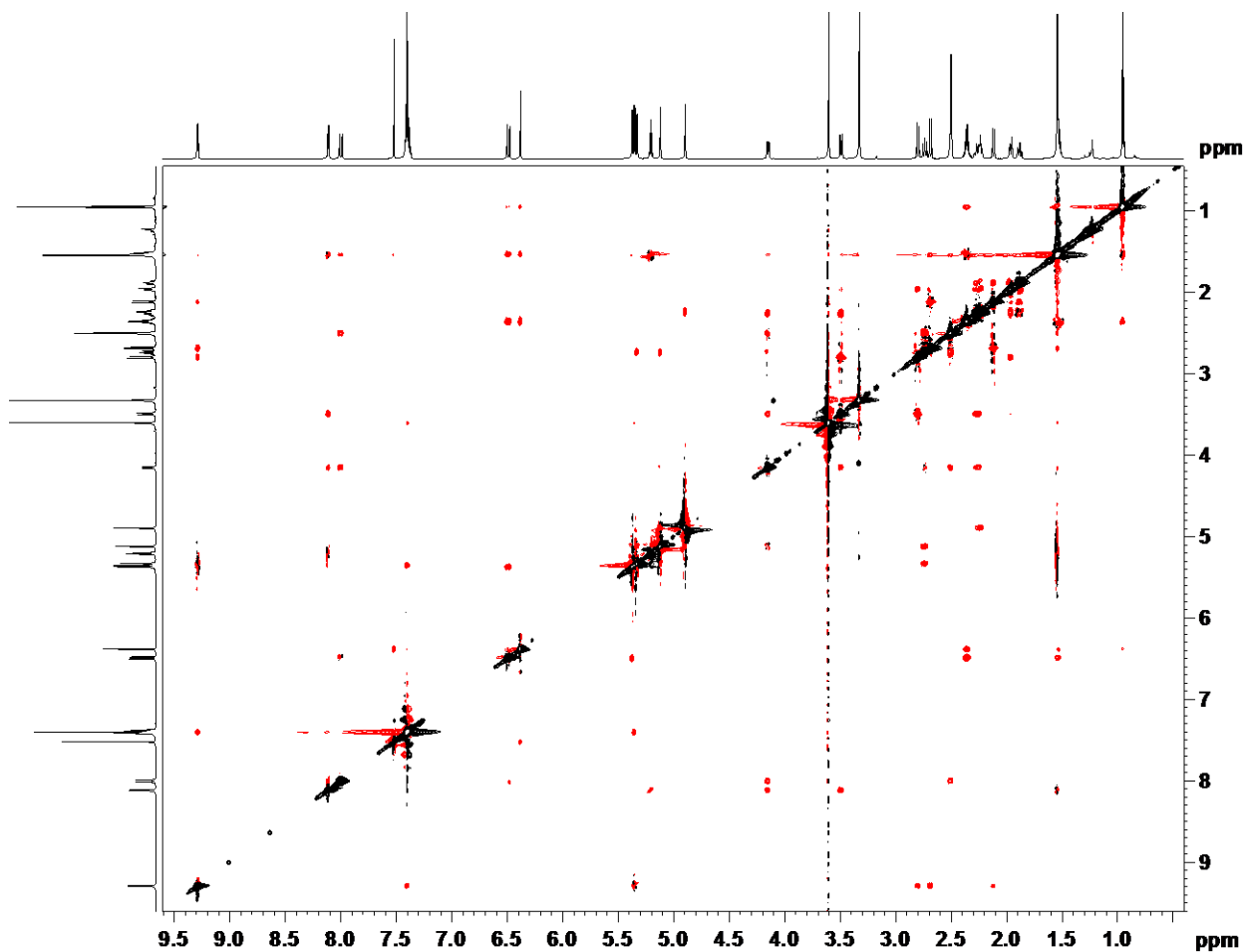


Fig. S25-RH. HR-MS (ESI) spectra of (*R*)-PGME-WSM A2

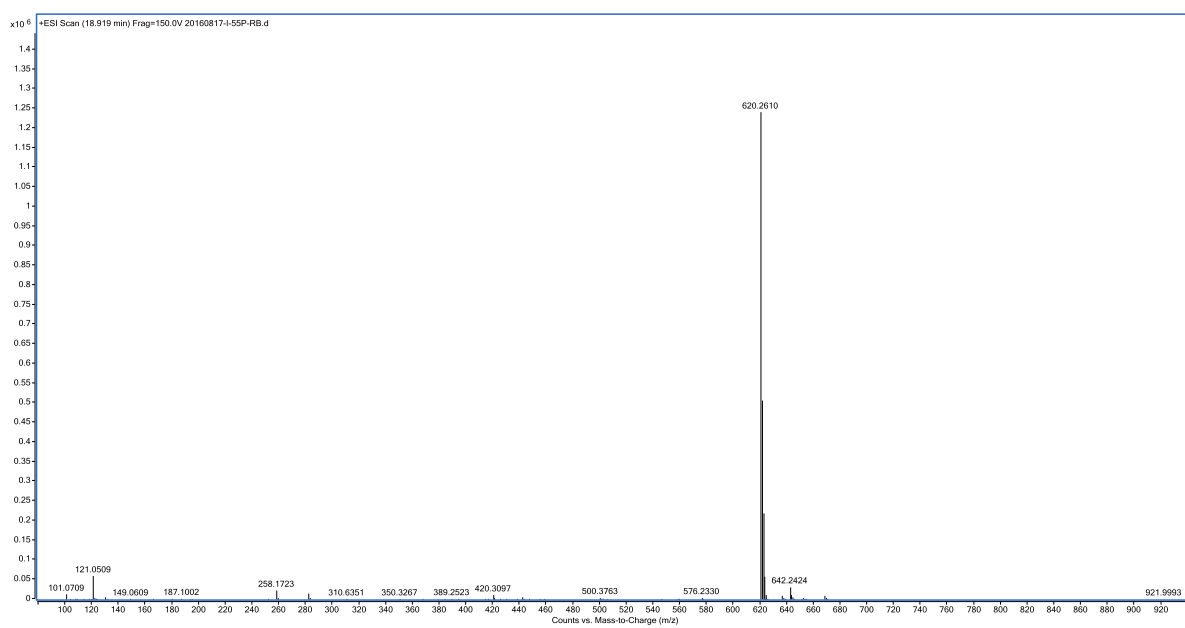


Fig. S26. Construction of the in-frame deletion mutant strains SB22002 (i.e. $\Delta wsmZ3$), and SB22004 (i.e. $\Delta wsmZ4$), and confirmation of their genotypes by Southern analysis. **(A)** Schematic representation for the deletion of *wsmZ3* in strain CB02120-2 by homologous recombination. The probe (526 bp) for Southern blot was amplified with primers orfZ3-SBlot-5 and orfZ3-SBlot-3 using genomic DNA of strain CB02120-2 as the template. Apr^S, apramycin sensitive; Apr^R, apramycin resistance; *acc(3)IV*, apramycin resistance gene. **(B)** Southern blot verification of strain CB02120-2 wild type (1819 bp) and mutant strain SB22002 (1025 bp). Genomic DNAs were digested with *Apa*LI and then used for Southern analysis. Lane 1, DNA marker VII, DIG-labeled (Roche); lane 2, strain CB02120-2 wild type; lane 3, SB22002. **(C)** Schematic representation for the deletion of *wsmZ4* in strain CB02120-2 by homologous recombination. The probe (492 bp) for Southern blot was amplified with primers orfZ4-SBlot-5 and orfZ4-SBlot-3 using genomic DNA of strain CB02120-2 as the template. **(D)** Southern blot verification of strain CB02120-2 wild-type (2265 bp) and mutant strain SB22004 (1626 bp). Genomic DNAs were digested with *Kpn*I and then used for Southern analysis. Lane 4, DNA marker VII, DIG-labeled (Roche); lane 5, strain CB02120-2 wild type; lane 6, SB22004.

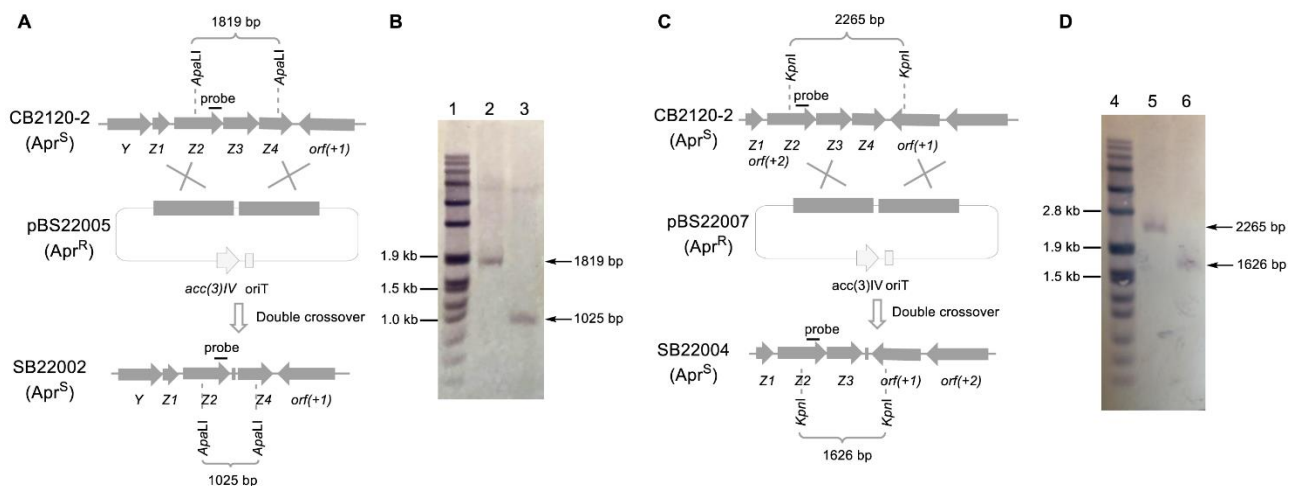


Fig. S27. Discovery of *S. sp.* CB01635 as an alternative LNM E1 producer. **(A)** Comparison of *lnm* gene cluster from *S. atroolivaceus* S-140 and *lnm*-type gene cluster from strain CB01635 revealing almost identical genetic organization. **(B)** The metabolite profile of strain CB01635 (I) in comparison with that of *S. atroolivaceus* S-140 that produces both LNM and LNM E1 (II). While LNM E1 production was reliably observed for both CB01635 and *S. atroolivaceus* S-140, LNM production was not detected in CB01635. **(C)** Confirmation of the identity of LNM E1 produced by strain CB01635 by HR-ESI-MS analysis: m/z 449.1562 [$M + H$]⁺ (calcd for $C_{22}H_{29}N_2O_4S_2$, 449.1563).

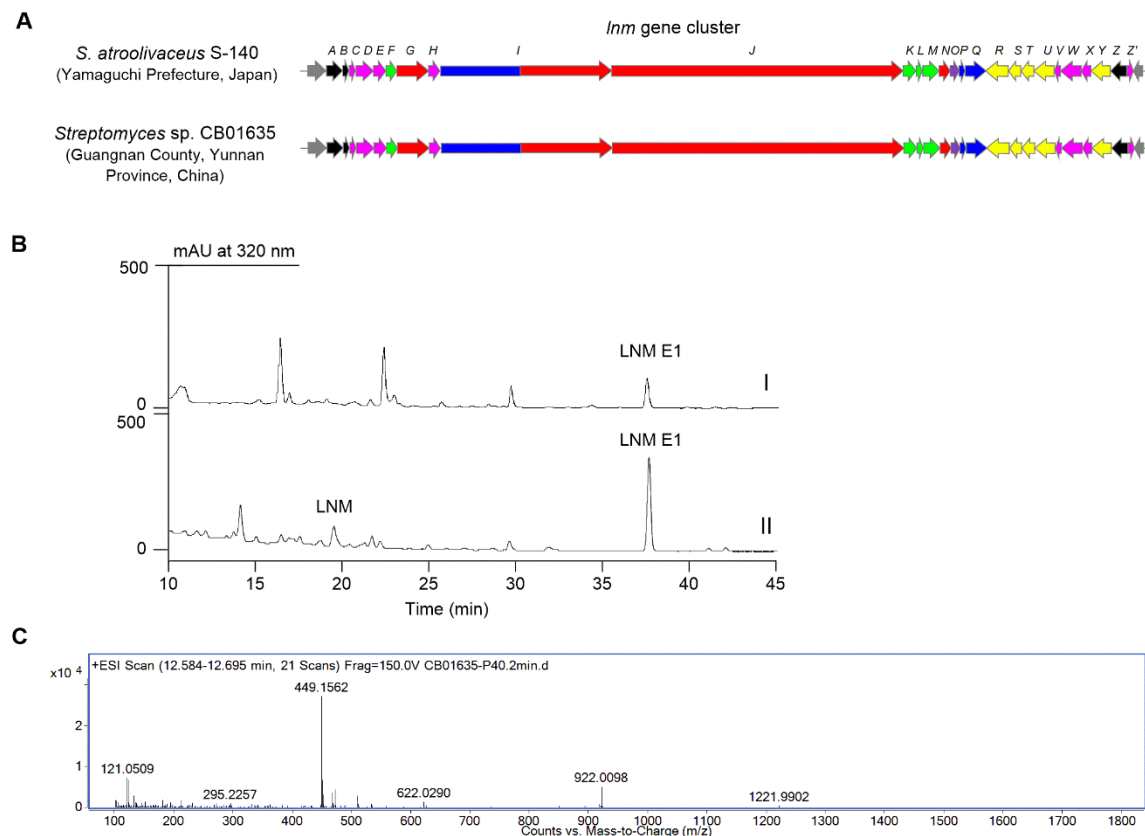


Fig. S28. Discovery of *Streptomyces* sp. NRRL F-5630 and *S. aureofaciens* NRRL B-2183 as alternative producers of GNM A and GNM B. (A) The *gnm*-like gene clusters from strains *Streptomyces* sp. NRRL F-5630 and *S. aureofaciens* NRRL B-2183 in comparison with the *gnm* gene cluster from strain CB01883. Geographical locations of the three strains (where they were originally isolated) were shown in the parentheses. (B) HPLC analysis of the metabolite profiles of CB01883 wild type (III), NRRL F-5630 (IV) and NRRL B-2183 (V) in comparison with the GNM A (I) and GNM B (II) standards.

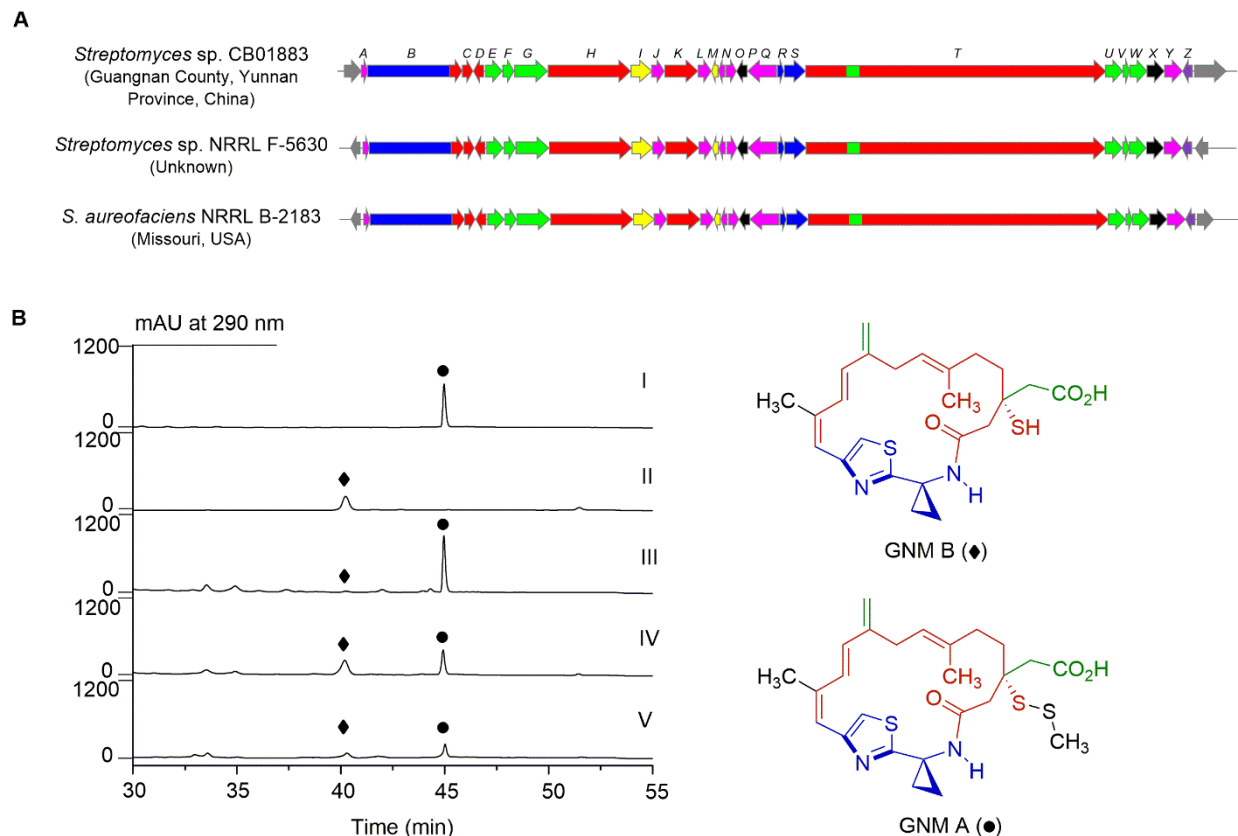


Fig. S29. Functional characterization of representative adenylation proteins from newly discovered LNM-type biosynthetic machineries. **(A)** SDS-PAGE analysis of the purified adenylation proteins. Lane 1, GnmS (59.8 kD); Lane 2, WsmQ (57.5 kD); Lane 3, Maur_X (A domain, 58.4 kD); Lane 4, CB01373_Q (A domain, 59.0 kD); Lane 5, CB02613_Z17 (A domain including an extra N-terminal with ~200 amino acid residues, 81.7 kD); Lane 6, CB02613_M (A domain including an extra N-terminal with ~200 residues, 80.6 kD); M, protein ladder. **(B)** The mechanism of hydroxylamine-trapping assay used in this study for probing the substrate specificities of the adenylation proteins (15). **(C)** Substrate specificities of the representative adenylation proteins from different LNM-type pathways. Under tested conditions, GnmS, WsmQ, Maur_X and CB01373_Q showed highest activities towards ACC (73% substrate conversion), D-Ala (32% substrate conversion), L-Thr (19% substrate conversion) and L-Thr (22% substrate conversion), respectively, while CB02613_Z17 and CB02613_M did not show obvious activity towards all the tested substrates (< 2% substrate conversion). The percentage of the substrate conversion was estimated based on the assumption that the UV absorbance of 3 mM DL-alanine hydroxamate complexed with FeCl₃ corresponded to the 100% substrate conversion. The relative activities of GnmS, WsmQ, Maur_X and CB01373_Q towards their best substrates were normalized to 100%, and the relative activities of CB02613_Z17 and CB02613_M towards different amino acids were calculated based on the activity of CB01373_Q towards its best substrate L-Thr.

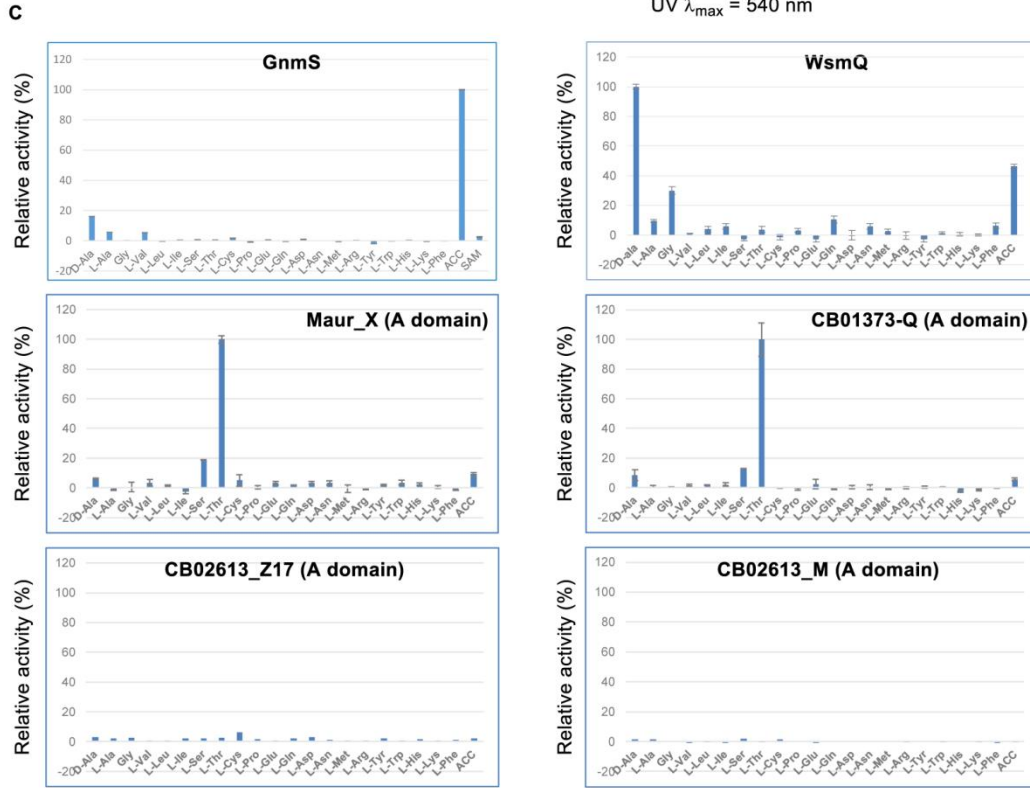
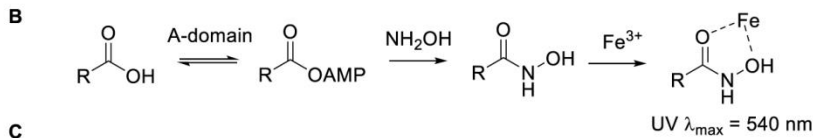
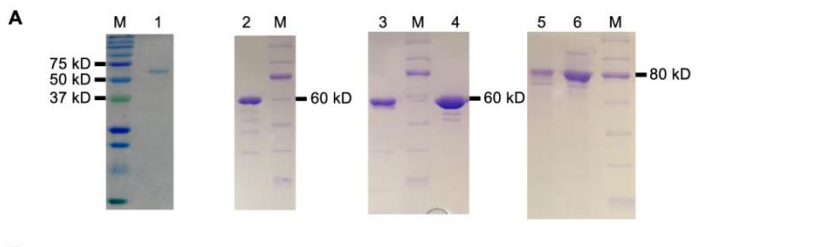


Fig. S30. Construction of the in-frame deletion mutant strain SB21003 (i.e. $\Delta gnmO$) and confirmation of its genotype by Southern analysis. **(A)** Schematic representation for the deletion of *gnmO* in strain CB01883 by homologous recombination. The probe (542 bp) for Southern blot was amplified with primers orf132-SBlot-5nn and orf132-SBlot-3nn using genomic DNA of strain CB01883 as the template. Apr^S, apramycin sensitive; Apr^R, apramycin resistance; *acc(3)/V*, apramycin resistance gene. **(B)** Southern blot verification of strain CB01883 wild type (1.7 kb) and mutant strain SB21003 (3.3 kb). Genomic DNAs were digested with *Aat*II and then used for Southern analysis. Lane 1, DNA marker VII, DIG-labeled (Roche); lane 2, strain CB01883 wild type; lane 3, SB21003.

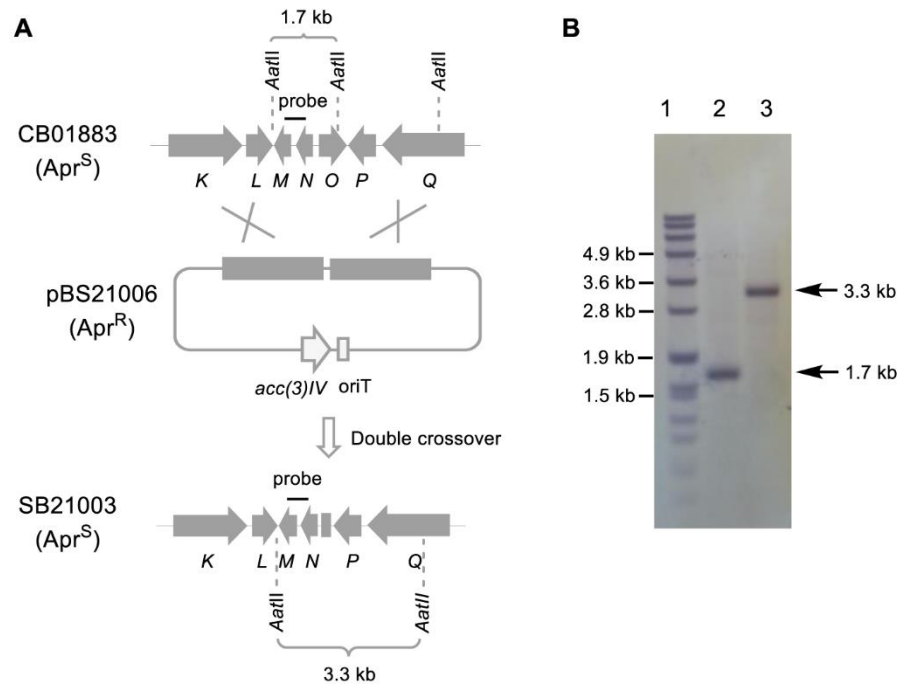


Fig. S31A. ^1H NMR spectra of GNM B1 (700 MHz, DMSO- d_6)

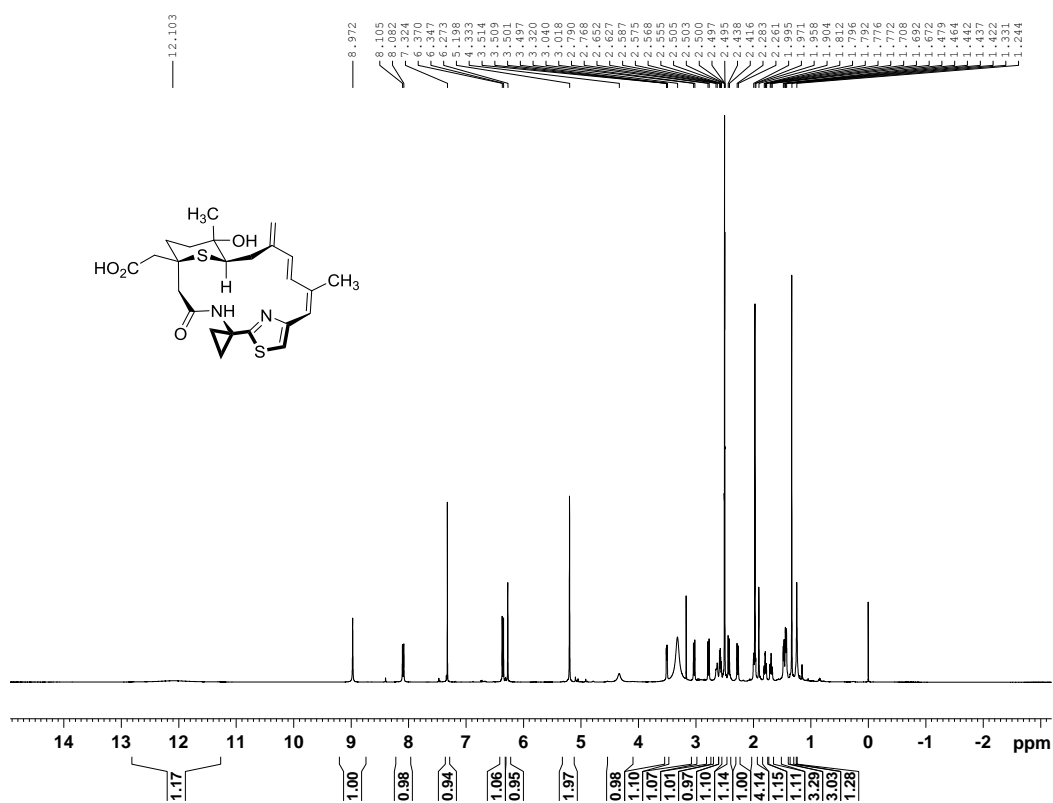


Fig. S31B. ^{13}C NMR spectra of GNM B1 (175 MHz, DMSO- d_6)

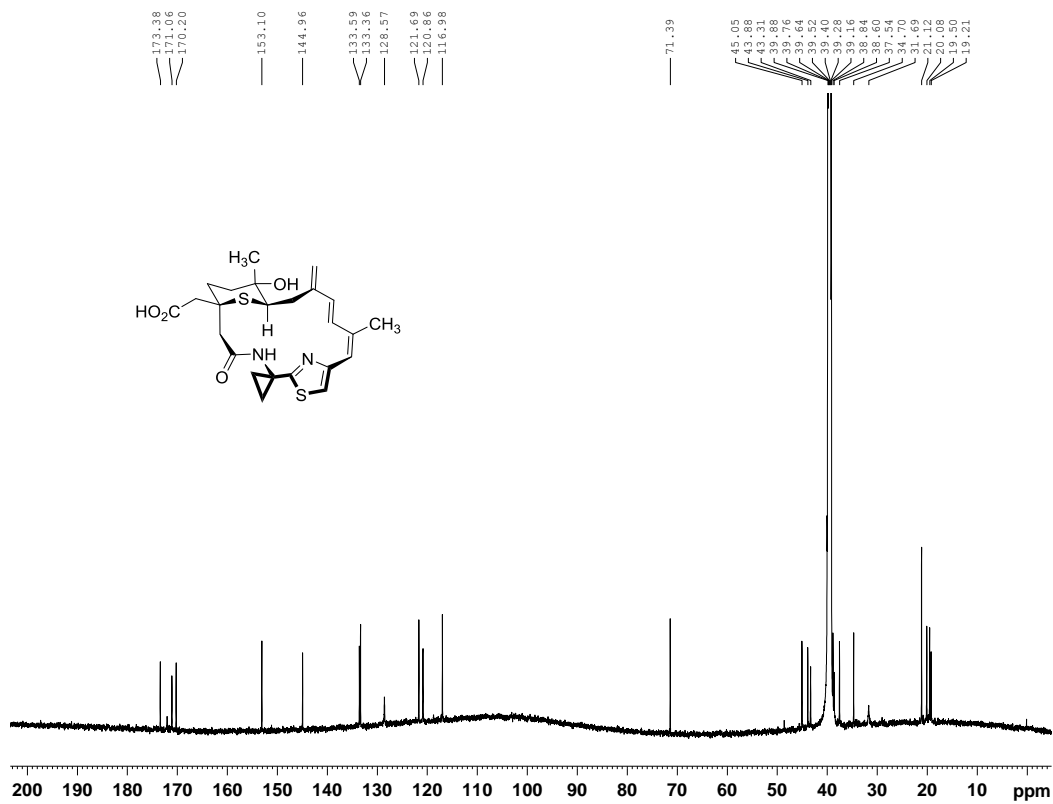


Fig. S31C. DEPT-135 spectra of GNM B1 (DMSO- d_6)

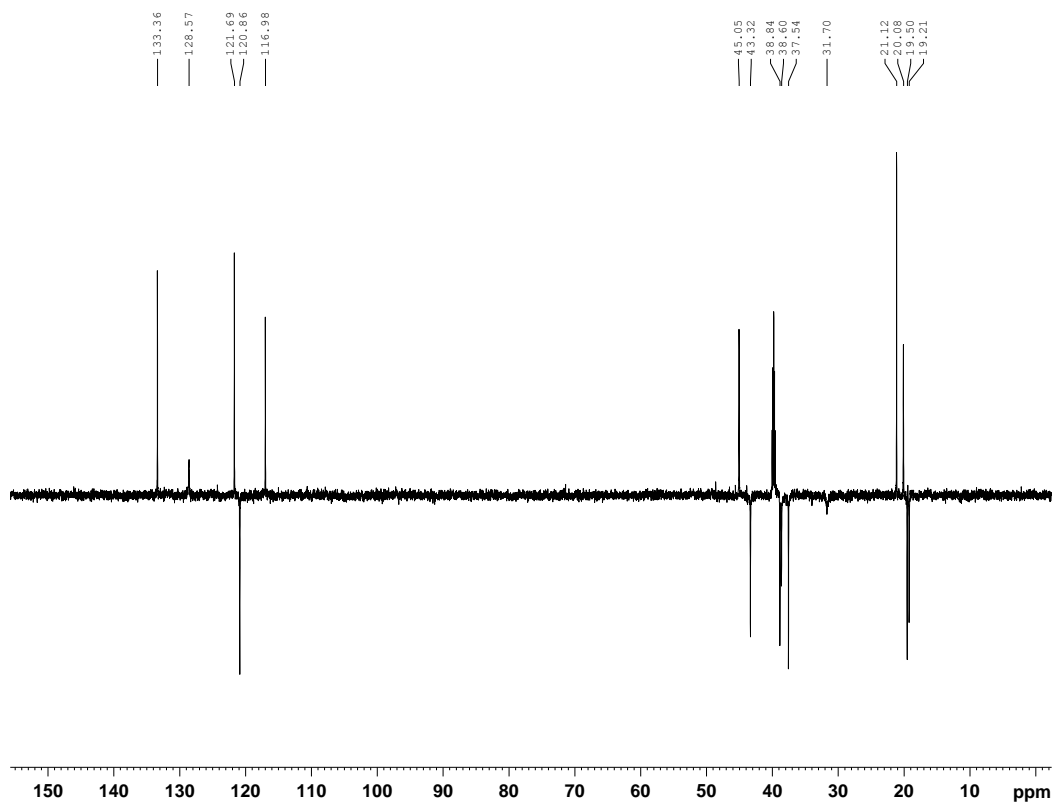


Fig. S31D. HSQC spectra of GNM B1 (DMSO- d_6)

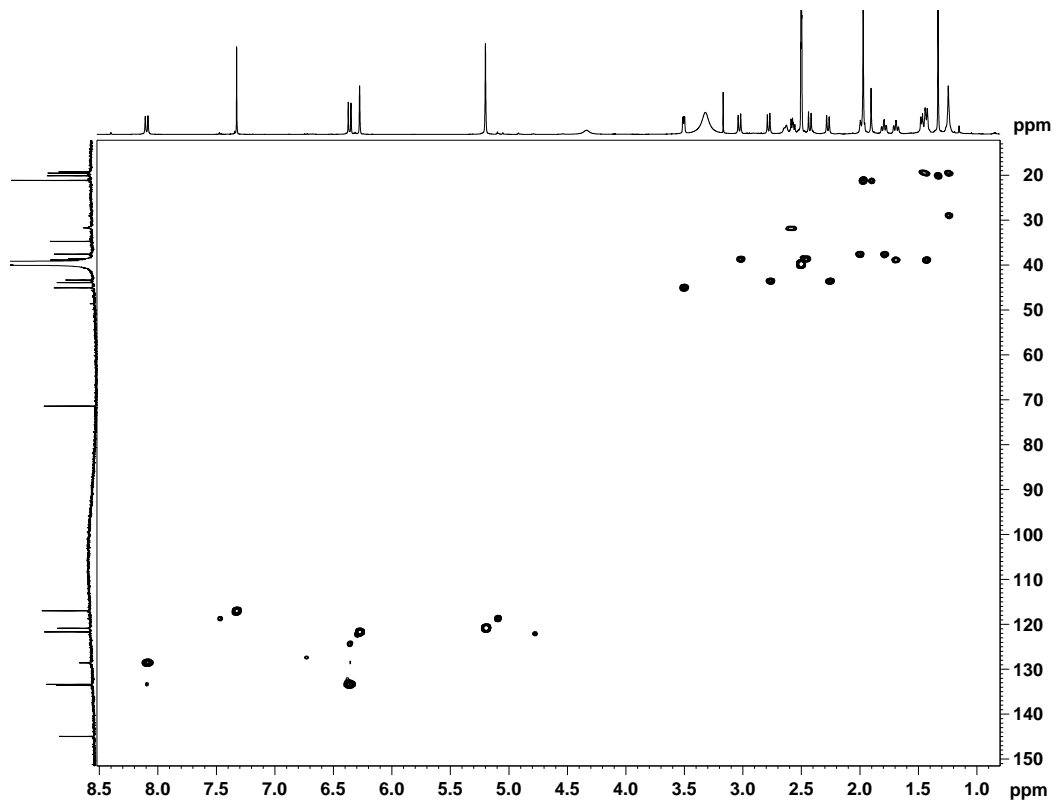


Fig. S31E. ^1H - ^1H COSY spectra of GNM B1 (DMSO- d_6)

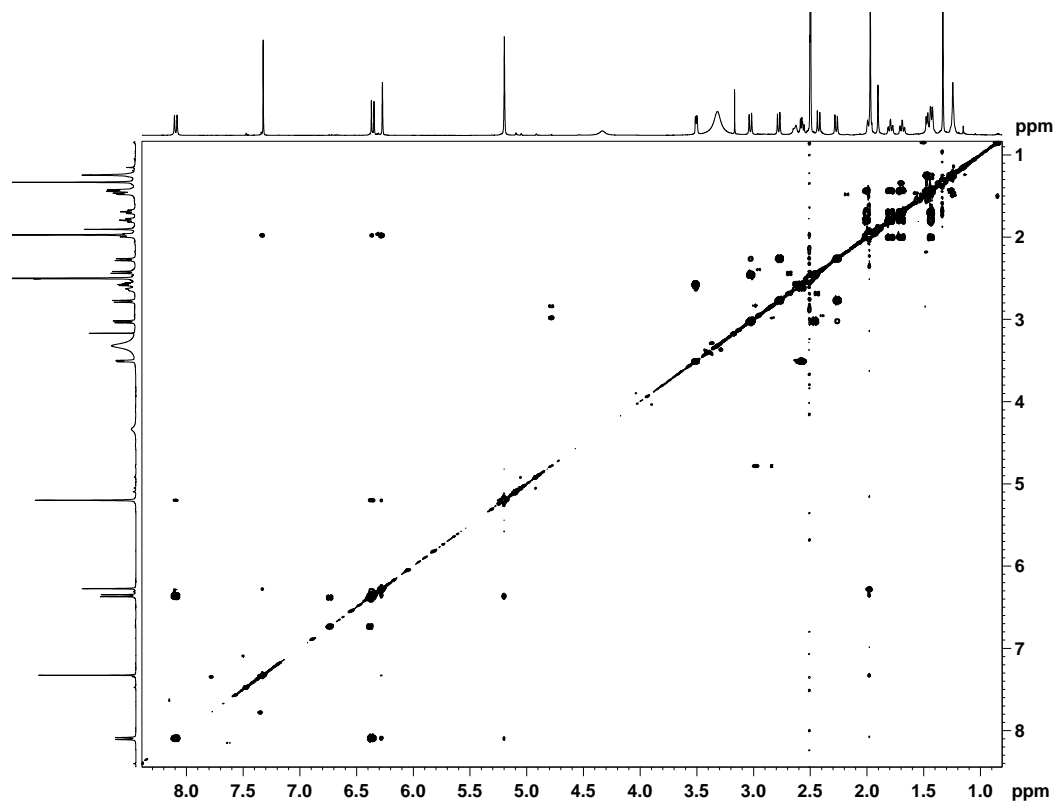


Fig. S31F. HMBC spectra of GNM B1 (DMSO- d_6)

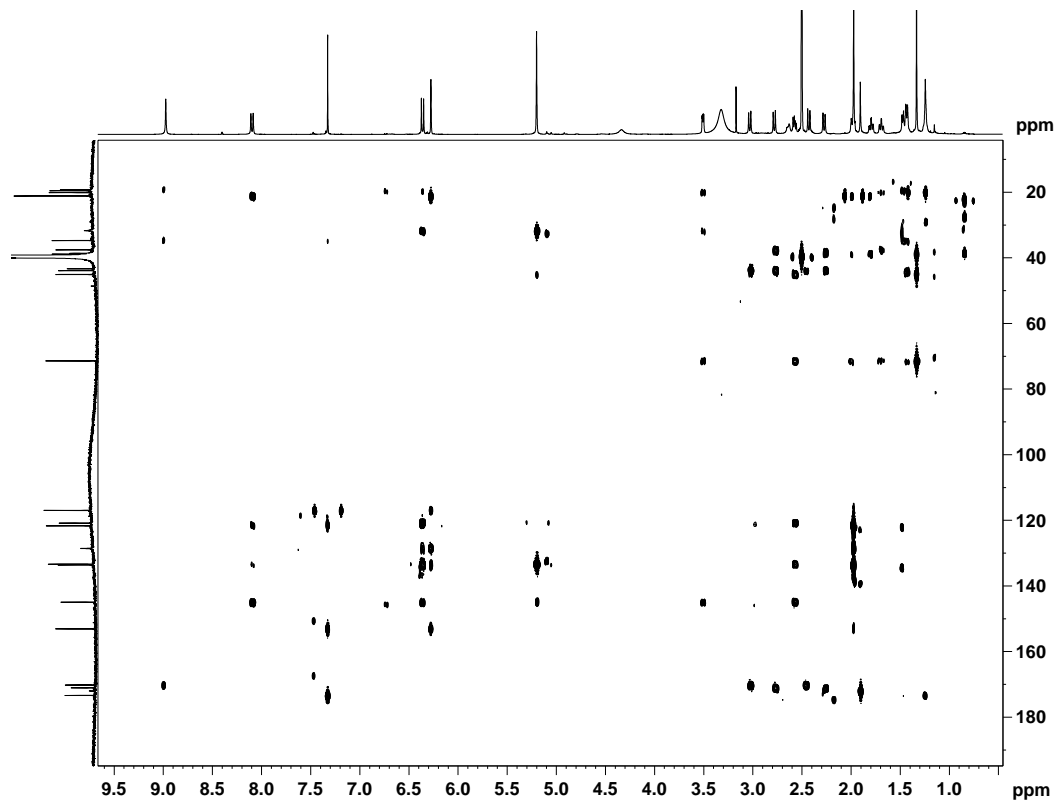


Fig. S31G. ROESY spectra of GNM B1 (DMSO- d_6)

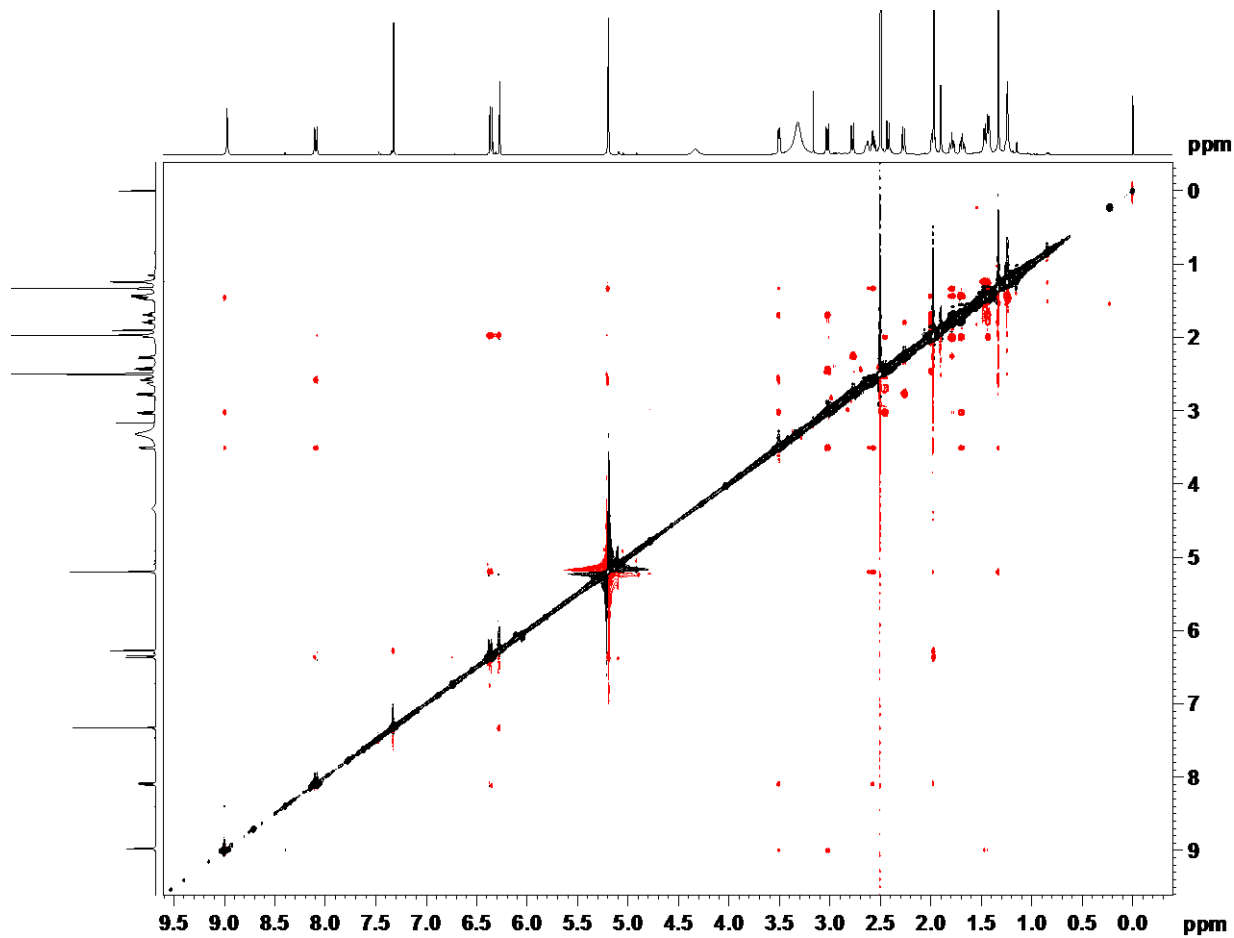


Fig. S31H. HR-MS (ESI) spectra of GNM B1

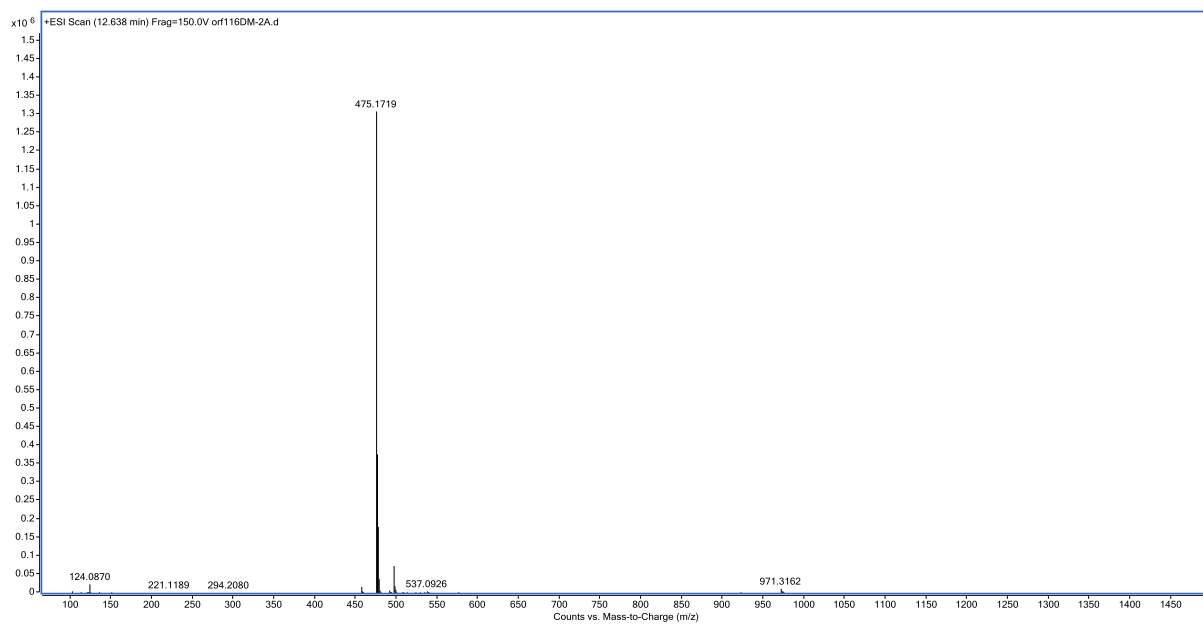


Fig. S32A. ^1H NMR spectra of GNM B2 (700 MHz, $\text{DMSO}-d_6$)

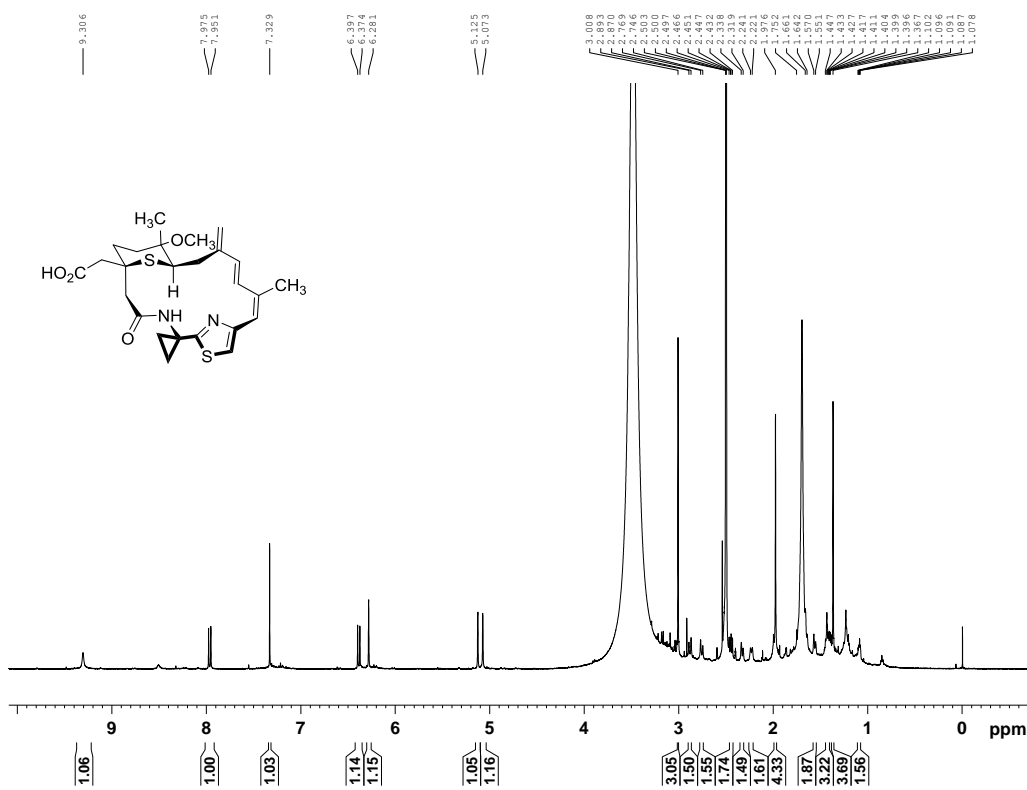


Fig. S32B. ^{13}C NMR spectra of GNM B2 (175 MHz, $\text{DMSO}-d_6$)

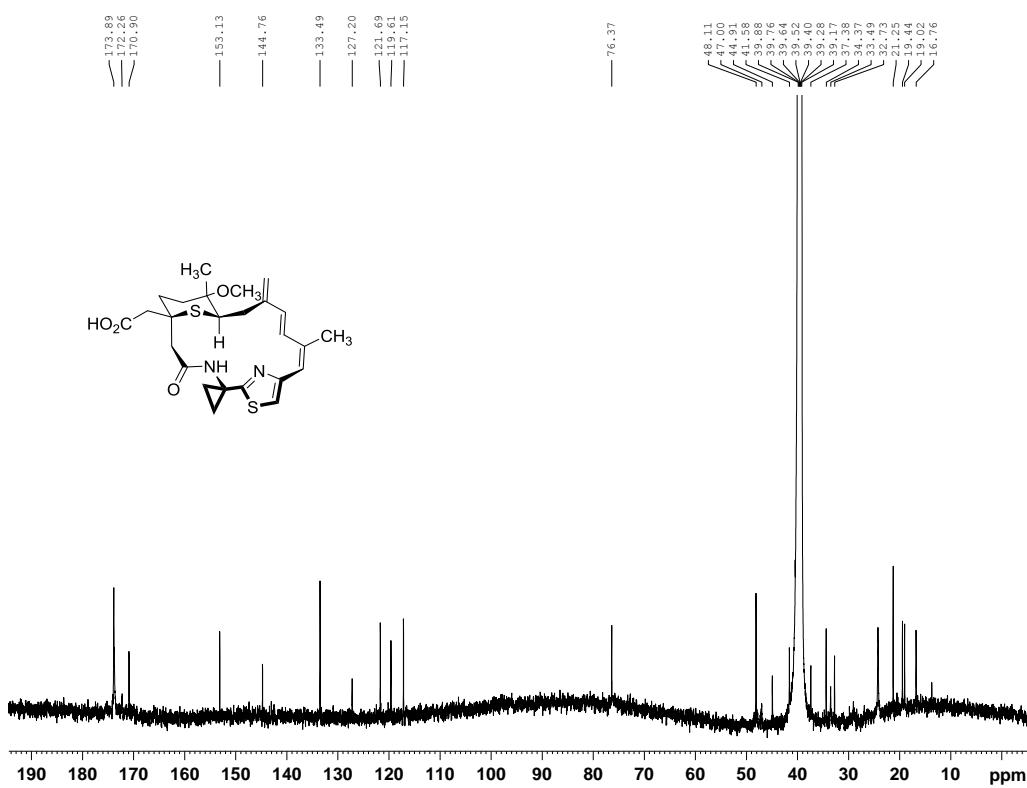


Fig. S32C. DEPT-135 spectra of GNM B2 (DMSO- d_6)

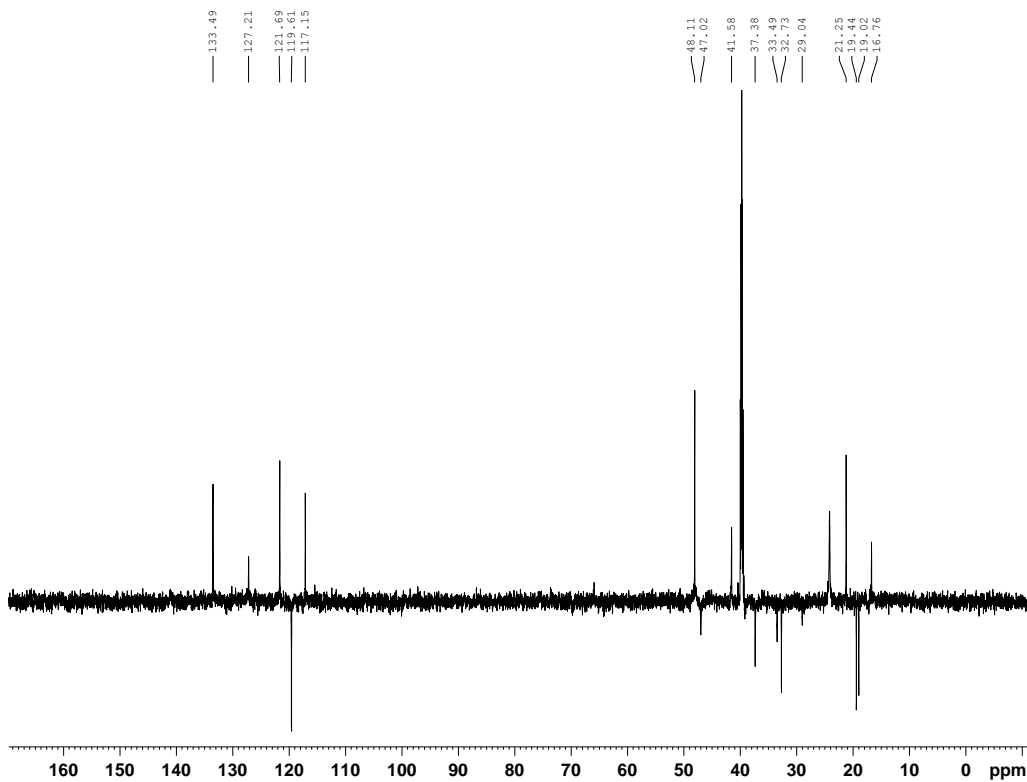


Fig. S32D. HSQC spectra of GNM B2 (DMSO- d_6)

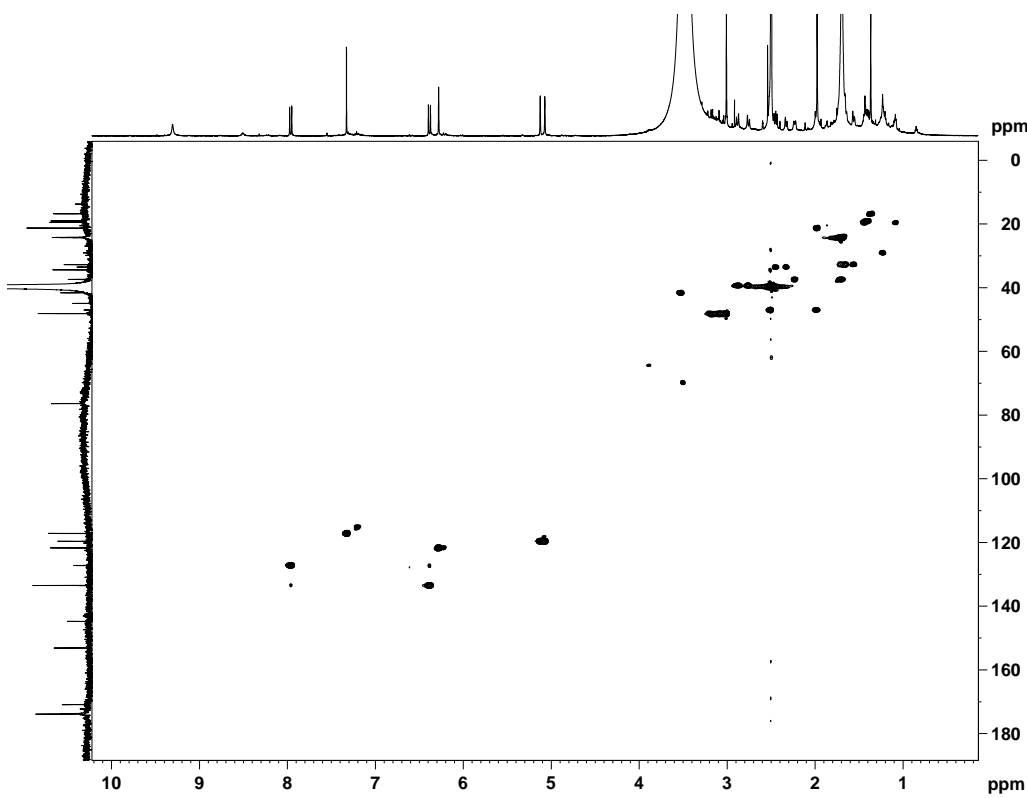


Fig. S32E. ^1H - ^1H COSY spectra of GNM B2 (DMSO- d_6)

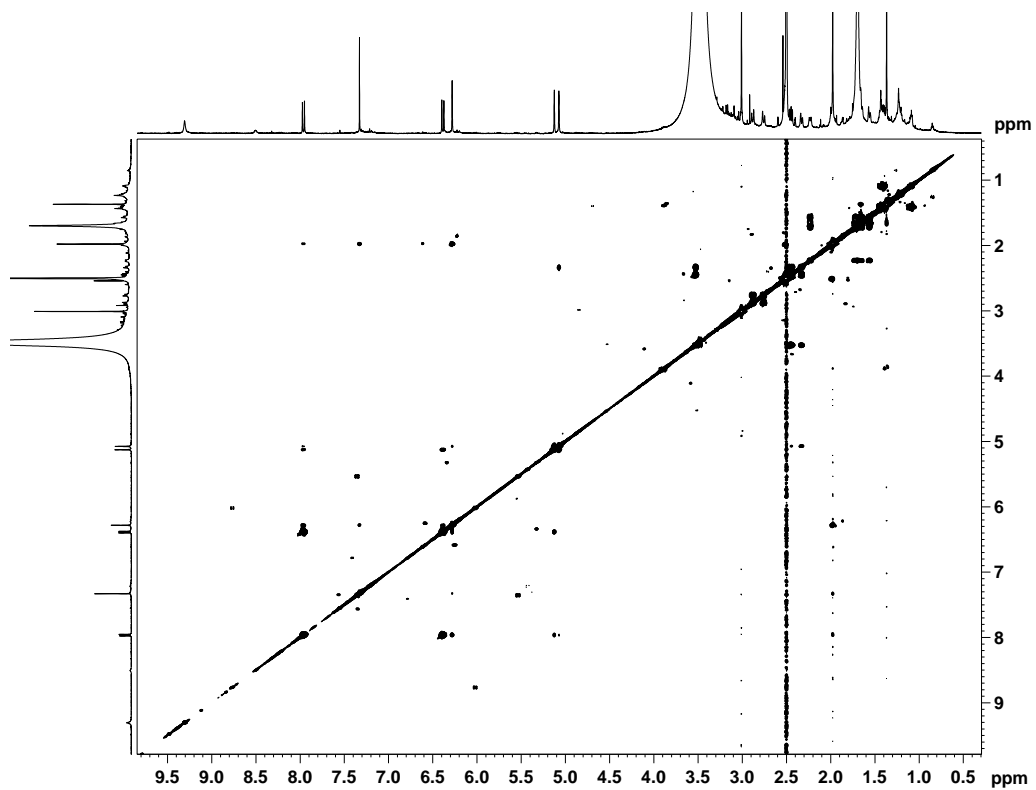


Fig. S32F. HMBC spectra of GNM B2 (DMSO- d_6)

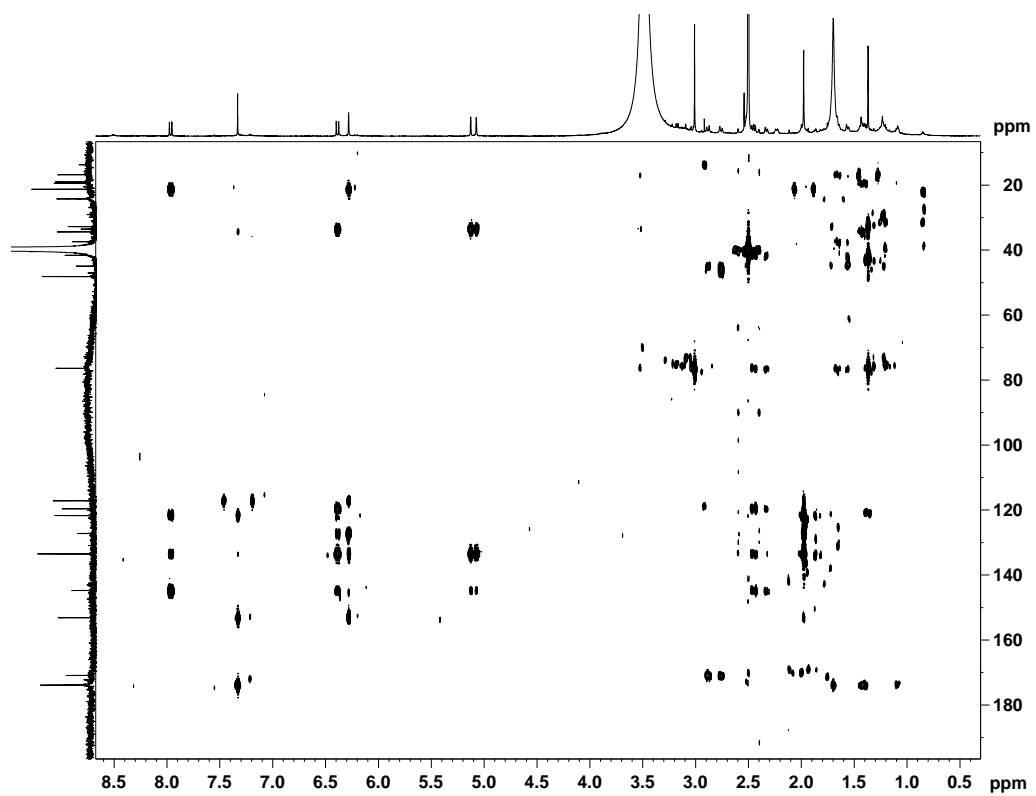


Fig. S32G. ROESY spectra of GNM B2 (DMSO- d_6)

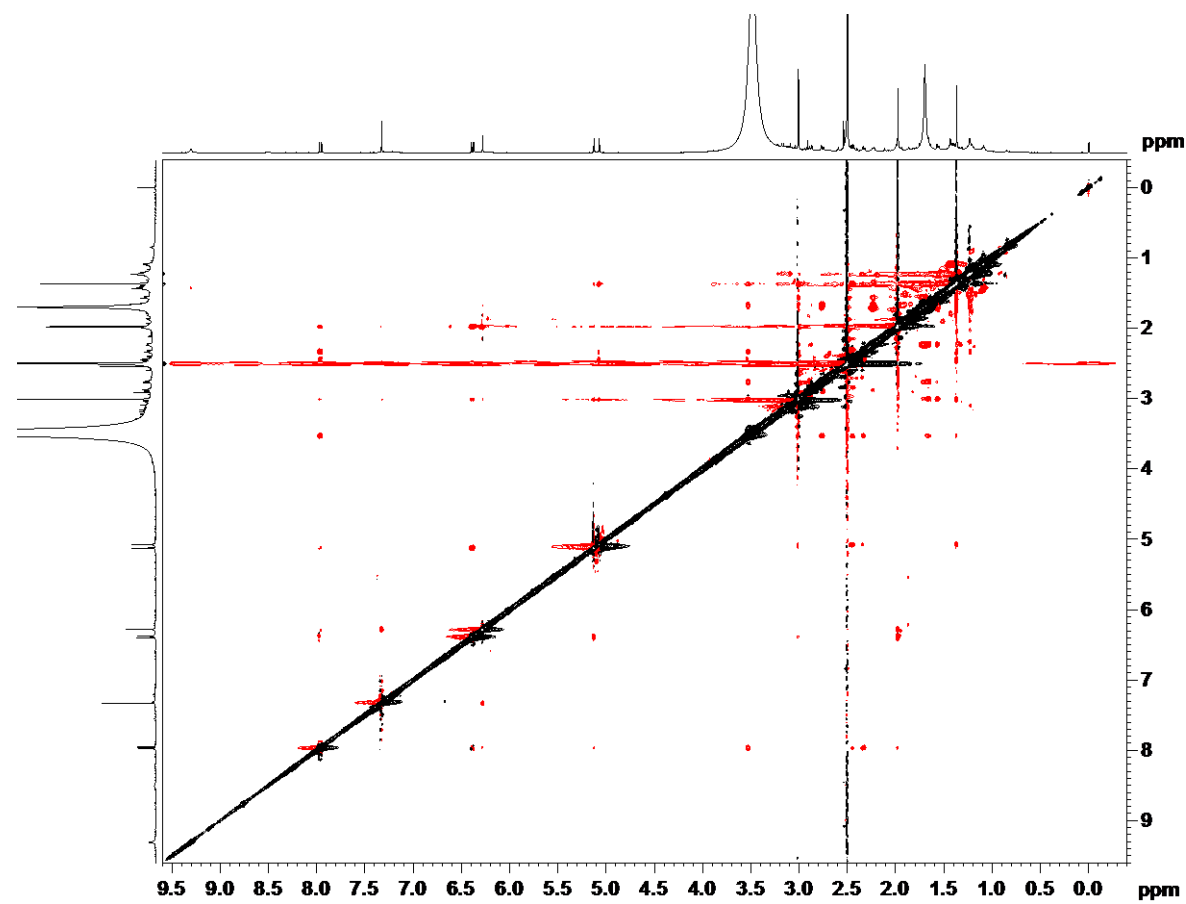


Fig. S32H. HR-MS (ESI) spectra of GNM B2

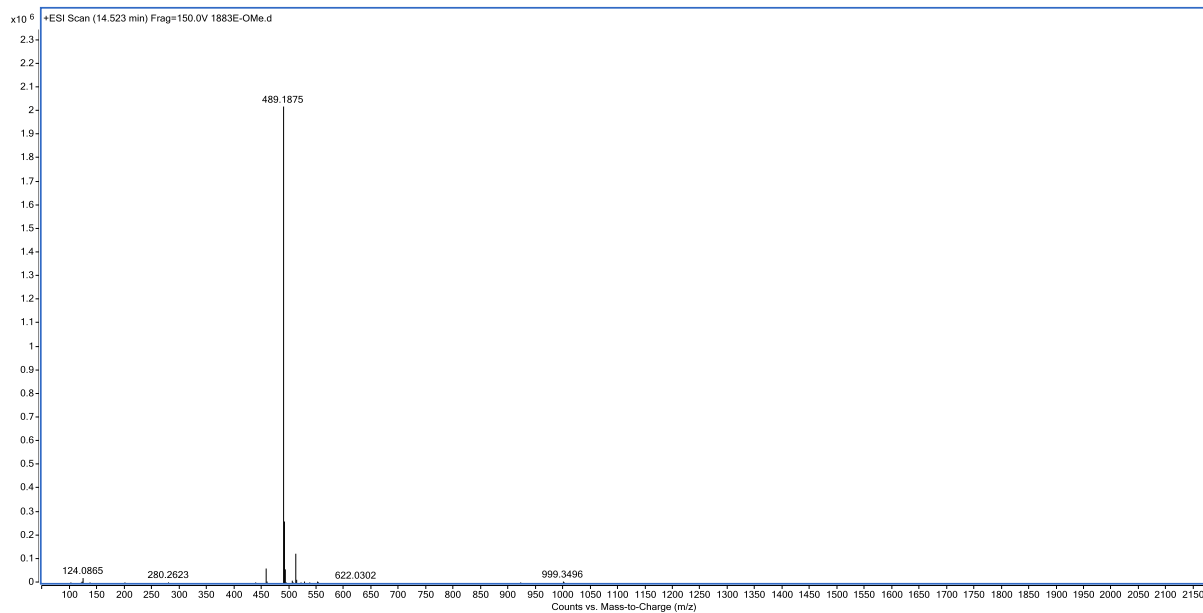


Fig. S33A. ^1H NMR spectra of GNM B3 (700 MHz, $\text{DMSO}-d_6$)

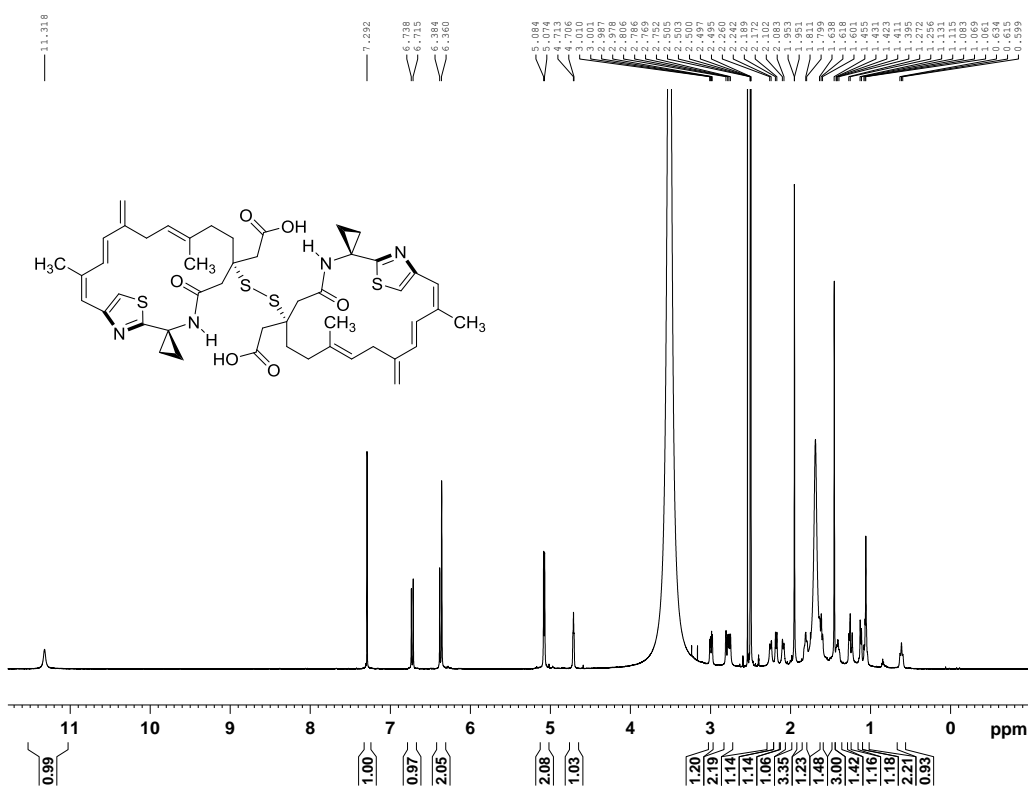


Fig. S33B. ^{13}C NMR spectra of GNM B3 (175 MHz, $\text{DMSO}-d_6$)

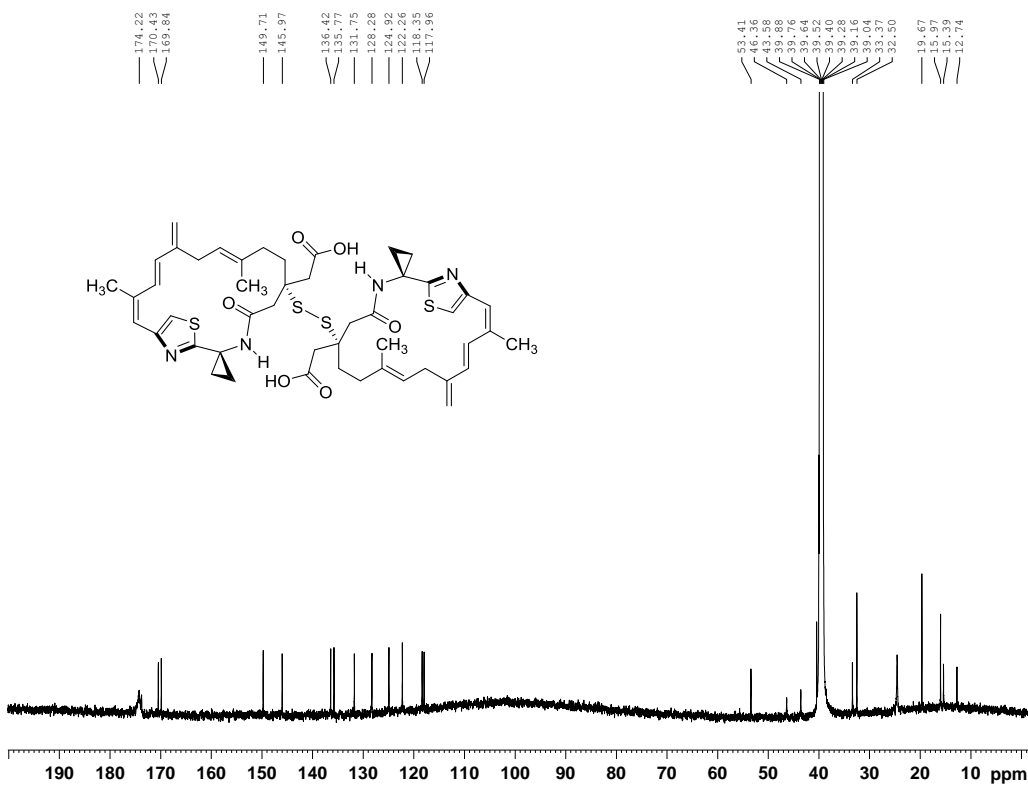


Fig. S33C. DEPT-135 spectra of GNM B3 (DMSO- d_6)

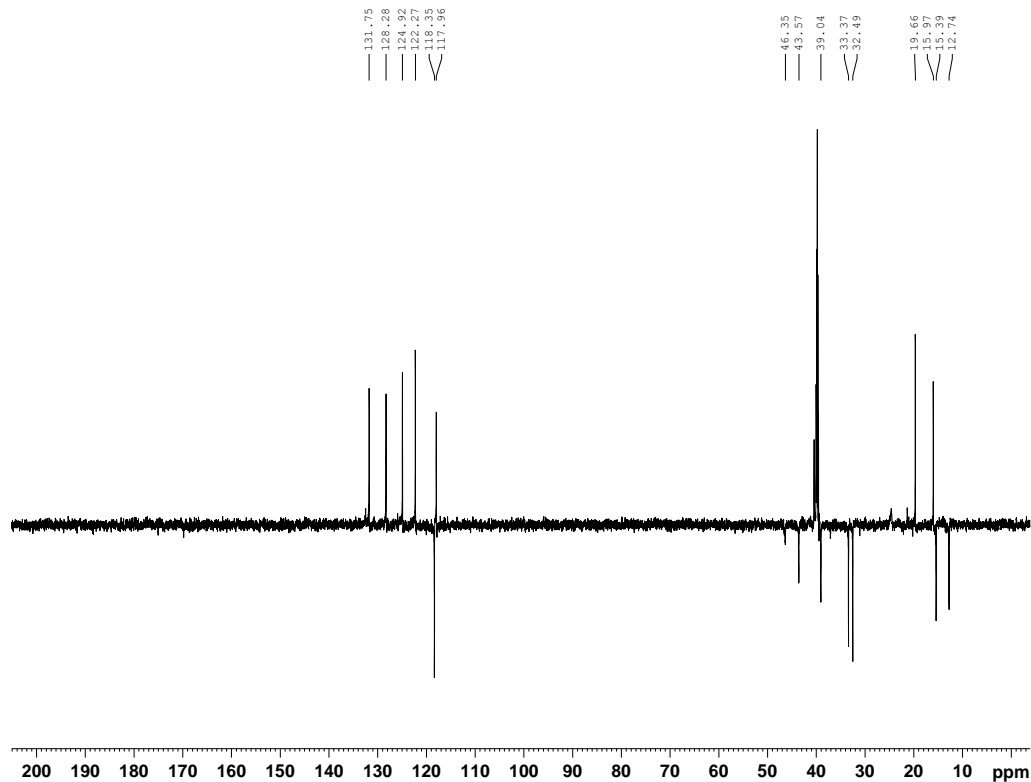


Fig. S33D. HSQC spectra of GNM B3 (DMSO- d_6)

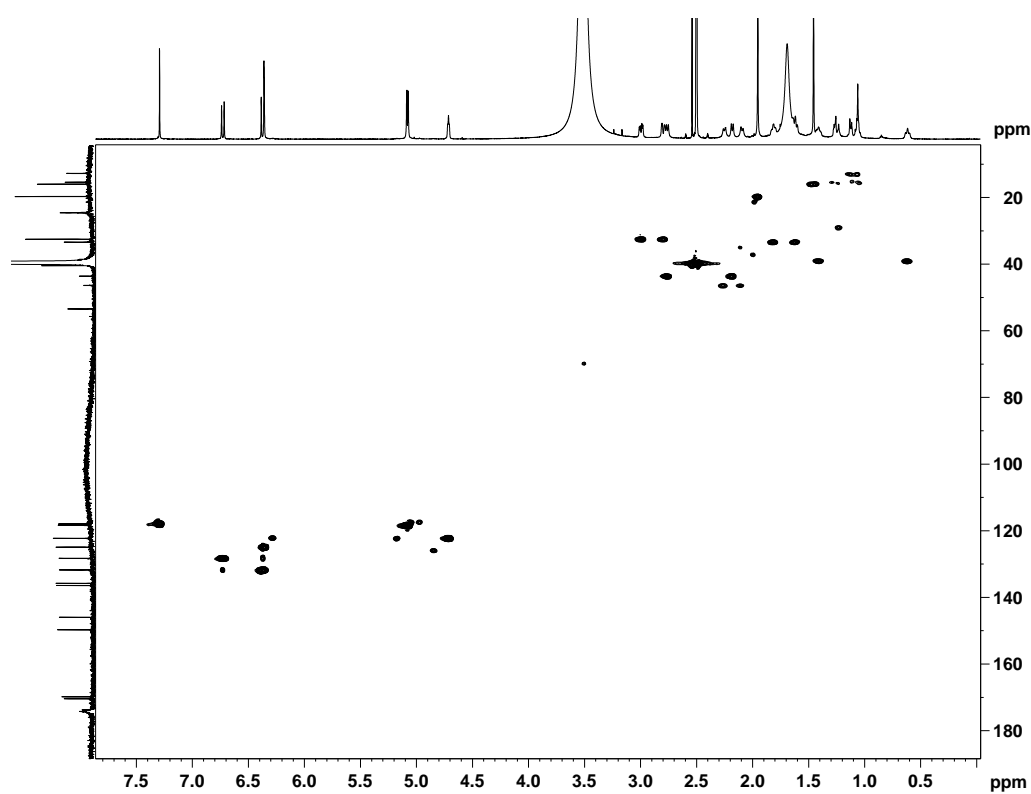


Fig. S33E. ^1H - ^1H COSY spectra of GNM B3 (DMSO- d_6)

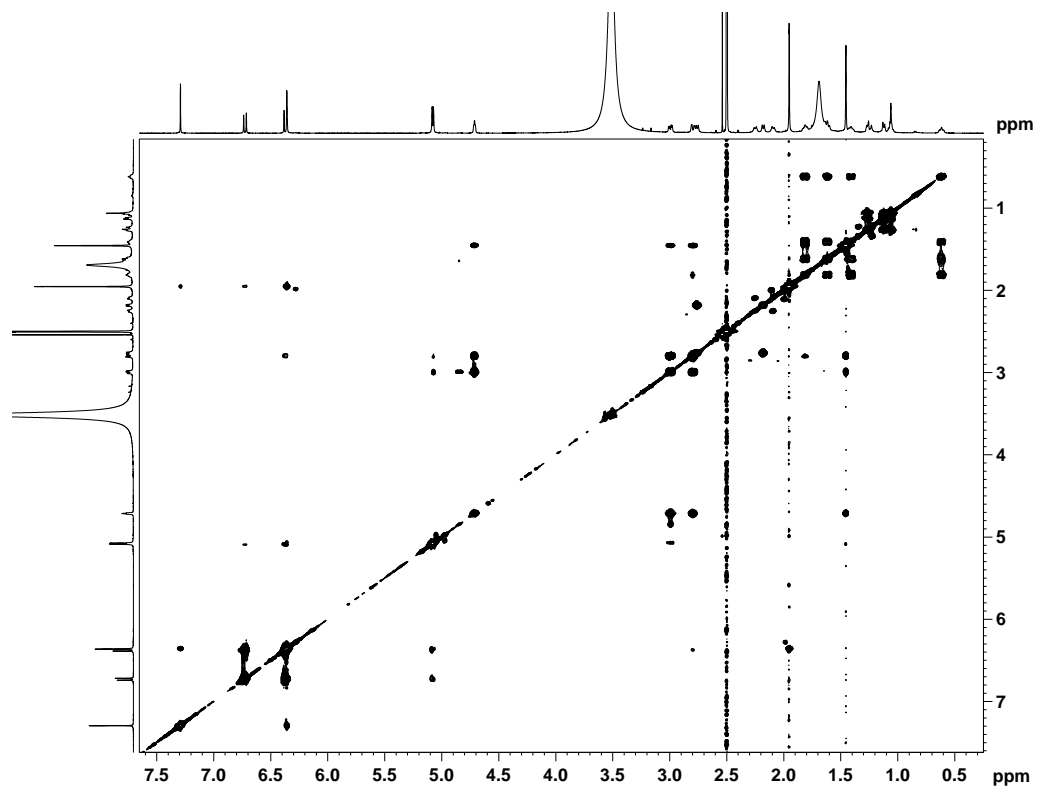


Fig. S33F. HMBC spectra of GNM B3 (DMSO- d_6)

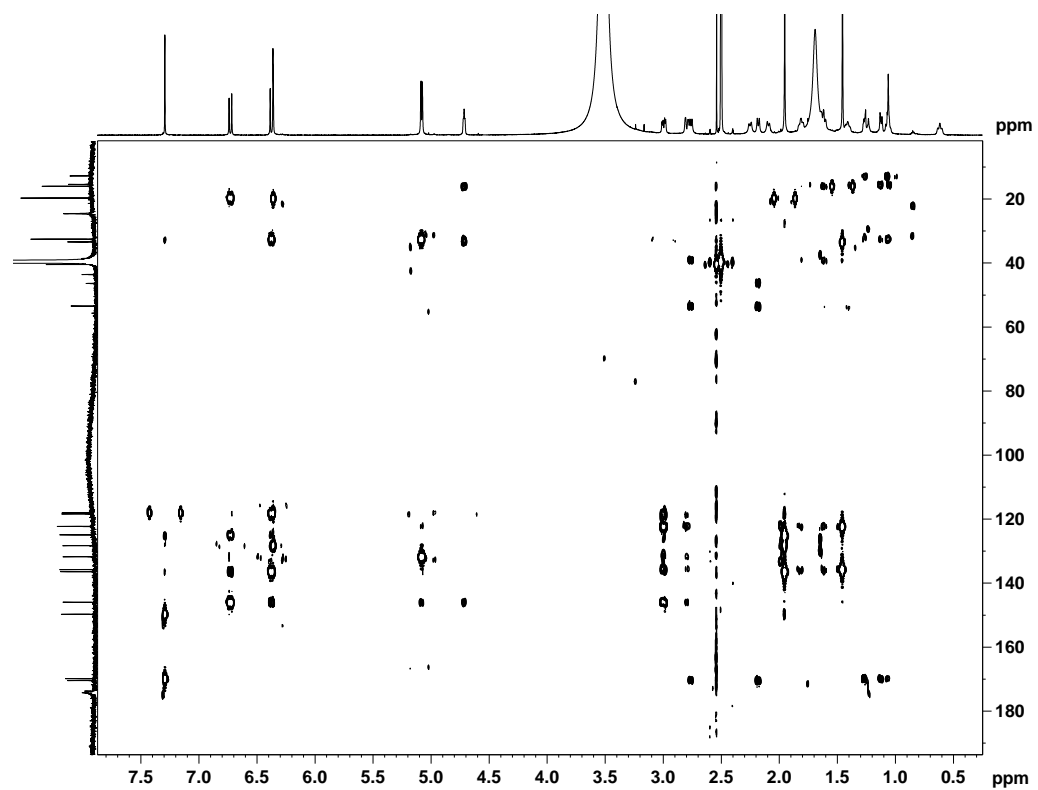


Fig. S33G. ROESY spectra of GNM B3 (DMSO- d_6)

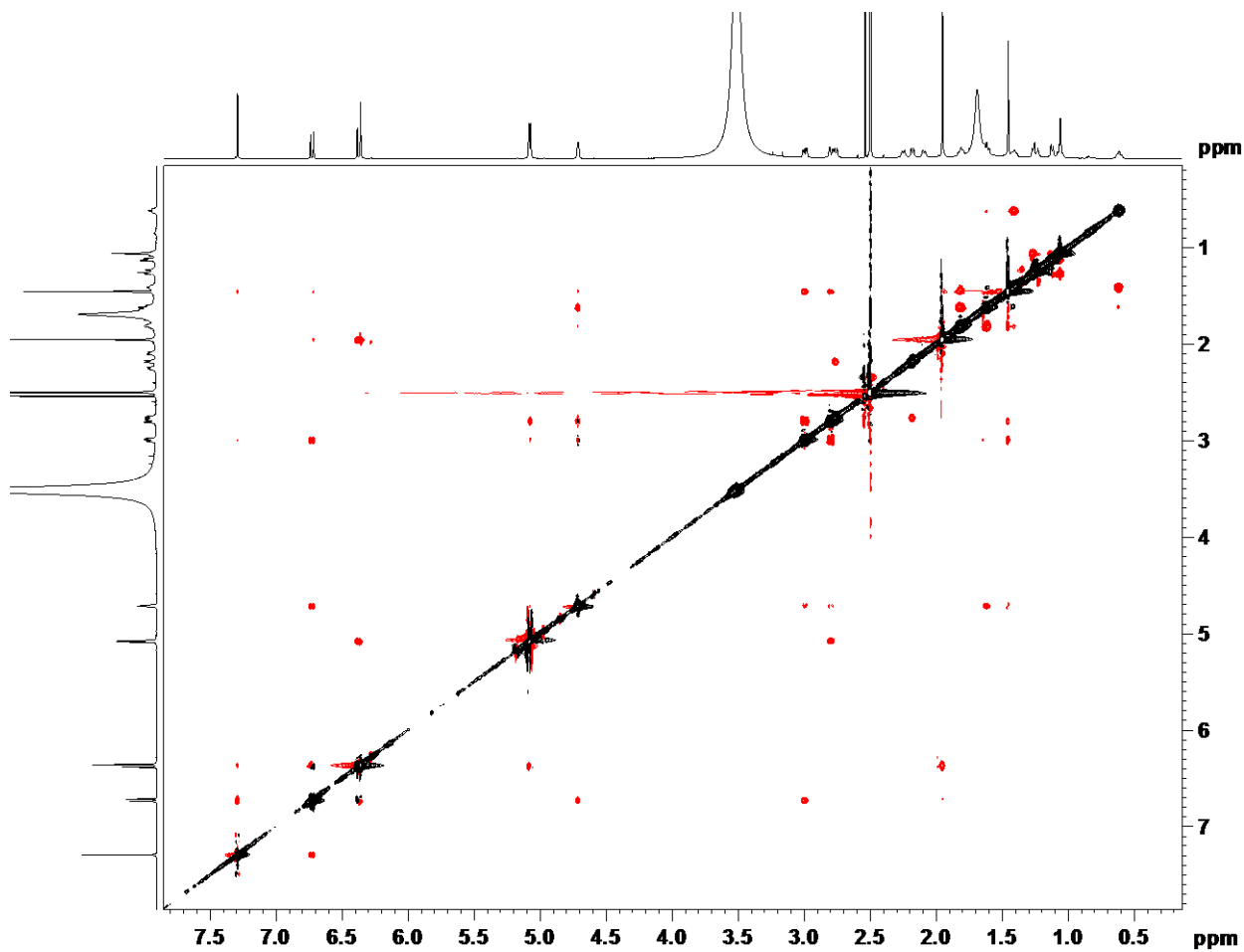


Fig. S33H. HR-MS (ESI) spectra of GNM B3

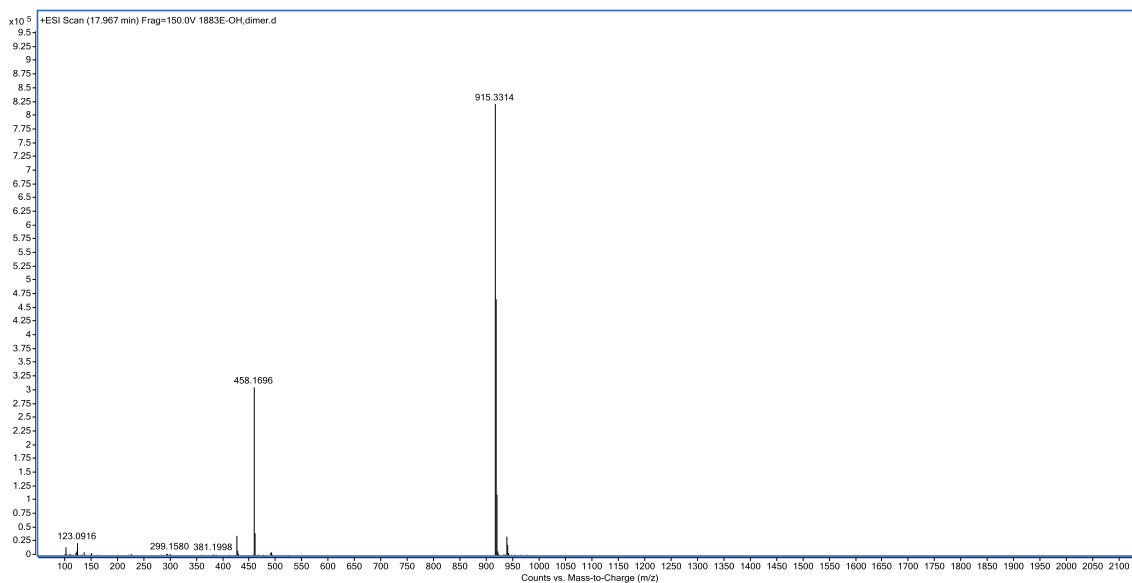
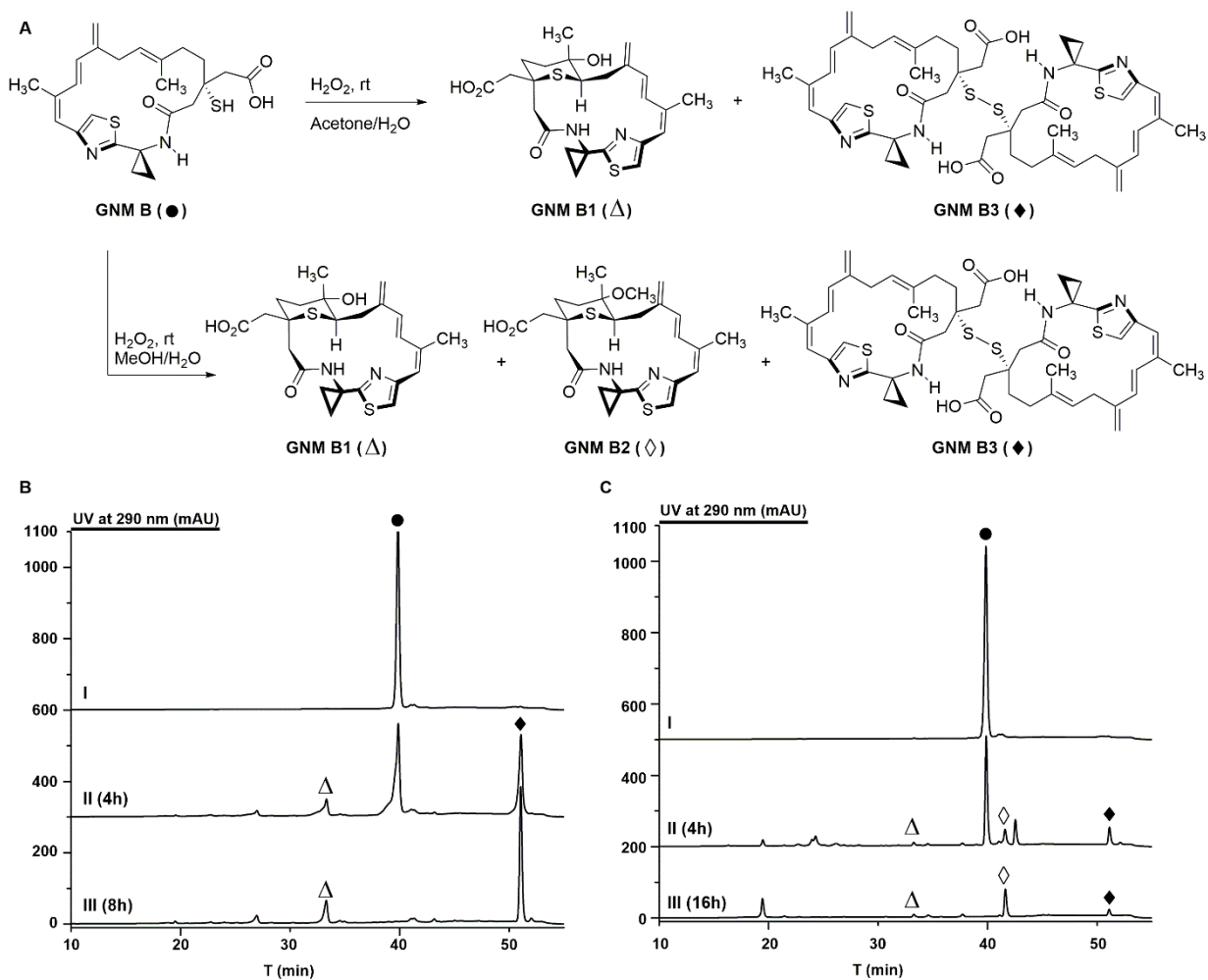


Fig. S34. Chemical transformation of GNM B to GNM B1, GNM B2 and GNM B3 (24). **(A)** Oxidation of GNM B with H_2O_2 . Conditions: A solution of GNM B (0.2 mg) in acetone/ H_2O (440 μL /15 μL) or in methanol/ H_2O (490 μL /5 μL) was added 5 μL H_2O_2 (30% in water), and the reaction mixture was stirred at room temperature for certain time as indicated. The reaction was followed by HPLC and LC-MS using the same conditions as that for the analysis of GNM A. **(B)** Oxidation of GNM B in acetone solution. I: GNM B standard; II: reaction for 4 h; III: reaction for 8 h. **(C)** Oxidation of GNM B in methanol solution. I: GNM B standard; II: reaction for 4 h; III: reaction for 16 h. GNM B (\bullet), GNM B1 (Δ); GNM B2 (\diamond); GNM B3 (\blacklozenge).



References

1. Sambrook J, Russell DW (2001) Molecular cloning: a laboratory manual, 3rd edn. Cold Spring Harbor Laboratory Press, NY.
2. Kieser T, Bibb MJ, Buttner MJ, Chater KF, Hopwood DA (2000) Practical Streptomyces genetics. The John Innes Foundation, Norwich.
3. Larkin MA, et al. (2007) ClustalW and ClustalX version 2. *Bioinformatics* 23:2947-2948.
4. Tamura K, Stecher G, Peterson D, Filipski A, Kumar S (2013) MEGA6: molecular evolutionary genetics analysis version 6.0. *Mol Biol Evol* 30:2725–2729.
5. Weber T, et al. (2015) antiSMASH 3.0-a comprehensive resource for the genome mining of biosynthetic gene clusters. *Nucleic Acids Res* 43:W237-W243.
6. Rudolf JD, Yan X, Shen B (2016) Genome neighborhood network reveals insights into enediyne biosynthesis and facilitates prediction and prioritization for discovery. *J Ind Microbiol Biotechnol* 43(2-3):261-276.
7. Hindra, et al. (2014) Strain prioritization for natural product discovery by a high-throughput real-time PCR method. *J Nat Prod* 77:2296–2303.
8. Boetzer M, Henkel CV, Jansen HJ, Butler D, Pirovano W (2011) Scaffolding pre-assembled contigs using SSPACE. *Bioinformatics* 27:578–579.
9. Boetzer M, Pirovano W (2012) Toward almost closed genomes with GapFiller. *Genome Biol* 13:R56.
10. Bierman M, Logan R, O'Brien K, Seno ET, Rao RN, Schoner BE (1992) Plasmid cloning vectors for the conjugal transfer of DNA from *Escherichia coli* to *Streptomyces* spp. *Gene* 116:43-49.
11. Li L, et al. (2017) Engineered jadomycin analogues with altered sugar moieties revealing JadS as a substrate flexible O-glycosyltransferase. *Appl Microbiol Biotechnol* 101:5291-5300.
12. Wang W, Li X, Wang J, Xiang S, Feng X, Yang K (2013) An engineered strong promoter for streptomycetes. *Appl Environ Microbiol* 79:4484–4492.
13. Cheng YQ, Tang GL, Shen B (2002) Identification and localization of the gene cluster encoding biosynthesis of the antitumor macrolactam leinamycin in *Streptomyces atroolivaceus* S-140. *J Bacteriol* 184(24):7013–7024.
14. Yabuuchi T, Kusumi T (2000) Phenylglycine methyl ester, a useful tool for absolute configuration determination of various chiral carboxylic acids. *J Org Chem* 65:397-404.
15. Lohman JR, Bingman CA, Phillips GN, Jr, Shen B (2013) Structure of the bifunctional acyltransferase/decarboxylase LnmK from the leinamycin biosynthetic pathway revealing novel activity for a double-hot-dog fold. *Biochemistry* 52(5):902–911.
16. Aslanidis C, de Jong PJ (1990) Ligation-independent cloning of PCR products (LIC-PCR). *Nucleic Acids Res* 18:6069-6074.
17. Kadi N, Challis GL (2009) Siderophore biosynthesis: a substrate specificity assay for nonribosomal peptide synthetase-independent siderophore synthetases involving trapping of acyl-adenylate intermediates with hydroxylamine. *Methods Enzymol* 458:431-457.
18. Röttig M, Medema MH, Blin K, Weber T, Rausch C, Kohlbacher O (2011) NRPSpredictor2-a web server for predicting NRPS adenylation domain specificity. *Nucleic Acids Res* 39:W362-W367.
19. Rausch C, Weber T, Kohlbacher O, Wohlleben W, Huson DH (2005) Specificity prediction of adenylation domains in nonribosomal peptide synthetases (NRPS) using transductive support vector machines (TSVMs). *Nucleic Acids Res* 33(18):5799-5808.
20. Stachelhaus T, Mootz HD, Marahiel MA (1999) The specificity-conferring code of adenylation domains in nonribosomal peptide synthetases. *Chem Biol* 6(8):493-505.
21. González-de-Castro Á, Broughton H, Martínez-Pérez JA, Espinosa JF (2015) Conformational features of secondary N-cyclopropyl amides. *J Org Chem* 80(8):3914-3920.

22. Hu DX, Grice P, Ley SV (2012) Rotamers or diastereomers? An overlooked NMR solution. *J Org Chem* 77:5198-5202.
23. Nagai Y, Kusumi T (1995) New chiral anisotropic reagents for determining the absolute configuration of carboxylic acids. *Tetrahedron Lett* 36(11):1853-1856.
24. Huang SX, et al. (2015) Leinamycin E1 acting as an anticancer prodrug activated by reactive oxygen species. *Proc Natl Acad Sci USA* 112(27):8278-8283.